UNIVERSITY OF SOUTHAMPTON

FACULTY OF SOCIAL AND HUMAN SCIENCES

Geography & Environment

Volume 1 of 1

Biogeochemical interactions in thermokarst lakes: investigations into methane processes and lake biota

By

Kimberley Leanne Davies

Thesis for the degree of Doctor of Philosophy

March 2015

UNIVERSITY OF SOUTHAMPTON

ABSTRACT

FACULTY OF SOCIAL AND HUMAN SCIENCES

Geography and Environment

Thesis for the degree of Doctor of Philosophy

BIOGEOCHEMICAL INTERACTIONS IN THERMOKARST LAKES: INVESTIGATIONS INTO METHANE PROCESSES AND LAKE BIOTA

Kimberley Leanne Davies

Processes in the cryosphere can trigger large-scale greenhouse gas flux to the atmosphere, including methane emissions via ebullition (bubbling) from thermokarst lakes. Methane emissions specific to thermokarst lakes have yet to be fully explored or quantified, and lake sediments hold potentially useful information about methane cycling. This study investigated the relationship between surface sediment properties and current patterns of large-scale methane emissions and how these emission patterns could be used to link methane availability to lake food webs in thermokarst lakes. Two main questions were addressed: how do sediment-based properties record the spatial distribution of methane production, and can we better understand how methane is utilised in lakes and lake food webs?

Samples were analysed from the surface sediments of two thermokarst lakes in Interior Alaska. The spatial distribution and stable carbon-isotope compositions of lipid biomarkers were used to assess the presence of methane oxidising bacteria (MOB) in the surface sediments. Based on other studies, it was hypothesized that MOB would be highest in the methane ebullition zone of a lake: this was the case in one lake but not in the other, which may reflect differences in source and mode of transportation of methane and affect the availability of methane for oxidation by bacteria.

Fossil chironomids were analysed to establish whether (i) chironomid assemblages varied with the strength of methane flux, and (ii) the stable carbon-isotope values of taxon-specific chironomid samples reflected assimilation of MOB that could be linked to areas of highest methane production. Assemblages showed subtle variations in composition. The $\delta^{13}C$ values were low, which might be linked to the assimilation of MOB; however, high within-lake and within-taxon variability in $\delta^{13}C$ values obscured any correlation with patterns of methane production and oxidation. This suggests there may be problems with using down-core $\delta^{13}C$ values of fossil chironomids to infer past methane production. Factors underlying the observed heterogeneity may be related to thermokarst dynamics or organic or inorganic sediment properties, and these require further exploration.

Table of Contents

List of tables

List of figures

DECLARATION OF AUTHORSHIP

I, Kimberley Leanne Davies, declare that this thesis titled:

BIOGEOCHEMICAL INTERACTIONS IN THERMOKARST LAKES: INVESTIGATIONS INTO METHANE PROCESSES AND LAKE BIOTA

and the work presented in it are my own and has been generated by me as the result of my own original research.

I confirm that:

1. This work was done wholly or mainly while in candidature for a research degree at this University;
2. Where any part of this thesis has previously been submitted for a degree or any other qualification at this University or any other institution, this has been clearly stated;
3. Where I have consulted the published work of others, this is always clearly attributed;
4. Where I have quoted from the work of others, the source is always given. With the exception of such quotations, this thesis is entirely my own work;
5. I have acknowledged all main sources of help;
6. Where the thesis is based on work done by myself jointly with others, I have made clear exactly what was done by others and what I have contributed myself;
7. None of this work has been published before submission:

Signed:

Date: 30/03/2015

Acknowledgements

First and foremost I would like to express my gratitude to my supervisors Prof. Mary Edwards and Dr. Pete Langdon. Not only did you both provide constant support, guidance and enthusiasm through the duration of PhD, but also throughout my undergraduate study. You both inspired me and gave me the confidence to try, and I will be forever grateful for the opportunities that you have provided.

Prof. Melanie Leng and Prof. Rich Pancost have contributed greatly towards this PhD by allowing me to use their laboratories and for helping to guide me through the often confusing but fascinating realm of organic geochemistry. I could not have done it without their expert knowledge, patience and support. I also thank Lidia Chaves Torres who was fundamental during my time in the OGU at the University of Bristol, and Hayley Essex for support in the PLUS lab.

In regards to financial support, I would like to thank Geography and Environment at the University of Southampton for funding this research and NERC Isotope Geoscience Facility and the QRA for a number of awards which made both labwork and fieldwork possible. I would like to thank Ben Gaglioti, Prof. Bruce Finney and Prof. Katey Walter Anthony and her team for sharing their data and knowledge with me. I also appreciate the support of Dr. Maarten van Hardenbroek, whose help during the final stages helped immensely.

Special thanks are given to Prof. Katey Walter Anthony, who, through her constant enthusiasm and passion for thermokarst lakes reinforced my own interest in the arctic environment. I am truly grateful for all the opportunities she has given me over the course of my PhD. Thanks are also given to Dr. Nancy Bigelow for her help and support whilst I spent time in Fairbanks.

I am indebted to Miriam Jones, Laura Brosius, Rob Collier, Tom Roland and Charlotte Clarke for help during trips to Alaska and Siberia and I am especially grateful to Charlotte and Alice Marks for help in the lab. I have appreciated the advice and help of Steve Brooks who has never failed to provide support and encouragement throughout the course of any of my academic endeavours.

I am grateful to all my close friends who supported me over the years. To those who I met during my time at Southampton: John Duncan, Ellie Tighe, Tom Bishop and Min Budimir; thank you all. To Jenni and John, for always

being on call for animated discussions and rehydration. I am also grateful to Cath Langdon, for always reminding me that ‘everything will be ok’.

Special thanks to Helen Mackay and Charlotte for all help during the final months. You made me smile when I didn’t think there was anything to smile about. The constant supply of tea and chatter was much appreciated.

Lastly, I would like to thank my family for all their encouragement and support. To mum and dad for always believing in me and helping in any, and every way they could; your love and care always keeps me going. To Felicity for helping me through tough times; thank you for keeping me on track. To Niall for unwavering support throughout; I will always appreciate your patience and care during stressful times. Thank you for always being there.

I couldn’t have done it without any of you.

Kim Davies
University of Southampton
March 2015

“Above all, don’t fear difficult moments. The best comes from them.”

- (Rita Levi-Montalcini, 1909 – 2012)

Chapter 1: Introduction, Research Process & Research Aim

1.1 Introduction

Arctic and sub-arctic regions are highly sensitive to climatic fluctuations and 21st century warming here is projected to be more pronounced than anywhere else on the Earth (Vaughan et al., 2013). These regions are dominated by near-surface permafrost and ice-rich soils which, when subjected to warming, are vulnerable to thaw (Jorgenson et al., 2006). Thawing of permafrost leads to the initiation and expansion of wetlands and water bodies (e.g. ponds and thermokarst lakes), and consequently the thaw and exposure of previously unavailable labile carbon sources (Zimov et al., 1997). Arctic and sub-arctic wetland areas are estimated to contribute a quarter of total greenhouse gas (GHG) emissions due to the anaerobic decomposition of Pleistocene carbon sources and subsequent methane generation (Walter et al., 2001; Walter et al., 2006; Zimov et al., 2006a; McGuire et al., 2006). The exposure of these 'new' carbon pools due to thawing permafrost means areas which were once considered carbon sinks are evolving into carbon and methane sources. This in turn, will lead to further temperature increases via a positive feedback loop enhancing climate warming induced problems (Walter et al., 2006; Zimov et al., 2006a; Schuur et al., 2008).

Northern-latitude thaw lakes (thermokarst lakes) have recently been identified as sources of biogenic methane emissions which have not previously been included in regional or global methane budgets, nor as a source of emissions in climate models, due to the uncertainty associated with large variability in the position and rate of methane emissions via ebullition (bubbling) within thermokarst lakes (Walter et al., 2006; Zhuang et al., 2009). Thermokarst lakes are a predominant feature of high-latitude landscapes, for example, they are believed to cover 22-48% of the Arctic tundra landscape in the Arctic Coastal Plain in Alaska (Hinkel et al., 2003). Under current warming conditions the area covered by these lakes in continuous permafrost regions is likely to increase.

Methane production that is specific to thermokarst lakes occurs in areas of more recently thawed permafrost underneath the lake. Understanding the

spatial and temporal evolution of methane production from thermokarst lakes is essential for developing a better understanding of the carbon cycle, the accuracy of global carbon budgets and subsequently, future climate projections. The current model for thermokarst lake evolution shows the majority of methane is generated and released at the expanding margins. Walter et al, (2008a) demonstrated that ~ 95% of methane produced in active thermokarst lakes is released via ebullition with high emissions at thermokarsting margins where carbon-rich sediments are exposed to anaerobic decomposition. The quantitative values derived from Walter et al's. (2006) study have yet to be validated by others, but the conceptual model of methane emissions from these lakes is widely accepted. First, frozen, carbon-rich sediment of Pleistocene age underlying the lake is exposed to relatively warm water and subsequently thaws leading to biogenic methanogenesis. Second, overlying bank material is deposited and incorporated into the littoral lake sediments which, under anoxic lake conditions, can be another potential source for methanogenesis at the lake margin. As the lake expands, the area of highest methane production within the lake will remain closest to the shores, therefore if a record of methane cycling is preserved in lake sediments its temporal and spatial distribution will alter depending on the location of a sediment core. Theoretically, a complete lake sediment record taken from the centre of a lake should show high methane levels at lake initiation, when the margins were much closer to the centre of the lake and thawing began, then decreasing activity over time as margins expand and carbon stocks in the centre of the lake diminish.

The model of methane generation in thermokarst lakes suggests lateral movement of carbon-rich margins over time with expansion of the lake. The speed of lateral movement over time, for example, whether the area moves at a similar rate to lake expansion, remains unknown. It is important to establish stability of a carbon-rich area especially on measurable timescales as this will determine whether patterns of methane generation and presence can be established through lake sediments.

Methane can be produced in the deep sediments underneath the lake or in sediments that have slumped in at the margins due to lateral expansion of the lake. This methane is emitted to the atmosphere via ebullition (bubbling). Bubbles form in the sediment and create tubes which allow a constant release

of methane to the lake water and atmosphere above. Here, these bubble tubes are defined as ebullition-seeps. In many thermokarst lakes methane emissions are not restricted to a single ebullition-seep but many will form within a highly localised region of newly exposed carbon as the lake expands. Although the length of seep stability is still unknown, observational data over the last decade has demonstrated that large seeps in lakes have remained stable over this time (Walter Anthony and Anthony 2013). A seep remains spatially stable until the underlying carbon source is exhausted and it is likely they have remained stable over the period contained in a surface sediment sample (usually a 0.5-1cm slice from a gravity core). It has also been observed that these seeps can be large enough and consistent in emissions that holes in winter lake ice (1-2m thick) can be maintained (Walter et al., 2008b).

The proportion of methane which is not released via ebullition is readily oxidised by methane oxidising bacteria (MOB) in the sediments and water column (Trotsenko and Khmelenina, 2005; Liebner and Wagner, 2007). This could mitigate methane emissions to the atmosphere to some extent; however, the amount of methane that is oxidised is still poorly understood. MOB and their tracers such as biomarkers could be utilised in order to understand any spatial patterns of methane oxidation which could be linked to areas of high production and increased supply rates of methane to the lake food web. Biogenic methane produced in lakes has a highly depleted isotopic signal in comparison to its source material (Whiticar, 1999) and in thermokarst lakes values as low as $\delta^{13}C_{CH4}$ -70‰ have been reported (Walter et al., 2007a). This suggests that $\delta^{13}C$ may be a proxy for methane within thermokarst lakes, if, for example, this highly depleted carbon can be followed through the food web and provided there is a good knowledge of the current patterns of biogeochemical cycling within the lake.

Recent studies have shown the ability of some chironomid (non-biting midges) taxa to utilise MOB as a viable food source within lakes (Deines et al., 2007a; Jones and Grey, 2011). This has been measured through the $\delta^{13}C$ values of larvae with displacement of as much as -64‰ reported in some cases (Grey et al., 2004b). Studies suggest assimilation of MOB and thus isotopically depleted $\delta^{13}C$ is taxon-specific with taxa such as *Chironomus* displaying very low values (Jones et al., 2008). As yet, little work has been completed on the relationship of methane to $\delta^{13}C$ of chironomid head capsules, but previous studies have

suggested that a methane signal can be determined through the $\delta^{13}C$ values of chironomid head capsules (van Hardenbroek et al., 2010; Wooller et al., 2012).

To summarise, large-scale methane production in thermokarst lakes has been identified via emissions which requires *in-situ* physical measurements. Therefore our understanding of thermokarst lake methane production in the past is limited by the length of the records. Recently the $\delta^{13}C$ values of MOB lipid biomarkers and chironomid larvae have been linked to patterns of methane availability in lakes and may provide an indirect means of establishing past conditions in thermokarst lakes. A detailed description of how this thesis will contribute to the scientific knowledge in this area is given below.

1.1.1 The Research Process

This section gives an overview of how the research project developed over time in order to provide context in terms of the final research aims and objectives and how each of the data chapters contributes to the overall research project. A detailed review of the important aspects of the project such as the importance of thermokarst lakes and the viability of the chosen techniques is provided in chapter 2.

1.1.2 Thesis development: the initial rationale

Initially, the primary focus of this project was to use chironomid remains in a palaeoenvironmental context to understand the availability of methane in thermokarst lake over geological timescales (the Quaternary).

Chironomid larvae are abundant in modern thermokarst lakes and their head capsules are well preserved in sediments. Chironomid head capsules could provide an indirect measure of methane production regions and supply to the food web in two ways: i) by their assemblage characteristics and ii) their $\delta^{13}C$ isotopic signal. First, chironomids are highly sensitive to environmental conditions and taxon-specific feeding preferences suggest assemblages are likely to alter depending on food source (Jones et al*.,* 2008). Second, the isotopically distinct signal of biogenically produced methane, along with further isotopic displacement created by MOB biosynthesis, in comparison to other potential food sources such as algae and detrital sediments, suggest that if MOB is an important food source, this isotopically light signal will be passed

along the food chain to chironomids, whose $\delta^{13}C$ signal is determined by their food source (DeNiro and Epstein, 1978).

At the time of the development of the research project, it was thought that due to the large-scale of methane production in thermokarst lakes, the supply of methane to the food web would be great also, therefore the signal of methane-derived carbon in lake organisms such as chironomids would be clear.

A modern pilot study was set up using a small dataset from across the surface sediments of two thermokarst lakes to simply confirm the early assumptions with the idea that much of the following focus would be on downcore records. During this first phase of analysis however, it became clear the results were complicated and although the rationale behind using chironomid remains was still robust, further work was needed to understand the cycling of methane in modern systems to a greater degree especially with regards to methane production, transportation and supply to lake food webs via MOB.

1.1.3 Further development of the research project

After the pilot study, it was deemed critical that the factors outlined above were taken into account as part of the research, hence the project evolved over time to include a number of different analyses in order to construct a model of the cycling of methane in thermokarst lakes, the modern distribution of organisms within the lake food web and the biogeochemical interactions as a whole.

Figure 1.1 highlights the pathways of methane within a lake, from production in anoxic sediments to flux to the atmosphere and recycling within the lake food web. This highlights that although the basic principles as outlined above may appear straightforward, there are a number of steps in between the production of methane and the utilisation by organisms in the food web which become increasingly more complex.

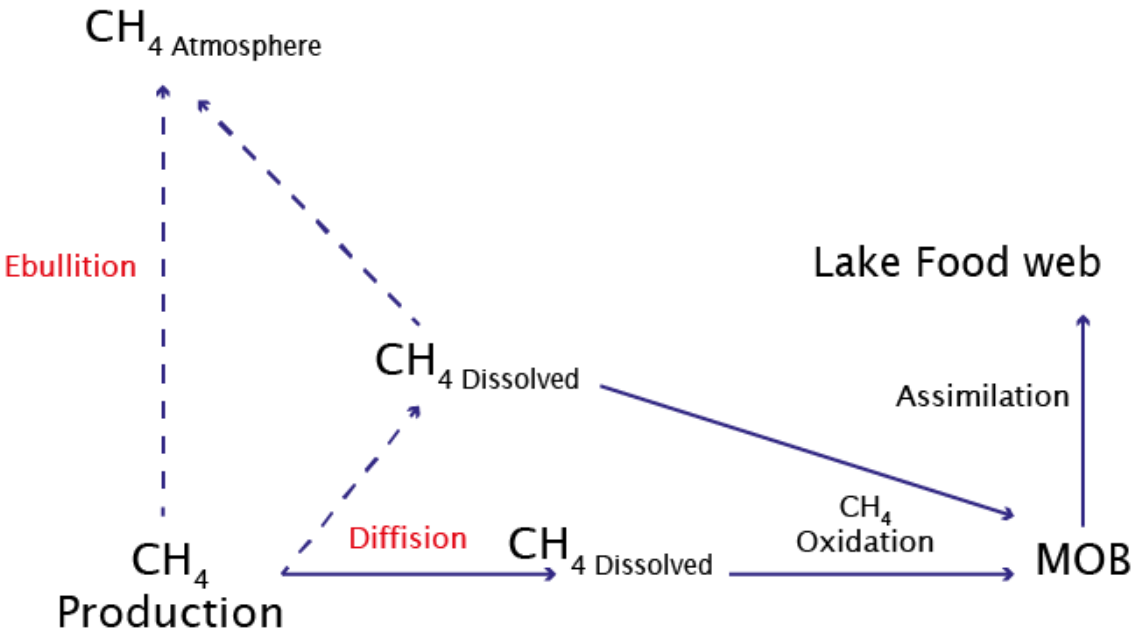

Figure 1.1 Flow diagram of methane cycling in lakes. Dashed lines indicate transport pathways which do not directly interact with organisms in the lake. Transportation mechanisms are highlighted in red.

Despite evidence to suggest MOB is likely to be a food source for chironomid larvae, a number of factors need to be taken into consideration. Are MOB concentrations high enough to alter chironomid assemblages in lakes or will other variables such as lake temperature and depth override any MOB signal? In order to gain a low $\delta^{13}C$ signal in chironomid head capsules, MOB would have to make up a large part of their diet. This will depend on the concentration on MOB in the surrounding sediment, how many of these are then consumed by chironomid larvae and the overall distribution of MOB within methane-rich areas.

Determining the presence and concentration of MOB can be achieved through tracers such as lipid biomarkers. The very low $\delta^{13}C$ signal of specific lipid biomarkers can determine the presence of MOB in thermokarst lakes and whether they are a viable food source for chironomid larvae. When compared a number of variables such as other food sources, chironomid concentrations water temperatures, which often control biological communities, a better understanding of driving factors of chironomid assemblages and isotopic

patterns can be derived along with measurement and analysis of biogeochemical interactions in these environments as a whole.

As well as knowledge of MOB, the project would benefit from the classification of the limnological systems, including the spatial distributions in organic matter within a lake which will affect the potential pool of carbon sources available to lake organisms. Contemporary patterns of methane emissions within lakes and across lakes, MOB presence and concentration, lake sediment classification and chironomid assemblages and isotopic will be studied in detail using a number of different techniques (as outlined within each chapter below).

1.2 Research Aim

The overarching aim of this thesis is **to investigate the biogeochemical interactions between methane and organisms within the food web of thermokarst lakes.**

This will be achieved through a series of focused objectives:

- Development and refinement of an appropriate sampling strategy for obtaining biological organisms from thermokarst lakes accounting for the fact that methane emissions are heterogeneous across the lake (addressed throughout all chapters).
- Classification of the relative contributions of different sources of organic matter to the surface lake sediments across a highly resolved spatial scale using a number of appropriate geochemical techniques (Chapter 4).
- Collection of data from surface sediments to establish the presence and stable isotopic signatures of lipid biomarkers which can be used as tracers of MOB (Chapter 5).
- Collection of data from surface sediments on chironomid assemblage distributions to establish changes within a lake and between lakes associated with methane production (Chapter 6).
- Collection of data from the surface sediments on the stable carbon isotope signatures of chironomid remains to establish the contribution of methane-derived carbon to their diets (Chapter 7).
- Synthesise all datasets to establish the links between methane and the lake food web (Chapter 8).

These analyses will be undertaken using samples from lakes in Alaska which are geographically close, facilitating assessment of the extent to which the relationships recognised are controlled by site-specific factors. This research is exploratory, yet vital in furthering our ability to understand production and emissions of methane from thermokarst lakes; it will be a crucial stepping-stone towards generating an inventory of methane which is recycled in the lake food web thus improving our understanding of GHG-lake system interactions.

Specific questions will guide the focus of each data chapter and allow each dataset to contribute valuable information towards the main research aim. Each data chapter is outlined below with the chapter title, methods employed and relevance to the main thesis aim.

- Chapter 4 – '**Examining the provenance and spatial distribution of organic matter in lake sediments'**.
  Both distribution and type of organic matter across bulk surface sediments in the study sites will be determined through multiple analyses: loss-on-ignition, stable carbon isotopes, C/N ratios and lipid biomarkers. Through the different analyses, the contribution of terrestrial organic matter in lake sediments can be determined. This is important, as knowledge of organic carbon sources in the lake allow a greater understanding of carbon cycling in the lake food web. By establishing the available carbon sources and their stable carbon isotope values the potential importance of methane-derived carbon in the food web can be determined.
- Chapter 5 – '**Spatial variability of diploptene δ^{13}C values in thermokarst lakes: the potential of a novel proxy to analyse the complexity of lacustrine methane cycling'**.
  The presence and stable carbon isotope values of MOB biomarkers will be studied in order to determine MOB presence in the sediments. Relative concentrations of MOB in the sediment will highlight whether their abundance is high enough to provide a feasible food source for chironomid larvae and that this food source be detectable in the stable isotopic signature of chironomid larvae and head capsules. Determining the stable carbon isotope composition of diploptene will allow a better understanding of the traceability of methane oxidation that is occurring in the surface sediments across the lakes in this study specifically.

- Chapter 6 – '**Spatial distributions of chironomid assemblages: the role of methane in chironomid community structure'**.
  Chironomid assemblages will be analysed in surface sediments across the study sites. This will highlight whether methane dynamics play a role in habitat partitioning of chironomid larvae in thermokarst lakes and whether particular taxa are associated with areas of high methane

production. This may highlight whether specific taxa are influenced by methane more than others. By analysing both the methane oxidation patterns and the chironomid assemblage patterns, a better understanding of the relationship between the two variables can be gained.

- Chapter 7- '**Stable isotope signatures of taxon-specific chironomid samples as indicators of methane supply to the lake food web in thermokarst lakes'**.
  The stable carbon isotope values of both chironomid larvae and chironomid head capsules will be measured in order to highlight the contribution, if any, of ^{13}C-depleted carbon to their diet. This will highlight whether MOB might be utilised in the diets of specific taxa and thus be seen in the assemblage patterns and stable isotope values of chironomid larvae and head capsules.

Chapter 2: Literature Review

2.1 High-latitudes: definition and overview

Arctic and sub-arctic regions can be defined in a number of ways depending on the chosen control; for example for the arctic: the 10˚ isotherm or the northern limits of the treeline, while for the sub-arctic: the southern limits of permafrost or the temperature of permafrost (Prowse, 1990). For the purpose of this study, the areas in question will be termed 'high-latitude' and will encompass both arctic and sub-arctic areas and high northern latitudes dominated by snow, ice and permafrost processes. This includes areas of discontinuous and sporadic permafrost and covers the Arctic tundra and boreal biomes. Definitions and further detailed descriptions of permafrost are given below.

2.1.1 High-latitudes: Climatic history of Beringia

2.1.1.1 Beringia in the Pleistocene

During past glacial cycles, vast areas of the northern hemisphere were glaciated. The lowlands of Beringia however, a region which encompasses the areas between the Lena river in northeast Russia and the Mackenzie River in Canada and thus incorporates much of Alaska, remained ice free (Elias and Brigham-Grette, 2004). During the Last Glacial Maximum (LGM ~ 25,000-14,000 ^{14}C yrs BP; Anderson et al., 2003), the build-up of ice within high-latitude regions surrounding Beringia led to a drop in sea level of between 120-130 m (Lambeck et al., 2002) and the exposure of the continental shelf between Siberia and Alaska known as the Bering land bridge. This is the most recent exposure of the land bridge and is suggested to have existed for 10,000 years from 30,000 – 20,000 cal yrs BP (Elias and Brigham-Grette, 2004). The expansion of the Laurentide ice sheet during the LGM created strong southerly winds along the western margin of the ice sheet creating warmer than present winter conditions in Alaska and Northwest Canada but lower than present CO_2, sea levels and insolation meant summer temperatures were likely to be lower than today, and overall created a cold, continental climate in Beringia (Bartlein et al., 1991).

Climatic reconstructions based on pollen concur with the theory of an arid Alaskan climate during the LGM, with the evidence suggesting a largely dry tundra landscape (Anderson and Brubaker, 1994). During the LGM glacial extent across Alaska was minimal. The largest area covered with ice was the Alaska Range. The Brooks Range had some glaciers whilst the Interior remained ice free. Increased aridity caused widespread loess deposition in the interior during the LGM (Anderson et al., 2003) and due to this aridity, lake levels were 40-75% lower than present (Barber and Finney, 2000). From 13,500yrs BP conditions remained cooler than present and it wasn't until 10,000yrs BP that conditions in Alaska altered to warmer and drier than present (Edwards, 2001). Additional evidence such as loess deposition and sand wedge development indicate a drier climate, whilst mountain glaciers and lowland ice wedge development indicated decreased temperatures (Hopkins, 1982).

An understanding of the past climate of Beringia is important as it is during this time period that the fine-grained substrate (loess) and labile carbon (tundra and grassland vegetation) were laid down, creating a basis for contemporary system functioning.

2.1.1.2 Contemporary factors

Temperature and precipitation play an important role in high-latitude hydrology and limnology, and regional differences will have an impact on many factors relating to lake processes. For example, lower temperatures maintain surface permafrost, limiting subsurface water storage capabilities thus maintaining lake levels (Rouse et al., 1997). Despite regional variation in both amount and timing of minimum and maximum annual precipitation, a key factor for lake hydrology in high-latitude regions is associated with storage of precipitation as snow and ice and its release during spring break-up. Spring melt dominates the hydrology of most high-latitude regions of Alaska and eastern Siberia and will play a large role in lake formation and dynamics, for example, lake level alterations, oxygen levels due to spring overturn, and allochthonous sediment input.

Terrestrial vegetation cover can affect a number of hydrological parameters within high-latitude regions, such as surface run-off and the depth of permafrost active layers (Walker et al., 2003). Clear links between vegetation,

climate, soils and the active layer have been identified (Klene et al., 2001), which suggest vegetation is likely to affect lake development through hydrological, permafrost and fire dynamic and affect lake status through nutrient and organic inputs.

2.1.2 High-latitude permafrost coverage and importance

The understanding of the many complex variables across high-latitude regions is further complicated by the presence of permafrost which, as stated previously, will have a large impact on the vegetation and hydrology especially lake formation and persistence in the landscape (Smith et al., 2005). Permafrost, defined as soil which remains at or below 0˚C for two or more years, dominates high-latitudes and covers ~ 24% of the northern hemisphere (Zhang et al., 1999). Permafrost can be characterised as continuous (90-100%), discontinuous (50-90%) and sporadic (10-50%) and generally shows a progressive reduction in continuity from north to south latitudes. Contemporary permafrost mostly developed under past glacial conditions and its current distribution is a product of both this past development and modern day heat exchange between the Earth's surface and below ground (Williams and Smith, 1989), therefore climate is the major factor conditioning permafrost stability.

Evidence suggests that many areas of continuous permafrost in high-latitude regions are thawing due to temperature increases at depth, with rates of 0.04-0.10 m yr^{-1} observed in terrestrial uplands (Osterkamp, 2005). This expansion of thaw into continuous permafrost zones is increasing the northerly extent of high-latitude wetlands which, in turn, is increasing the total area available for carbon and methane emissions. Permafrost is highly variable, even in areas of continuous coverage. For example, the Arctic Coastal Plain of Alaska is dominated by ice-rich sediments and underlain by continuous permafrost of depths from 300-600m (Brown et al., 1997 cited in Hinkel et al., 2005).

2.1.2.1 Yedoma

High-latitude soils, defined as soils within circumpolar permafrost regions and up to 300m in depth, are thought to sequester ~1,672 Pg of organic carbon, with over three-quarters stored in permafrost (Tarnocai et al., 2009). Of particular relevance, is what's known as Yedoma. The term yedoma has

evolved several times, from describing geomorphic relief in Siberian permafrost regions formed by thermokarst erosion (Schirrmeister et al., 2008), to the term *yedoma suite*; a strict definition of a stratigraphical horizon representing the Late Pleistocene in northeastern Siberian Lowlands (Sher, 1971), through to currently where the term is used in the literature to describe Pleistocene loessic sediments. The *yedoma suite* spans the periods of MIS 2 and 3 and is characterised as a number of buried cyrosols (Schirrmeister et al., 2011). High ground-ice content and large syngenetic ice wedges mean that the yedoma suite is categorised as having very high ice content (80% volume; Schirrmeister et al., 2011). The type site for the Yedoma Suite is the Duvanny Yar in the Kolyma Lowlands and the presence of the Yedoma Suite is closely linked to mountain ridges in north eastern Siberia (Schirrmeister et al., 2013). This area is dominated by ice-rich soils and carbon rich loess deposits (~4% organic carbon) and is estimated to contain ~450 Pg of labile carbon (Zimov et al., 1997) which, if thawed, could be subject to anaerobic decomposition and subsequently produce a large amount of methane. The characteristic features of the Yedoma suite have been observed in other high-latitude regions but to a lesser extent (Zimov et al., 2006b), thus the term yedoma is used here to describe the deposits that underlie the thermokarst lakes in the study.

2.1.3 High-latitudes lakes and their importance

Current evidence suggests that climate warming over the next century within high-latitude regions will be the most pronounced and occur at a greater rate than anywhere else globally, therefore understanding the significance of its effects is crucial (Meehl et al., 2007). The thawing of permafrost and subsequent wetland formation is increasing with rising temperatures. Wetlands, and more specifically lakes, are already widely distributed throughout Arctic and sub-arctic regions and provide valuable resources for both biological and human communities. High-latitude lakes are important due to recent evidence highlighting them as potentially un-quantified sources of carbon dioxide and methane (Kling et al., 1992; Walter et al., 2006; Walter et al., 2007a), which has global significance for future environmental change through increased levels of GHG emissions. Such lakes have been effectively used to understand past climate regimes (Kaufman, 2004; Miller et al., 2010);

however, it has yet to be determined whether a palaeo-gas flux can be derived from these lakes.

High-latitude lakes are widely abundant and diverse. A number of lake types can be identified, from freshwater to saline, which display a wide range of thermal and chemical regimes (Vincent et al., 2008). The complexity of the system is often a function of latitude, with lakes generally decreasing in complexity towards the poles. The factor that has the largest influence on lake system development in high-latitude regions is the seasonality of climate conditions (Hinzman et al., 2005). Low air temperatures and prolonged snow and ice cover alter catchment processes which ultimately feedback to lake functionality and productivity. A number of other variables can be identified which are important factors in influencing lake systems and are unique to high-latitude environments. These include irradiance, water supply and nutrient supply (Vincent et al.,2008). It should be noted, however, that climate across high-latitudes is highly variable and therefore regional disparity is common. The above factors have an underlying impact on lake development that need to be taken in to consideration.

2.2 Thermokarst lakes

Thermokarst lakes are the most widely distributed and abundant lake type in regions where continuous and discontinuous permafrost is present. Alterations within the current vegetation system due to climate change, for example the decline in white spruce due to increased temperatures (Barber et al., 2000) or increased frequency of extreme fire years (Soja et al., 2007), are expected to negatively alter the carbon budget. Alternations such as those above can also negatively affect thermokarst lake dynamics through active layer depth changes and moisture balance changes (Oechel et al., 1997). Therefore, vegetation dynamics within regions are important in thermokarst lake formation and permanence.

These lakes are a dominant feature of lowland areas within Siberia and northern Alaska. For example, in the Yukon River Delta there are an estimated ~ 200,000 thaw lakes (Maciolek, 1989). As well as their importance as indicators of permafrost disturbance, thermokarst lakes, along with other types of lakes, have been proposed as sources of carbon and methane (Kling et al., 1992), and have more recently been identified as a previously un-quantified source (Walter et al., 2007b).

2.2.1 Origins and development

The genesis of thermokarst lakes is still not fully understood; however, most thaw lakes display a generic cyclic pattern from formation, through growth to rapid drainage. In general it is postulated formation occurs due to degradation of previously stable ice-rich permafrost or ice wedges and the development of small ponds which leads to lateral expansion through retrogressive thaw slumping (French 2007). Rapid drainage often occurs where lake expansion cross-cuts other unfrozen water bodies such as streams and rivers, or ice wedge failure (Jorgenson and Shur, 2007). The longevity of thermokarst lakes is highly variable from only a few days to hundreds of years. Their stability is strongly controlled by regional climate, for example Davis (2001) argues a warming in climate is responsible for initiation and development of contemporary thermokarst lakes. Local factors such as underlying substrates and hydrology are also thought to play a large role in controlling thermokarst lake dynamics (Pienitz et al., 2008)

Thermokarst lakes display highly varied morphometric features; frequently they are shallow (~5m) and have a relatively small area, but some grow substantially and reach diameters of 1-2km (French, 2007) and depths up to 20m (West & Plug, 2008). West and Plug (2008) identify three main types of thaw lakes described in the literature based on bathymetry; broad lakes with a deep pool and shallow littoral shelf, bowl shaped lakes and flat bottomed lakes. Much of the literature that is important for this study is focused on the latter two lake types.

2.2.1.1 The thaw bulb

Critical to the understanding of thermokarst lakes position in the arctic carbon cycle is knowledge of talik or thaw bulb formation underneath the lake and of how active the thermokarst margins are. If mean annual lake bottom temperatures exceed 0˚C, sediment underneath the lake will thaw and remain this way until lake drainage or lake level reduction allows bottom waters to freeze. Thaw bulb depths are a function of ground ice content (permafrost coverage) and lake size. Their depths are highly variable but studies have reported values between ~32 and 73 metres (Hunter et al. 1981 in: West and Plug 2008). The thaw bulb extends around the margin of the lake and as described previously, lake expansion is due to the thawing of ice-rich permafrost along the lake's margin. Importantly, the thaw bulb is often formed in yedoma, described in detail in section 2.1.2.1, which when thawed provides a good environment for the bacterial production of methane. Equally, material that enters the lake due to slump can also be subject to methanogenesis; especially deep, bowl shaped thermokarst lakes. This bacterial methane production underneath thermokarst lakes is discussed in more detail below.

2.3 Methane

Atmospheric methane is the second most important anthropogenic GHG after carbon dioxide (CO_2). Currently the average tropospheric concentration is 1,800 ppb; these are the highest levels observed in the last 800,000 years, as seen in Antarctic ice core records (Loulergue et al.,2008). The level of methane in the atmosphere is determined via feedback loops between sources and sinks, and currently global methane emissions are between 500-650 Tg CH_4 yr^{-} (Denman et al., 2007; Kirschke et al., 2013). Methane is the product of anaerobic respiration performed by methanogens and the largest recognised single terrestrial source of atmospheric methane is wetlands (Denman et al., 2007); however, 60-70% of methane emissions between 2000-2005 were anthropogenic. The largest identified sink of methane on decadal timescales is oxidation with the hydroxyl (OH) radical in the troposphere. Increases in atmospheric methane will also lead to increased CO_2 as this is a direct by-product of methane oxidation.

2.3.1 Methanogenesis & methane oxidation in high-latitude freshwater systems

Atmospheric methane released from high-latitude wetlands and freshwater ecosystems is derived from organic carbon and forms part of the carbon cycle. It is mostly produced by methanogenesis in strictly anoxic conditions by *Archea*, the methanogens, which use substrates such as CO_2, carbon monoxide (CO), methanol (MeOH) and acetate ($C_2H_3O_2^{-}$) to produce methane (CH_4). There are at least two different pathways for methanogenesis in freshwater systems: CO_2 reduction, (Equation 2.1),

$$CO_2 + 4H_2 \rightarrow CH_4 + 2H_2O \quad \text{(EQ 2.1)}$$

or acetate fermentation (Equation 2.2)

$$CH_3COOH \rightarrow CH_4 + CO_2 \quad \text{(EQ 2.2)}$$

With the latter being responsible for twice as much methanogenesis in soils and sediments (Conrad, 1999).

Methane oxidation usually takes place under aerobic conditions (Equation 2.3),

$$CH_4 + O^2 \xrightarrow[\text{monooxygennose}]{} CH_3OH \rightarrow HCHO \rightarrow HCOOH \rightarrow CO_2 + H_2O \quad \text{(EQ 2.3)}$$

but it can occur in anoxic environments (Pancost et al., 2000a; Sanseverino et al., 2012). In these conditions, a different oxidising compound such as sulphur is the electron acceptor; the chemical reaction is given in equation 2.4

$$CH_4 + SO_4^{2-} \rightarrow HCO_3^- + HS^- + H_2O \quad \text{(EQ 2.4)}$$

In marine settings, methane production in environments such as cold seeps and methane hydrates takes place in anoxic sediments and the anaerobic oxidation of methane (AOM) is considered a major global sink of methane (Knittel et al., 2005; Reeburgh, 2007). AOM may be important in thermokarst lakes, as methane is produced in the thaw bulb deep beneath the lake, it may be oxidised in the sediments prior to reaching the surface. We know that even if this does happen, not all methane is oxidised below the surface. AOM may also play a role in oxidation above the thaw bulb, as anoxia due to stratification is common under winter ice and at the end of summer, however its importance will depend on the abundance of sulphate-reducing bacteria which are required in order for a reaction to take place (Briggs et al., 2011)

Biogenic methane, and the consequent carbon molecules, produced in wetlands and freshwater systems are easily distinguishable from other sources of carbon in these systems as its stable isotope composition is characterised by highly depleted $\delta^{13}C$ values). The $\delta^{13}C$ values of biogenic methane are on average between -60 and -80‰ (Whiticar, 1999; Conrad et al., 2007) whereas other sources of carbon such as allochthonous plants and phytoplankton have $\delta^{13}C$ values ranging from -25 to -35‰ (Peterson and Fry, 1987; Vuorio et al., 2006).

Lacustrine sediments have recently been identified as an important source of methane production (Bastviken, 2004; Walter et al., 2006; Bastviken et al., 2011), and it is suggested that 20-56% of organic matter degradation in freshwater lakes is associated with methane production (Bastviken, 2009). For atmospheric methane emissions, it is argued littoral sediments are more important than profundal due to the likelihood that the methane will reach the atmosphere (Bastviken et al., 2008), as once it reaches the oxic/anoxic

interface in freshwater ecosystems it can be oxidized by methanotrophs to CO_2. The level of methane emissions from freshwater ecosystems will ultimately depend on the ability of bacteria to produce and oxidise it, both in the sediments and the water column which will, in turn, link to higher levels of a lake food web (Grey et al., 2011). The anoxic/oxic interface will change position in the lake depending on the conditions in the lake. For example, this may be high in the water column in summer if stratification occurs or at the sediment-water interface in well-oxidised conditions. Methane production and oxidation in freshwater environments is dependent on a number of factors: temperature, hydrology (e.g. soil moisture in peatlands), availability of suitable organic material and ecosystem growth (Megonigal et al., 2005).

Methane oxidising bacteria (MOB), or methanotrophs, are of the phylum Proteobacteria (Figure 2.1) and mostly spilt into two classes; Gamma Proteobacteria, or 'Type I' methanotrophs, and Alpha Proteobacteria, or 'Type II' methanotrophs which are based on carbon assimilation pathways, phylogeny and internal cell structure (Madigan and Martinko, 2006). MOB are present throughout both terrestrial and aquatic environments wherever there is a constant methane source. As mentioned above methane is produced in anoxic parts of lacustrine systems and is oxidised by MOB at the oxycline converting methane to CO_2 and cell material (Madigan and Martinko, 2006). Quantifying methane oxidation in lakes is important for the both the understanding of methane contribution to pelagic food webs and the amount of methane that reaches the atmosphere. Due to fractionation, the stable carbon isotope signature of MOB is usually lower than the $\delta^{13}C$ values of the original source of carbon and some studies reported $\delta^{13}C$ signatures of MOB which were up to 30‰ more depleted than the CO_2 carbon source (Jahnke et al., 1999; Templeton et al., 2006). This means that MOB-derived carbon can be traced through trophic levels in the food web if it contributes to the diets of higher consumers.

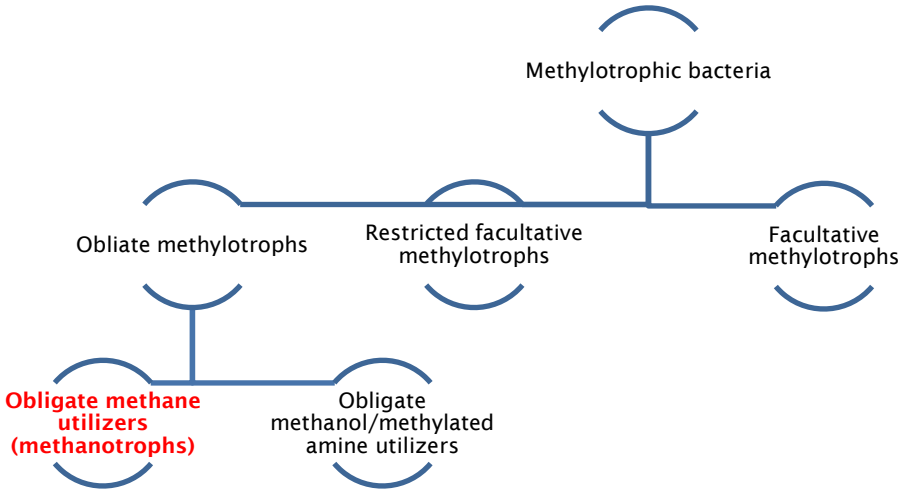

Figure 2.1 Subdivisions of methylotrophic bacteria (Adapted from Green., 1992)

2.3.2 High-latitude wetlands and methane emissions

High-latitude wetlands which include water bodies, especially thermokarst lakes that are often a continuation of hydrological cycling in high-latitude wetlands, account for only a small percentage of the global land surface, yet they are thought to be a considerable carbon sink and a natural source of methane production (Schuldt et al., 2012). The largest high-latitude wetland areas are found between 50˚ N and 70˚ N and are classified as largely bogs and fens (Reddy and DeLaune, 2008). Estimates of high-latitude peatland carbon storage are wide ranging (250-621Pg C) but still indicate a large volume of carbon that has accumulated over the Holocene (Gorham, 1991; Smith et al., 2004; Jones and Yu, 2010; Yu et al., 2010). High-latitude peatlands are a large carbon sink which are increasingly becoming a source through wetland expansion. Methane emissions from these wetland areas are suggested to be between 32-112 Tg CH_4 yr^{-1} (McGuire et al., 2010).

High-latitude wetlands emit both CO_2 and methane and the ratio between the gases depends on two main factors: the degree of aeration (mainly of peatlands) and the microbial methane production and oxidation (Kamal and Varma, 2008). Once methane is produced, it is moved to the atmosphere in a

number of ways: diffusion, plant mediated transport and ebullition (Bastviken et al., 2004).

These pathways have also been identified in thermokarst lakes, however quantitative levels have not been given for diffusion and plant mediated transport, nor has oxidation in thermokarst lakes been fully quantified. Walter et al. (2006) suggest ~95% of methane produced in actively expanding thermokarst lakes in Siberia is released via ebullition. Alternatively, it is argued that once thermokarst lakes stabilise, the overall level of methane emissions are reduced and the diffusive component is increased (Walter Anthony et al., 2010). Furthermore, little work has been completed on the internal utilisation and storage of methane-derived carbon within thermokarst lake systems. Wooller et al. (2012) and van Hardenbroek et al. (2012) use the stable isotopes of various aquatic organisms to highlight changes in methane availability over time, however the connections between methane production, transport, atmospheric flux and utilisation within the lake water column was not fully studied. Further work is required in order to fully understand the interactions between different modes of methane emissions and cycling within the lake in thermokarst lake systems.

2.4 Thermokarst lakes and methane emissions

2.4.1 Source of methane emissions in thermokarst lakes

As highlighted in Section 1.1, thermokarst lakes have recently been identified as a source for methane emissions. In terms of methane emissions, ebullition is the main route for methane to the atmosphere and in thermokarst lakes this can be split into three pathways: background, point source and hotspots (Walter et al., 2008a; figure 2.2).

Walter et al., (2008a) studied a number of thermokarst lakes from both Alaska and Siberia and suggest that of the lakes studied, background ebullition was most closely associated with acetate fermentation methanogenesis whilst point source and hotspot ebullition is positively correlated to CO_2 reduction pathways.

In thermokarst lakes methane is predominantly produced in the talik bulb or in sediments which have slumped into the lake at the margin due to thermal erosion and not the surface sediments (Walter et al., 2008a). This is important as the organic material found in the talik bulb is highly labile and therefore more susceptible to the processes associated with decomposition. An important factor associated with the ability of methanogens to produce methane is the stability of insoluble compounds to decay. The organic compounds in the loess-derived talik bulb deposits will have been subject to destruction in the past which means they are more amenable to autotrophs and subsequent methanogenesis than those in the surface sediments. Mazéas et al., (2009) highlight that is it important to consider the nature of the sediments that are being exposed to decomposition, as organic carbon content can be highly variable, therefore the level of methane production will alter accordingly.

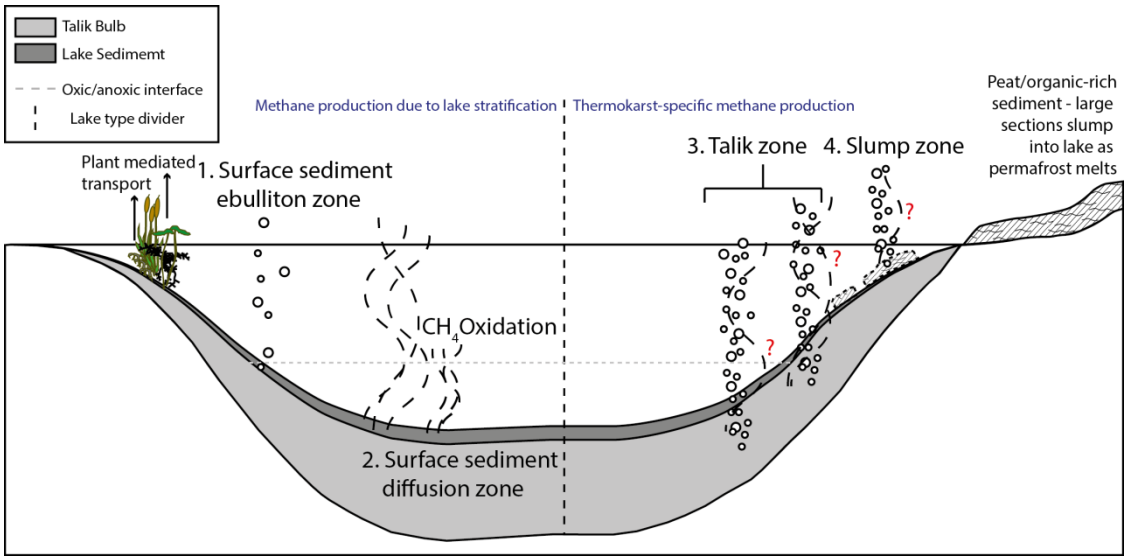

Figure 2.2 Illustration of methane production zones and emission pathways in lakes alongside thermokarst-specific zones and pathways.
1) Surface sediment ebullition. Methane that is produced in the anoxic surface sediments is released via ebullition, usually near the margins (Bastviken et al., 2004). (2) Surface sediment diffusion. Methane is produced in the anoxic surface sediments and diffuses into the sediments above and into the water column. Some of this methane will reach the water surface-air interface but a large amount is likely to be oxidised by MOB (Kankaala et al., 2006). (3) Talik zone. Methane is produced in the deeper talik sediments underneath the lake and is released via ebullition-seeps (Walter et al. 2008a). Often this is a higher flux which is more constant than (1). This production zone and pathway is a thermokarst lake-specific process. (4) Slump zone. Methane production in the surface sediments is increased due to the introduction of large volumes of slumped sediments. This methane is also released via ebullition-seeps. Often, the flux from these ebullition-seeps is higher than surface sediment ebullition but not as high as talik ebullition. This process might occur in lakes which have dynamic margins and high erosion rates, however it is likely that this process is most common in thermokarst lakes due to the melting of permafrost so is termed thermokarst-specific. Red ?'s indicate where methane diffusion from the sediments has not been studied in detail.

2.4.1.1 Anomalous Holocene methane fluxes

Studies of ice cores and other records highlight a sharp increase in methane emissions in the northern hemisphere after the Younger Dryas chronozone in the early Holocene (~ 9.5 – 11.5ka). Emissions appeared to almost double in comparison with LGM emissions from ~ 30 during LGM to 60 Tg CH_4 yr^{-1} (Chappellaz et al., 1990; Kennett et al., 2003). The source of this pulse in methane emissions is still debated but some have attributed it to the high-latitude wetlands (Smith et al., 2004; Valdes, 2005). Much of the argument is based on the theory that, despite the known immature stages of the North American peatlands' at this time, peat initiation prior to 8,600 yrs BP across vast areas of high-latitude regions might have represented a major carbon sink at the beginning of the Holocene and may have contributed to the peak in methane flux during a thermal maximum (Smith et al., 2004; Jones and Yu, 2010). However some have highlighted errors in the findings associated with the proposed chronologies (Reyes and Cooke, 2011). Reyes and Cooke (2011), demonstrated that from nearly 300 published ^{14}C basal dates from the work completed by Jones and Yu (2010), only half were deemed acceptable to reconstruct initiation. This early Holocene methane flux, coincides with a thermal maximum in the early Holocene, a period of increased warming in high latitudes (Kaufman, 2004), which might be cause for an increase in thermokarst lake development during this period. The increase in thermokarst lakes might cause a pulse of methane emissions under hypothesised scenarios discussed in previous sections and therefore could be considered a source for methane emissions during the early Holocene (Walter et al., 2007b). Exposures of drained thermokarst lakes, which initiated during this period, can be found across high-latitude regions and enable us to explore the idea that thermokarst lakes may have contributed to the methane emissions in the early Holocene.

2.5 Chironomids

This section will provide an introduction to chironomids and their role in lacustrine ecology and review their use as both modern and palaeoecological proxies. Previous studies of chironomids and methane in lakes will be discussed in order to place the current study in context.

2.5.1 General ecology

Chironomidae (chironomids or non-biting midges) is a family of two winged flies (Insecta: Diptera) with ~ 8,000 – 20,000 species thought to exist worldwide (Coffman, 1995). Chironomids occupy a wide geographical distribution and, along with species-specific tolerances along large environmental gradients, the dispersive abilities of adults and short life cycles mean that they are highly sensitive indicators of environmental change, (Armitage et al., 1995; Porinchu and Macdonald, 2003). The larvae are highly abundant in freshwater ecosystems and are often the dominant macroinvertebrate in both the littoral and profundal zones of lakes, as such they are a valuable food source for fish and birds and are an important component of freshwater food webs (Eller et al., 2007). In high-latitude regions chironomids are considered not only one of the dominant communities but also one of the most diverse (Oliver and Dillon, 1997). Since the early 1900s, chironomids have been noted as an important part of lake ecosystems and were one of the first elements of the biota to be used in lake classification by Thienemann in 1918. Due to their importance within lakes, chironomid larvae have been used by ecologists and limnologists in lake classification as indicators of lake trophic status and oxygen concentration (e.g. Walker et al. 1991; Larocque et al. 2001; Little and Smol 2001) and more recently temperature and water depth (e.g. Brooks and Birks 2001; Kurek and Cwynar 2009).

2.5.1.1 Classification

The chironomid family is globally distributed with species found in aquatic environments from the tropics to the Arctic and Antarctic. Classification of chironomids began over one hundred years ago, yet is a continual process of re-interpretation with new descriptions added frequently. The family can be

divided into eleven subfamilies, of these, only three are common in northern hemisphere freshwater ecosystems; these are the Orthocladiinae, Tanypodinae and the Chironominae (Oliver and Roussel, 1983). From these subfamilies ~ 22 tribes have been identified in the literature (Cranston, 1995), however as with many taxonomic classifications, the exact number alters frequently depending on the discovery of new species, increased taxonomic resolution, regional differences in techniques and species interpretations. Previously the adult stage has provided the basis for identification, therefore our knowledge of the immature aquatic stages is often incongruent between tribe, genus and species and in some cases missing completely (Ferrington, 2008). However, according to Ferrington, (2008) the Nearctic currently has 211 genera and 1,092 recorded species of Chironomidae, which are defined as having aquatic immature stages. Taxonomic resolution in palaeo records is often reduced due to limited identifiable features on the head capsules. Much larval taxonomy is based on modern larvae and therefore when bodies are not present the ability to coherently identify to species level is lost. The level to which the taxonomic resolution is important will depend on the question being answered in the study. Brooks and Birks (2001) suggest increased taxonomic resolution will allow greater predictability of transfer functions, however others suggest that uncertainty might be increased at higher taxonomic resolution due to lack of consistency in identification and amplified noise (Brodersen et al., 2001)

The main features of a fossil chironomid head capsule which are used for identification are the mentum, ventromental plates and mandibles; however, the latter are not always present. In the Holarctic region, the recent taxonomic key published by(Brooks et al., 2007), provides a standardised taxonomy for palaeoenvironmental research. However, it is not comprehensive and should therefore supplemented with older and more detailed keys (e.g. Wiederholm 1983 and Oliver & Roussel 1983).

2.5.1.2 Morphology and life cycle

Chironomids are holometabolous and have four life-cycle stages: egg, larva, pupa and adult, with all but the adult stage being aquatic in the majority of species (Tokeshi, 1995). Development from egg to larvae is dependent on conditions in the lake with variables such as salinity, pH and oxygen concentration affecting the process (Porinchu and Macdonald, 2003).

Characteristic features of chironomid larvae include a segmented body and a non-retractile head capsule (Cranston 1995). The head capsule is comprised of chitin ($C_8H_{13}O_5N$), which has a greater resistance to decay than the fragile body tissue. The larval stage is often the longest with four phases of ecdysis (shedding of the exoskeleton) known as instars. The first instar is usually planktonic, whilst the 2nd, 3rd and 4th instars are typically benthic. However, species such as *Sergentia coracina* (Zetterstedt) are thought to be partially planktonic in the latter instars also (Walker 2001). Length of time at each cycle progressively increases, with the longest period spent at the 4th instar phase. In temperate regions, more species are univoltine, meaning only one life cycle per year, whilst others can cycle up to three times per year (Tokeshi 1995). In high-latitude regions a cycle of between two and three years is not uncommon as the pupation and emergence phase in high-latitude lakes can take a number of years with studies showing life cycles of up to seven years in cold tundra environments (Butler, 1982). From 1st - 4th instar the exoskeleton remains in the sediment, however of this only the heavily chitinised head capsule is preserved over time, and this is used in palaeoecological studies. The preservation of the 1st and 2nd instars is often reduced as chitin is recycled to the latter stages (Iovino, 1975), therefore, the early instars can be missing completely from a palaeo record. If 1st- 2nd instars are present they are usually part of an assemblage table as an increase in numbers or sudden presence of is likely to indicate a shift in environmental conditions even if it is just a change in preservation but these instars would not usually be included in a temperature reconstruction.

2.5.2 Habitat

Chironomid distribution within the lake will depend on a number of factors including potential food sources, competition and species-specific preferences such as preferred food types and substrates. A gradient of assemblage change can be present, from the littoral to the profundal, depending on the tolerance of a species to variables such as temperature and oxygen levels. For example, unlike any other genus, some species of the genus *Chironomus* have haemoglobin and can therefore withstand periods of anoxia, which allows them to survive in the deep waters of the profundal zone or highly eutrophic lakes. Other taxa such as *Sergentia coracina* and *Tanytarsus lugens* have been

identified as indicators of deep water, whilst *Dicrotendipes and Polypedilum* are indicative of shallow systems (Walker and MacDonald, 1995). Macrophyte abundance has been identified as an important factor influencing littoral chironomid distributions (Brodersen et al., 2001), and chironomids can be used to inform us about past changes in macrophyte distribution and abundance (Langdon et al., 2010).

As yet, no studies have looked at the relationship between chironomid assemblage distributions and methane production within lakes. It is highly likely that disentangling a signal of methane production from chironomid assemblage's changes will be difficult as other factors such as depth, temperature and anoxia are likely to co-vary with methane in many lakes, especially bowl shaped thermokarst lakes or where the signal of methane is not very strong. On the other hand, chironomid assemblages may be able to distinguish environmental patterns that could be associated with methane emissions in lakes. Studying lakes with consistently flat bottoms mean that other variables such as depth and temperature can be eliminated and the effects of methane in the system can be seen more clearly.

2.5.3 Chironomid food sources

Chironomid larvae are mostly detritivores and analysis of their gut content suggests that under normal conditions detritus constitutes 50-90% of their overall diet (Johnson, 1987). As such, chironomid larvae play a large role in the 'recycling' organic matter in lakes. Detrital material is largely composed of phytoplankton but can often include other autochthonous and allochthonous material. Some species are plant miners, whilst others graze on bacteria and algae (Walker, 2001). Individuals may have more than one feeding mode, for example, scraping, shredding or piercing. The method of gathering food will depend on a number of factors such as larval size and stage, food quality or competition. In general, profundal larvae collect and filter fine organic detritus that sinks through the water (Berg, 1995). Planktonic primary productivity is seasonally variable; therefore algae and other phytoplankton may not provide a constant food source for macro invertebrates as other forms of detritus.

2.5.4 Taxon-specific feeding preferences

Although many generalisations are made about chironomid larvae, many habits and tolerances are species-specific. Many Chironomini create tubes which they keep oxygenised and clean through body movements (Walshe, 1951). The genus *Chironomus* is among the tube dwellers, however individual taxa often have different feeding preferences. For example *Chironomus plumosus*-type is considered primarily as a filter feeder, but it utilises detritus when food availability is low (Johnson, 1987; Goedkoop et al., 2006). *Chironomus anthracinus*-type is a deposit feeder of detritus around the tube mouth. Its feeding mechanism includes 'sweeping' the sediment surface surrounding its tube using the anterior part of body, and it feeds down to the interface between oxidised and reduced sediment (Grey & Deines 2005). The subfamily Tanypodinae is considered predatory and feeds on protozoans, crustacean larvae and other chironomid larvae (Walker, 2001; Merritt et al., 2008) which means this subfamily may not be useful for this study as they are unlikely to consume MOB directly. The Orthocladiinae contain a large number of species but are mostly considered littoral taxa which feed on algae found on plants or rock surfaces which might highlight this subfamily as inappropriate for looking at ingestion of MOB as it is likely most MOB are in the detrital sediment. It is important to distinguish the feeding preferences of chironomids in order to establish the potential carbon sources which a chironomid might ingest and how likely it is that MOB will contribute to the diets of the individuals sampled in the study.

2.5.4.1 Bacterial contribution to chironomid diets

Despite the high proportion of detritus in chironomid larvae diet, its nutritional value for macroinvertebrates is questionable and therefore other food sources, such as bacteria, might provide greater nutritional importance (Grey & Deines, 2005). The partial contribution of bacteria to chironomid diets has long been known (Johnson, 1987; Goedkoop and Johnson, 1992), but the level of importance is dependent on a number of variables. The contribution and importance of bacteria in chironomid diets varies seasonally within lakes and differing lake status (Grey & Deines, 2005), and it is also likely to be affected by the species specific feeding habits of the larvae. The importance of bacterial contributions will also be greatly affected by the bacterial communities

themselves, and the amount of bacterial carbon contribution to the chironomid diet will also be determined by the oxygen content of the lake and the ability of the bacteria to survive. Seasonal patterns in growth and availability of food will affect the availability of bacteria as a food source. It is important to consider the possible shifts in bacterial communities to understand their potential as a carbon source in lake food webs.

2.5.5 Chironomids as palaeoenvironmental indicators

As stated above, the head capsules of chironomid larvae are heavily chitinised and are therefore well preserved in lake sediments and identifiable to a relatively high taxonomic resolution. The larvae develop *in-situ* within lacustrine sediments and therefore fossil assemblages will closely represent the extant faunal assemblage at the time of deposition (Brooks et al., 1997b; Brodersen and Lindegaard, 1999). Chironomids are a relatively new proxy in palaeoecological studies, having only been employed for the last two decades, in comparison to other proxies such as coleopteran which have been used since the 1950s and others such as pollen and macrofossils, which have been utilised for over a hundred years. As with any ecological indicator, chironomids are likely to be influenced by a number of variables at one time. Therefore, despite the usefulness of individual variable reconstructions, caution should always be used when interpreting the results. A consideration of these other factors which might influence chironomid population structures is imperative (Langdon et al., 2010).

A brief overview of the main variables which are likely to influence chironomids in thermokarst lakes along with previous studies and findings are discussed below in order to contextualise the role and importance of methane to a chironomid larvae in a thermokarst lake.

2.5.5.1 Temperature

Most commonly chironomid head capsules are used as a proxy for high-resolution temperature reconstructions which is argued as the most important variable in controlling chironomid populations (Walker et al., 1991). Early work by Walker et al. (1991; 1997) highlighted the potential of the aquatic larval stages of chironomids as temperature indicators in Canadian lakes. A large portion of the life cycle is spent in the aquatic environment and water

temperature will influence egg and larval development, often with a positive relationship between temperature and development (Mackey, 1977). Air temperatures will influence the distribution of chironomids during their adult stage and have been closely correlated with surface water temperatures in lakes which do not have strong thermal stratification (Livingstone and Lotter, 1998; Lotter, 1999). Therefore temperature is likely to play a large role in chironomid distributions and chironomid head capsules are a good proxy reconstructing past temperatures(Walker et al., 1991; Brooks, 2006).

Following this work, many qualitative interpretations of chironomid assemblages in relation to climate were made, demonstrating consistent assemblage patterns across latitudinal gradients (Brooks, 1996; Brooks et al., 1997a; Brooks et al., 1997b; Lowe et al., 1999; Brooks and Birks, 2000). Recognition of the variability in annual surface temperatures led to the development of mean July-air temperature inference models using surface sample training sets and weighted averaging techniques, for North America (Walker et al., 1997) and northern European regions (Larocque et al., 2001; Brooks and Birks, 2001), providing quantified values of late-glacial and early-Holocene temperature changes.

As with any palaeo proxy, uncertainties are associated with chironomid transfer functions. One of the main issues is the ability to reconstruct the fairly stable Holocene temperatures. Often temperature fluctuations across this period have been small in relation to the statistical uncertainties in the transfer function. Despite this, reliable reconstructions from northern latitude regions have been achieved (Larocque et al., 2001; Larocque and Hall, 2003; Barber and Langdon, 2007; Chase et al., 2008; Langdon et al., 2011).

2.5.5.2 Lake status

More recently chironomid head capsules have been used to understand lacustrine ecological processes over time such as changes in lake trophic status, pH and macrophyte variations. Lake nutrient status has been reconstructed using chironomids relationships to dissolved oxygen (Quinlan and Smol, 2001; Brodersen and Quinlan, 2006) total phosphorus (Brooks et al., 2001; Langdon et al., 2006) and chlorophyll *a* (Brodersen and Lindegaard, 1997; Ruiz et al., 2006). Langdon et al., (2010) highlight the influence of macrophyte communities in shallow lakes on chironomids, suggesting that

they may be used to understand alterations in macrophyte habitat. Chironomids have been used to establish catchment disturbances, for example (Mayer and Johnson, 1994), calculated environmental degradation due to pollution.

2.5.5.3 Lake depth and thermal regime

Water depth has been identified as one of the most important variables influencing chironomid communities(Walker and MacDonald, 1995). As highlighted above, species-specific tolerances to depth suggest an assemblage relationship to depth and many studies have shown this is statistically significant (Larocque et al., 2001). However, past studies have highlighted the difficulty of establishing the impacts of this variable as it is closely linked to water temperature. Lake-depth inference models are also influenced by the thermal regime of lakes. For example, Quinlan et al. (2012) developed a lake depth model for north western Ontario, Canada but found the model predicted consistently shallower maximum depths than observed. They then developed a thermal regime model and concluded that a period of increased mixing in the past was identifiable and the potential cause of the shallow lake depths generated by the depth inference model. This study highlights that although lake depth is an important variable in chironomid assemblage distributions, the relationship is not clear cut and may actually reflect other factors such as the thermal regime (Quinlan et al., 2012).

2.5.6 Stable isotopes as palaeoenvironmental indicators from chironomids

The sections below will briefly outline the previous work where the stable isotopes from chironomids have been used to infer past and present conditions within a lake and its surrounding environment.

2.5.6.1 Lake food webs

Stable isotopes are increasingly being used in order to establish aquatic ecosystem food web interactions through the understanding of carbon isotopes ($\delta^{13}C$) in the tissues of organisms (Bunn and Boon, 1993; Jones and Grey, 2004). The $\delta^{13}C$ values should reflect that of the organism's food source and therefore carbon can potentially be traced through the aquatic food web to

some taxon-specific levels. Utilisation of such techniques has provided valuable information about food sources and predator prey relations in aquatic ecosystems.

Studies suggest the average $\delta^{13}C$ values of C_3 and C_4 plants are ≈ -28‰ and -13‰ respectively (Peterson and Fry 1987), but these can vary depending often on the ecosystem in question. The range of $\delta^{13}C$ values of food sources within aquatic ecosystems and those in relation to chironomid larvae feeding preferences are shown in figure 7.1, however the values given cover the maximum possible range for each source rather than an average, and these ranges are likely to encompass global extremes. Therefore it is necessary to understand more specifically the $\delta^{13}C$ from the system in question, in this case the high-latitudes, so the values reflect real environments more closely.

Experiments using *Chironomus spp.* larvae suggest that ~ 94% ± 6.9% of their carbon is obtained from food (Akerblom and Goedkoop, 2003). Therefore the $\delta^{13}C$ values of chironomid larvae should closely reflect the values of the initial food type. For chironomid larvae, if it is assumed their diet is composed mostly of organic detritus, then their isotopic composition, at least during the 4th instar stage, will reflect this. Recent studies have highlighted that the $\delta^{13}C$ signal is also transferred to the exoskeleton and therefore the signal can be traced through the fossil record and retain signature of the whole organism (van Hardenbroek et al., 2010). As shown in figure 7.1, distinguishing between certain carbon sources such as terrestrial and aquatic plant material is potentially unachievable, but when the carbon source is different enough, for example MOB, the carbon signal of chironomids will likely change to reflect the contribution of this material.

2.5.6.2 Isotopic uncertainties

An important factor to consider in isotope studies, especially those dealing with biological proxies, is fractionation and the resultant $\delta^{13}C$ values. Studies have indicated there is large variability in fractionation at the base of aquatic food webs in $\delta^{13}C$ from -2.1‰ to 2.8‰ (Zanden and Rasmussen, 2001) and inconsistency in carbon accumulation through the different stages of the chironomid life cycle is also important. As stated previously, chitin, and as a result carbon, in chironomid head capsules accumulates over time and from

instar to instar, therefore fractionation may alter the $\delta^{13}C$ values slightly depending on the instar.

Other factors to consider will include those associated with both biological and ecological aspects. For example, in order to fully comprehend the end member $\delta^{13}C$ values, understanding of specific food sources which are assimilated by herbivores or detritivores is needed, and this is often limited (Goedkoop et al., 2006). Natural variability will always be present in studies of biological organisms and has been shown to alter $\delta^{13}C$ values from chironomids by ~1‰ (van Hardenbroek et al., 2012b). However the level to which natural variability will be an issue for understanding carbon flow through lake food webs will depend on the sample size and sample repetition and in the context of some isotope studies it is unlikely to alter results greatly. Problems might arise where taxon-specific repeat samples have differing values, therefore understanding statistically significant differences in populations and what is natural variability is important.

Once food is ingested, microbial conditioning, e.g. the colonisation of microbes on food particles within the gut, often occurs and therefore should be taken into consideration. Many studies have suggested that the gut content of chironomid larvae is a large source of error in stable isotope studies (Grey et al., 2004) and it is strongly suggested gut purging prior to analysis is important (Goedkoop et al., 2006). Chironomid larvae have the ability to alter the part of the plant they utilise for energy (and consequently the source of $\delta^{13}C$) if, for example, they are in a period of starvation. This means chironomids are digesting the part of the plant with the most energy to increase efficiency. Doi et al. (2007) suggest that during a starvation period, *Chironomus acerbiphilus* metabolized somatic components, which have high $\delta^{13}C$ values than fatty acid components, which will alter the isotopic composition of the larvae. The overall shift in isotopic signatures due to these feeding alterations may only be a few per mill at most, which is unlikely to be a significant or measurable alteration in the context of most isotope studies.

2.5.6.3 Methane and methane oxidation bacteria

Recently, stable isotope studies have hypothesised about the contribution of carbon from methane sources, for example in the form of MOB to the diets of profundal chironomid larvae (Grey et al., 2001; Bastviken et al., 2003; Eller et

al., 2007; Jones et al., 2008) and it is suggested chironomids could provide a proxy for past methane fluxes from lacustrine environments (Jones & Grey 2011). In order to establish the validity of this suggestion, a detailed review of previous studies is given below.

As discussed in section 2.3.1 methane oxidation in lakes is important in controlling methane emissions to the atmosphere and leads to a significant microbial biomass which might be utilised as an internal carbon source for macroinvertebrates, namely chironomids (Eller et al., 2005). Fractionation of carbon by methanogenic archaea leads to highly depleted methane (-50‰ to -80‰) which is then further depleted during oxidation which provides a good tracer through the food web (Whiticar 1999).

Early studies of chironomid larvae highlighted depleted $\delta^{13}C$ values in comparison to bulk particulate organic matter (POM), for example Bunn and Boon (1993) found chironomid larvae in Australian Billabongs with values of -38‰ where POM values of around -25‰ to – 30‰. Previous studies have noted strongly depleted $\delta^{13}C$ values in chironomid larvae in comparison to POM (Grey et al., 2001; Kiyashko et al., 2001). Grey et al., (2001) found values as low as -41‰ in Loch Ness and -53.5‰ in Esthwaite Water, whilst other studies highlight filter feeding species such as *Chironomus plumosus*-type with $\delta^{13}C$ values ranging between -40 and 75‰ (Grey et al., 2004a; Jones and Grey, 2004; Grey et al., 2004b; Kelly et al., 2004; Deines et al., 2007b). Unexpectedly low $\delta^{13}C$ values compared to POM have led to the idea that chironomid larvae are incorporating other sources of carbon into their diet, namely bacteria involved in the methane cycle as biogenic methane is characterised by significantly depleted $\delta^{13}C$ values in comparison to other resources within the freshwater system (Bunn and Boon, 1993; Whiticar, 1996). As stated previously most sources of carbon within the lake have $\delta^{13}C$ values between -8 & -35‰, therefore further depleted $\delta^{13}C$ values in zooplankton and chironomid larvae have been attributed to partial assimilation of methane via MOB (Bastviken et al., 2003; Kelly et al., 2004). Jones et al. (2008) studied 87 lakes across a large geographic range and highlighted a strong negative relationship between dissolved oxygen concentrations and depleted $\delta^{13}C$ values of the larvae suggesting stratification is an important process for methane oxidation and thus accumulation of MOB in the profundal lake environment. Deines et al. (2007b) were able to identify chironomid larvae had assimilated MOB through

^{13}C-labelled methane and phospholipid fatty acid detection laboratory experiments.

Depending on the level of depletion, carbon isotope values alone may not provide enough evidence to suggest MOB as a carbon source. Field based evidence based on both carbon and hydrogen isotopes however, has been able to distinguish not only uptake of methane but also the source of the methane (Deines et al., 2009).

The idea that some biological organisms create an environment where interdependent relationships can be sustained has long been known. In the case of methane utilisation, marine studies have highlighted the potential of symbiotic relationships between bacteria and other organisms, resulting in depleted carbon values of organisms near to hydrocarbon vents and seeps (Grey & Deines, 2005). Hershey et al. (2006) suggest the tube-dwelling nature of some chironomids may allow increased utilisation of methanotrophs, this is somewhat validated as Eller et al. (2005) noted high potential methane oxidation rates in deeper sediments and attributed this to bioturbation, specifically that associated with chironomid behaviour enhancing growth conditions for their food source (e.g. MOB). Further to this Eller et al. (2007) suggest that the oxic/anoxic interface of the chironomid larval tube may provide an ideal microhabitat for MOB and that this may provide a constant food source for chironomid larvae. While Eller et al. (2007) did not find evidence to indicate chironomid larvae were feeding on MOB or that they shared a symbiotic relationship with the bacteria, they did not rule out that this might be the cause of depleted δ^{13}C values. They conclude the evidence may not be apparent due to rapid degradation of bacteria in the gut or that chironomid feeding habits are more variable than previously thought. The study did however indicate that chironomid larval habits of bioturbation promoted the growth of microorganisms which are part of their diet.

Eller et al. (2005) estimated the contribution of methane-carbon to the diet of *C. plumosus*-type using a two-source isotope mixing model in two lakes (dimictic and polymictic). The results suggested between 16-30% of larval biomass was comprised of methane-derived carbon. Other mixing models have also highlighted an increase in the percentage of carbon derived from methane in chironomid biomass with distance from the littoral environment. Ravinet et

al. (2010) indicated values increased from zero in the littoral to 28% in the profundal, further suggesting profundal, tube dwelling chironomid taxa such as *C. plumosus*-type and *C. anthracinus*-type appear to aid the growth of MOB communities through habitat and feeding preferences.

It is important to note that such mixing models do not account for all sources of MOB assimilation, for example the direct assimilation of MOB or assimilation of other organisms feeding on MOB (which is likely to be true for certain subfamilies such as Tanypodinae) and therefore interpretations should be viewed with some caution, despite this, it might be possible to suggest at least partial assimilation by MOB through a mixing model approach. Recent studies have added to the body of work which suggests that not only is the assimilation of MOB geographically specific within lakes, but is taxon-specific. van Hardenbroek et al. (2012b) studied chironomid head capsules from a Swedish lake and highlighted a negative correlation between diffusive methane fluxes and Chironomini $\delta^{13}C$ values and suggest this tribe are sensitive to methane in the surrounding sediment. They also indicated depleted $\delta^{13}C$ values for the subfamily Tanypodinae, suggesting this group feeds on prey with depleted values.

In summary, from the current literature, a clear picture of the validity and importance of MOB in chironomid larvae diet is still to be determined. The results of the studies discussed above suggest a highly variable signal in terms of chironomid diet and the ability to pick out a clear methane signal is difficult. The results above however, all pertain to lakes where methane production is not a dominant process within the lake. Many of the lakes from previous studies will have seasonal variations in methane production and oxidation and the level to which MOB will contribute to the chironomid diet will be subject to these seasonal variations. In thermokarst lakes methane production and oxidation, at least in the thermokarsting zone, is often constant and although some seasonal factors may influence oxidation, for example ice cover, the supply of MOB to chironomids in this zone is likely to be more consistent than in other lake settings. If assimilation of methane- based carbon in chironomids is higher in a thermokarst lake due to larger scale production and oxidation, it is likely this will be picked up in the $\delta^{13}C$ values of the chironomid larvae.

2.5.6.4 Other sources of isotopic depletion

In many cases, the $\delta^{13}C$ values found are only a few parts per mille more depleted than POM and bulk sediment, this is especially the case with fossil head capsules. Although most cases make strong arguments for uptake of methane as the cause of the difference, other methods of generating depleted isotopic values cannot be ruled out.

Studies have highlighted isotopically lighter chironomid larvae compared with POM and have attributed this alteration to accumulation of lipids in tissues (Grey et al., 2004) which can be as much as 8.4‰ lighter than the material from which they are synthesised (DeNiro & Epstein, 1977). Lipids are suggested to contribute 17-23% of larval dry weight (Hamburger et al., 1995) and have been put forward as possible reasons for isotope displacement (Grey et al., 2004a). The decay of organic matter within lakes generates CO_2 with depleted $\delta^{13}C$ values, but the process of incorporating this carbon into chironomids is not straightforward and therefore may not be the most plausible explanation (Wooller et al., 2012). Other potential means for isotopically depleted $\delta^{13}C$ values in chironomid larvae include consumption of chemoautotrophs, which via a number of processes result in bacterial $\delta^{13}C$ values as low as -50‰ (Kohzu et al., 2004).

2.5.7 Chironomids as indicators of methane in thermokarst lakes

As yet, there has been very little work completed on the role of MOB in the diets of chironomid larvae from thermokarst lakes. Little to no work has been completed on the different sources of methane oxidation within thermokarst lakes and whether this affects the subsequent uptake by chironomid larvae.

A study completed on surface samples from ten Siberian thermokarst lakes highlighted a taxon-specific relationship between chironomid head capsules and methane flux with the most depleted $\delta^{13}C$ values found in the lakes with the highest methane fluxes (van Hardenbroek et al., 2012a). van Hardenbroek et al. (2012a) suggest that variability in the $\delta^{13}C$ values of fossil chironomid head capsules over time may reflect change in past methane fluxes. However, the study highlights that these lakes appear to be anomalous as a consistent methane emission zone could not be identified nor were the levels of methane flux as high as noticed in other studies of thermokarst lakes. The study also

used samples taken from the deepest point of each lake, which is suggested to be most representative of the lake overall. However in thermokarst lakes this might not be the case. As noted in above, the highest level of methane flux is found at the edge of the lake (Walter et al., 2008b), which is very different compared with non-thermokarst lakes where methane is produced mostly in the profundal zone, for example through reducing processes. Therefore a central position may not reflect thermokarst based methane fluxes but those produced under general limnological conditions. In order to establish patterns associated with thermokarst lakes, samples taken from a methane flux location and compared with non-methane flux areas would be most suitable.

Further work by Wooller et al. (2012) highlighted depleted values in fossil capsules from a thermokarst lake in northern Alaska. The study shows a fluctuating methane derived contribution to chironomid head capsules of between 10 and 25% from ~12,000 to 3000 yrs BP, after which the percentage carbon derived from methane increases to 30% with individuals showing values as high as 50% (Wooller et al., 2012). After 10,000 yrs BP, temperatures increased, in line with a rise in methane-derived percentage carbon which may be due to increased thermokarsting at the lake margin and therefore increased methane generation (Wooller et al., . 2012). This study used an integrated chironomid assemblage and therefore any taxon- specific values will have been averaged into one. If previous studies are correct and chironomid feeding preferences are different this may mean a methane-derived carbon signal is masked by other taxa. The data from this study show that the most depleted average $\delta^{13}C$ value was found in the modern surface samples and was -35.2‰ which is very much still within the range of values derived from a non-methane carbon source. This value was also averaged from a range between -40.5 to -29.5‰ which suggests high spatial variability even at a constant temporal scale. The data may simply represent taxon variability due to taxon-specific feeding and habitat preferences and may not be indicative of past methane changes. Caution should be taken when making palaeoclimatic interpretations from a single, homogenised chironomid HC sample.

2.6 Biomarkers

Lipid biomarkers are preserved in the geological record and represent digenetic markers of organisms and therefore environmental conditions at the

time of lipid production. As highlighted above, CO_2 and methane are important GHGs and understanding of the biochemical carbon cycle, both in the past and present, will aid the understanding of future changes to the cycle due to anthropogenic impacts. Processes such as photosynthesis, methanogenesis and methane oxidation are carried out by bacteria and Achaea which will bio-synthesise molecules. These molecules and their degradation products are recognisable in the sedimentary record and consequently these can provide a proxy for tracing carbon pathways and environmental conditions in a number of settings using features such as their chemical structure, relative distributions and stable isotopic composition (Pancost and Sinninghe Damsté, 2003).

A number of biomarkers can be used to understand environmental conditions in lake systems, these will be discussed below. In both marine and terrestrial environments, lipids from prokaryotes, such as hopanoids are some of the most abundant compounds found in sediments both in modern and fossil environments. Bacteria and *Achaea* have a diverse range of carbon compositions and functions and therefore the biomarkers of such organisms can be linked to specific processes and are constantly being developed as proxies for carbon pathways. The isotopic composition of the biomarkers allows an understanding of the chemical and biological interactions of complex ecosystems. The interpretation of the $\delta^{13}C$ values of biomarkers can be complex due to the number of controls of carbon composition such as: carbon assimilation (van Der Meer et al., 2001), lipid biosynthesis (Sakata et al., 1997) and the source of substrate carbon (Pancost and Sinninghe Damsté, 2003). For detailed reviews of biomarkers in relation to carbon cycling, the reader is directed to Pancost and Sinninghe Damsté (2003).

2.6.1 *n*-alkanes as indicators of terrestrial and aquatic organic contribution to lake sediments

Bulk sediments in lakes offer an integrated signal of organic input from a number of different sources. Understanding the individual sources is important in order to interpret the bulk signal. Compound-specific isotope analysis of lipid biomarkers such as *n*-alkanes can help to disentangle the bulk organic sediment signal (Ficken et al., 1998).

Short chain *n*-alkanes (C_{14} – C_{22}) are produced mainly by bacteria and algae (Grimalt and Albaigés, 1987), mid chain *n*-alkanes (C_{20} – C_{25}) are thought to be derived mainly from aquatic macrophytes (Ficken 2000) whereas long chain *n*-alkanes (C_{27} – C_{33}) with a predominance of odd-over-even (OEP) carbon numbers are attributed to terrestrial plants (Eglinton and Calvin, 1967; Ficken et al., 1998). Patterns, although not always as simplistic as suggested, in the abundance of terrestrial, aquatic and algal biomarkers in lakes can be used to assess the relative sediment accumulation from different sources and potential changes in, for example, terrigenous input.

2.6.2 Biomarkers as evidence of methane and methane oxidation

Of the major compound classes, four are commonly encountered in the identification of methane oxidation, or methanotrophs, in environmental settings, the most common of which will be discussed below.

2.6.2.1 Hopanoids

Hopanoids are pentacyclic triterpenoids and are part of the membrane of many bacteria such as cynobacteria, methanotrophs and aerobic heterotrophic bacteria (Rohmer et al., 1993). Diplopterol and bacteriohopanpolyol (BHPs) are two of the most common derivatives and due to this common occurrence may not be deemed useful bacterial biomarkers when regarding concentrations in samples, whilst methylhopanoids have been noted as highly diagnostic with some being specific to MOB (Zundel and Rohmer, 1985).

Originally hopanoids were associated solely with aerobic bacteria (Ourisson et al., 1987), recently however, a number of observations of hopanoid biosynthesis in anaerobic bacteria have been made; for example Fischer et al., (2005) found them in anaerobic cultures of *Geobacter* sp., whilst their occurrence in anaerobic planktomycetes was noted by Sinninghe Damsté et al. (2004). These observations led to a better understanding of previous studies which had observed geohopanoids in anaerobic environments (Pancost et al., 2000b; Thiel et al., 2003) and highlighted that hopanoids cannot be indicative of aerobic organisms alone (Talbot and Farrimond, 2007).

Until recently both diplopterol and BHPs had been considered to hold little diagnostic information about carbon sources due to their ubiquitous nature in

many aerobic bacteria (Pancost et al., 2003). Talbot and Farrimond (2007) used a newly developed method (multi stage ion trap mass spectrometry, and demonstrated that both modern and past environmental settings have a diverse range of BHPs which can be used to identify bio and geochemical processes and organic matter from a range of organisms (Talbot and Farrimond, 2007).

Diploptene is a diagenetic derivative of diplopterol and is often present in both contemporary and ancient sediments in diverse environments and is mostly thought to be derived from bacterial sources (Wakeham, 1990) where it is associated with the rigidity of the cell membranes (Rohmer et al., 1993).

2.6.2.2 Fatty Acids

Phospholipid fatty acids (FAs) are common in bacteria in both the bound and free form, for example C_{16} and $C_{18,}$ and therefore they do not provide evidence of specific prokaryotic processes (Pancost and Sinninghe Damsté, 2003). However, more specific FAs have been identified, such as those of both 'type I' and 'type II' MOB as introduced above. Previously, FAs in MOB have been used to understand the contribution of methane-derived carbon in the diets of zooplankton, which suggests FAs can be used to understand carbon and methane transfer through the lake food web (Sanseverino et al., 2012).

2.6.3 Carbon assimilation in bacteria

The mechanism for carbon assimilation in bacteria is, in principle, the same as that for higher order organisms such as algae or chironomids. As discussed above, the carbon isotopic signature of an organism is primarily based on the carbon content of the source material and how this is assimilated. In typical limnological environments, the $\delta^{13}C$ values of dissolved inorganic carbon (DIC) or other potential bacterial carbon assimilation sources are between -10‰ and 1‰ (Pancost and Sinninghe Damsté, 2003). Where the DIC is primarily derived from organic matter or methane oxidation the $\delta^{13}C$ values can be significantly depleted. Little work has been completed on the relationship between heterotrophic bacterial biomass and its $\delta^{13}C$, thus the understanding of the process of carbon assimilation in these organisms remain fairly poor. In principle however, the isotopic composition of the source material is likely to be reflected in the organisms which are utilising this carbon source(Pancost

and Sinninghe Damsté, 2003), or due to the fractionation process the organism may have a more depleted carbon isotope signal than the original substrate.

Peat bogs, especially those associated with high-latitude wetlands, provide shallow, anoxic wetland areas where prokaryotic processes can degrade the organic material and produce methane. Peat bogs therefore provide a good environment to understand methane cycling (Pancost 2000). Pancost et al., (2000) used the $\delta^{13}C$ values of both hopaniods of aerobic bacteria and ether-bound isoprenoid lipids in order the understand carbon degradation pathways and organisms involved in the process of organic degradation. The study highlights the applicability of biomarkers to understanding carbon cycling in peat bogs but also the complexity of the use of such a proxy in palaeoenvironmental settings. A strong understanding of the system is needed in order to utilise biomarker proxies to their full potential.

Marine methane seeps provide the closest analogue for methane ebullition-seeps in thermokarst lakes (although they are very different systems). Studies of these environments have identified diploptene as a methanotrophic biomarker in microbial mats which is linked to the seeps (Pancost et al., 2000a; Elvert et al., 2001a). Furthermore, other studies have identified diploptene in lake sediments and have attributed its low $\delta^{13}C$ values to the presence of MOB.

Studies have demonstrated the ingestion of MOB by organisms such as chironomids through the use of phospholipid fatty acids (PLFAs), which were detected in the tissue of chironomid larvae (Sanseverino et al., 2012) and confirmed the transfer of MOB carbon to the remains of chironomids (Deines et al, 2007a). If methane is being oxidised in thermokarst lakes and subsequently ingested by chironomid larvae, this might be detectable in the fossil remains. Behavioural traits of taxon-specific larvae such as *C. plumosus*-type mean they feed on both benthic and pelagic MOB and are likely to promote MOB growth (Deines et al., 2007a).

2.7 Summary

Studies quantifying methane production and emission from thermokarst lakes have identified these environments as an important aspect of the arctic carbon

cycle. However, a number of areas which need to be studied in more detail have been identified in this chapter.

It is clear that thermokarst lake-specific methane production and emission is high but the amount of methane that is recycled within the lake is still to be quantified and the importance of ebullition-seeps for biogeochemical interactions within the lake remains unknown. In order to move towards understanding these aspects, a number processes are outlined and will be addressed throughout this thesis.

Methane that is produced either in the deep talik or from old carbon that has slumped into the bottom of the lake has been studied at the lake surface and is largely transported via ebullition. However, transport pathways remain poorly understood. Furthermore, the role of diffusion in the transport of dissolved methane in relation to areas of high methane production has yet to be determined.

Studies have indicated that MOB are present in the surface sediments of thermokarst lakes and that a number of biological organisms utilise methane-derived carbon as a food source in these lakes also. These biogeochemical interactions have yet to be studied in detail spatially, nor has the role of thermokarst-specific methane in the within lake methane cycle.

Overall the evidence from previous studies highlights the applicability of techniques such as stable carbon isotopes in lipid biomarkers and chironomids for testing the presence and consumption of MOB in the surface sediments of thermokarst lakes.

Chapter 3: Study sites and sampling strategy

3.1 Site selection

A number of criteria were outlined which had to be met prior to fieldwork. Firstly and most importantly, the lakes included in the study needed to have strong methane emissions in the form of seep-ebullition which was easily detectable from ground-based observations. This was deemed important as large-scale methane production should allow a clearer insight into the supply of methane to the lake food web as opposed to environments where the level of methane emissions were unclear. Secondly, in order to understand the lake methane dynamics further, it was preferable that the sites were part of the long-term methane emission monitoring project at the University of Fairbanks, Alaska. Other criteria which were preferable but not crucial included: previous knowledge on the limnology and lake development and accessibility.

3.1.1 Study sites: catchment overview

The study sites are located to the west of Fairbanks at a latitude of 65˚N. The region has a continental climate with average annual temperatures ranging from approximately -30˚C in January to over 23˚C in July and mean annual precipitation of 25 cm (U.S Climate Data, 2015).

Ace and Smith L.s are part of the Happy Creek hydrological basin which drains into the larger Chena River network. Both sties lie between 500 and 600 m elevation a.s.l. The areas immediately surrounding both lakes is relatively flat rising with little change in elevation. The area is in the *Picea-Populus-Betula* boreal forest typical of the continental Interior. In general the study catchment is sparsely populated with little development in the area, however Smith L. lies within the University experimental farming area and Ace L. has a number of houses located near to its eastern shore.

The area is underlain with discontinuous permafrost which varies in thickness from 10-185 m (French, 2007). The surficial geology of much of the

surrounding area is dominated by retransported Pleistocene loess deposits (Péwé, 1975). It is this sedimentary unit which, when thawed underneath the lakes, provides the labile carbon for methanogenesis.

The lakes are both considered thermokarst in origin (Alexander and Barsdate, 1971; Alexander and Barsdate, 1974), although the rate of current thermokarst erosion is unknown. Both lakes show evidence for recent (past 50 yrs) thermokarst action at one 2015 margin. They have been part of many previous studies and are currently part of a long term monitoring project run by the University of Alaska, Fairbanks (UAF) which aims to understand current levels GHG emissions from thermokarst lakes.

Lakes were chosen prior to fieldwork based on a measure of methane output from thermokarst zones. The study lakes are part of a long-term monitoring project set up by Katey Walter Anthony at the University of Alaska, Fairbanks and are characterised by areas of both high methane and low methane emissions, with zones of high methane ebullition located at the thermokarst margins and quiescent zones in the central areas. GPS coordinates of the high methane zone (K.Walter Anthony *Pers Comm*) and personal observational data from previous field seasons were used to define the limits of the high methane zone.

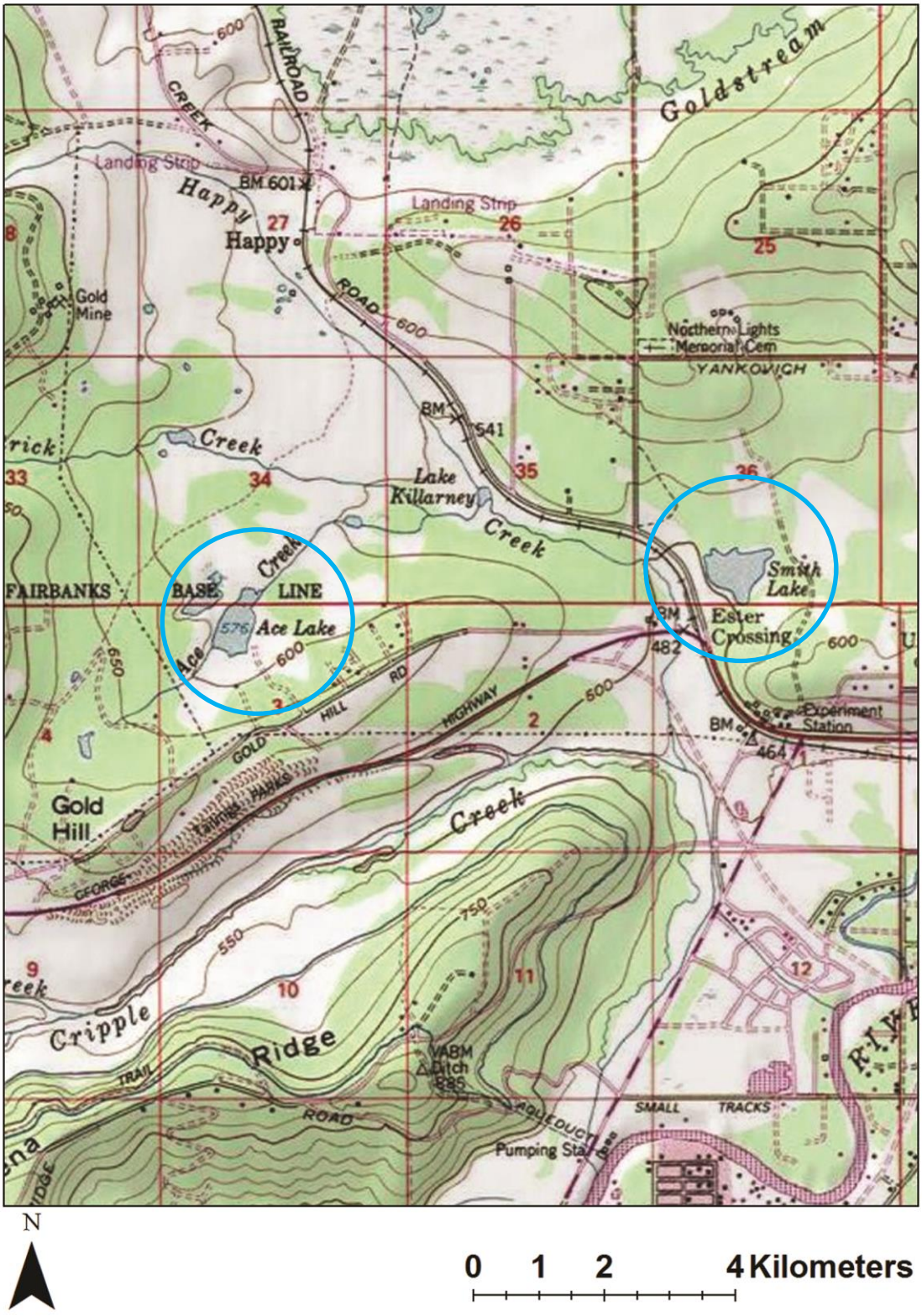

Figure 3.1 Map of study sites in Interior Alaska. Both lakes are highlighted in blue circles.

3.1.1.1 Ace Lake

Ace L. (64˚51'45.49N, 147˚56'05.69W) is part of the Ace-Deuce Lake system (Alexander and Barsdate, 1974) situated on Gold Hill at the margin of the Tanana Valley, west of the UAF (Figure 3.1). Both lakes in this system are thermokarst in origin and formed through melting ice bodies in the loess landscape. Ace has two major water input mechanisms; outflow from Deuce and surface runoff during spring. The outflow from Ace feeds other lakes as part of the Happy Creek hydrological system. The Ace-Deuce Lake system has high nutrient levels and therefore Ace L. can be described as a eutrophic lake with a strong seasonal nutrient cycle (Alexander and Barsdate, 1974). Ace L. is approximately 1km long, 400m wide and has a maximum depth of 8m (photo 3.1). The depth across Ace is highly variable and the current margin of thermokarst erosion might be associated with the melting of an ice wedge under that section of lake. Figure 3.2 shows the basic bathymetry of the lake, highlighting the deepest point towards the centre of the lake but also the deep section likely created by the melting ice wedge towards the northern margin.

Previous studies show that the primary productivity is sustained throughout the summer season; however, the algal population in the lake is dominated by blue-green algae throughout most of this time (Alexander & Barsdate, 1974). Ace L. is somewhat unusual compared to other Interior or thermokarst lakes. Alexander and Barsdate (1974) describe Ace as monomictic, whereas many lakes of the Interior are typically dimictic. A basal date obtained from wood of 1000yrs BP (Gaglioti *pers comm)* at Ace L. suggests this has a longer residence time and is more stable than traditionally thought for thermokarst lakes (Finney *pers comm*.). The increased residence time might be due to the discontinuous nature of the underlying permafrost in the region.

These features make Ace L. an interesting and highly useful study site as thermal stratification often leads to laminated sediments, especially in the deeper parts of the lake, providing a well resolved environmental record, while Ace's age means this record can be resolved over a long temporal record.

Photo 3-1 Ace L., July 2012. The view is toward the north-east. The thermokarst margin can be seen at the far end of the lake.

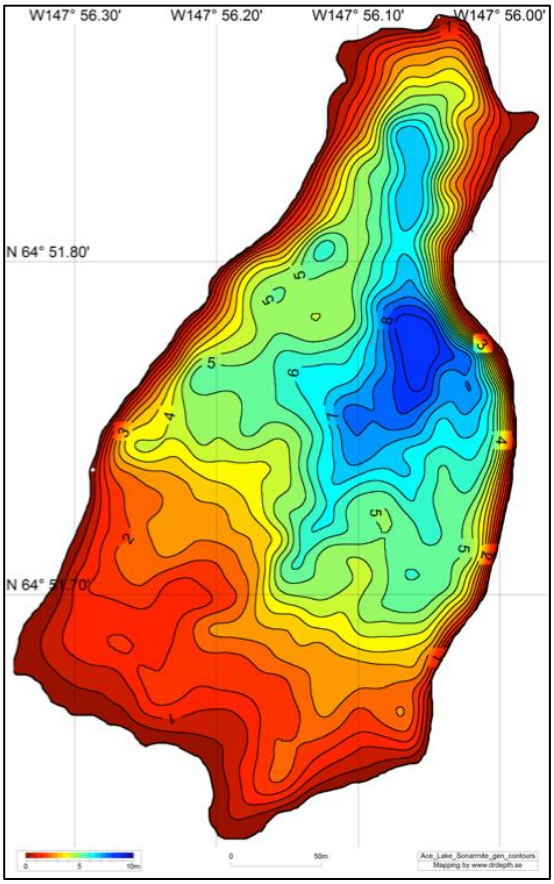

Figure 3.2 Bathymetry map of Ace L.. Courtesy of B. Gaglioti

3.1.1.2 Smith Lake

Smith L. (64°51'55.23N, 147°51'59.48W) is at a lower elevation (~80m lower) in the Tanana Valley from Ace L. and may have once been part of the same drainage system prior to the building of infrastructure such as the railway line and main roads (figure 3.1). It has a larger surface area than Ace and is approximately 1km by 1km (Photo 3.2). It is situated close to UAF experimental agricultural and wildlife sites and there is no permanent flow through the lake. Inlets and outlets dry up through the summer season. Smith L. is considered to be dimictic (Hutchinson 1957), however Alexander and Barsdate (1974) argue that the spring overturn often does not fully complete. Like Ace, Smith has an irregular depth profile which is attributed to its formation through ice body melt; however, the average depth profile is fairly uniform across the lake, ranging from 1.0–3.0m (Alexander and Barsdate, 1971; personal observation). Figure 3.3 shows a detailed bathymetry map for Smith. Its relatively uniform depth allows modern methane emissions and chironomid assemblages to be studied whilst removing anoxia as a permanent variable which might exhibit a strong influence on chironomid community structure. During summer months, primary productivity is high with blue-green algae dominating the algal community (personal observation).

As with Ace, Smith has an obvious zone of methane emission in the south-west segment of the lake. Radiocarbon dating of the methane emissions from this zone highlight that it is much younger (2.5 ka yrs; Walter Anthony *pers comm*) than expected when compared to measurements from other thermokarst lakes (Walter et al, 2008a). This suggests that the source of carbon for methane production at Smith might be the Holocene peat into which the lake is expanding or shallower sediments underlying the lake (shallower than those where methane is produced in Ace L.). Melting of permafrost causes slumping of bank material (evident in the form of 'drunken' trees which are a well-documented sign of thermokarst erosion) which enters the lake and provides a new source of carbon for methanogenic bacteria. The degree to which the active margin contributes sediment to the lake is considered in more detail in chapter 4.

Photo 3-2 Smith L., July 2013. The view is toward the south. The Thermokarst margin can be seen in the background. Photo courtesy of T. Roland

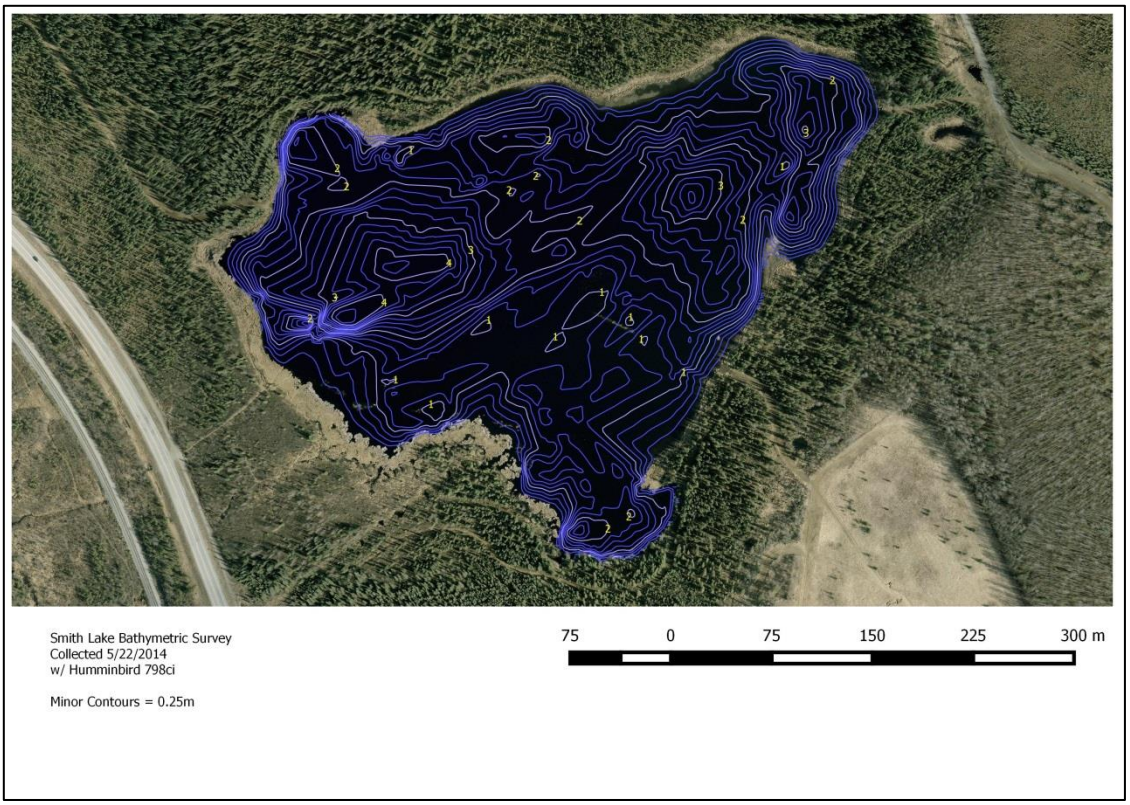

Figure 3.3 Bathymetry of Smith L.. Courtesy of: K, Walter Anthony

3.2 Sampling Strategy

Due to the large number of different samples and techniques utilised, the specific samples used in each chapter across the lakes are not provided here, but a diagram is included in each data chapter to maintain clarity.

3.2.1 Thermokarst zone designation

The thermokarst zone designation was based on quantitative observations of methane ebullition seeps in the lake. The zone boundary was placed beyond the furthest observed ebullition-seep in the lake (with distance from the thermokarst margin). Evidence for slumping or erosion of terrestrial material at the margin was observed through 'drunken trees' which are so called because thawing and slumping causes the trees to lean towards the lake (Photos 3.3 and 3.4). Samples taken outside of the thermokarst zone were classified as 'centre' or 'littoral' depending on their position in the lake. Littoral referred to samples that where close to any margin apart from the thermokarst margin, thus samples could not be both littoral and in the thermokarst zone.

3.2.2 Surface sediment collection

Samples were collected on field expeditions in 2011, 2012 and 2013. Samples retrieved in 2011 were collected in April through the ice, whilst those from 2012 and 2013 were collected in June and July in ice-free conditions.

All surface sediment samples were retrieved in Perspex tubes using a gravity corer. The cores were extruded at either 0.5 or 1 cm intervals, labelled appropriately and stored in plastic bags. Once the samples were shipped back to the UK they were kept in cold storage (4˚C) until required for further analysis.

All analysis was completed on the upper most sediment depths (maximum depth of 1.5 cm) and for the majority of samples the 0-0.5 cm interval provided adequate material for analysis. Repeat samples were completed either of extra material from the same depth or using the 0.5-1 cm interval.

Photo 3-3 Evidence for thermokarst thaw at Ace L.. Photo is taken from the north west margin looking south east.

Photo 3-4 'Drunken trees' at the thermokarst margin in Smith L. Photo taken from the south east margin looking north west. Photo courtesy of T. Roland

Chapter 4: Examining the provenance of organic matter in thermokarst lake sediments

4.1 Outline

This chapter presents results and interpretation of an in-depth study of the organic content of surface sediments of both study lakes. Firstly a review of the relevant techniques used to identify the amount and type of organic matter is provided. The results are presented for each technique separately to describe the patterns, and then compared to assess the ability of each method. Finally the data are discussed in the context of overall patterns of carbon cycling in thermokarst lakes.

4.2 Introduction

Organic matter preserved in lake sediments is important for understanding changes within both a lake and the surrounding catchments over geological timescales. Organic matter is composed of particulate detritus from plants and animals that settles on the lake bottom but escapes remineralisation over time. The source of organic matter in lakes is both allochthonous (derived from the area surrounding the lake) and autochthonous (from sources within the lake) and can be broken down into groups: terrestrial higher plants, aquatic higher plants, algae, animal matter and bacteria. The relative contribution of each of these groups will be affected by factors such as catchment topography and lake bathymetry. The size of the lake and fetch will affect the spatial distribution of each group within the lake.

Establishing the source and type of organic matter is important for a variety of reasons: firstly, organic matter in lakes is important as it provides a food source for many organisms which dwell in the lake. Establishing the various components and relative prevalence of the identified groups of organic matter types can help understanding of lake food webs and carbon cycling through trophic levels. Secondly, understanding the source of organic matter can provide useful palaeoecological and palaeoenvironmental records over long

temporal timescales (Meyers, 1994). The different organisms occurring within a watershed have unique biochemical components which can be used to understand changes in community structure over time (Meyers and Ishiwatari, 1993). Finally, understanding spatial differences in organic matter composition and source across lake sediments might aid process identification, for instance, slumping or regions of fluvial inflow.

A number of geochemical approaches have be used to successfully highlight the source of organic material in lake sediments; these include quick and cheap techniques which can be implemented on bulk sediment samples (which might be referred to as more 'traditional') and more advanced methods which focus on extracting information at the molecular level (a more novel approach). The reader is directed to Meyers and Ishiwatari (1993) and Meyers (2003) for full reviews of the common methods of establishing the source and type of organic matter in lake sediments; however, the methods that are applied in this chapter are described in brief below.

The total amount of organic matter can be measured through both loss on ignition (LOI) and total organic carbon (TOC). LOI estimates the percentage of organic matter in a sample compared to inorganic material. TOC measures the amount of organic carbon in a sample; organic matter on average contains about 50% carbon (Meyers, 2003). These techniques allow an understanding of the abundance of organic matter in lakes.

The abundance of different sources of organic matter will differ across a lake due to reasons such as preservation preferences and delivery processes (Meyers 2003). The contribution of allochthonous material can diminish with increasing distance from the lake shore in large lakes (Tenzer et al., 1997). In small, shallow lakes, it might be expected that terrestrial organics are more homogeneous due to frequent mixing of water. The utility of techniques such as LOI and TOC is often increased when used alongside other techniques such as the $\delta^{13}C$ values of the bulk organic sediments or the C/N ratios.

The $\delta^{13}C$ values of organic matter are most useful in distinguishing between C3 and C4 plants. C3 plants have lower $\delta^{13}C$ values due to preferential uptake of the lighter ^{12}C isotope compared to C4 plants (Meyer, 1994). C3 plants have an average $\delta^{13}C$ value of -27‰ whilst C4 plants have a higher average value of -14‰ (Meyers, 1994). Algae which use dissolved CO_2 which is in equilibrium

with the atmosphere (currently -8‰), will have $\delta^{13}C$ values which are very similar to other C3 plants (Meyers and Lallier-Verges, 1999). In some cases, dissolved CO_2 that enters the lake is isotopically light, which results in very low $\delta^{13}C$ values of algae (-47‰; Rau, 1978).

The $\delta^{13}C$ value of bulk sediment can be an important technique for assessing the type of organic matter that settles as lake sediments. Usually though, in environments with a variety of plants, the initial individual $\delta^{13}C$ signatures are homogenised in the bulk sediment $\delta^{13}C$ value. Understanding the $\delta^{13}C$ values of both the bulk sediment and the living plant material in the catchment of interest is often useful, especially for research regarding carbon cycling through lake food webs. Bulk sediment $\delta^{13}C$ values which are lower than what is considered as typical, if the organic matter contribution is from expected sources, can help to highlight changes in isotopic fractionation or carbon cycling in lakes.

The $\delta^{13}C$ values of organic matter can help to distinguish the type of plant matter from which it is derived (e.g. C3 versus C4 plants) but they do not necessarily highlight the source (e.g. terrestrial or aquatic). C/N ratios from 20-50 are associated with terrestrial land-based plants whereas algae typically have values under 12 (Meyers, 1994; Leng, 2006). Meyers and Lallier-Vergés (1999) suggest C/N ratios of 13-14 in lake sediments indicated an equal contribution of algal and vascular plant organic matter. Changes in C/N ratios over space and time can highlight shifts in the relative importance of autochthonous and allochthonous organic matter contributions to lake sediments. For example, Kaushal and Binford (1999) reported increases in C/N ratios which they linked to increased terrestrial carbon input to the lake due to deforestation.

Finney et al. (2012) use all of the techniques outlined above to understand changes in carbon cycling across the Holocene in a lake in Alaska. They argue that large fluctuations in $\delta^{13}C$ values over time are the result of changes in the input of ^{13}C-depleted, catchment respired CO_2. Subsequently, this carbon is fractionated further by phytoplankton, resulting in $\delta^{13}C$ values of phytoplankton which are highly ^{13}C-depleted. If plankton makes a significant contribution to organic matter, these low $\delta^{13}C$ values will be reflected in the bulk sediment $\delta^{13}C$ values. A good understanding of the causes of variability

of $\delta^{13}C$ values in organic matter (both in the living organisms and bulk sediment) is important for studies using $\delta^{13}C$ values as ecological tools, especially if the organisms being studied are of a higher trophic level.

The presence of specific *n*-alkane chain lengths has been used to investigate the source of organic material in lakes (e.g. Cranwell et al. 1987; Pearson et al. 2007). For example, short chain odd numbered *n*-alkanes (C_{15} – C_{19}) are more indicative of algal sources, mid chain lengths (C_{23} to C_{27}) are associated with aquatic macrophytes (Ficken et al., 2000) and long chain *n*-alkanes (C_{29} to C_{33}) are usually associated with higher terrestrial plants (Collister et al., 1994), although the patterns are not always straightforward. Often, distinguishing aquatic macrophytes can be difficult. Ficken et al., (2000) provide an equation which can highlight the relative contribution to the high molecular weight (HMW) compounds from both aquatic macrophytes and terrestrial higher plants. The equation is given in the methods section (EQ 4.1). Ficken et al., (2000) propose values of <0.1 indicate terrestrial plants, 0.1-0.4 are submerged/floating macrophytes and 0.4-1 reflect emergent vegetation. However, they highlight that values of between 0.1 and 0.4 likely indicate a mixture of all the sources; terrestrial, emergent and submerged macrophytes (Ficken et al., 2000). Silliman and Schelske, (2003) report a rapid shift in organic matter dominance as reflected in changes in the abundance of *n*-alkanes in Lake Apopka, Florida. They hypothesise the change was associated with anthropogenic phosphorus loading. Thus, the relative abundance of *n*-alkanes alongside various ratios of terrestrial/aquatic geolipids can be used to highlight the source and type of organic matter in lake sediments.

4.2.1 Thermokarst Lake Sediments

To date, little work has been completed on understanding sediment input into thermokarst lakes in a contemporary setting. Improving our understanding of sediment input and transport in contemporary thermokarst lakes is crucial in order to reliably reconstruct past changes in these systems. In particular, knowledge of organic sediments will also help to increase the understanding of the contribution of methane to the lake food web.

Thermokarst lakes, by the nature of how they develop, are likely to have a high amount of terrestrial input compared with many other lake types, especially in the early stages of development (Murton, 1996). Sediment that enters a thermokarst lake by way of thaw slumping could be composed of a mixture of organic and inorganic material with a wide range of ages. The amount of permafrost in the soils surrounding the lake, as well as the presence of massive ice structures such as ice wedges, will affect the stability of the lake margins and the depth of thaw and, therefore, the amount of material that enters the lake.

Surficial soils and living plants that slump into the lake might have a significant impact on the ratio of terrestrial to aquatic matter. However, this will depend on geomorphic settings. For example, thermokarst lakes located in boreal forest catchment will have a larger input of trees and higher plants as opposed to those located on the Arctic Coastal Plain in the arctic tundra zone, where vegetation composition is dominated by shrubs, herbaceous vascular plants and mosses. Thermokarst action at the lake edge can also increase the amount of Holocene or Pleistocene sediments that enter the lake. In Interior Alaska, deposits of both Pleistocene and Holocene are formed of loess (except for Holocene peat deposits), composed of fluvial silts (95%) and fine organics (from tundra-steppe environments), which means the amount of inorganic sediments entering the lake could also be high.

The distribution of terrestrial lake sediments will vary among thermokarst lakes due to differences in size and also bathymetry. It might be expected that the contribution of terrestrial organic matter to lake sediments will be highest close to the thermokarst margin. However, if the lake is small and processes of sediment transportation are high then the terrestrial organic matter might be homogenised across the lake. The signal of slumped material from terrestrial sources should be distinguishable from aquatic organic matter in lake sediments using the techniques outlined above. This chapter details an in depth examination of the amount and types of organic matter forming the surficial sediments of two thermokarst lakes in Interior Alaska. A range of methods, as outlined above, are compared in order to highlight the contribution of organic matter in the chosen lakes which will enable a good understanding of the carbon sources and their respective $\delta^{13}C$ values that are available to organisms within the lake food web.

4.3 Design

The objective of this chapter is to measure the organic composition of lake sediments over space in two thermokarst lakes to establish the relative contribution of different sources of organic matter. A number of techniques are used to gain not only a better understanding of the distribution of organics in the lakes, but to assess the reliability of each, if used on an individual basis. Surface samples across the lakes were taken to highlight, among other things, the spatial distribution of organic matter in lake sediments and whether this distribution could be used to distinguish important thermokarst lake processes (e.g. sediment slumping) or sources of carbon for the lake food web.

Three predictions about what might be occurring in the study lakes were made:

1. The concentration of terrestrial-derived organic matter will be higher close to the thermokarst margin. If the thermokarst margins are active and large amounts of fresh plant matter and terrestrial soils enter the lake, a large proportion of this will remain at the edge as often the size of the material entering the lake will make redisposition within the lake difficult.
2. Organic matter will be heterogeneous across the study lakes. In the opposite argument to above, strong internal lake processes (e.g. stratification) could lead to high heterogeneity in overall organic sediment distribution. The relative size of the lakes means they are sheltered, and not subjected to processes (such as strong fetch or sediment focussing) which might cause an accumulation of fine suspended material in one region of the lake.
3. In contrast to above, organic matter within the lakes will be homogenised across the lake due to transportation processes (such as bottom currents or water column mixing).

4.3.1 Sampling strategy

The full description of the study sites and background to the lakes can be found in chapter 3. Figure 4.1 shows the sampling points relevant to this chapter. Most of the sample points have been used for multiple analyses. No biomarker samples were retrieved from the centre of Ace L.

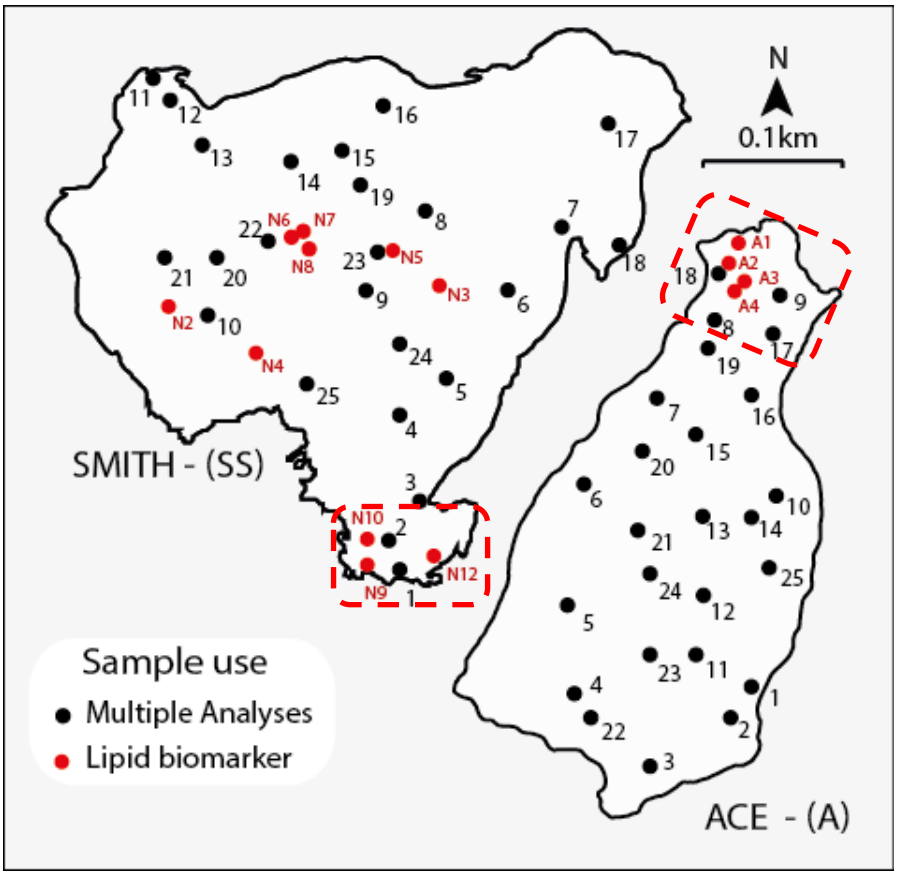

Figure 4.1 Sample locations in the study sites. Black dots represent samples that were used for a number of analyses and red dots represent samples used for biomarker analysis.

4.3.2 Methods

4.3.2.1 Loss on ignition

The surface sediment's organic content, total organic carbon (TOC) and the carbonate content were estimated from loss on ignition. Briefly, sub samples (~1g, 0-1 cm depth) were dried in the oven at 105˚C overnight, left to cool

and weighed. The dry samples were placed in the furnace at 550˚C for two hours, left to cool and weighed (organic content). The samples were returned to the furnace at 950˚C for four hours, left to cool and weighed (carbonate content).

4.3.2.2 Stable carbon isotopes, total organic carbon and C/N mass ratios of bulk sediment

Stable carbon analysis of bulk organic matter was completed at the NERC Isotope Geochemistry Laboratory. Samples were exposed to 5% HCL for 12 hours to remove carbonates. The samples were rinsed with 30ml of de-ionised water through Whatman no.41 filter paper. The filter paper was dried at 50˚C and the remaining sediment was ground using a pestle and mortar. 50ug of sediment was weighed into tin capsules and crushed. $^{13}C/^{12}C$ analyses were performed by combustion in a Costech Elemental Analyser (EA) on-line to a VG TripleTrap and Optima dual-inlet mass spectrometer. Stable carbon isotope values were calculated to the VPDB scale using a within-run laboratory standards calibrated against NBS18, NBS-19 and NBS 22. Replicate analysis of well-mixed samples indicated a precision of + <0.1‰ (1 SD). C/N ratios and TOC were measured at the same time as $^{13}C/^{12}C$ analyses. C/N ratios were calibrated against an Acetanilide standard. Replicate analysis of well-mixed samples indicated a precision of + <0.1.

4.3.2.3 Stable carbon isotopes of plant material

A number of plant samples were retrieved from the lake shore and within the lake. Stable carbon isotope analysis was performed at the UC Davis Stable Isotope Facility following standard laboratory procedures for solid materials.

4.3.2.4 Stable carbon isotopes of *n*-alkanes

Surface samples (1-2 cm depth) were subsampled for biomarker analysis. Samples were freeze-dried and ground. Subsequently, samples were extracted with a sequence of organic solvents to obtain the total lipid extract (TLE). The TLE was split into different fractions according to polarity via column chromatography. All fractions were analysed by GC/MS and additionally, compound-specific stable carbon isotope analysis was performed on the apolar fraction and selected samples from the phospholipid fraction (the latter

is not discussed here). The methods describe below relate to extraction of the apolar (*n*-alkane) fraction only. Figure 4.2 highlights the methods described below and highlights the relevant branches for this study.

4.3.2.4.1 Solvent-based extractions

Two sequential extractions were performed upon the samples. First, a modified Bligh and Dyer, adapted from Bligh and Dyer (1959). Briefly, buffered water was prepared adjusting a solution of 0.05M KH2PO4 in water to pH 7.2 through the addition of NaOH pellets. Subsequently, a monophasic solvent mixture was made up with buffered water, CHCl3 and MeOH (4:5:10 v/v). Samples were sonicated in Blligh-Dyer solvent mixture for 15 minutes and then centrifuged at 3000 rpm for 5 minutes. Supernatant was collected in a round bottom flask. This step was repeated twice and all supernatants were combined and dried to obtain TLE1. Post-extraction sediment residues were air-dried.

The Bligh-Dyer post-extraction residues were sonicated in dichloromethane (DCM) for 15 minutes and centrifuged at 3000 rpm for 5 minutes as previously described. This step was repeated first with DCM:MeOH (1:1, v/v) and then with MeOH. Supernatants were combined after every step of sonication-centrifugation to obtain TLE2. Both TLE1 and TLE2 were then combined to get the final TLE (TLE3).

4.3.2.4.2 Column chromatography

TLE3 was split into three fractions of increasing polarity as described previously (Oba et al., 2006; Pitcher et al., 2009). Briefly, silica gel columns (0.5 g, 60 Å particle size) were prepared and conditioned with 4 ml of *n*-hexane:ethyl acetate (3:1, v/v). The TLE was then loaded on top of the column and different fractions were collected with the following eluents: first, 3 ml of *n*-hexane:ethyl acetate (3:1, v/v) to obtain the simple lipid fraction; second, 3 ml of ethyl acetate to separate glycolipids; finally, 10 ml of MeOH to obtain the phospholipid fraction. Every fraction was subsequently blown down under nitrogen until dry.

The simple lipid fraction was further split into the neutral lipid and the fatty acid fractions. First, a solution of $CHCl_3$ saturated with NH_4OH ($CHCl_3$ sat) was prepared. Two volumes of $CHCl_3$ were extracted with one of NH_4OH 12% (2x).

The organic phase was then collected into a round bottom flask and Na_2SO_4 anhydrous was added until complete removal of water. The resulting $CHCl_3$ sat was then decanted for further use. Second, silica gel columns (again, 0.5 g, 60 Å particle size) were prepared and conditioned with 4 ml of the recently prepared $CHCl_3$ sat solution. The simple lipid fraction was then loaded onto the column and subsequently, the neutral lipid fraction was eluted with 9 ml of $CHCl_3$ sat; followed by the fatty acid fraction, which was eluted with 9 ml of $CHCl_3$:acetic acid, 100:1. The two different collected fractions, neutrals and fatty acids, were blown down until dry.

A third column chromatography was performed to separate the neutral fraction into apolar and polar lipids. Columns were prepared with ~0.5 g of activated alumina (Al_2O_3) and conditioned with 4 ml of *n*-hexane:DCM (9:1, v/v). The neutral fraction was then loaded onto the column and the apolar fraction was collected after elution with 4 ml of n-hexane:DCM (9:1, v/v)), followed by the polar fraction with 3 ml of DCM:MeOH (1:2, v/v). The resulting fractions were blown down until dry.

4.3.2.4.3 GC/MS analysis

Prior to instrumental analysis two different chemical treatments were performed to make the lipid biomarkers GC/MS amenable. First, intact polar (IP) head groups were covalently cleaved to remove glyco- and phophor-moieties attached to the lipid hydrocarbon. Second, derivatization of carboxylic and hydroxyl groups contained within the lipid structure was performed. The organic phase was separated and blown down until dry.

GC-MS analyses of extracts were performed using a Thermoquest Finnigan Trace GC and MS. The GC was fitted with an on-column injector and the stationary phase was CP Sil5-CB. Detection was achieved with electron ionization (source at 70 eV, scanning range 50-580 Daltons). The temperature program consisted of three stages: 70-130 ˚C at 20 ˚C/min rate; 130-300 ˚C at 4 ˚C/min; and 300 ˚C, temperature held for 10 min. Data processing was performed by Xcalibur 2.0. The internal standard for quantification utilized was 2-hexadecanol, except for the apolar fraction, in which no internal standard was added because only ratios of compounds were examined.

4.3.2.5 GC/C/IRMS

Gas chromatography combustion isotope ratio mass spectrometry (GC/C/MS) was performed after GC/MS biomarker analysis, upon samples from the apolar fraction and selected samples from the phospholipid fraction. Samples had been previously made GC/MS amenable, therefore, only TMS was necessary max. 24 h prior to GC/C/MS. The analyses were carried out in a ThermoScientific Trace GC Ultra coupled to a Conflo IV interface and DeltaV mass Spectrometer. The mass analyser consisted of 3 Faraday cup collectors m/z 44, 45 and 46). The GC was fitted with a CP Sil 5 CB capillary column (50 m x 0.32 mm x 0.12 μm) and He was the carrier gas at 2 ml min-1 flow rate. The combustion reactor of NiO/Ni/CuO was maintained at 1000 ºC. Calibration was achieved using CO2 reference gas of known isotopic composition and sample delta ^{13}C values were expressed against the standard vPDB. The GC temperature program is the same as the one previously described for GC/MS analyses. All measurements were performed in duplicate and the software for data processing was IsoDat 3.0 from ThermoFisher Scientific.

4.3.2.6 Ratios

A number of different ratios were used to estimate the various contributions of organic matter types from the *n*-alkane compounds. Usually the ratios are applied to concentration data. However, in the absence of concentration data, the integrated peak area for each compound was used. Within each sample run, the area under each compound peak is a proportion of the total area under all measured peaks. In a single run, all peaks are relative to one another so a bigger peak area value will represent a higher concentration of the given compound compared to a smaller peak area (in the same run). Therefore, any ratios should still estimate the relative proportion of each group of interest.

The ratio (P_{aq}) was used to determine the relative contribution of terrestrial and aquatic plants in the sediments (Ficken et al 2000). The P_{aq} ratio is calculated as follows:

$$P_{aq} = (C_{23} + C_{25})/(C_{23} + C_{25} + C_{29} + C_{31}) \qquad \text{(EQ 2.1)}$$

The carbon preference index (CPI) can be used to assess the likelihood that the higher molecular weight (HMW) *n*-alkanes in the sample are derived from higher plants. Low HMW CPI values can indicate contamination or microbial or algal inputs (Clark Jr and Blumer, 1967). The CPI is calculated as follows:

$$0.5\left(\frac{\sum_{\text{odd}} C_{25-33}}{\sum_{\text{even}} C_{26-34}} + \frac{\sum_{\text{odd}} C_{25-33}}{\sum_{\text{even}} C_{24-31}}\right) \quad \text{(EQ 2.2)}$$

4.3.2.7 Vegetation characterisation

The potential sources of organic matter in the study lakes were characterised and the most common vegetation types were sampled for bulk $\delta^{13}C$ analysis. Terrestrial vegetation was sampled in accessible locations as close to the lake margin as possible. Aquatic vegetation was sampled from the boat alongside sediment retrieval. Vegetation samples were frozen until analysis. The samples were thawed and washed with DO water to remove contaminants, placed in glass vials and freeze dried. The freeze-dried samples were ground using a pestle and mortar, weighed and placed into tin capsules. The samples were analysed at the UC Davis Stable Isotope Facility using the standard protocols for lab.

4.3.2.8 Particulate Organic Matter (POM)

Particulate organic matter (POM) was sampled from the centre of Ace L. throughout 2013 by B.Gaglioti of UAF. At the time of writing, the full details of the methods used to collect and process the samples were not available.

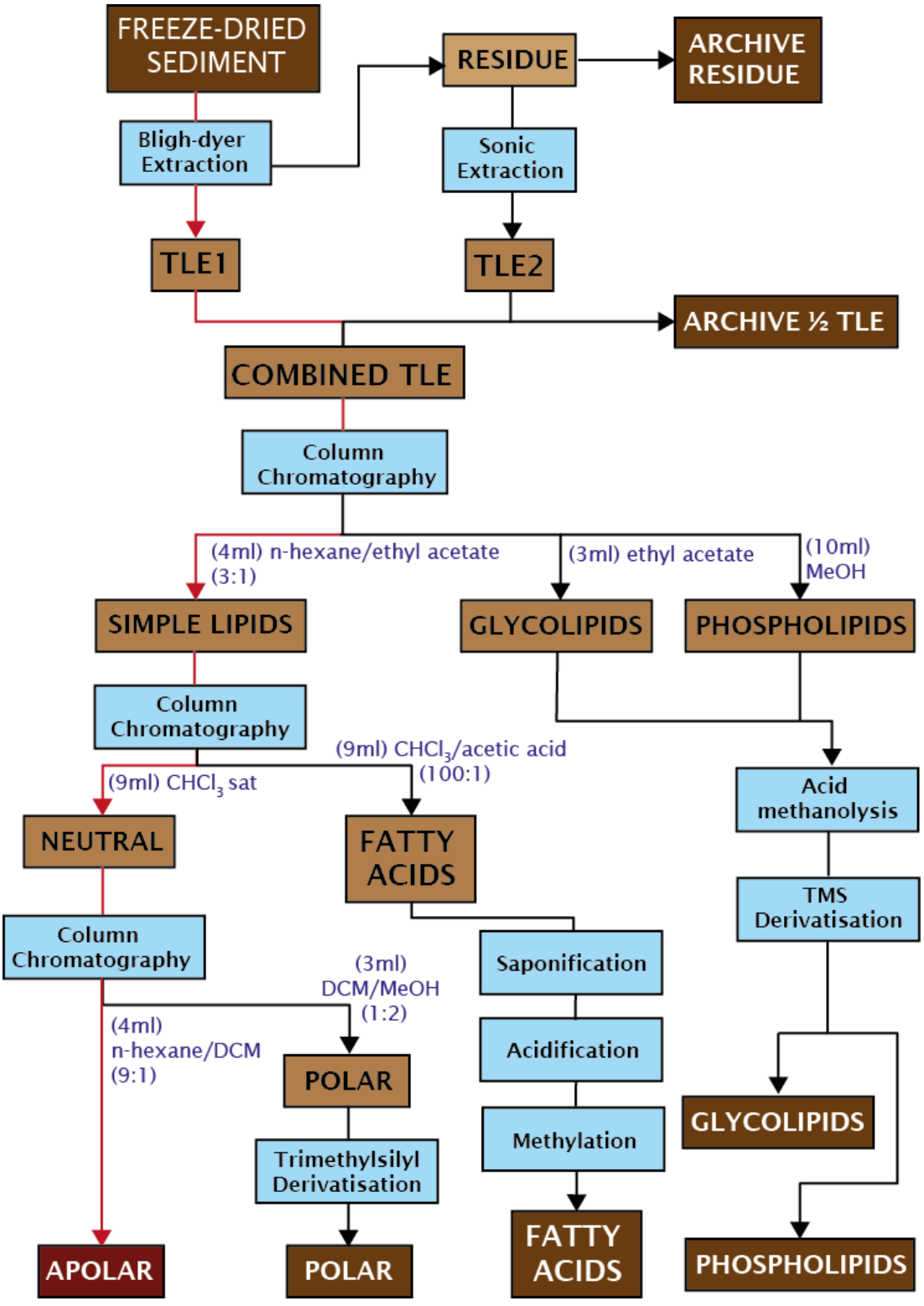

Figure 4.2 Biomarkers methods flow diagram. Red lines indicate the method pathway for this chapter

4.4 Results

Chapter 5 deals with the diploptene results separately; however, the distribution and $\delta^{13}C$ values of diploptene are placed into context with the *n*-alkane results here to highlight the importance of the more detailed study of the diploptene stable isotope results.

4.4.1 Sources of organic material in lakes and $\delta^{13}C$ values of vegetation

Due to the close proximity of the study sites, similar vegetation communities are present at both lakes: typical interior boreal forest, plus wetlands along drainage networks and near the lake shore. *Picea glauca* and *Picea mariana* are the dominant tree species. In areas of disturbance or sparse tree cover *Potentilla sp.*, *Ledum latifolium*, *Vaccinium uliginosum* and *Chamerion angustifolium* are common. Grasses and sedges also frequently occur, especially in the wetter areas near drainage networks. Areas in drainage networks have some peat development. At Smith L. peat has developed near to the Thermokarst zone, whilst at Ace, patches are associated with the drainage network. Peat is typically dominated by *Sphagnum sp.* and unidentified brown mosses.

The aquatic macrophyte vegetation at both lakes is similar, with greatest vegetation development at shallow (~2m) water depths. At Ace L. it is restricted to littoral areas whilst at Smith L. a significant amount is found across the entirety of the lake. Common emergent and semi emergent plants include *Equisetum sp., Nymphaea sp., Sparganium sp.* and *Typha Latifolia.* Submerged plants were not recorded due to sampling constraints. At Smith L. blue-green algal blooms were prevalent in summer, whilst at Ace L. large areas of the littoral zones were covered in algal blooms. These blooms are likely seasonal, only being present during certain periods of the ice-free season. Figure 4.3 shows some of the common plant types and their bulk $\delta^{13}C$ values alongside the $\delta^{13}C$ values from bulk sediments at both study sites. Overall the $\delta^{13}C$ values from the vegetation samples range from -36.8 to -21.1‰. At Smith L., the bulk sediment $\delta^{13}C$ values have a tight range which fits well with the vegetation $\delta^{13}C$ values. Ace L. has a wider range, which is driven by two outliers that are not within 2 standard deviations (S.Ds) of the

mean (*Sparganium sp.* and unidentified brown moss). On average, Ace L. bulk sediment values are more depleted than Smith L. and are at the lower edge of the observed vegetation $\delta^{13}C$ values.

The relationship between bulk sediment $\delta^{13}C$ values and water depth was tested using regression analysis (Figure 4.4). The results indicated a correlation between increasing water depth and decreasing $\delta^{13}C$ values (r^2= 0.6 p = 0.05).

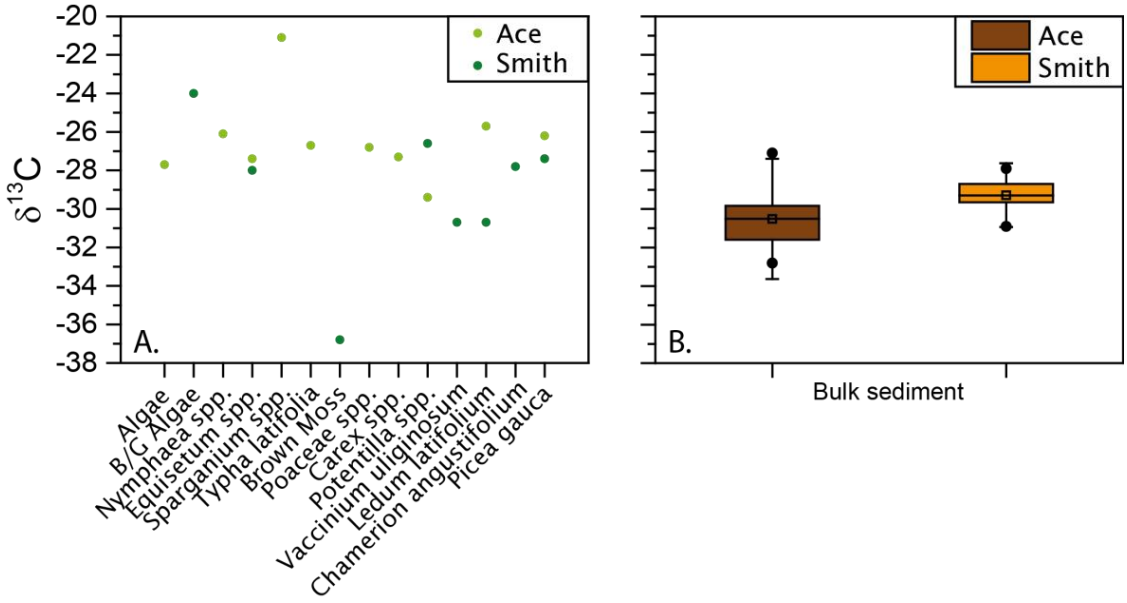

Figure 4.3 $\delta^{13}C$ values of different sources of organic matter in lake sediments.. a) Common vegetation in and around the lakes. Vegetation is presented from aquatic to terrestrial (left to right). A standard instrumental error of ±0.1‰ is incorporated in the size of the data points. b) box plot of bulk sediment samples at Ace L. and Smith L..

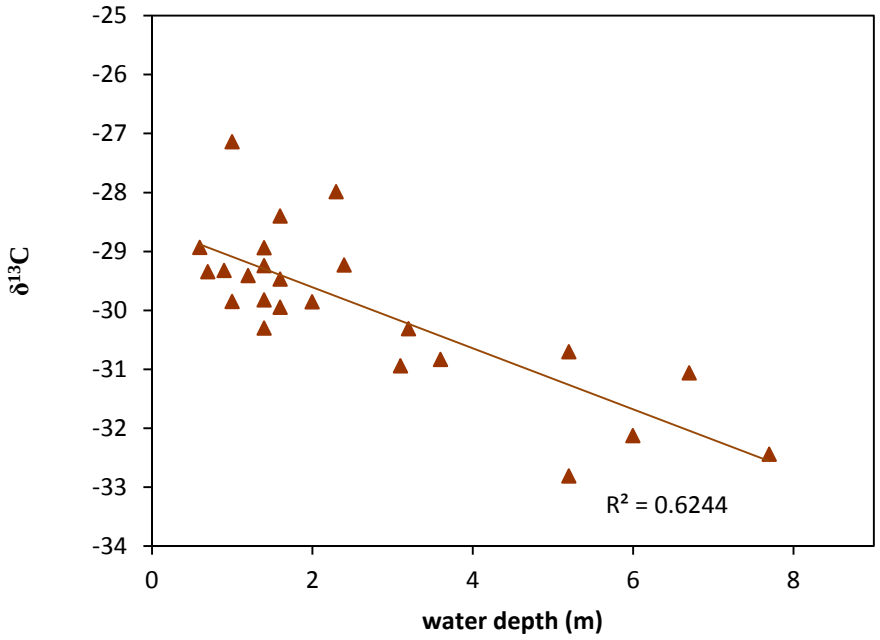

Figure 4.4 Bulk sediment $\delta^{13}C$ values plotted against water depth (p = 0.05).

4.4.2 POM

The seasonal profile of $\delta^{13}C_{POM}$ across the given timeframe shows high variability and a trend from ^{13}C-depleted values (-37.3 to -35‰; Table 4.1; Figure 4.5), to more enriched (-23.6‰) and then a trend of decreasing values over time (decreasing from -30.5 to -33.2‰). For the most part, repeat samples are very similar but even these are at least a 1‰ different.

Table 4.1 POM $\delta^{13}C$ values from the centre of Ace L.

Sample Code	Sampling date (2013)	$\delta^{13}C$	C/N Ratios
20	16 April	-35.02	10.7
35	16 April	-37.34	8.2
36	7 June	-23.62	7.4
39	19 June	-30.56	8.8
40	19 June	-31.72	8.5
42	12 July	-31.61	6.5
43	12 July	-32.76	6.4
4/13 2	3 August	-32.54	6.7
4/13 1	3 August	-33.26	4.9

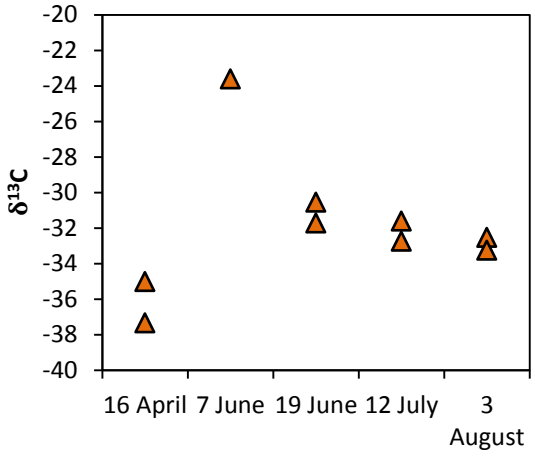

Figure 4.5 POM $\delta^{13}C$ values measure throughout 2013. Repeat samples were taken for all but one month.

4.4.3 Organic content, TOC and C/N mass ratios.

The differences in the contribution of organic material as determined by LOI are shown in figure 4.6 and with TOC in table 4.2. The results highlight that for the most part Smith L. has higher LOI and TOC values than Ace L.. Most samples at Smith L. have an organic content of 30% and above and TOC values over 10%, whilst at Ace L. almost all samples have below 30% organics and 10% TOC. Altogether the organic content of the samples ranged from 8.6 to 73.7%, a difference of 65% between minimum and maximum values. TOC ranges from 3.6 to 29.5%, a difference of 26%. In general, central samples at Smith L. are higher than the rest of the lake and are less variable.

The spatial patterns show the centre and some littoral areas of Smith L. had some of the highest organic content values (figures 4.6 and 4.7, table 4.2; however values were highly heterogeneous. The lowest values (samples s13-11 and a13-3) were located in the littoral zones of both Ace L. and Smith L. with organic contents below 10%. The high variability in values in both the thermokarst and littoral samples could be reflecting large inputs of both organic matter and silts.

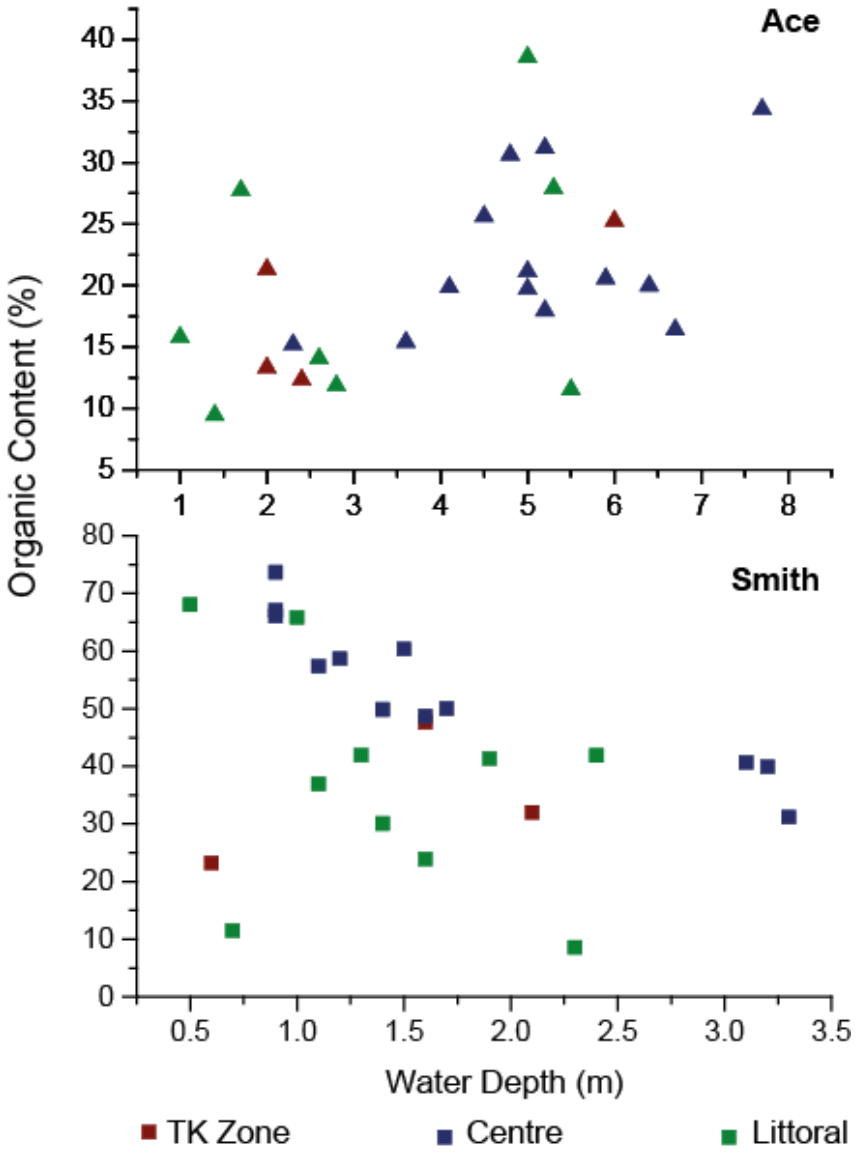

Figure 4.6 Organic content (%) across Ace L. and Smith L..

Table 4.2 Bulk sediment organic content, organic carbon content and water depths across Ace L. and Smith L..

		Sample Code	LOI (%)	TOC* (%)	Water Depth (m)
Ace L.					
	TK Zone	A13-8	25.3	10.1	6
		A13-9	21.3	8.5	2
		A13-17	13.3	5.3	2
		A13-18	12.3	4.9	2.4
	Centre	A13-5	15.2	6.1	2.3
		A13-10	16.4	6.6	6.7
		A13-11	19.9	7.9	4.1
		A13-12	19.7	7.9	5
		A13-13	34.3	13.7	7.7
		A13-14	20.0	8.0	6.4
		A13-15	30.6	12.3	4.8
		A13-19	18.0	7.2	5.2
		A13-20	21.1	8.5	5
		A13-21	25.6	10.3	4.5
		A13-23	15.4	6.2	3.6
		A13-24	31.2	12.5	5.2
		A13-25	20.6	8.2	5.9
	Littoral	A13-1	11.9	4.7	2.8
		A13-2	14.1	5.6	2.6
		A13-3	9.5	3.8	1.4
		A13-4	27.7	11.1	1.7
		A13-6	11.5	4.6	5.5
		A13-7	38.6	15.4	5
		A13-16	27.9	11.2	5.3
		A13-22	15.8	6.3	1
Smith L.					
	TK Zone	S13-1	23.2	9.3	0.6
		S13-2	47.6	19.0	1.6
		S13-3	32.0	12.8	2.1
	Centre	S13-8	50.0	20.0	1.7
		S13-9	66.1	26.4	0.9
		S13-10	49.8	19.9	1.4
		S13-14	60.4	24.1	1.5
		S13-15	57.4	22.9	1.1
		S13-19	48.7	19.5	1.6
		S13-20	31.2	12.5	3.3
		S13-21	39.9	16.0	3.2
		S13-22	40.7	16.3	3.1
		S13-23	58.7	23.5	1.2
		S13-24	67.1	26.8	0.9
		S13-25	73.7	29.5	0.9

Littoral	S13-4	68.0	27.2	0.5
	S13-5	65.8	26.3	1
	S13-6	41.9	16.8	2.4
	S13-7	41.9	16.8	1.3
	S13-11	8.6	3.4	2.3
	S13-12	11.5	4.6	0.7
	S13-13	41.3	16.5	1.9
	S13-16	30.1	12.0	1.4
	S13-17	23.9	9.6	1.6
	S13-18	36.9	14.8	1.1

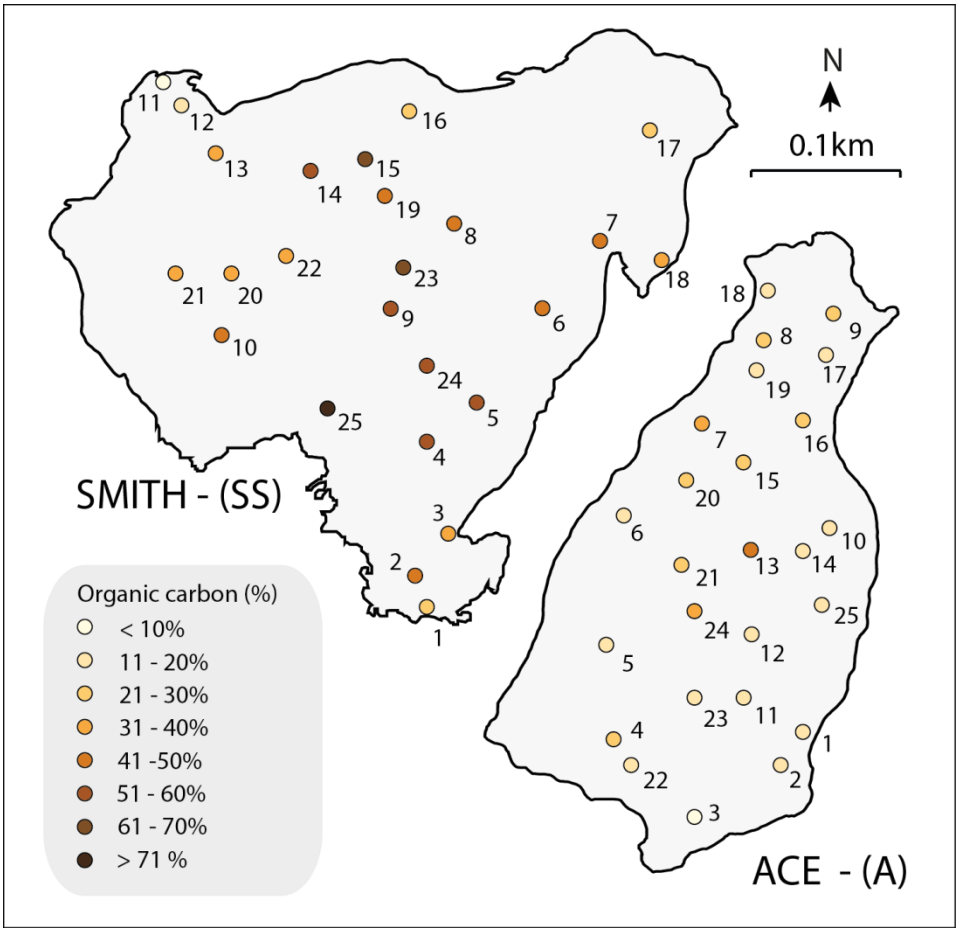

Figure 4.7 Bulk sediment organic content (%) spatial distribution across Ace L. Lake and Smith L.

4.4.4 Profiles of $\delta^{13}C$ and C:N ratios of bulk sediment

All samples have a C/N mass ratio of between 9 and 22 (Table 4.3). Smith L. has the highest ratios overall, ranging from 11.2 to 15.7. Ace L. has lower ratios (9.1 to 11.9) apart from sample A11-2 which has the highest ratio of all samples at 21.8 (Figure 4.8). The lowest C/N ratios are found across Ace L. and show little connection to a single zone.

Table 4.3. Bulk sediment $\delta^{13}C$ values and C/N ratios

		Sample Number	$\delta^{13}C_{bulk}$	C/N Mass Ratios	Water Depth (m)
Smith L.					
	TK Zone	S13-1	-28.9	14.6	0.6
		S13-2	-28.4	14.6	1.6
		S11-10	-28.9	14.4	1.4
	Centre	S11-3	-29.2	15.5	1.4
		S13-19	-29.5	13.8	1.6
		S13-22	-30.9	11.2	3.1
		S13-23	-29.4	13.8	1.2
		S13-24	-29.3	13.7	0.9
	Littoral	S13-11	-28.0	15.3	2.3
		S13-12	-29.3	12.8	0.7
		S13-16	-30.3	11.6	1.4
		S13-17	-29.9	15.7	1.6
Ace L.					
	TK Zone	A11-2	-27.1	21.8	1.0
		A13-18	-29.2	11.9	2.4
		A13-9	-29.9	11.4	2
		A13-8	-32.1	9.9	6
		A11-6	-30.3	11.5	3.2
	Centre	A13-19	-30.7	10.8	5.2
		A13-24	-32.8	9.1	5.2
		A13-23	-30.8	11.2	3.6
		A13-13	-32.4	9.8	7.7
		A13-10	-31.1	11.0	6.7
	Littoral	A13-3	-29.8	10.8	1.4
		A13-22	-29.9	9.9	1

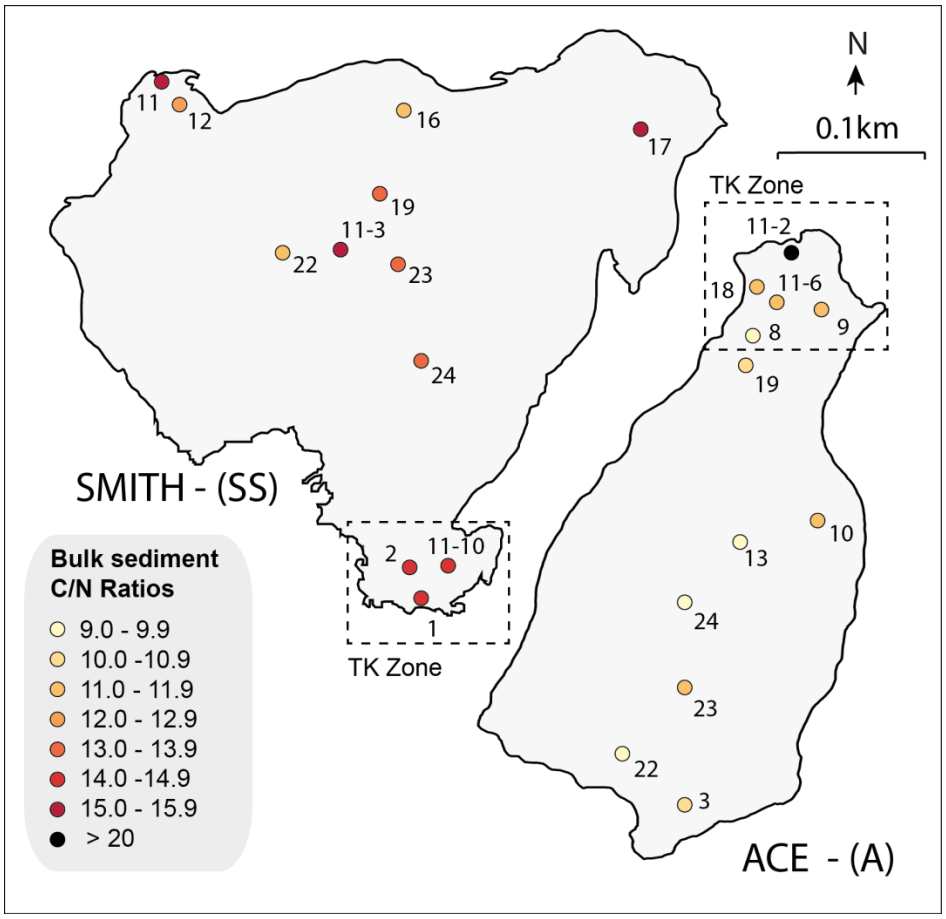

Figure 4.8 C/N ratios of bulk sediment

Stable carbon isotope values of bulk sediment ranged from -27.1 to -32.8‰ (Table 4.3) which equates to almost 6‰ difference between bulk sediment samples. The most negative $\delta^{13}C$ values are found in the centre and in the thermokarst zone of Ace L. (figure 4.9) and overall Ace L. has the most heterogeneity.

The bulk sediment C/N mass ratios and the $\delta^{13}C$ value show a positive correlation with some of the most negative $\delta^{13}C$ values corresponding to the lowest C/N mass ratios (Figure 4.10). There is greater correlation at Ace L. than at Smith L. and the relationship is statistically significant at Ace L. ($r^2 = 0.5$, $p = 0.02$; $r^2 = 0.2$, $p = 0.07$ for Ace L. and Smith L. respectively).

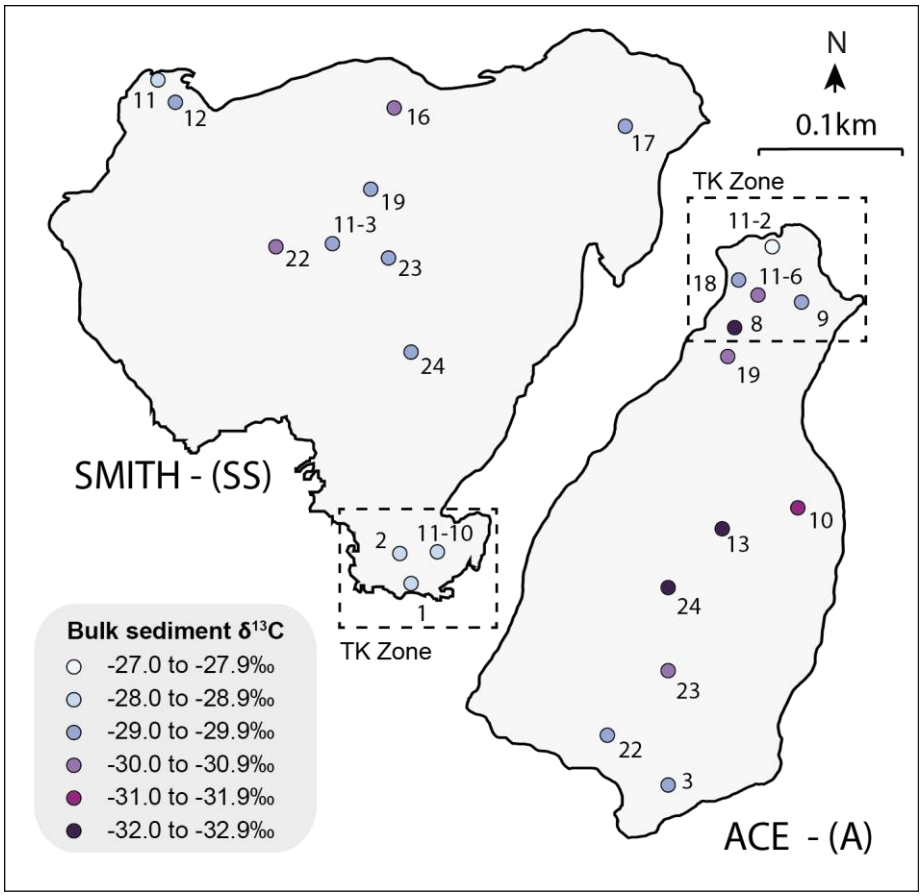

Figure 4.9 Bulk sediment $\delta^{13}C$ values at Ace and Smith L.

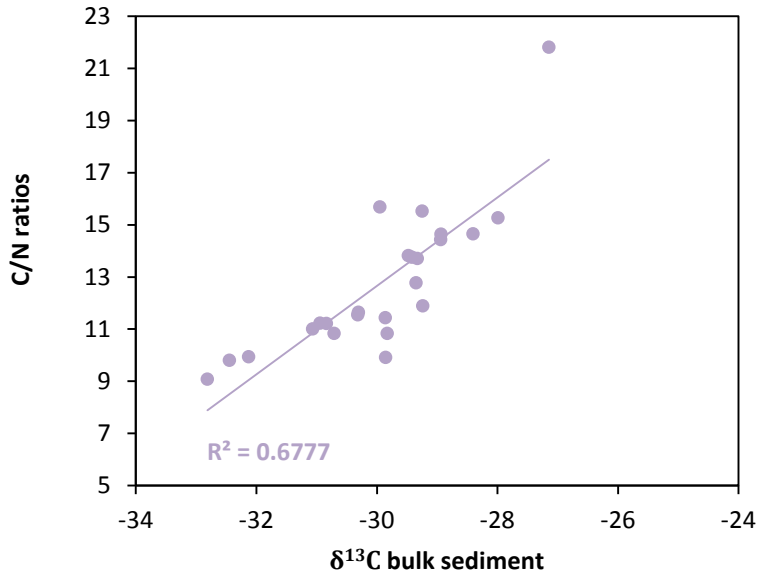

Figure 4.10 Bulk sediment $\delta^{13}C$ values against C/N ratios (r^2 = 0.6 p = <0.05)

4.4.5 *n*-alkane distributions and $\delta^{13}C$ values

A total of 18 samples were analysed across both lakes. All identifiable *n*-alkane peaks were integrated and quantified as peak area (Appendix A). The integrated peak area for each odd carbon numbered compound is presented against the total integrated peak area as a ratio. The ratio showed the proportion of each compound compared to the total of the measured compound amount within each sample (Table 4.4).

The shortest chain length that could be confidently integrated was $C_{17,}$ but this was not possible in all samples as the signal to noise ratio was too low to distinguish clear peaks. The smallest ratio is C_{17}:total_compounds (0.001) at sample point S12-N3. The highest ratio is found at Ace L. is C_{27} (0.304). Overall, C_{25} to C_{29} appeared dominant, whilst C_{17} and C_{19} were low in relative abundance. There is little to distinguish between lakes or between the thermokarst zone and the centre at Smith L.. The ratio data highlight the highest proportions of odd chain length compounds are found at Ace L. but for the most part the data suggest a fairly homogenous distribution across all samples (Figure 4.11).

Diploptene was initially characterised from its mass signal and its eluting position in relation to other compounds. It fitted well with previous studies that identify diploptene(Pancost et al., 2000b). As with the *n*-alkane ratios, the proportions of diploptene do not appear to correlate with a specific location within the lake or between the two thermokarst zones.

P_{aq} ratios ranged between 0.25 and 0.63. In Ace L. the ratios indicate a dominance of submerged/floating macrophytes whilst at Smith L. emergent macrophytes are important in almost half the samples. All CPI values were over 5 which indicate a strong signal of higher plants and the values ranged from 7.7 to 24.7. The average chain length (ACL) ranged from 26.8 to 27.3 and 25.8 to 28.3 for Ace and Smith L. respectively, and highlighted increased variability in the dominant compounds at Smith L.

Table 4.4. Ratio of individual compounds against all *n*-alkane integrated peaks including diploptene

Site		Sample Number	Dip:$C_{sum\_n\text{-}alkanes}$	C_{17}:$C_{sum\_n\text{-}alkanes}$	C_{19}: $C_{sum\_n\text{-}alkanes}$	C_{21}: $C_{sum\_n\text{-}alkanes}$	C_{23}: $C_{sum\_n\text{-}alkanes}$	C_{25}: $C_{sum\_n\text{-}alkanes}$	C_{27}: $C_{sum\_n\text{-}alkanes}$	C_{29}: $C_{sum\_n\text{-}alkanes}$	C_{31}: $C_{sum\_n\text{-}alkanes}$	C_{33}: $C_{sum\_n\text{-}alkanes}$
Ace												
		A1	0.06	0.013	0.008	0.024	0.078	0.166	0.279	0.184	0.135	0.016
		A2	0.23	N/A	0.003	0.025	0.069	0.149	0.252	0.191	0.153	0.031
		A3	0.09	N/A	0.003	0.023	0.081	0.202	0.304	0.184	0.112	N/A
		A4	0.17	0.004	N/A	0.027	0.076	0.164	0.247	0.173	0.163	0.039
Smith												
	Centre	S12-N1	0.08	0.007	0.009	0.071	0.214	0.156	0.222	0.135	0.083	0.007
		S12-N2	0.09	N/A	0.008	0.048	0.116	0.150	0.212	0.167	0.149	0.030
		S12-N3	0.08	0.001	0.003	0.030	0.087	0.152	0.219	0.168	0.173	0.044
		S12-N4	0.13	N/A	N/A	0.043	0.110	0.174	0.223	0.145	0.143	0.033
		S12-N5	0.06	N/A	N/A	0.016	0.062	0.119	0.186	0.180	0.241	0.073
		S11-N6	0.05	N/A	0.002	0.020	0.059	0.128	0.225	0.195	0.210	0.060
		S11-N7	0.07	N/A	0.002	0.024	0.077	0.132	0.211	0.184	0.199	0.057
		S11-N8	0.03	N/A	N/A	0.000	0.047	0.099	0.226	0.224	0.222	0.047
	TK	S12-N9	0.08	0.010	0.007	0.031	0.075	0.138	0.248	0.215	0.148	0.032
		S12-N10	0.06	0.003	0.004	0.027	0.060	0.093	0.164	0.214	0.235	0.082
		S12-N11	0.08	0.002	0.005	0.028	0.070	0.129	0.212	0.200	0.177	0.053
		S12-N12	0.04	N/A	N/A	0.073	0.239	0.116	0.148	0.137	0.138	0.043
		S12-N13	0.09	N/A	0.027	0.042	0.135	0.164	0.235	0.183	0.143	N/A
		S11-N14	0.04	0.002	0.003	0.022	0.064	0.126	0.205	0.198	0.213	0.063

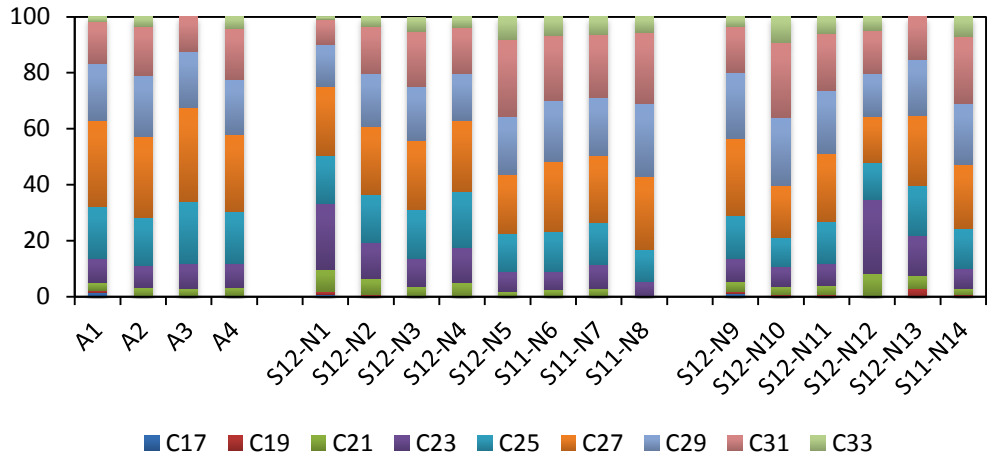

Figure 4.11 Odd chain length *n*-alkanes. The ratio of each compound against the total odd chain length *n*-alkanes was calculated as a percentage.

Table 4.5 CPI, Average chain lengths and P_{aq} values calculated from compound-specific integrated peaks

			CPI (C_{25} – C_{33})	ACL (C_{21}-C_{34})	P_{aq}	P(wax)
Ace						
		A1	13.9	27.1	0.43	0.71
		A2	8.5	27.3	0.39	0.73
		A3	14.1	26.8	0.49	0.68
		A4	10.9	27.3	0.42	0.71
Smith						
	Centre	S12-N1	14.2	25.8	0.63	0.54
		S12-N2	11.0	26.8	0.46	0.66
		S12-N3	8.6	27.4	0.41	0.70
		S12-N4	8.4	26.9	0.50	0.64
		S12-N5	8.2	28.2	0.30	0.77
		S11-N6	10.5	27.9	0.32	0.77
		S11-N7	9.2	27.8	0.35	0.74
		S11-N8	7.7	28.2	0.25	0.82
	TK Zone	S12-N9	14.5	27.3	0.37	0.74
		S12-N10	8.3	28.3	0.25	0.80
		S12-N11	8.9	27.7	0.35	0.75
		S12-N12	N/A	N/A	N/A	N/A
		S12-N13	24.7	26.6	0.48	0.65
		S11-N14	10.8	27.9	0.32	0.76

Compound specific $\delta^{13}C$ values of *n*-alkanes (odd chain numbers from C_{17} to C_{33}) across Ace L. and Smith L. range from -39.2 to -23.2‰ which is a 16‰ difference between minimum and maximum values of different *n*-alkanes (Table 4.6). However, due to the reduced resolution of compounds of LMW the few that were resolved have not been included in further interpretation. The range of $\delta^{13}C$ values within a single chain-length between samples is much lower, with the average difference between minimum and maximum values for the same chain length being 4.9‰. The $\delta^{13}C$ values of *n*-alkanes are offset from the $\delta^{13}C$ values of bulk sediment by an average of 2‰ which is likely due to biological fractionation.

The compound specific *n*-alkane $\delta^{13}C$ values do not appear to vary with regard to a specific area within the lake and the small amount of difference in the $\delta^{13}C$ values is likely due internal variation within each sample and is not necessarily linked to the sample's location (Figure 4.12).

The $\delta^{13}C$ values of diploptene are a lot lower than the $\delta^{13}C$ of the *n*-alkanes (Figure 4.12). The average *n*-alkane $\delta^{13}C$ value is -32.6% whilst the average $\delta^{13}C$ of diploptene is -50.2‰, which is a 17‰ difference. While the results of the diploptene $\delta^{13}C$ values are discussed independently (Chapter 5), it is important to highlight here the clear difference in $\delta^{13}C$ values. The lower values of $\delta^{13}C$ in diploptene suggest that the organisms from which diploptene derives might have a carbon source other than *n*-alkanes and that further exploration of the reasons for ^{13}C-depleted diploptene is warranted.

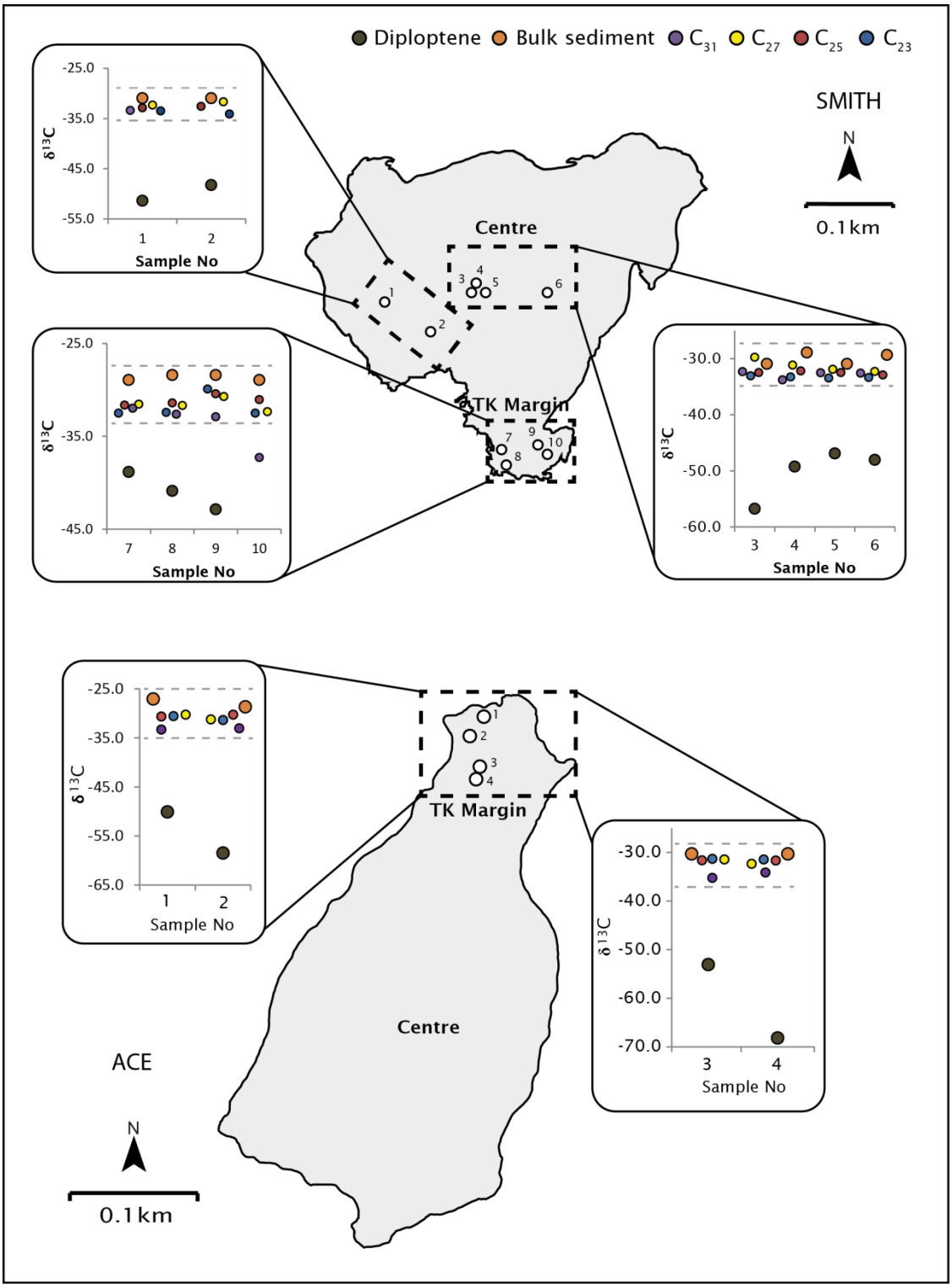

Figure 4.12 *n*-alkanes and diploptene. Diploptene and bulk sediment are represented by larger filled circles for ease of identification

Table 4.6 $\delta^{13}C$ values of *n*-alkanes across the study sites. Bulk sediment and diploptene $\delta^{13}C$ values are included for reference

		Sample No.	C_{17}	C_{19}	C_{21}	C_{23}	C_{25}	C_{27}	C_{29}	C_{31}	C_{33}	Bulk Sediment	Diploptene
Ace													
		A1	-34.5	-30.1	-31.4	-30.6	-30.7	-30.3	-32.1	-33.3	-32.4	-27.1	-50.1
		A2	--	-23.2	-33.0	-31.4	-30.3	-31.3	-33.9	-33.1	-32.8	-28.7	-58.5
		A3	--	--	-32.2	-31.3	-31.6	-31.5	-32.9	-35.3	-31.9	-30.3	-53.1
		A4	-39.2	--	-32.7	-31.5	-31.7	-32.4	-34.8	-34.2	-33.2	-30.3	-68.2
Smith													
	Centre	S12-N2	--	--	-35.4	-33.5	-32.9	-32.4	-34.3	-33.4	-33.0	-30.9	-51.4
		S12-N4	--	--	-36.1	-34.1	-32.6	-31.7	-32.8	-	-31.9	-30.9	-48.3
		S12-N3	--	--	-35.0	-33.4	-32.9	-32.3	-33.6	-32.6	-31.7	-29.3	-48.0
		S11-N6	--	--	-34.8	-33.3	-32.2	-31.2	-33.1	-33.8	-32.9	-28.9	-49.2
		S11-N7	--	--	-35.2	-33.1	-32.5	-29.7	-34.5	-32.3	-33.2	-30.9	-56.8
		S11-N8	--	--	--	-33.5	-32.5	-31.9	-33.7	-32.5	-32.2	-30.9	-46.9
	TK zone	S12-N9	--	--	-33.0	-32.4	-31.4	-31.7	-33.4	-32.6	-31.4	-28.4	-40.9
		S12-N10	--	-32.4	-32.1	-32.5	-31.6	-31.5	-32.5	-32.0	-31.4	-28.9	-38.8
		S12-N12	--	--	-29.8	-29.9	-30.4	-30.7	-32.6	-32.9	-31.0	-28.4	-42.9
		S11-N14	--	--	-34.9	-32.5	-31.0	-32.4	-36.8	-37.3	-36.6	-28.9	--

4.5 Discussion

4.5.1 The source of organic matter

The results of this chapter highlight that both macrophytes and algae are dominant sources of organic matter in the study sites. The level to which they contribute to the sediment is highly heterogeneous across the lake surface; however, some potential patterns are highlighted and discussed below. Organic matter from terrestrial sources appears to be a small fraction of the total, and there does not appear to be an increased contribution in close to the thermokarst margin.

As described in section 4.2, there are three main sources which can contribute to organic matter in lake bottoms: terrestrial and aquatic higher plants, soil (sediment) and algae. It was anticipated that the contribution of terrestrial plants to the organic matter in thermokarst lake sediments would be greatest in samples from closest to the thermokarst margin. The results of this study show that in the lakes in this study this is not the case and, as such, this idea can be rejected. The source of organic matter and reasons for heterogeneity within the study sites is discussed in more detail below.

Typically the $\delta^{13}C$ values of bulk sediment should reflect an average signal of organics in the lake catchment (Benson et al. 1991, Meyers 1994). The bulk sediment $\delta^{13}C$ values are within range of those measured from the vegetation samples; however, on average the bulk sediment values were offset from the vegetation, being 1-2‰ more negative. There is a weak, negative correlation ($r^2 = 0.62$, $P = 0.05$, $n= 23$) between the $\delta^{13}C$ values of bulk sediment and water depth, with more depleted $\delta^{13}C$ values at greater water depths (Figure 4.4). A number of possibilities are discussed: firstly what might be driving the low bulk sediment $\delta^{13}C$ values and secondly why these vary with water depth.

Low $\delta^{13}C$ of bulk sediment might be driven by seasonal changes in fractionation of carbon by phytoplankton. Algae utilise dissolved CO_2, which is usually in isotopic equilibrium with atmospheric CO_2 (Meyers 1994) and will therefore have a similar $\delta^{13}C$ profile to that of other vegetation types. This may alter if the system is not in equilibrium. POM values from Ace L. show $\delta^{13}C$ values are more depleted than the measured vegetation types. A single

measurement of $\delta^{13}C$ of algae was recorded at each lake. At Ace L., this consisted of a bulk sample taken from an algal mat in late June 2013. The $\delta^{13}C$ value of this algal sample fits between the $\delta^{13}C$ of POM measured in early June and early July, increasing the justification that POM at Ace L. is predominantly algae or phytoplankton. This may indicate the importance of seasonality and an isotopically light carbon source for algae in Ace L.. In marine environments, $\delta^{13}C$ values of phytoplankton become more depleted with higher concentrations of CO_2 as photosynthetic isotopic fractionation is greater (Hayes, 1993). Furthermore Kling et al. (1992) suggest CO_2 builds up under the ice over the winter in high-latitude lakes, which might explain the most depleted $\delta^{13}C$ POM values immediately after ice break up. Meyer (1997) indicates that preferential uptake of ^{12}C during thermal stratification can lead to an isotopically depleted algal signal and might explain the gradual decrease in $\delta^{13}C_{POM}$ across the summer at Ace L. Furthermore Finney et al. (2012) highlight low $\delta^{13}C$ values of POM in a number of Alaskan lakes, including Ace L., and Gu et al. (1996) found low $\delta^{13}C$ values of POM or phytoplankton in Smith L. indicating that low $\delta^{13}C$ of POM in at the study sites it plausible.

The correlation between $\delta^{13}C$ values of bulk sediment and water depth is likely due to a dominance of phytoplankton or POM in the organic matter in sediments from deeper waters. This could be linked to both the lack of mixing of the lake waters and the limited amount of macrophyte growth below 2-3m depth. The C/N ratios of POM suggest a large contribution of algae to the signal, and are also correlated to water depth. Meyers (1994) highlights the C/N ratios of various plant types and shows terrestrial plants have C/N ratios of >20 whilst algae generally range between 4 and 10. Given the high primary productivity, aquatic plant growth and terrestrial plant input to both Ace L. and Smith L., it is the likely that the intermediate C/N ratios of bulk sediment are reflecting a mixed signal. The C/N ratios reflect a relative increase in the algal component with depth at Ace L. The relationship however, is not as clear in Smith L., but this is likely due to shallower overall depth profile in the latter.

n-alkanes have been used to highlight the dominant sources of organic matter in lake sediments through the use of carbon chain-lengths. Often, however, this can be an over simplification of the provenance of *n*-alkanes as the same

compound can be produced by a number of plants. In this study, a strong odd-over-even pattern (OEP) of *n*-alkanes is found in all samples and the ratios suggest a dominance of high molecular weight compounds (C_{27} to C_{31}). The values of CPI are high (7.7 to 24.7) suggesting a dominance of higher plants (Eglinton and Hamilton, 1967; Muri et al., 2004). Some studies have highlighted that C_{21} to C_{25} *n*-alkanes can be derived from blue-green algae (Pearson et al., 2007) as well as the aforementioned aquatic plant sources. In a lake such as Smith, where both blue-green algae and aquatic macrophytes dominate, the proportional partitioning of the *n*-alkane compounds among plant types might be difficult. Overall though, the results of the *n*-alkanes at Smith L. suggest a dominance of submerged/floating and emergent species, which is consistent with observational data which suggests aquatic macrophytes are an important component of the system. This is in agreement with results of other approaches and the other techniques which suggest a low contribution of terrestrial organic matter.

At both study lakes, the *n*-alkane data appears to show a negligible amount of low molecular weight (LMW) compounds. The other techniques suggest that an algal component might be quite important. It is likely the lack of LMW compounds is due to large differences in the concentrations between the short and the long chain *n*-alkanes. Environments that are known to have high levels of primary productivity and very little allochthonous input (e.g. the Black sea) have TOC values which are very low, suggesting even when autochthonous production is relatively high, the overall concentration of autochthonous material is still very low in terms of detectability. Studies have highlighted that the preferential degradation of algal material and the overall production of carbon chains in algae is lower than higher plants (Wetzel, 2001). This leads to the HMW compound concentrations masking the LMW compounds. Different methods should be utilised in order to extract the short-chain *n*-alkanes which are potentially present but in much reduced concentrations. Further work on other lipids such as the fatty acids, sterols and phytols will also elucidate any variations in organic source material across the lake.

4.5.2 The spatial distribution of organic matter

The organic content (%) as estimated by the LOI is within the broad range of values that have been estimated from other boreal and thermokarst lakes (e.g. (Anderson and Brubaker, 1994; Larocque et al., 2001; Anderson et al., 2003). The data suggest a high amount of heterogeneity in the amount of organic matter and TOC across the surface sediments of both lakes. In Ace L., the overall lower organic content has been attributed to the reduced amount of aquatic macrophyte growth in comparison to Smith L.. Sediment focusing, as is common in many lakes with a deeper central zone (e.g. Anderson and Brubaker 1994), does not appear to be occurring at the study sites. In Ace L., if sediment focusing were occurring, it might be expected that the highest organic matter values would be in the deepest samples. A negative relationship between water depth and organic content (%) is found in the centre of Smith L. (R^2 = 0.8, p = <0.05) with organic content decreasing with increasing water depth, but this is based on very few samples and along a very short depth gradient (data not displayed in graph form). It is proposed that the lack of sediment focusing and the high heterogeneity of TOC, C/N ratios and bulk sediment $\delta^{13}C$ values across both lakes are linked to infrequent mixing of the water column. Detailed studies of the lakes have highlighted strong stratification across an annual timeframe, with winter ice and high summer temperatures causing strong thermal and oxygen gradients (Alexander and Barsdate, 1971; Alexander and Barsdate, 1974; Gu et al., 1994). As discussed above, the C/N ratios and bulk sediment $\delta^{13}C$ values indicate that the waters in Ace L. are unlikely to mix frequently. In Smith L., the high heterogeneity of organic matter could be linked to mesoscale heterogeneity in aquatic vegetation stands. If the organic matter is deposited at the site where it is formed, then the sediment profiles will reflect the *in-situ* vegetation and algal communities. Interestingly, organic content, TOC and C/N values suggest high inter-lake and intra-lake variability yet the *n*-alkane ratios are somewhat homogenous, and the ratios are fairly consistent throughout the dataset.

In Ace L., the C/N ratio and bulk sediment $\delta^{13}C$ value taken from the sample closest to the thermokarsting margin suggest that this sample is dominated by terrestrial material. If more samples were taken from very close to the margin, further evidence of terrestrial input might be seen. Although it is only

one sample, it does suggest that slumping at the thermokarst margin might be contributing to the organic matter signal in Ace L. At the very least, it can be argued that the relative contribution is higher in Ace L. than in Smith L., which is consistent with the more extensive and steeper nature of the thermokarst margin at Ace L.

To summarise, the spatial distribution of organic matter in the study lakes can likely be attributed to their limnological profiles; the stratification of lake waters mean that sediment is infrequently redistributed and therefore the organic content is patchy across the lake surface sediments.

4.5.3 Sediment cycling in thermokarst lakes

The results highlight a high amount of complexity in the distributions of organic material within both lakes. Overall, the results from the different methods indicate that the input of terrestrial material from the slumping of the thermokarst margin is not significant, or at least, that the within-lake productivity is proportionally much higher. Reasons for the lack of terrestrial vegetation at the thermokarst margin are discussed below.

One reason for the lack of terrestrial organic matter in the thermokarst zone might be that slumped material might not solely comprise modern terrestrial matter. Although a large amount of modern (and Holocene) organic matter is displaced into the lake via the thaw and subsequent slumping of material due to thermokarst erosion, in lakes such as Ace and Smith, which are located on Pleistocene loess, a relatively large amount of older inorganic material might enter at the same time. For example in Smith L., photo 4-1 shows a large amount of soil and underlying sediment entering the lake. These sediments have lower organic content and TOC values (Walter et al., 2008a). A study by Schleusner et al. (2015) on Lake El'gene-Kyuele in Arctic Siberia, highlighted that the thermokarsting margin was distinguishable by the input of large amounts of inorganic sediments (Schleusner et al. 2015). If this were the case for Smith L. or Ace L. then we might expect lower organic content and TOC in the thermokarst zone. Ace L. has a higher input of inorganic material than Smith L. but this cannot be clearly linked to the thermokarst zone. Therefore, it is likely that any terrestrial input into the study lakes is fairly equal in terms of organic and inorganic contributions. The size of the lake studied by

Schleusner et al. (2015; over 2km long) and the catchment dynamics (low vegetation growth in a tundra environment) are very different to those in this study.

Another explanation might be that the thermokarst margin is more stable than was first assumed. At Ace L., terrestrial material dominates a single sample close to the thermokarst margin, indicating that this section may still be actively slumping. The fact that this is the only sample close to the margin (< 3m) suggests that the area which is currently slumping might be small or that the material from the slump is not effectively dispersed beyond the shoreline. At Smith L. however, the lack of terrestrial material (both organic and inorganic) contributing to the surface sediments suggests that the thermokarst margin is currently relatively stable at this point in time, which is not unreasonable, based on visual inspection over recent years. Although Photo 3-4 suggests large areas of the margin entering the lake, the photo was taken in 2011 and there was little change over the following sampling seasons.

4.6 Conclusions

This chapter looked at the important sources of organic matter in thermokarst lakes.

The evidence suggests that within-lake sources are the most important contributors of organic matter to the surface sediments. At Ace L., the contribution of phytoplankton is apparent in the C/N ratios and bulk sediment $\delta^{13}C$ values whilst at Smith L. the aquatic macrophytes appear to be the most dominant source. The *n*-alkane analysis did not extract the right information for understanding the algal component of the organic matter but did highlight the relative importance of submerged/floating and emergent vegetation at both sites.

Bulk sediment $\delta^{13}C$ values showed that although the majority of bulk sediment appears to be vegetation, the algal component is important and can lower the $\delta^{13}C$ values of the bulk sediment. This has important implications for the chapters to follow as it highlights that other sources of depleted carbon are likely to be present in the lakes, or at least, in Ace L..

The results highlighted high heterogeneity across the surface sediments in both lakes which was attributed to the strong stratification present across much of the year at both lakes. The lack of water column mixing means that sediments settle *in-situ* instead of focusing as is common in many lakes, especially those with steep profiles such as Ace L..

The influence of the thermokarst margin appeared to be minimal at both lakes, although there is some evidence at Ace L. that terrestrial material is contributing to the lake surface sediments. It was concluded that in Smith L. the thermokarst margin was stable and therefore little terrestrial material was entering the lake. At Ace L., the results suggested that overall the thermokarst margin was stable, although small regions, which might contain ice bodies, might be active.

Chapter 5: Spatial variability of diploptene $\delta^{13}C$ values in thermokarst lakes: the potential to analyse the complexity of lacustrine methane cycling.

Foreword: This chapter is presented in the style of the journal it was written for. The content of the chapter is the most up to date version of the paper as was available at the time of thesis submission. For publication, figure 2.2 will be included in the final manuscript.

K. L. Davies[1], R. D. Pancost[2,3], M. E. Edwards[1], K. M. Walter Anthony[4] P. G. Langdon[1], 4, L. Chaves Torres[2,3]

[1]Geography & Environment, University of Southampton, SO17 1BJ, United Kingdom

[2]Organic Geochemistry Unit, School of Chemistry, University of Bristol, BS8 1TS, United Kingdom

[3]Cabot Institute, University of Bristol, BS8 1 UJ, United Kingdom

[4]Water & Environment Research Centre, University of Alaska Fairbanks, Fairbanks, Alaska, 99775, USA

5.1 Abstract

Cryospheric changes in northern high latitudes are linked to significant greenhouse gas flux to the atmosphere, including methane release that originates from organic matter decomposition in thermokarst lakes. The connections between methane production in sediments, transport pathways and oxidation are not well understood and this has implications for any attempts to reconstruct methane production from sedimentary archives. We assessed methane oxidation as represented by methane oxidising bacteria across the surface sediments of two interior Alaska thermokarst lakes in relation to methane emissions via ebullition (bubbling). The bacterial biomarker diploptene was present and had low $\delta^{13}C$ values (lower than -38‰)

in all sediments analysed, suggesting methane oxidation was widespread. The most ^{13}C-depleted diploptene was found in the area of highest methane ebullition emissions in Ace L. (δ^{13}C diplotene values between -68.2 and -50.1‰), suggesting a positive link between methane production, oxidation, and emission in this area. In contrast, significantly less depleted diploptene δ^{13}C values (between -42.9 and -38.8‰) were found in the area of highest methane ebullition emissions in Smith L. Lower δ^{13}C values of diploptene were found in the central area of Smith L. (between -56.8 and -46.9‰), where methane ebullition rates are low but methane diffusion appears high. Using δ^{13}C-diplotene as a proxy for methane oxidation activity, we suggest the observed differences in methane oxidation levels among sites within the two lakes could be linked to differences in source area of methane production (e.g. age and type of organic carbon) and bathymetry as it relates to varying oxycline depths and changing pressure gradients. As a result, methane oxidation is highly lake-dependent. The diploptene δ^{13}C values also highlight strong within-lake variability, implying that single-value, down-core records of hopanoid isotopic signatures are not secure indicators of changing methane flux at the whole-lake scale.

5.2 Introduction

Thermokarst and thermokarst-affected lakes (those formed and/or influenced by thaw and collapse of ice-rich ground) are now recognized as important past and present sources of methane flux to the atmosphere (Walter et al., 2006; Walter et al., 2008a; Shirokova et al., 2012; Wik et al., 2013). Under current scenarios of projected future climate warming in regions sensitive to thaw (Colins et al., 2013), these lakes are expected to remain a source of methane emissions to the atmosphere (Vincent et al., 2013). Predictions of the future contribution they will make to the dynamic global carbon cycle and any estimations of past emission rates are largely based on measurements recorded over the last 15 years (e.g. Brosius et al., 2012; Walter Anthony et al., 2014). Long-term (i.e. Holocene) variations in lake-derived methane flux to the atmosphere and changes in emissions during discrete climatic events in the past are less well understood (but see Walter Anthony et al., 2014; Walter et al., 2007b). A proxy for past gas flux from lakes would be an important development in better understanding long term carbon cycling, but we are far from understanding within-lake methane dynamics well enough for such a proxy to yet be reliable.

The broad term ‘thermokarst lakes’ encompasses a complex range of lakes types associated with different geographical and geomorphological settings in permafrost regions. Methane production within these lakes and fluxes to the atmosphere vary with lake type. Walter et al. (2008) and Brosius et al. (2012) divide thermokarst lakes into two main categories: yedoma lakes and non-yedoma lakes, where yedoma refers to late Pleistocene deposits of organic- and ice-rich silt, typically several or more metres deep (Zimov et al., 2006; Schirrmeister et al., 2013).

Methane production in thermokarst lakes can be classified by production type: production that occurs in anoxic surface sediments, as is common in most freshwater lakes and reservoirs, and production that occurs in deeper sediments, especially along the boundary of the "thaw bulb", which is specific to thermokarst lakes (Figure 1). Anoxia is caused by oxygen depletion associated with microbial decomposition of organic matter. Anoxic conditions are enhanced by thermal stratification in the water column and/or by rapid sedimentation that buries labile organic material before it can be processed at

the sediment surface. A common trait of thermokarst lakes is methane production via mineralisation of organic carbon from sources not found in other lakes. For example, methane emissions can occur where thermokarst-induced erosion leads to large-scale slumping of banks into the littoral zone; material is typically of Holocene age, but may be older (Figure 2.2). As well as the production from slumped material, yedoma lakes may feature high methane emissions related to the microbial processing of older, labile carbon in the deep thaw bulb (talik, i.e., an area of thawed permafrost sediment underneath the lake). Walter Anthony and Anthony (2013) suggest that yedoma thermokarst lakes typically produce more methane than non-yedoma thermokarst lakes owing to a higher availability of labile carbon in thick, thawed yedoma sequences.

Once produced, methane can be transported to the atmosphere through a number of pathways: ebullition (bubbling), turbulent diffusion and plant mediated transport (Bastviken, 2004). Several studies have focused on these emission pathways, assessing methane production and emission levels in freshwater environments (e.g. Bastviken, 2004; Bastviken et al., 2011; Delsontro et al., 2011; Joyce and Jewell, 2003).

Thermokarst-specific methane ebullition seeps have been observed and measured using GPS mapping and submerged bubble traps and described as persistent, spatially explicit fluxes at the water-air interface (Sepulveda-Jauregui et al., 2014; Walter et al. 2006, 2008; Walter Anthony and Anthony 2013). Ebullition seeps are thought to be fairly stable due to the development of conduits or ‘bubble tubes’ (Greinert et al., 2010; Scandella et al., 2011), which are point sources from which methane is emitted to the atmosphere repeatedly at the sediment-water interface. Nearly always, such seeps are densest near to actively eroding lake margins, which we call the "thermokarst zone". Here, methanogenesis is high due to thermokarst-specific sources of methane production: thawing of fresh talik and bank collapse (Figure 1; Kessler et al., 2012). Walter Anthony et al. (2010) postulate that most methane production that is specific to thermokarst lakes is transported to the atmosphere via seep ebullition (due to high rates of methane production in dense, thick talik sediments), although the diffusive flux component can be relatively high in older, more stable thermokarst lakes that have accumulated Holocene-aged organic carbon in near-surface sediments.

Less work has focused on methane production in surficial sediments of thermokarst lakes, dissolution and diffusion of methane from the sediments to the water column, and resultant diffusive emission, particularly in thermokarst zones. This paper reports an analysis of carbon isotopes in sedimentary bacterial biomarkers in relation to different forms of atmospheric methane flux from two lakes near Fairbanks, Alaska, with the aim of improving our understanding of methane cycling in thermokarst lake systems and assessing the effectiveness of biomarkers as a proxy for methane cycling in lakes.

5.2.1 The link between methane ebullition and methane diffusion from sediments

A significant fraction of methane produced in lake sediments can be oxidized and recycled within the lake, processes that offset methane emissions. Methane that has diffused from the sediments is subject to aerobic microbial oxidation by bacteria (Bastviken et al., 2002; Trotsenko and Khmelenina, 2005; Liebner and Wagner, 2007). Aerobic methane oxidation (MO) is thought to considerably reduce methane emissions from water bodies (Reeburgh, 2007). MO studies in lakes have mostly been carried out under stratified water column conditions (Bastviken et al., 2002; Kankaala et al., 2006). As with diffusive methane flux (Sepulveda-Jauregui et al., 2015), little work has focused on aerobic MO in thermokarst lakes (Martinez-Cruz et al., 2015). Understanding the link between MO and observed fluxes is crucial for developing a proxy for past methane production in thermokarst lakes.

In studies based on deep marine environments there is a correlation between widespread methane, released via cold seeps through sediments, and MO, as indicated by the presence and $\delta^{13}C$ values of specific bacteria and compounds (Pancost et al., 2000b; Elvert et al., 2001a; Pancost et al., 2001). In these environments both anaerobic (Alperin and Hoehler, 2010; Briggs et al., 2011) and aerobic (Elvert and Niemann, 2008; Birgel and Peckmann, 2008) methane oxidation processes have been identified and are important for mediating methane flux to the atmosphere. As well as a link between methane ebullition-seeps and methane diffusion in deep marine settings, a study carried out in a shallow (9m) near-shore bight linked the formation of bubble tubes with increased methane diffusing from the sediments (Martens and

Klump, 1980), the argument being that bubble tubes create an increased surface area that enhances methane diffusion, even though methane transported via ebullition is taken directly to the atmosphere and is not subject to oxidation. While derived from different environments than thermokarst lakes, the deep and shallow marine results suggest a positive relationship between transport via ebullition and methane diffusion from sediments, which may also occur in thermokarst lakes.

He et al. (2012) provide evidence that suggests a possible correlation between a coal-bed sourced methane ebullition seep and MO in the non-yedoma thermokarst lake, L. Qalluuraq, Alaska. The highest MO potentials occurred near the coal-bed sourced ebullition-seep and were associated with the presence of type I MOB in the sediments at the seep location. He et al. (2012) also observed high spatial variability of MO potentials and methanotroph communities and highlighted the need for further investigation of MO in thermokarst lakes.

In contrast, based on $\delta^{13}C$ and δD stable isotope values and radiocarbon ages of methane in bubbles, Walter et al. (2008) and Walter Anthony et al. (2014) suggest that methane emitted by ebullition originating in deep thaw-bulb sediments by-passes aerobic MO and that the majority of deep-sourced methane is transported through ebullition seeps as opposed to escaping sediments via diffusion. We therefore have two contrasting conceptual models (hypotheses): an enhancement model and a by-pass model. In the enhancement model, the thermokarst zone of a lake, where ebullition seeps are most abundant, would have higher levels of deep-sourced methane diffusion from sediments when compared with “quiescent” areas that are virtually ebullition seep free. In the by-pass model, where diffusion of deep-sourced methane out of sediments is thought to be minimal, we expect no difference between thermokarst-zone and lake-centre diffusion of deep-sourced methane from sediments, or, conceivably, less diffusion in the seep-rich area. A potential confounding factor is diffusion of methane that is formed in near-surface sediments, which can have variable and contrasting patterns across lakes, independent of spatial patterns of ebullition seeps.

Past methane emissions may be addressed qualitatively by using indirect proxies, for example, features related to the cycle of methane through the

lacustrine food web. Biogenic methane has highly depleted $\delta^{13}C$ values (usually -50 to -80‰, Whiticar, 1999), depending on the methane production pathway and substrate availability. These depleted $\delta^{13}C$ values can be traced through the food web, for example, in low-level heterotrophs such as invertebrates. Previous studies have linked depletion in the $\delta^{13}C$ values at various stages in the food web to the incorporation of carbon from of methane oxidising bacteria (MOB; van Hardenbroek et al., 2010; Jones and Grey, 2011; Sanseverino et al., 2012). Recent studies have demonstrated that some chironomid (non-biting midge) taxa utilise MOB as a food source within lakes (Deines et al., 2007a; van Hardenbroek et al., 2010). In thermokarst lakes, depleted $\delta^{13}C$ values in larvae and fossil head capsules have been linked to increased methane flux (van Hardenbroek et al., 2012a). Wooller et al. (2012) also interpret negative shifts in $\delta^{13}C$ values of fossil chironomids and daphnia as an increase in methane availability.

MOB have been identified in sediments from a wide range of terrestrial and aquatic environments. They are known to synthesise a number of specific compounds that can be isolated. In particular, the compound diploptene (17 β(H), 21 β(H)-hop-22 (29)-ene), a hopanoid hydrocarbon derived from a range of bacterial sources, has been identified as a methanotrophic biomarker via low $\delta^{13}C$ values in marine sediments and microbial mats associated with methane seeps (Pancost et al., 2000a; Pancost et al., 2000b; Elvert et al., 2001b) as well as Holocene peat (van Winden et al., 2010; Zheng et al., 2014). Diploptene and the related diplopterol have been used to establish past patterns of MO from marine sediment records (Jahnke et al., 1999; Pancost et al., 2000a) as well as lake sediments (Spooner et al., 1994; Schouten et al., 2001), and peat deposits (Kip et al., 2010; van Winden et al., 2012; Zheng et al., 2014).

To oxidise methane effectively, MOB require access to dissolved methane in sediments and lake water. The assumption is, therefore, that isotopic depletion at or near the base of the food web indicates oxidation of dissolved methane. The extent to which isotopic signals can be used as a proxy for past methane ebullition flux in thermokarst lakes depends on the relationship between ebullition and diffusion and the sensitivity of the isotope signal to changing methane supply. In order to investigate these issues, we applied the approach used to identify MO at deep marine vents and seeps—lipid

biomarkers from bacteria—to different areas associated with known ebullition emission patterns in two Alaskan lakes. MOB are a more direct proxy for methane than organisms higher in the food chain, and their use should allow a better understanding of methane diffusion from sediments, particularly in areas of ebullition seeps. The presence and $\delta^{13}C$ values of diploptene were used firstly to establish if MO was occurring at levels detectable by biomarkers, and secondly to assess the degree of MO observed in areas characterized by different modes of methane production and transport to the atmosphere.

5.3 Regional context & Study sites

Yedoma-like deposits that are similar to those described in, and common to, Siberia (Schirrmiester et al 2011) can be found in Interior Alaska. These sediments can have a relatively high organic content (Péwé, 1975) and are rich in excess ice. Thermokarst lakes that develop in landscapes dominated by these deposits have been placed into the yedoma or non-yedoma types (as described above) in previous studies (Walter et al., 2008; Brosius et al., 2012; Sepulveda-Jauregui et al., 2015). Two lakes were sampled in April 2011 and July 2012 (Figure 5.1). Ace L. represents a yedoma-type lake (Sepulveda-Jauregui et al., 2015), where the permafrost soils surrounding the lake and eroding into the lake along its NE margin are predominantly yedoma. Smith L. is classified as a non-yedoma lake in which Holocene-aged deposits are likely the main source of organic matter fuelling methane production.

Smith L. (64˚51'55.92"N, 147˚52'0.70"W; figure 2) is a shallow (≤4 m), productive lake located in Interior Alaska. It has a gentle bathymetric profile with average water depths between 1-3m. The lake is not subject to a strong fetch or high energy inflow or outflow. Observations during the ice-free periods suggest high primary productivity, with blue/green algal blooms predominant throughout the summer months (KLD, personal observation). The lake likely originated by thermokarst processes (Alexander and Barsdate, 1971); comparisons of lake shorelines between the 1950s and today suggest that segments of the southern and western margins have been actively thermokarsting during recent decades, and tilting trees currently lining the margin of a bay on the southeast shore are further evidence of localized thermokarst. Smith L. is a useful study site as its shallow profile reduces the potential of production or storage of methane due to stratification. Ace L. (64˚51’45.49N, 147˚56’05.69W) is part of the Ace-Deuce Lake system (Alexander and Barsdate, 1974) situated within an area covered by the Pleistocene Gold Hill and Goldstream loess formations (Pewe 1975). Ace L. is thermokarst in origin and formed through the thawing of ice bodies in the loess. The Ace-Deuce Lake system has high nutrient levels, and therefore Ace L. can be described as a eutrophic lake with a strong seasonal nutrient cycle (Alexander and Barsdate, 1974).

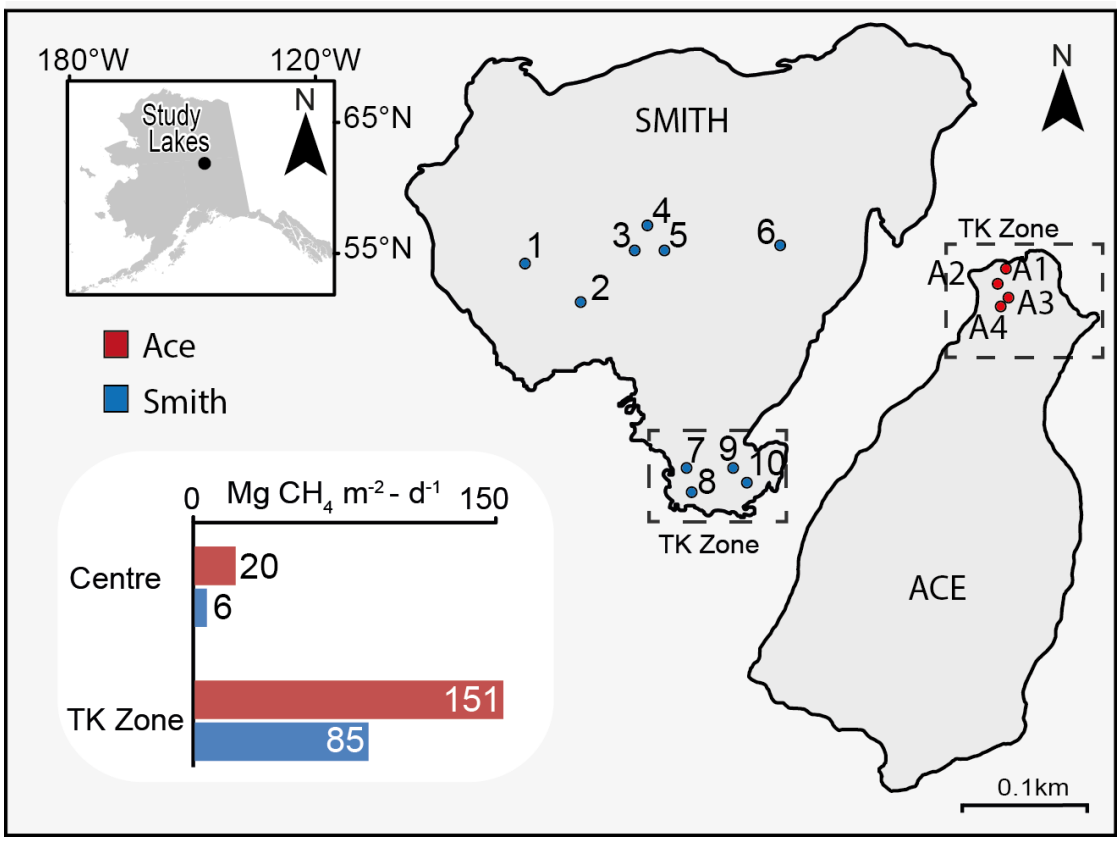

Figure 5.1. Locations of the study lakes in Alaska and the sample points within each lake.

5.4 Methods

5.4.1 Establishing sample regions

Walter Anthony and Anthony (2013) defined the 'thermokarst' zone for a number of lakes, and we continue to use this definition here. The thermokarst zone was the region of active thermokarst margin expansion observed using historical aerial photographs obtained during the past 60 years. In most lakes, the density of ebullition seeps is higher in thermokarst zones compared to non-thermokarst zones (Walter Anthony and Anthony, 2013). In Ace and Smith L., ebullition emissions were quantitatively monitored through a combination of winter-time ice-bubble surveys and bubble-trap flux measurements via previous studies (Sepulveda-Jauregui et al., 2015) and our own summertime bubble counts (figure 5.2). We obtained surface sediment cores well within the zone boundaries and as close to observed ebullition seep locations as possible. At Ace L., bubble counts may have been underrepresented due to fetch-mediated surface turbulence disturbing visual counts of bubbles. However this was an issue at all count sites, such that, any error encountered will be associated with the overall scale of emissions measured and not with bias between zones.

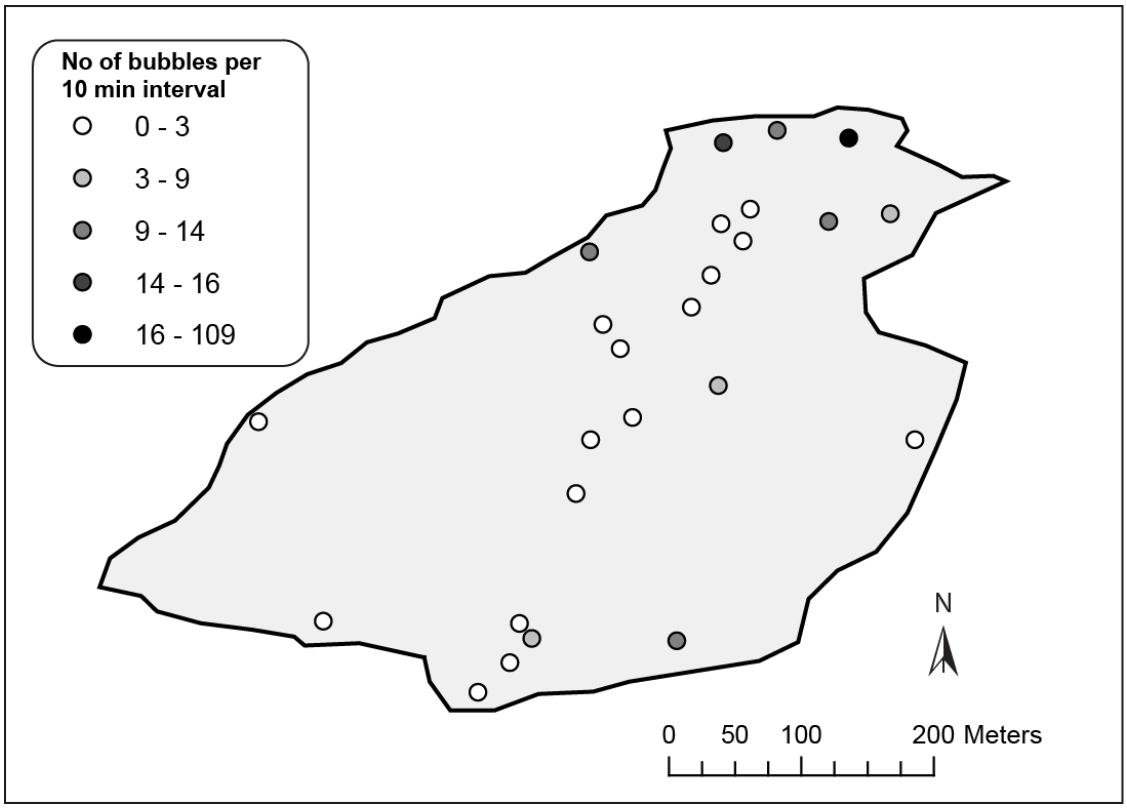

Figure 5.2 Bubble counts at Ace L.. A tally of all bubbles which broke at the water surface within a 2m radius of an anchored location.

5.4.2 Methane monitoring

Ebullition gas samples were collected from the thermokarst zone in the manner described in Walter Anthony et al. (2012) for determination of bubble methane concentration, stable isotope analyses, and radiocarbon dating. Gases were collected from submerged bubble traps into 60-ml glass serum vials following Walter et al. (2008), sealed with butyl rubber stoppers, and stored under refrigeration in the dark until analysis in the laboratory. We measured methane concentration using a Shimadzu 2014 equipped with an FID at the Water and Environmental Research Centre at University of Alaska Fairbanks (UAF). We determined $\delta^{13}C_{CH4}$, using a Finnegan Mat Delta V, and δD_{CH4} on a Delta XP at Florida State University. Subsamples of gas were combusted to CO_2, purified, and catalytically reduced to graphite (Stuiver and Polach, 1977), and the $^{14}C/^{12}C$ isotopic ratios were measured by accelerator mass spectrometry at the Woods Hole Oceanographic Institution's National Ocean Sciences AMS Facility. Stable isotope compositions are expressed in δ (‰) = 103 (($R_{sample}/R_{standard}$)-1), where R is $^{13}C/^{12}C$ or D/H and standards refer to

the Vienna Pee Dee Belemnite (VPDB) and Vienna Standard Mean Ocean Water (VSMOW), respectively. The analytical errors of the stable isotopic analyses are ± 0.1 ‰ $\delta^{13}C$ and ± 1.0 ‰ δD. We express radiocarbon data as percent modern carbon pmC (%) = $((^{14}C/^{12}C)_{sample}/(^{14}C/^{12}C)standard) \times 100$, which is the percentage of $^{14}C/^{12}C$ ratio normalized to $\delta^{13}C$ = -25‰ and decay corrected relative to that of an oxalic standard in 1950 (Stuiver and Polach, 1977).

5.4.3 Biomarker analysis

Surface sediment samples were retrieved using a gravity corer and the 0-5cm sequence was extruded at 1-cm resolution and retained for analysis; the 1-2 cm slice was subsampled for biomarker analysis. Two sequential extractions were performed upon the samples. The first step was a modified Bligh and Dyer extraction (Bligh and Dyer, 1959). Briefly, buffered water was prepared adjusting a solution of 0.05M KH_2PO_4 in water to pH 7.2 through the addition of NaOH pellets. Subsequently, a monophasic solvent mixture was made up with buffered water, $CHCl_3$ and MeOH (4:5:10 v/v). Samples were sonicated in Bligh-Dyer solvent mixture for 15 minutes and then centrifuged at 3000 rpm for 5 minutes. Supernatant was collected in a round bottom flask. This step was repeated twice and all supernatants were combined and dried to obtain the total lipid extraction (TLE) labelled TLE1. Post-extraction sediment residues were air-dried. The Bligh and Dyer post-extraction residues were sonicated in DCM for 15 minutes and then centrifuged at 3000 rpm for 5 minutes. This step was repeated first with DCM:MeOH (1:1, v/v) and then with MeOH. Supernatants were combined after every step of sonication-centrifugation to obtain TLE2. Both TLE1 and TLE2 were then combined to yield the final TLE.

The TLE was split into three fractions of increasing polarity using silica flash column chromatography (Oba et al., 2006; Pitcher et al., 2009). Silica gel columns (0.5 g, 60 Å particle size) were prepared and conditioned with 4 ml of *n*-hexane:ethyl acetate (3:1, v/v). Fractions were eluted with 3 ml of *n*-hexane:ethyl acetate (3:1, v/v) to obtain the simple lipid fraction, 3 ml of ethyl acetate to obtain glycolipids and 10ml of MeOH to obtain phospholipids. The simple lipid fraction was further split into neutral lipid and the fatty acid fractions. The organic phase was then collected into a round bottom flask and Na_2SO_4 anhydrous was added until complete removal of water. Silica gel

columns (again, 0.5 g, 60 Å particle size) were prepared and conditioned with 4 ml of the recently prepared $CHCl_3$ sat solution. The simple lipid fraction was then loaded onto the column and subsequently, the neutral lipid fraction was eluted with 9 ml of $CHCl_3$ sat. Finally, the neutral lipids were separated into apolar and polar lipid fractions. Columns were prepared with approximately 0.5 g of activated alumina (Al_2O_3) and compounds eluted with 4 ml of *n*-hexane:DCM (9:1, v/v) and 3 ml of DCM:MeOH (1:2, v/v) to yield the two fractions, respectively. Here, we focus on analyses of the neutral lipid apolar fraction.

5.4.3.1 Compound identification and Compound-specific $\delta^{13}C$ isotope analysis

GC-MS analyses were performed using a Thermoquest Finnigan Trace GC and MS. The GC was fitted with an on-column injector and the stationary phase was CP Sil5-CB. Detection was achieved with electron ionization (source at 70 eV, scanning range 50-580 Daltons). The temperature program consisted of three stages: 70-130 ˚C at 20 ˚C/min rate; 130-300 ˚C at 4 ˚C/min; and 300 ˚C, temperature held for 10 min.

Gas chromatography combustion isotope ratio mass spectrometry (GC-IRMS) was performed using a ThermoScientific Trace GC Ultra coupled to a Conflo IV interface and DeltaV mass Spectrometer. The GC conditions and program were the same as for GC-MS analyses. Calibration was achieved using CO_2 reference gas of known isotopic composition and sample $\delta^{13}C$ values were expressed against the standard VPDB. All measurements were performed in duplicate.

5.4.3.2 Mass balance equation

A carbon isotopic mass balance equation (Equation 5.1), or two-part mixing model, was developed to evaluate the contribution of MOB to the total bacterial biomass, and therefore, the relative amount of oxidation occurring at each sample location. The resulting end member values are given in table 5.1

$$f_{mob} = \frac{\delta^{13}C_{dip} - \delta^{13}C_{hetero\_hopane}}{\delta^{13}C_{mob\_hopane} - \delta^{13}C_{hetero\_hopane}} \quad \text{(EQ 5.1)}$$

f_{mob} is the fraction of diploptene generated by MOB and $\delta^{13}C_{dip}$ is the stable carbon isotopic composition of diploptene in a given sample. $\delta^{13}C_{hetero\_hopane}$ is the $\delta^{13}C$ value of the hopanoids derived from heterotrophic bacteria, the inferred other primary source of hopanoids in this setting, and is expressed as the $\delta^{13}C_{bacterial\ biomass} - \Delta^{13}C_{biosynthesis}$ (~4‰). Heterotrophic bacteria will primarily reflect the values of the substrate carbon; however a ~2 to 4‰ shift can occur during lipid biosynthesis (Pancost and Sininnghe Damsté 2003, and references therein). $\delta^{13}C_{mob\text{-}hopane}$ is the value of the hopanoids derived from MOB. It is calculated from the $\delta^{13}C_{methane}$ minus the fractionation that occurs during carbon uptake by methanotrophs (0-30‰; Jahnke et al., 1999) minus the biosynthetic fraction during lipid synthesis ($\Delta^{13}C_{biosynthsis}$; ~10‰). MOB can be significantly depleted in comparison to the source carbon they utilise (Whiticar 1999); isotopic differences can be as large 30‰ (Jahnke et al., 1999). With little information available on the fractionation of hopanoids during their biosynthesis by MOB, we assumed a conservative value of 10‰ for our study. Four end-member values were calculated, taking into account maximum and minimum extremes for $\delta^{13}C_{dip}$ and $\delta^{13}C_{hetero}$ (Table 1). A threshold of 10% was used arbitrarily to identify the point at which we considered MOB to be contributing to the diploptene signal.

Table 5.1 Mixing model end member values and $\delta^{13}C$ values of the primary variables used to calculate the proportion of MOB at each sample point. $\delta^{13}C_{bulk}$ is the average bulk sediment value from each lake, ± indicates the standard deviation of the $\delta^{13}C_{bulk}$. MOB and heterotrophic bacteria have been assumed to have maximum levels of lipid biosynthesis occurring (10 and 4‰ respectively. $\delta^{13}C_{mob\text{-}hopane\_min}$ is the estimated minimum stable isotope value given the $\delta^{13}C$ value of methane at each lake and the maximum potential fractionation of carbon by MOB. $\delta^{13}C_{mob\text{-}hopane\_max}$ is the estimated value of MOB with no fractionation during assimilation. $\delta^{13}C_{hetero\text{-}hopane\_max}$ is the maximum estimated stable isotope value of heterotrophic bacteria if no fractionation is occurring during assimilation and the bulk sediment is +1Standard deviation from the mean at each lake. $\delta^{13}C_{hetero\text{-}hopane\_min}$ represents the minimum value for heterotrophic hopanes given maximum possible fractionation during assimilation and if bulk sediment is -1S.D from the mean.

	$\delta^{13}C_{bulk}$ (‰)	±	$\delta^{13}C_{mob\text{-}hopane\_min}$ (‰)	$\delta^{13}C_{mob\text{-}hopane\_max}$ (‰)	$\delta^{13}C_{hetero\text{-}hopane\_min}$ (‰)	$\delta^{13}C_{hetero\text{-}hopane\_max}$ (‰)
Ace L.	-30.8	2.1	-104.6	-74.6	-36.9	-32.7
Smith L.	-29.3	0.8	-100.9	-70.9	-34.1	-32.5

5.5 Results

Early-winter ice-bubble surveys combined with bubble-trap measurements of ebullition flux and bubble methane concentration revealed that ebullition seeps occur with high density in the thermokarst zone (2.27 seeps m^2 and 4.2 seeps m^2 for Smith L. and Ace L., respectively) compared to the rest of the lake (0.35 seeps m^2 and 0.67 seeps m^2 for Smith L. and Ace L., respectively). Seep ebullition values in the thermokarst bays were 85 and 151 mg CH_4 m^2 d^1 for Smith L. and Ace L., respectively (Figure 5.1). In the rest of lake (lake centre and non-thermokarst margins) seep ebullition was 6 and 20 mg CH_4 m^{-2} d^{-1} for Smith L. and Ace L., respectively. The $\delta^{13}C$ values for methane in bubbles collected from seeps in the thermokarst zones were -60.9‰ and -64.6‰ for Smith L. and Ace L., respectively. At Smith L., the radiocarbon age of methane in ebullition bubbles collected adjacent to the margin was ~2ka, indicating a dominant Holocene carbon source (likely decomposing near-surface peat). No radiocarbon dates of methane were available at Ace L.

Diploptene was detected in all but one of the samples analysed (Table 5.2; figure 5.3). This sample was not part of further analysis. In the Ace L. thermokarst zone, diploptene values ranged from the lowest value for the whole dataset of -68.2‰ to -50.1‰. The most negative value was found at the greatest water depth (3.2m) and was the only sample that does not lie within 1 standard deviation of the mean. However, another sample at the same depth was far less depleted (-50.1‰), which suggests the low $\delta^{13}C$ value is not explained by water depth. In Smith L., diploptene $\delta^{13}C$ values ranged from -56.8‰ to -38.8‰. Samples from the centre and edge of Smith L. (n=6, n=3 respectively) were compared and a Mann-Whiney U test applied (H0: diploptene $\delta^{13}C$ values are not different). The values for Smith L. indicates that the MOB proportional contributions to the total bacterial communities differed significantly between the two sample zones, values from the thermokarst zone of Smith L. being higher (-42.9 to -38.8‰) than those in the lake centre (-56.8 to -46.9‰).

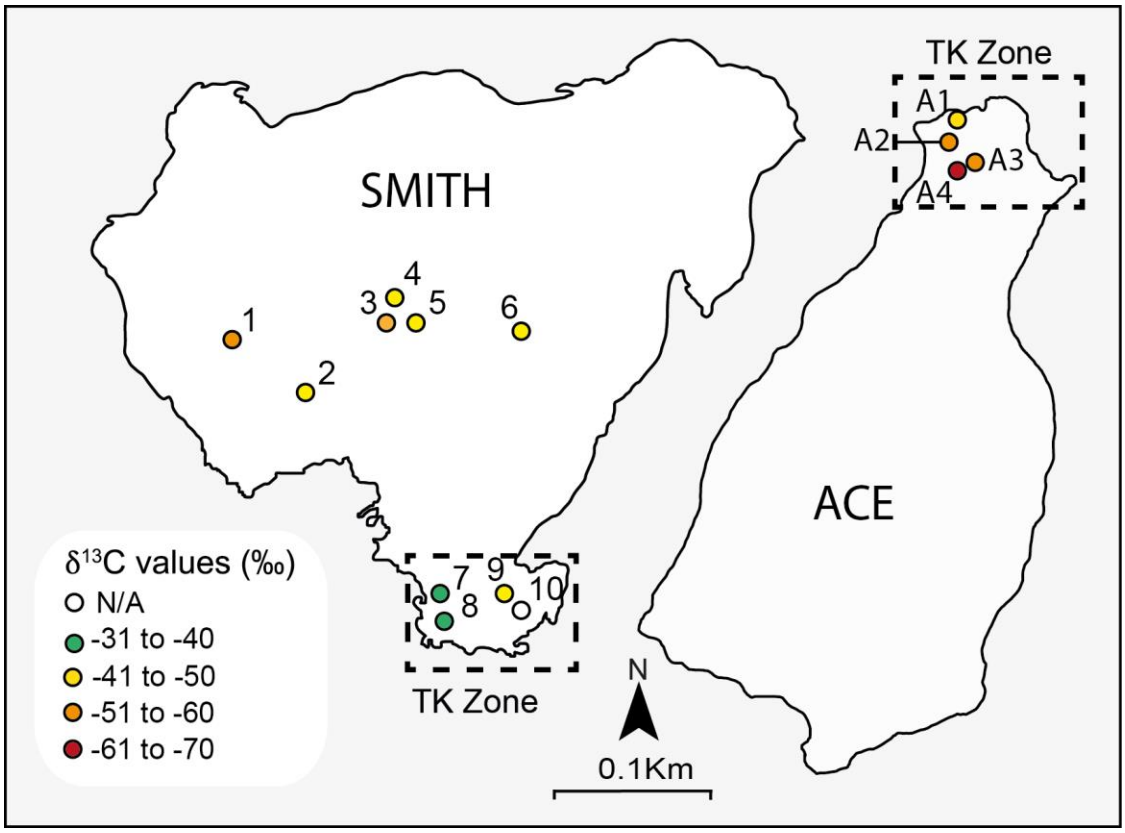

Figure 5.3 Diploptene $\delta^{13}C$ values at Smith L. and Ace L.. In general the most depleted values are found in Ace and in the centre of Smith. The Thermokarst zone at Smith has the least depleted values for the whole dataset.

Diploptene $\delta^{13}C$ values in the thermokarst zone of Ace L. are similar to those of the lake centre at Smith L., and values from Smith L. thermokarst zone are higher than both of these. Thermokarst zone diploptene $\delta^{13}C$ values at Ace L. were more negative than those at Smith L. by at least 10‰, despite methane $\delta^{13}C$ values being less than 5‰ different. However, the samples in the thermokarst zone of Ace L. and the centre of Smith L. (n=4, n=6 respectively) were not significantly different according to a Mann Whitney U test.

The potential contributions of MOB, under different end-member assumptions, to the diploptene signal are shown in Table 3. The minimum and maximum possible contributions range from 19 to 85%, 7 to 27% and 19 to 63% for Ace L. thermokarst zone, Smith L. thermokarst zone and Smith centre, respectively.

Table 5.2 $\delta^{13}C$ values of diploptene at the study sites.

		Sample Number	$\delta^{13}C_{dip}$ (‰)	SD
Ace				
	TK zone	a1	-50.1	1.5
		a2	-58.5	2.0
		a3	-53.1	0.4
		a4	-68.2	0.1
Smith				
	Centre	1	-51.4	2.7
		2	-48.3	0.0
		3	-56.8	N/A
		4	-49.2	1.0
		5	-46.9	1.8
		6	-48.0	0.1
	TK zone	7	-38.8	0.3
		8	-40.9	0.2
		9	-42.9	0.1
		10	N/A	N/A

Table 5.3 Estimated contribution of MOB to the diploptene signal. Calculations assume fractionation due to biosynthesis of 10‰ for MOB and 4‰ for heterotrophic bacteria. f_{mob_min} was calculated assuming the highest fractionation for both MOB and heterotrophs (30 and 4‰ respectively). f_{mob_max} assumes no fractionation during assimilation. $f_{mob\_average}$ was calculated using average $\delta^{13}C$ values for $\delta^{13}C_{mob\text{-}hopane}$ and $\delta^{13}C_{hetero\text{-}hopane.}$

		Sample Number	f_{mob_min}	f_{mob_max}	$f_{mob\_average}$
Ace					
	TK zone	a1	0.19	0.42	0.28
		a2	0.32	0.62	0.43
		a3	0.24	0.49	0.33
		a4	0.46	0.85	0.61
Smith					
	Centre	1	0.26	0.49	0.34
		2	0.21	0.41	0.28
		3	0.34	0.63	0.45
		4	0.23	0.44	0.30
		5	0.19	0.37	0.26
		6	0.21	0.40	0.28
	TK zone	7	0.07	0.17	0.11
		8	0.10	0.22	0.14
		9	0.13	0.27	0.18

5.6 Discussion

5.6.1 Distribution of ebullition seeps

The spatial distribution of ebullition-seeps at Ace L. and Smith L. adheres to the general pattern of seep occurrences as described in other studies, (Walter Anthony and Anthony, 2013), in that the highest density of methane ebullition seeps were found in the thermokarst zone.

5.6.2 The presence and spatial variability of MOB

The $\delta^{13}C$ values of diploptene ranged from -68.2 ‰ to -38.8 (Figure 5.3), values similar to those that have been previously invoked as evidence for methanotrophy in lacustrine sediments (-64‰ to -55‰; Spooner et al., 1994; Naeher et al., 2014), marine sediments (-62‰ to -35‰; Freeman et al., 1994; Thiel et al., 2003) and in wetlands (-40‰ to -30‰ to; van Winden et al., 2010; Zheng 2014). Therefore, we conclude that diploptene $\delta^{13}C$ values are reflecting the presence of MOB bacteria in lake sediments. The lowest values in Ace L. are among the lowest reported for lacustrine (or other terrestrial), suggesting a relatively high degree of methanotrophy in those sites. In the thermokarst zone at Ace L., the diploptene values were highly variable but all suggested MO was occurring, and the fraction of diploptene derived from MOB was >10% even under the most conservative assumptions (Table 3).

The results of the mixing model suggest that MOB can contribute anywhere between 7-83% of the diploptene production across all sampled areas (Table 3). We note that there are some important caveats to using this mixing model. Crucially, diploptene is not derived from all bacteria nor even all methanotrophic bacteria (Rohmer et al., 1987). Nor does it likely occur in constant biomass-to-lipid ratios in those organisms from which it can derive, such that extrapolations from a diploptene mass balance to inferring bacterial biomass distributions should be done cautiously. They are best considered semi-quantitative. Nonetheless, a MOB contribution to total biomass of ~10 to 80% is similar to that derived from other studies (11-80%; Bastviken et al. 2003; Sundh et al. 2005; Kankaala et al. 2006). Regardless of absolute MOB estimates, our data show that the centre of Smith L. and the thermokarst zone at Ace L. have the highest proportion of MOB in the total bacterial biomass.

The data presented here allow us to develop, alongside other studies, models of methane production and emission pathways in thermokarst lakes. At Ace L., MOB biomass was high relative to other samples collected in this study and in the context of previous studies. Ace L.is a 'yedoma-type' lake and has a high methane ebullition flux (151 mg m^2 d^1), likely derived from older (e.g. Pleistocene), deeper sediments in the talik bulb (Walter et al., 2008; Sepulveda-Jauregui 2015). Given the coincidence of high bubble counts and high estimated MOB biomass, it could be assumed that the supply of dissolved methane and therefore MO is high in the thermokarst zone.

Ace L. appears to be representative of the enhancement model, whereby methane ebullition flux from bubble tubes increase the amount of methane diffusion from the sediments. In Ace L., and by extension other yedoma-type thermokarst lakes, where methane is produced in deep sediments the increased contact time with sediment (both over distance and time taken for bubbles to reach the sediment-water interface) may allow for increased methane diffusion in adjacent sediments. Alternatively, thermokarst erosion of yedoma-type permafrost is also known to supply nitrogen and phosphorus to lakes (Walter Anthony et al. 2014), enhancing primary production, which in turn can fuel methanogenesis and MO from contemporary (atmospheric) carbon (Martinez-Cruz et al., 2015). We cannot definitively distinguish between these alternatives since the carbon utilised by MOB observed in Ace L. could be derived from deep, ^{14}C-depleted methane and/or from shallow-sediment, contemporary methane.

Within the thermokarst zone at Smith L. the δ^{13}C values of diploptene were less variable (range: 10‰) than the Ace L. thermokarst zone (18‰) and the δ^{13}C values were overall more enriched (-42.9 to -38.8‰). In fact, the thermokarst zone in Smith L. had the lowest proportion of MOB for the entire dataset, with a MOB contribution to diploptene being equivocal for most of these samples. Conversely, samples from the centre of Smith had diploptene δ^{13}C values that were similar to those of the Ace thermokarst zone. The differences between the centre and the thermokarst zone could arise from alterations in the microbial community that manifest as different MOB expressions of hopanoids, for example, Smith L. thermokarst zone MOB might not be biosynthesising diploptene or its precursor. Alternatively, there may be differences in the balance of MO for energy versus biomass

production. Another explanation for the difference in $\delta^{13}C$ values, which could be validated through further investigation, could be due to differences in the methane production pathways as highlighted by Walter et al. (2008). The higher $\delta^{13}C$ values of diploptene could be due to more enriched methane formed through acetate fermentation. The most direct interpretation given the currently dataset, however, is that MOB are more abundant in the centre of the lake than at the thermokarst margin and, by extension, more MO is taking place in the lake centre. Given the pattern of high MO in the centre of Smith L. and less MO at the edge but more flux to atmosphere via ebullition, it seems that Smith methane dynamics are more akin to those of 'clastic' lakes or other, non-thermokarst boreal lakes (e.g. Bastviken et al,. 2004). The patterns at Smith L. also suggest that methane dynamics in the thermokarst zone follow the by-pass model in which methane ebullition is an independent process that interacts weakly with the lacustrine system.

Overall, the Smith thermokarst zone had lower methane ebullition rates (85 mg CH_4 m^{-2} d^{-1}) and less negative $\delta^{13}C$ of methane as measured from ebullition flux (-60.9‰) than Ace L. It is possible that this methane is not produced in the talik, but in near-surface sediments likely derived from peat slumping at the margin. This is supported by the late Holocene radiocarbon date of ebullition seep methane. The large size of the sediment blocks and the early stage of decomposition of the organic material that slump into the lake may mean there is less exposed substrate surface area and less methane production, as compared to yedoma-lake production from the fine-grained and more labile sediments. Production in shallower sediments (and often shallow water depths) means reduced partial pressure and faster release of bubbles from the sediment. Here, if bubble tubes initiate in shallower sediments (that are shallower than the talik bulb but deeper than the anoxic surface sediments) and the overall number, size and intensity of bubble tubes is reduced, then the connection between ebullition and diffusion could be decoupled. Whether there is a reliable connection between ebullition flux and high diffusion in the thermokarst zone is still to be determined, but the results of this novel but preliminary study highlight the need to continue research in this area.

5.6.3 Assessing past and current carbon cycling in thermokarst lakes

A crucial outcome of this study is the large variability seen in the $\delta^{13}C$ values of diploptene across small spatial distances. This is an important finding, as often whole lakes can be represented by a single sampling site in palaeoenvironmental studies. Such large fluctuations in $\delta^{13}C$ values in surface sediments, which were taken as replicates (e.g. repeat samples from the same zone within a lake), highlight the need for caution when interpreting shifts in $\delta^{13}C$ values through time (i.e., down a single sediment core).

While the differences in diploptene $\delta^{13}C$ values between chosen study zones discussed above are statistically significant, the sample number is small, and this topic could benefit from further sampling. There is a large degree of heterogeneity in the values in all three study areas. Interestingly, previous studies of MOB in lake sediments also show large variability in bacterial communities across small spatial extents (Kankaala et al., 2006). This could have implications for interpretation of not only biomarkers but also other geochemical records. For example, it is unclear how high spatial and temporal variability in MOB biomass affects the isotopic composition of consumers higher in the food web. The biological and geochemical connections between MOB and higher trophic organisms need to be better understood in order to interpret past methane emissions.

5.7 Conclusions

A primary aim of our research was to contribute towards the understanding of the links between methane production, transport and recycling in thermokarst lakes. Diploptene $\delta^{13}C$ values were used as a proxy for MO that could be linked to variations in methane supply via diffusion in thermokarst lakes. Diploptene was present in almost all samples and its $\delta^{13}C$ values were highly variable. A two-part mixing model highlighted potential variation in total MOB biomass with almost no MOB contributing to bacterial biomass in some samples but forming over half the total bacterial population in others. Like methane production, MO is highly complex, both in terms of its spatial distribution and in relation to the type of substrate available. A single model for thermokarst lakes is unlikely to capture all patterns present at both the inter-lake and intra-lake level. Thus, it is crucial that interpretation of diploptene $\delta^{13}C$ values (and other MO proxies) in palaeoenvironmental investigations take into lake type (e.g., yedoma or non-yedoma) and possible spatial heterogeneity in methane production pathways. Moreover, future work should examine localized spatial variability of MO within lakes and how spatial variation is integrated temporally, as this may critically affect observed down-core patterns of biomarkers and their isotopic signals. We conclude that diploptene biomarkers have considerable potential to help reconstruct patterns of methane cycling in lakes and, with certain caveats, particularly attention to context, past methane dynamics.

Chapter 6: Spatial distributions of chironomid assemblages: the role of methane in chironomid community structure

6.1 Outline

This chapter presents results and interpretation of site-specific chironomid assemblage patterns in relation to areas of high methane production. Firstly a review of methane emission and cycling in thermokarst lakes and how they are predicted to impact chironomid community structure is provided, along with the sampling strategy and relevant methods. Following this, the results are presented for each lake separately to describe the site-specific patterns, then as a comparative dataset to assess inter-lake similarities and differences. Finally, three key factors are discussed: the influence of methane on chironomid community structure; the relationship between chironomid communities and other environmental variables in lake systems; and the implications for further research.

6.2 Introduction

It is widely predicted that the impacts of climate change will be most strongly experienced in high-latitude regions, especially in hydrological freshwater systems (Prowse et al., 2006). Increased thawing of the ground ice is likely to accelerate the formation of new lakes, including thermokarst, and increase the rate of expansion of existing water bodies via slumping of thawed bank material into the littoral zones of thermokarst lakes. Underlying and surrounding these newly formed lake conditions, are sources of organic-rich sediments which, as has already been demonstrated in previous studies (Walter et al., 2006; Walter et al., 2007b; Walter Anthony and Anthony, 2013; Sobek, 2014) are subject to microbial decomposition and large-scale production of methane, which is produced and released to the atmosphere via ebullition at the water-air interface. A proxy for environmental conditions within the surface sediments which might occur due to methane emissions via

ebulltion would enable a greater understanding of the importance of these lakes within the global carbon cycle.

As highlighted in section 2.2 the main source of methane emissions in thermokarst lakes is from ebullition-seeps which are defined as areas where methane bubbles (bubbles which have high concentrations of methane gas within them) form conduits in the sediments thus allowing a preferential flow channel from source of production to release at the sediment surface (Varadharajan, 2009). These ebullition-seeps are a spatially explicit source of methane (Walter et al., 2007b, 2008) which are persistent on short temporal scales (Walter et al. 2010) and mostly exclusive to thermokarst lakes. Often many ebullition-seeps are grouped within the active thermokarst area where newly thawed carbon is available for methanogenesis (Figure 2.2). This area is termed the thermokarst zone and it is hypothesised that methane ebullition is likely to have an impact on the biogeochemistry of this area. In turn, this may be reflected in the biological communities within the lakes, for example macroinvertebrates such as chironomids. Chironomid larvae develop *in-situ* and therefore fossil assemblages will closely represent the extant faunal community (Brooks et al., 1997b; van Hardenbroek et al., 2011). Particularly where sediment focusing is not strong, such as in shallow lakes or in littoral areas, changes in the environmental conditions due to methane emissions via ebullition-seeps may be highlighted through changing chironomid community composition.

This study assesses whether methane emission via ebullition-seeps has a discernible effect on the ecosystem, either directly through physical changes to the sediments or biologically; by altering the base level components of the aquatic food web. These hypothesised impacts are discussed in more detail below.

6.2.1 Physical

The constant, rapid and large-scale emission of methane as bubbles is predicted to have an impact or interaction with the unconsolidated surface sediments and water column through which they are passing.

Bubble sizes from 1-100 cm have been measured in the lake ice above thermokarst lakes to calculate total methane flux (Walter Anthony and

Anthony 2013); however the larger bubbles in this study are an accumulation of multiple bubbles so it is unlikely that the largest of the measurements will represent actual diameters as they leave the sediment. Walter Anthony and Anthony (2013) suggest an average single bubble size of 1-40 cm but again they suggest that those over 25 cm could be merged. Even if each bubble were less than 5 cm in diameter when released from the sediment, it is hypothesised that the constant release of even small bubbles would result in disturbance to sediments on a scale that might impact aquatic organisms close to ebullition-seeps such as chironomids, whose average sizes range from a few mm to a few cm. This may manifest as a shift in habitat partitioning with a change in the chironomid community towards taxa which thrive in disturbed habitats. The disturbance may create an environment conducive for larval development, such as aerated sediments with increased oxygen availability. Alternatively it may result in a complete reduction in overall chironomid numbers with few taxa inhabiting these areas. For example, tube dwelling chironomids such as *Chironomus* spp. may be unable to build tubes in these bubble-rich environments.

6.2.2 Biological

A key hypothesis to be tested is that high methane ebullition flux such as that which occurs in the thermokarst zone leads to increased diffusion of methane from the sediments. This diffusive methane is either recycled in the lake or released to the atmosphere. A large portion of the methane that is produced in systems with high partial pressure is released as bubbles, Walter et al., (2007b) estimate 95% of thermokarst-specific methane is released via bubbles, but no studies have explicitly tested this. Even if diffusive methane was only 5% of the total methane production, in these thermokarst zones this is likely to still be a significant amount.

Previous studies from the shallow coastal environment have highlighted a positive correlation between ebullition seeps and diffusive methane (Martens and Klump, 1980). It is hypothesised that in a setting such as a shallow thermokarst lake, where the oxycline is often at the sediment-water interface, any diffusive methane might be quickly oxidised by methane oxidising bacteria (MOB). It is estimated that between 11-80% of methane that diffuses from the sediments is oxidised by MOB (Bastviken et al., 2003; Sundh et al.,

2005, Kankaala et al., 2006) It is hypothesised that this would lead to an increase in the methanotrophic bacterial biomass adjacent to ebullition-seeps.

Recent studies have shown a change in the stable carbon isotope composition of some lacustrine biota such as chironomids which has been attributed to use of MOB as a carbon source (Jones and Grey, 2011). Jones et al, (2008) suggest chironomid larvae to have depleted $\delta^{13}C$ values as a result of increased consumption of MOB. Other studies have also highlighted taxon-specific depletions in $\delta^{13}C$ values in chironomid taxa which were adapted to specific conditions in deep lakes (Grey, 2001, van Hardenbroek et al., 2013).

If thermokarst zones were to cause an increase in the MOB biomass on a large enough extent that it is evident in the $\delta^{13}C$ values and if chironomid taxa are feeding on MOB biomass generated by ebullition-seeps, it might also cause changes in assemblages across a lake associated with feeding preferences.

6.3 Design

Studies having acknowledged the assimilation of MOB by some chironomid taxa (Jones and Grey 2011), and attempts have been made to use changes in $\delta^{13}C$ values of chironomids to reconstruct past methane emissions (Wooller et al., 2012). van Hardenbroek et al. (2013) have highlighted a correlation between low $\delta^{13}C$ values of specific chironomid taxa and increased methane availability. As yet, little work has been completed to establish if methane production, specifically on a scale large enough for constant ebullition-seeps to develop, is acting as an environmental variable which is driving community changes (as opposed to stable isotope composition of taxa) within a lake. It is hypothesised that methane production and release may be acting as an environmental variable which could be driving changes in biota and chironomid communities within a lake. The objective of this chapter was to establish the influence, if any, of methane in controlling chironomid communities in two thermokarst lakes from Interior Alaska. Chironomid assemblages and environmental parameters (including the location of samples with regard to the thermokarst zone) were measured at various locations within the lakes in relation to areas of high methane production. Statistical techniques were used to assess the most important environmental and limnological factors controlling chironomid distributions both within and between the lakes. Should a link between chironomids and thermokarst zones be present, it is likely to be visible in both the chironomid abundance diagrams and the results of the ordination testing.

6.3.1 Sampling Strategy

A detailed description of the study sites can be found in Chapter 3. Figure 6.1 shows the sample points relevant specifically to this chapter. Samples were taken from across both lake surfaces in order to gain the greatest spatial coverage and resolution.

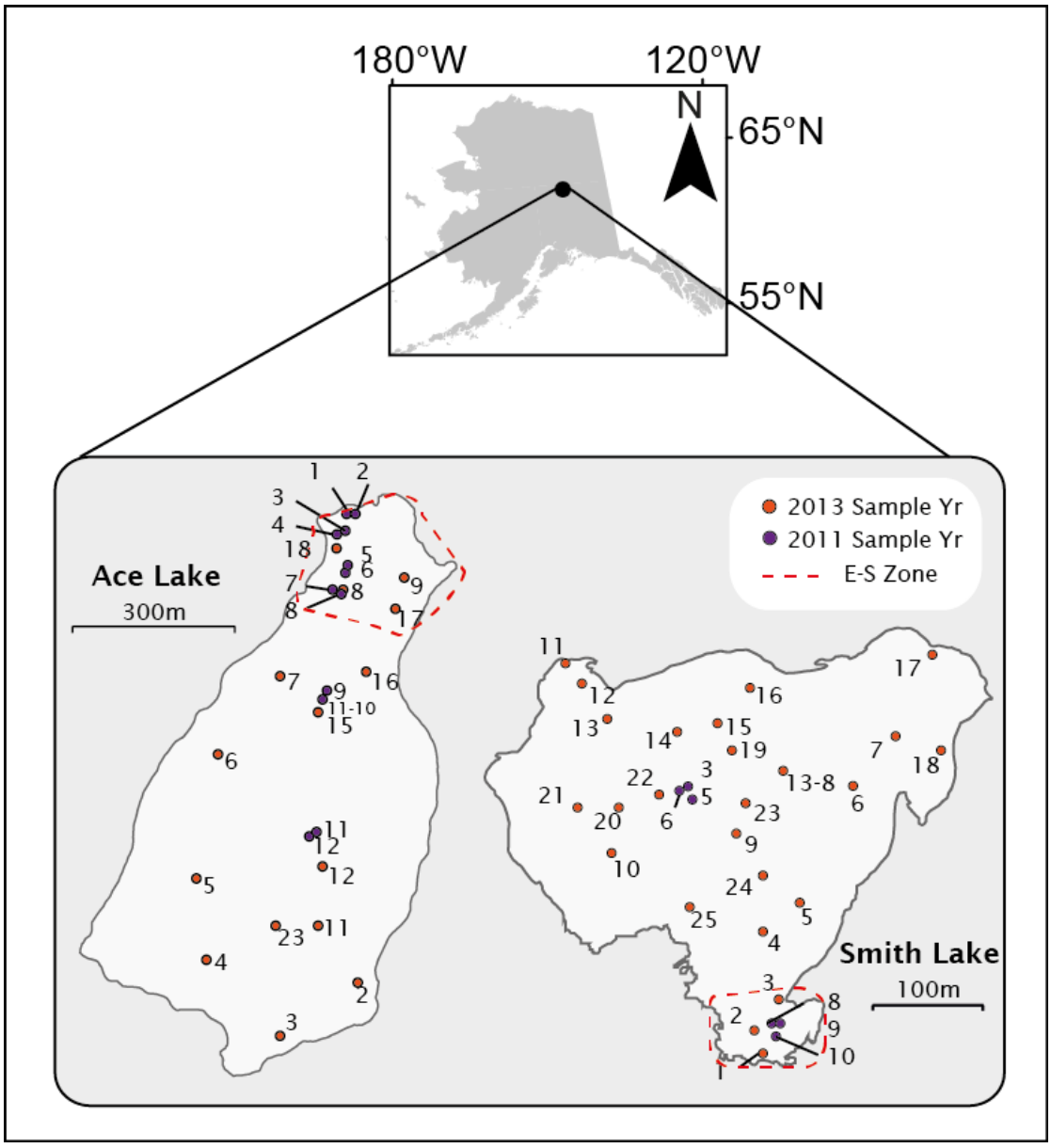

Figure 6.1 Study sites and sample locations. The different sample points represent different sampling years. The thermokarst zone is highlighted by dashed red lines.

6.3.1.1 Sample preparation and statistical testing

6.3.1.1.1 Chironomid assemblage preparation

All chironomid samples were prepared at the Palaeoenvironmental Laboratory, University of Southampton (PLUS). Where possible samples were weighed and dried prior to chironomid preparation. When this was not possible, dry sample weights have been calculated using an average water loss value of 82% which is derived from the values of the dry surface samples used in this study.

Methods for chironomid preparation followed those given in Brooks et al. (2007). Sediments were sieved through nested sieves of 180 and 90µm respectively, to remove the finer sediment fraction. This was done using distilled water when specimens were required for stable isotope analysis.

If HCs were not required for further analysis (stable isotope analysis) the standard method for chironomid preparation was used which included a deflocculation step. In this instance, sediments were placed into beakers and 10% potassium hydroxide (KOH) was added. The samples were heated to 70-75˚C and stirred for 3 minutes before being passed through the sieves.

6.3.1.1.2 Head capsule processing: picking, mounting & identification

Head capsules (HCs) were picked from both size fractions using a Bogorov sorting tray (Gannon, 1971) and fine forceps under stereomicroscope. HCs were placed under cover slips in distilled water for identification where further analysis was required. In this instance, the standard mounting agent Hydromatrix© was not used to avoid contamination as HCs were then placed into taxon-specific labelled vials for stable isotope analysis. When not required for more analyses, HCs were mounted in Hydromatrix© under 6mm coverslips and identified to the highest resolution possible using a Nikon e2100 microscope at x400 magnification using Brooks (2007) and Wiederholm (1983) as references. However, a slightly lower taxonomic resolution was achieved with those which were permanently mounted in hydromatrix© resulting in higher than normal undifferentiated specimens.

6.3.1.1.3 Confidence criteria

First, all samples in Ace L. were analysed as a single dataset, regardless of HC numbers or spp. abundance. It was clear that there were two distinct populations which were defined by the sampling years (Figure 6.2). It was clear that not all samples were suitable for statistical testing.

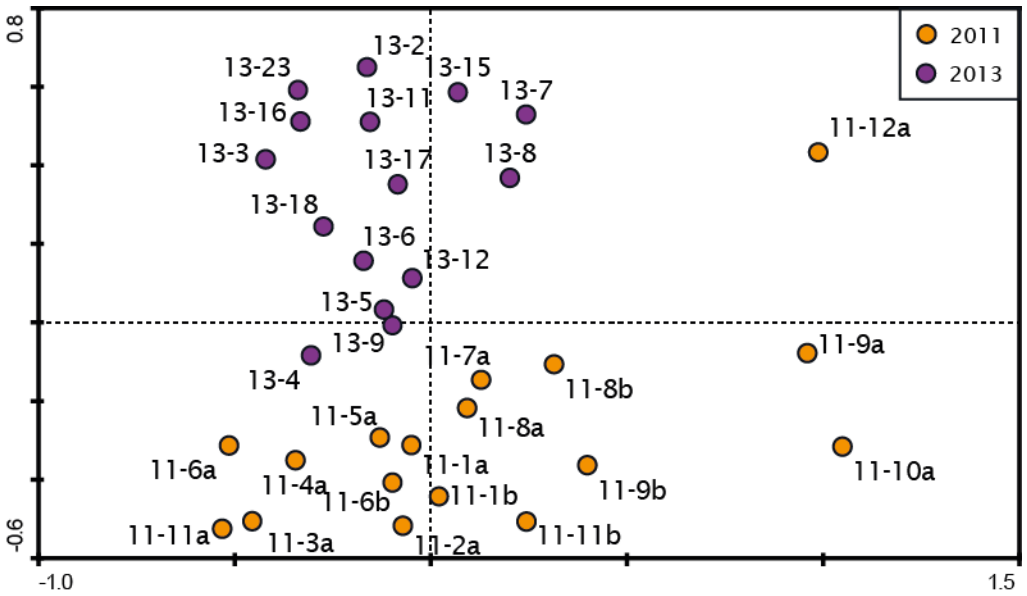

Figure 6.2 PCA using all samples from Ace L., a clear division based on sample year can be seen.

Therefore, a number of criteria were outlined, whereby all had to be met for a sample to be used, in order to increase the reliability of the final dataset:

- Samples with less than 30 HCs were excluded as they were deemed to have insufficient numbers to provide useful results.
- Within each sample, taxa with less than 2% overall abundance and single occurrences were removed to reduce the influence of rare taxa.
- Samples with more than 25% of the total counts undifferentiated were removed as such high numbers were deemed to be an artefact of the lower resolution when water was used, rather than a real ecological influence.

After applying the confidence criteria, 18 samples were taken forward from Ace L. and 30 from Smith L. Figure 6.3 shows the samples from Ace selected using the confidence criteria. Although the problems caused by different sampling years or methods cannot be ruled out completely, using a number of criteria greatly increased reliability of the dataset.

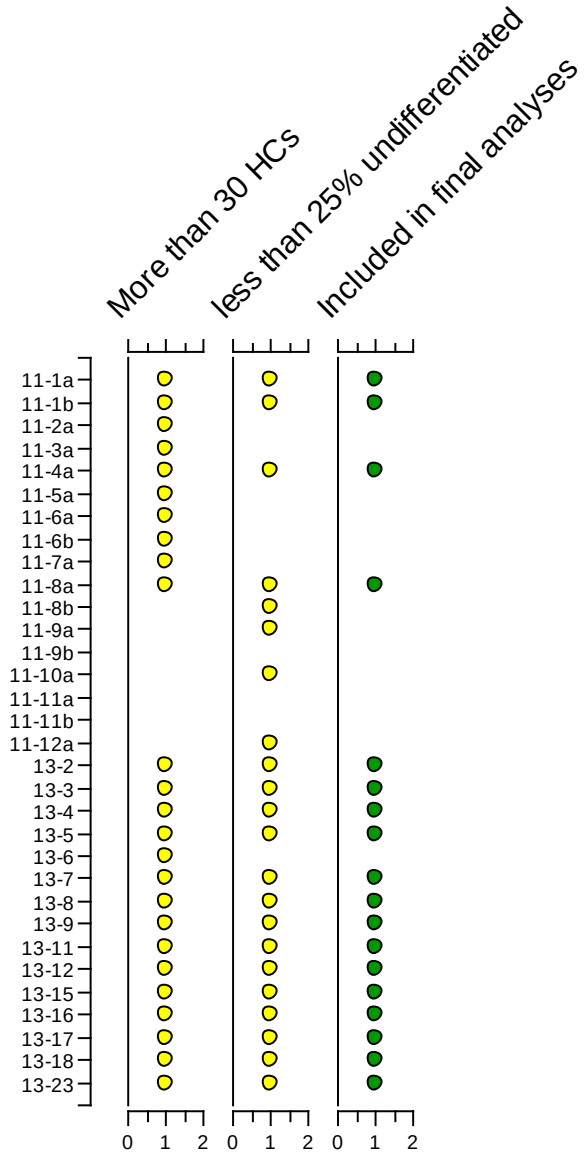

Figure 6.3 Selection criteria for Ace L. samples. Circles indicate yes. Samples required two yes answers to be present in the final dataset.

6.3.1.2 Total organic carbon (TOC)

Loss on ignition (LOI) was used to determine the organic carbon content (TOC) of the sediments using standard methods as presented by Heiri et al. (2001). Surface samples from both sampling years (2011 and 2013) were weighed and placed in the oven at 105˚C to dry overnight. Once dried the samples were placed in pre-weighed crucibles, weighed and fired at 550˚C for two hours, cooled and re-weighed.

6.3.1.3 Environmental variables

A number of variables were deemed important for this study: water depth, water temperature, dissolved oxygen (%DO), conductivity and whether the samples were in the thermokarst zone or not. Due to limited resources, not all variables were measured at both study sites. Environmental variables were collected for Ace L. in the July 2011 using a YSI probe by a team at the University of Alaska, Fairbanks (Gaglioti *pers comm*). Environmental data from Smith L. was collected during July 2013. At Ace L., measurements were taken every metre from 1 – 8m depth. The water depth from which a given sample was extracted was estimated using linear interpolation (at 0.1m intervals) between measurement points.

Thermokarst zones were defined by previous research and observational data collected during each sampling trip. Bubbles were observed and counted across the lake. The limit of thermokarst zone was defined as a line beyond which little to no bubbles could be counted using a set time interval. The limits are highlighted in figure 6.1

6.3.1.4 Statistical testing

All identifiable chironomid HCs were included in the total count diagrams and values expressed as relative abundances. The results are presented in a zonal diagram using C2 v1.5.1 (Juggins, 2007). Prior to ordination testing, some taxa were merged and those with less than 2% abundance or occurring in less than 2 samples were removed to remove the influence of rare taxa.

Environmental data were available at both lakes but the total number of measurable variables was limited. The methane data was added as a nominal variable with binary codes where samples were coded ‘0’ for not in the

thermokarst zone and '1' if they were inside this zone. Macrophyte presence at Ace L. was recorded in the same manner and coded as '1' where macrophytes were present and '0' when they were absent.

Ordinations were performed on the merged data using CANOCO v 4.5 (Ter Braak and Smilauer, 2002). The purpose of the ordination was to allow further exploratory analysis and, where possible, attempt to explain the variation in the data.

Detrended correspondence analysis (DCA) was performed using detrending by segments and square-root transformation of the data to calculate the gradient lengths of the ordination axes to establish if unimodal or linear techniques were most appropriate (Birks, 1998). The importance of down-weighting rare spp. was also tested. The down-weighting of rare species increased the gradient axes a little (a max of 0.3) but the gradient length remained less than 2 Standard deviations, suggesting a linear methods were most appropriate Principal components analysis (PCA) and Redundancy Analysis (RDA) were used to examine the variation in chironomid assemblages.

RDA was used to explain variation in the chironomid assemblages in relation to the measured environmental variables and to highlight any co-variance in the environmental variables. First, the test was run without testing statistical significance to examine the inflation factor of each variable. At Ace L. 4 of the 6 variables were considered to be strongly co-varying as indicated by the inflation factor (>20). Using the Ace L. dataset, the test was carried out a second time using automatic forward selection to remove the variables exhibiting co-variance. In Smith L. the variables all had low inflation factors (≤5) but TOC was not statistically significant (P = 0.148). Methane presence and water depth (m) were statistically significant (p = < 0.05). The results of the RDA for both lakes were used to explore the relationships further despite the lack of statistical significance or the co-variance of the environmental variables, the results of the RDA were used to explore the relationships but with the results are interpreted with some caution.

PCA with square-root transformation of the data was used on samples and species data only, first from both lakes separately, then in a combined dataset to determine relationships within the species data which might be linked to environmental variables through biological and ecological factors associated

with specific taxa. Finally PCA was performed with the environmental variables as an indirect gradient analysis (where the variables do not constrain the data) in an attempt to confirm any interpretations based solely on ecological information.

6.4 Results: Chironomid assemblages

6.4.1 Spatial distributions

6.4.1.1 Ace Lake

A total of 100 different groups were identified (Appendix B) and 40 had a relative abundance of more than 5% in at least one sample across the lake. Initially the results are split into zones to highlight any patterns associated with methane production (Figure 6.4).

In the thermokarst zone, six taxa were highly abundant; *Chironomus anthracinus*-type, *Chironomus plumosus*-type, 1st instar Chironomini, *Endochironomus albipennis*-type, *Chricotopus (isocladius) spp.* and *Psectrocladius sordidellus*-type. Both *Chironomus plumosus*-type and 1st instar Chironomini showed increasing abundance with distance from the north shore whereas *Chricotopus (isocladius) spp.* was highest nearer to this shore. *Polypedilum nubifer*-type had some of its highest occurrences in the thermokarst zone and overall the thermokarst zone was dominated by taxa of the tribe Chironomini and one or two taxa from the subfamilies Orthocladiinae and the Tanypodinae all of which were persistent throughout all samples. The Tanypodinae were consistently present in the thermokarst zone, although their relative abundance remained low (<10%). Of the taxa relative abundance was less than 5%, many were only present in single samples, and of these samples, a large number were found in the thermokarst zone, for example, *Lauterborniella*, *Xenochironomus* and *Stenochironomus* all of which appeared only once in separate samples in this zone.

In the central area of the south-central zone, similar taxa as in the thermokarst zone were abundant such as *Cricotopus (isocladius*) spp. and 1st instar Chironomini. *C.anthracinus*-type was almost completely missing whilst *C.plumosus*-type was at its highest relative abundance of any sample in the lake. *Cricotopus bicinctus*-type increased in relative abundance in the centre and in sample 11-10a it was almost 30% of the total population. Apart from the taxa described above, occurrences of other taxa in the centre of the lake were low with most only being present in one or two samples. Many of the taxa which were rare (a relative abundance of less than 5%) were absent in the

centre. A few taxa such as *Paracladius* and *Orthocladius oliveri*-type were present here and nowhere else in the lake. Overall this central region was characterised by high heterogeneity in presence and abundance of alomost all taxa that were found in this zone. In the southern region of this zone there were high abundances of *C.anthracinus*-type. 1st instar Chironomini declined in numbers in a southward direction towards the southern shore which mirrored its pattern in the thermokarst zone of increasing abundance away from the margin. *P.sordidellus*-type was missing from some samples, specifically: 11-11a, 11-11b, 11-12 and 13-12. In this zone *P.nubifer*-type was replaced by *Polypedilum nubeculosum*-type and *Parachironomus varus*-type was also abundant. *Orthocladius* type peaked in sample 11-11b and increased in relative abundance from low in a few samples, to a significant proportion of the total population. Frequent occurrences but low relative abundance of many of the taxa meant formulating a specific set of rare taxa for this zone was difficult.

6.4.1.2 Water depth

Figure 6.5 shows the same assemblages but arranged along a water depth profile. From the dominant taxa it is difficult to highlight a clear pattern; however, taxa such as *Tanytarsus mendax*-type and *P.nubeculosum*-type appear to be associated with deeper water, whilst *Paratanytarsus penicillatus*-type and *Tanytarsus glabrescens*-type were more abundant in the shallower samples. A somewhat clearer relationship with water depth was seen in the rare taxa (figure 6.6). *Paracladius* and *O.oliveri*-type are exclusive to samples in deeper water, whilst the genus *Phaenospectra* and those taxa included therein, *Pseudosmittia, Corynoneura edwardsi*-type and *Stenochironomus* were confined to the most shallow water depths.

Clear heterogeneity was found across samples, especially those which were sampled close together. Overall there is a core group of taxa which persist in relatively high abundance throughout the samples plus a large number of highly variable taxa in terms of proportion of the sample and presence/absence.

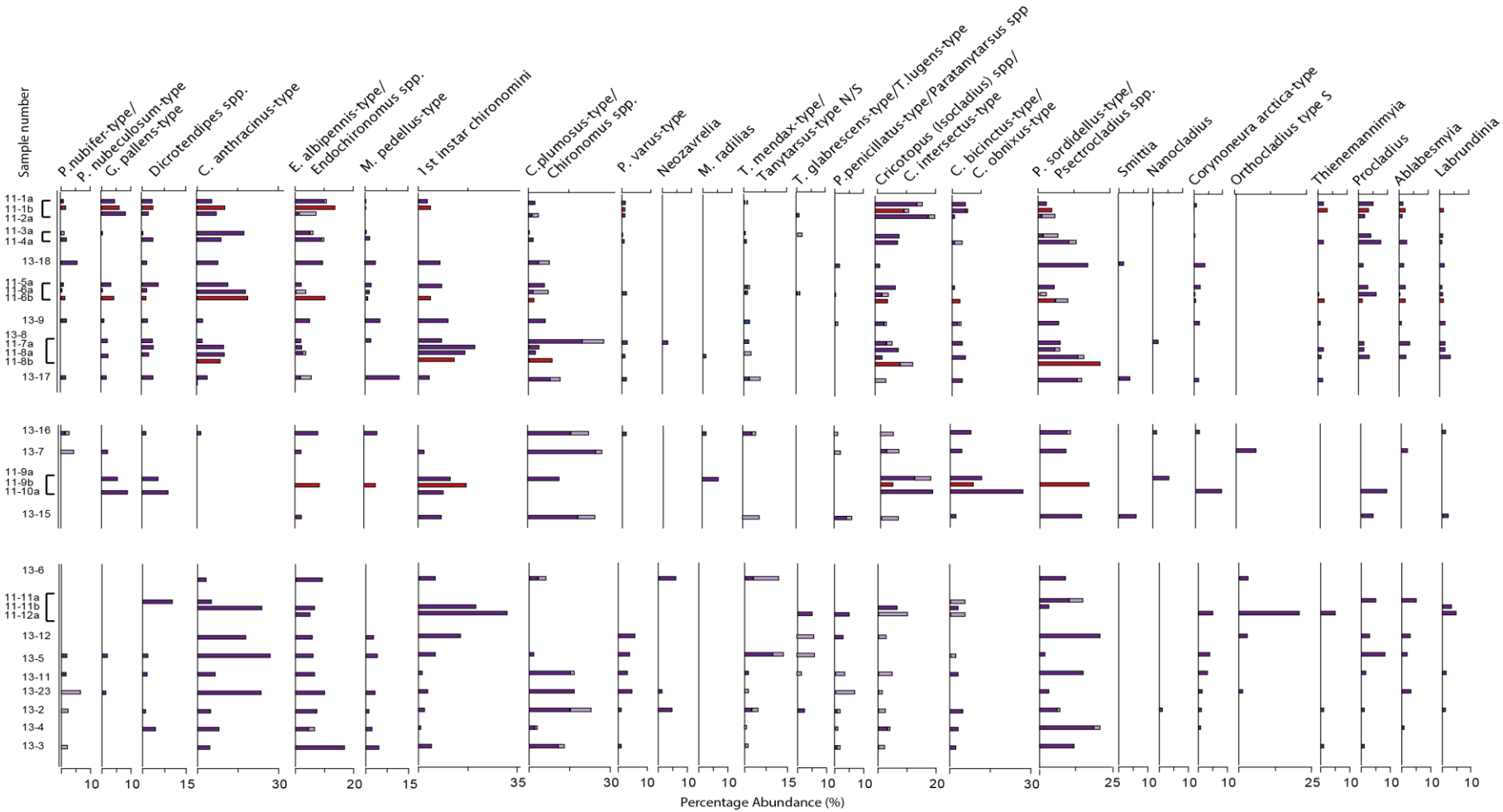

Figure 6.4 Ace L. chironomid assemblage diagram (0-1 cm depth). Light purple represents the 2nd second listed in the label (after the /). Red lines highlight samples which were at 1 cm depth. Only the taxa which were > 5% abundant are displayed.

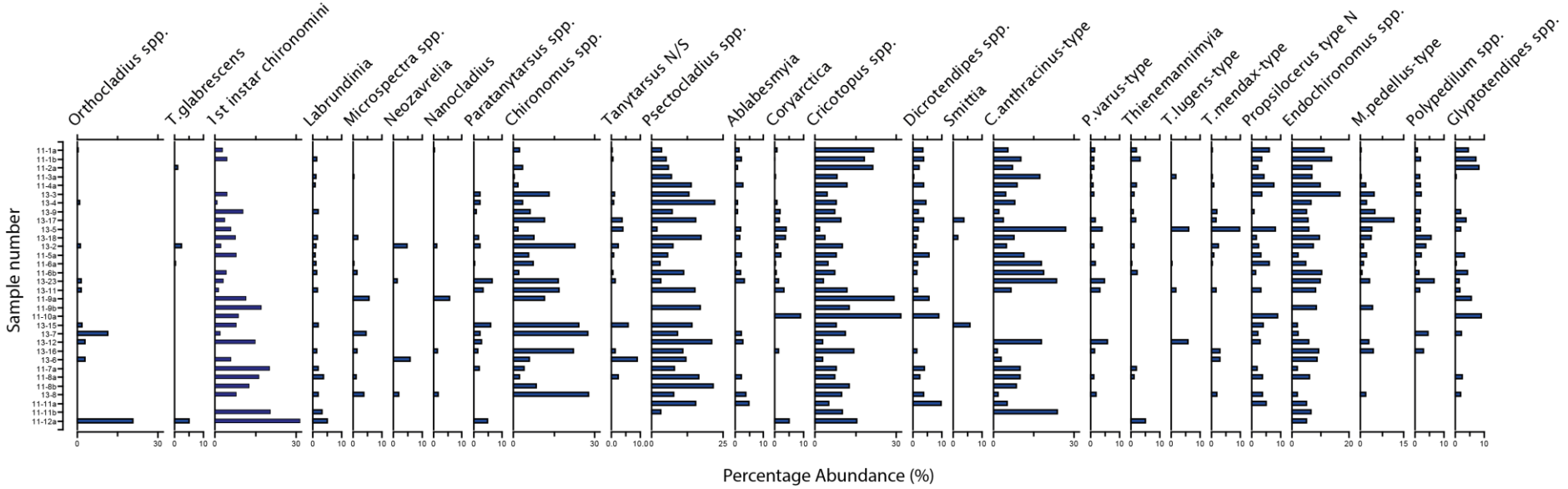

Figure 6.5 Chironomid assemblages, Ace L.. Only taxa which were > 5% abundant are displayed. Samples are arranged along a water depth profile from the deepest in the bottom left to the shallowest in the top right

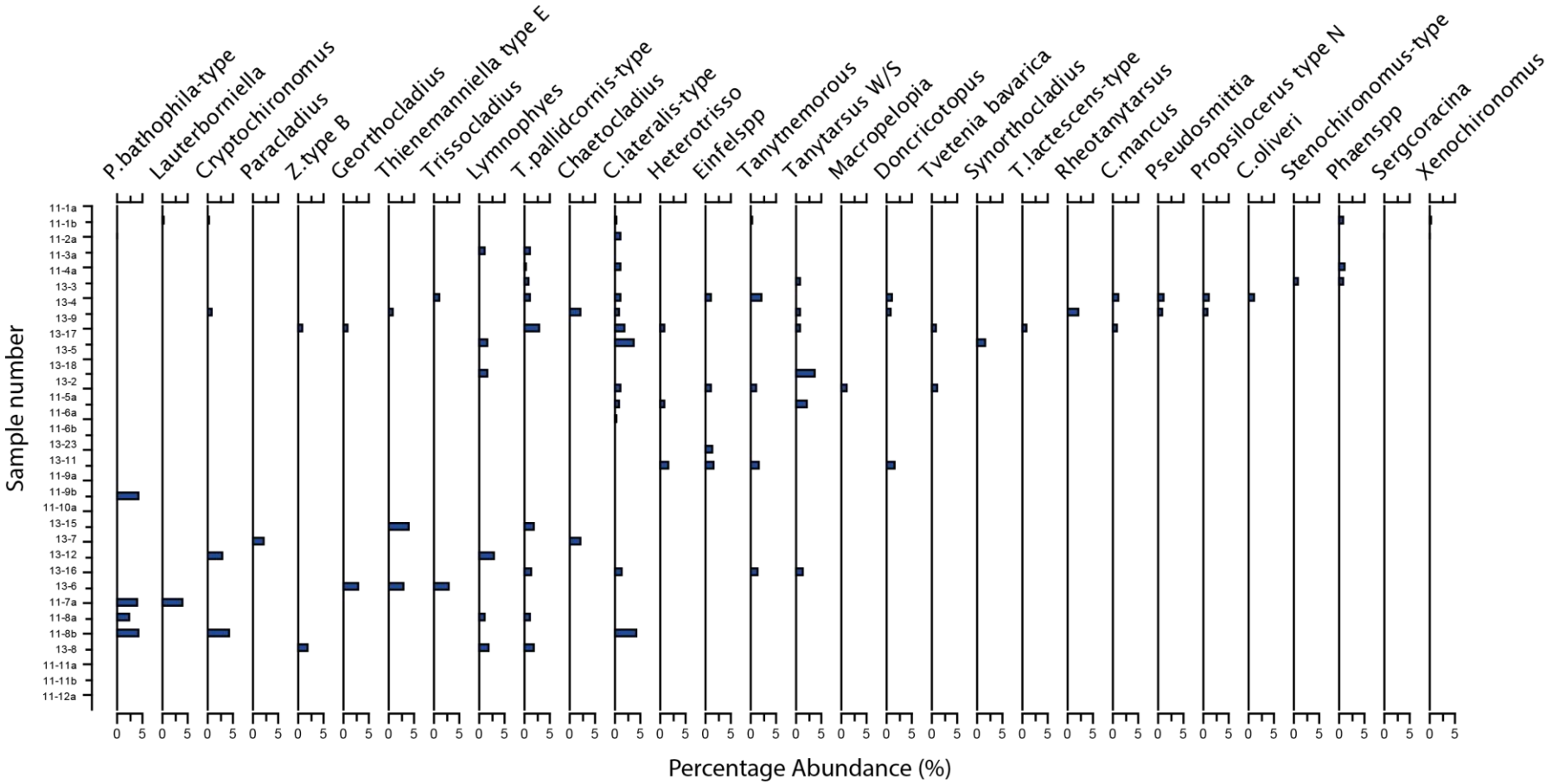

Figure 6.6 Chironomid assemblage diagram for Ace L.. Only taxa which were < 5% abundant are displayed. Samples are arranged along a water depth profile from the deepest in the bottom left to the shallowest in the top right.

6.4.1.3 Smith Lake

In Smith L., 87 taxa were identified in total with 31 taxonomic-specific groups with more than 5% abundance in at least one sampling location (Figure 6.7)

Of the taxa with low relative abundances (< 5%), many were exclusive to this zone, with taxa such as *P. bathophila*-type, *P. nubeculosum*-type and *Glyptotendipes severini*-type were found only in the thermokarst zone. *Procladius* had a higher abundance in the thermokarst zone than in the rest of the lake but this was only in a single sample; 11-8. Taxa in the genus *Chironomus,* specifically *C. anthracinus*-type and *C. plumosus*-type were two of the most abundant taxa with homogenous distributions across the lake. *M. pedellus*-type showed a similar distribution pattern to *Chironomus* but had a lower overall abundance.

The north-central zone at Smith L. was similar to the thermokarst zone, however the presence and relatively high abundance (>10%) of *T. lugens*-type was a key difference. In the Tanytarsini tribe most taxa had a relatively even distribution across the lake; however the overall numbers of taxa in this tribe which were more than 5% abundant were low. *T. lugens*-type and *M. insignilobus*-type only appeared in the centre of the lake and the latter was present in a small number of samples. There were a high number of 'Tanytarsus N/S' and 'Tanytarsini undifferentiated' which highlights the large number of specimens that were difficult to identify. Given the low number of taxa in this tribe present across the whole dataset, it is likely that many of the 'Tanytarsus N/S' were *T. lugens*-type which would widen its distribution across the lake, but this taxon would still be absent in the thermokarst zone. No clear changes in assemblage patterns were apparent from the data. The taxa which were rare (<5% relative abundance) had low occurrences. Some taxa were confined to the North-central zone, for example, *Pseudochironomus, Tanytarsus glabrescens*-type and *Paracladius* were found only in the North-central zone (Appendix B).

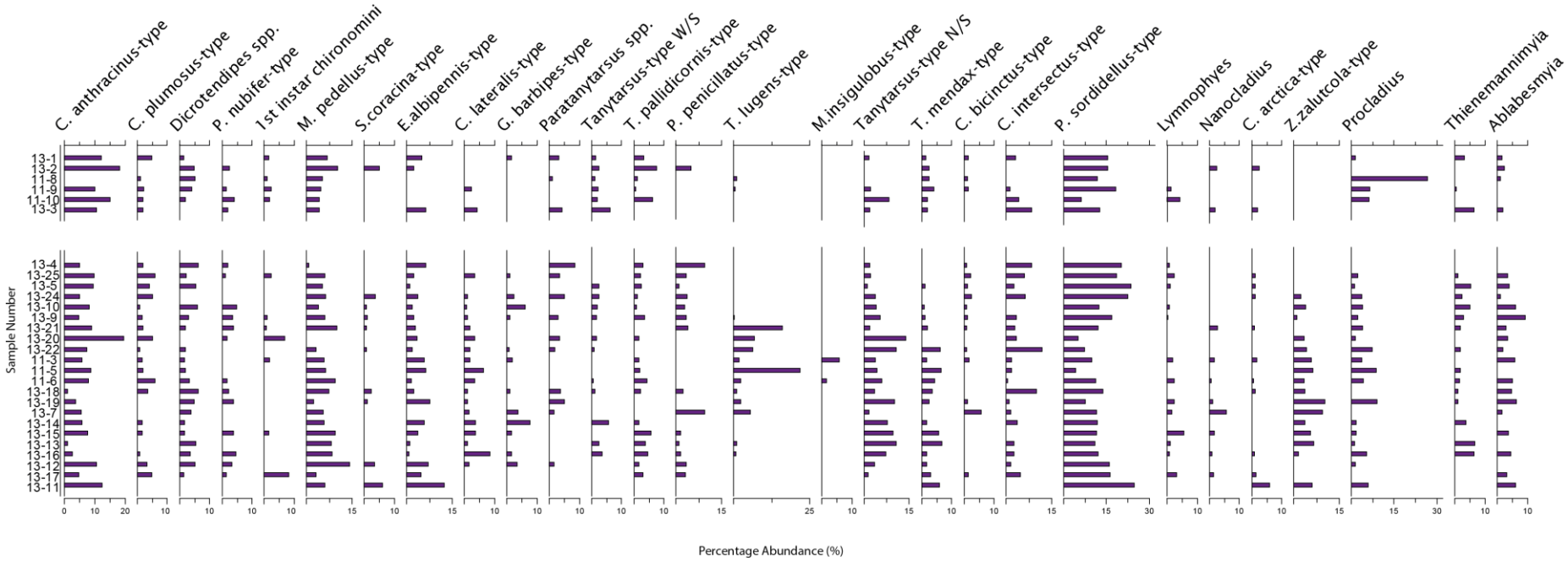

Figure 6.7 Chironomid assemblages from Smith L. Only the taxa which were > 5% abundant are displayed. Sample are arranged from thermokarst zone samples at the top of the diagram with samples becoming progressively distant from this zone with position on the y axis.

6.4.2 Inter-lake comparison

Similar taxa were present at both Smith and Ace, and the chironomid assemblages as a whole was similar in both lakes. Taxa such as *C. anthracinus*-type, *C. plumosus*-type and *P. sordidellus*-type were prominent and abundant across both lakes. When viewing the lakes as a whole, rather than with individual sample points, the lakes had similar abundances of Orthocladiinae and Tanypodinae but they had different numbers of Tanytarsini and Chironomini (figure 6.8). Ace L. showed a high number of Chironomini and a low percentage abundance of Tanytarsini, whereas Smith L. had much less variability between the subfamilies. However, the overall chironomid diversity at Smith was lower than in Ace, with fewer taxa present and with high abundances (>5% relative abundance). Both lakes showed variability in taxon presence or absence across different sampling locations, especially the taxa which were rare (<5% relative abundance). However there was greater variation in Ace L.

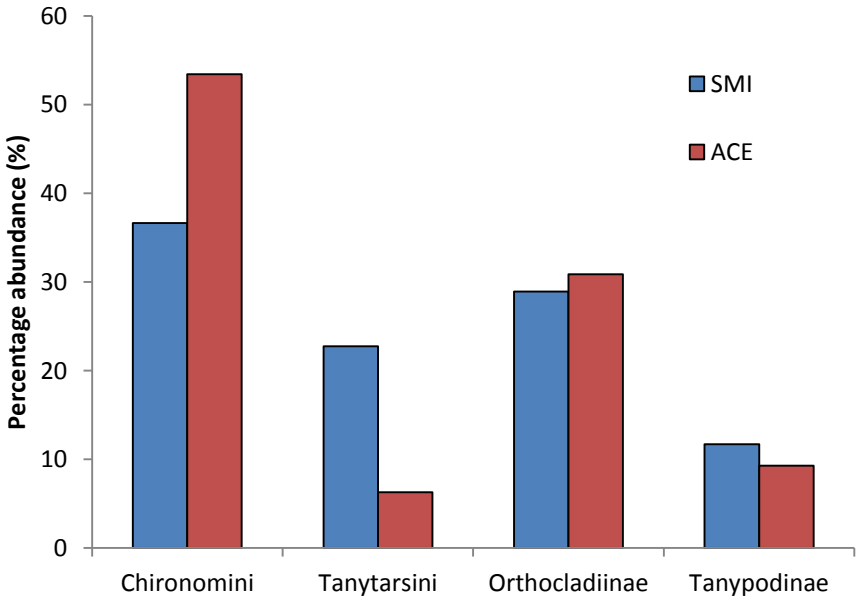

Figure 6.8 A comparison of the relative abundance of the major chironomid groups at Ace and Smith L.

Overall the concentration of HC's per gram of dry sediment (HC/G) was greater at Smith than at Ace and the range of concentrations was highest at Ace L. (Table 6.1)

Table 6.1 Chironomid head capsule concentrations calculated per dry gram of sediment.

	Sample code	HCs per 1g dry		Sample code	HCs per 1g dry
Ace			**Smith**		
	11-1a	N/A		13-4	439
	11-1b	251		13-1	198
	11-2a	28		13-12	159
	11-3a	76		13-9	781
	11-4a	N/A		13-24	331
	13-3	164		13-25	326
	13-4	425		13-5	322
	13-9	465		13-15	244
	13-17	255		13-18	745
	13-5	240		13-23	346
	13-18	255		13-7	254
	13-2	130		11-8	N/A
	11-5a	97		11-9	666
	11-6a	198		11-10	172
	11-6b	136		11-3	75
	13-23	74		11-5	64
	13-11	116		11-6	327
	11-9a	5		13-10	435
	11-9b	7		13-16	347
	11-10a	4		13-14	239
	13-15	123		13-2	189
	13-7	123		13-17	504
	13-12	165		13-19	374
	13-16	155		13-8	409
	13-6	66		13-13	308
	11-7a	11		13-3	225
	11-8a	51		13-11	31
	11-8b	16		13-6	439
	13-8	125		13-22	443
	11-11a	3		13-21	335
	11-11b	7		13-20	445
	11-12a	4			

6.4.3 Ordination results

The results of the DCA highlighted both lakes had short gradient lengths (<3 SDs) therefore a PCA was used (Table 6.2). Some of the taxa were merged in order to maximise the abundance at genus and sub-genus level. The data are presented at each lake separately then as a combined dataset.

Table 6.2 Summary table derived from ordination testing

		PC1	PC2	PC3	PC4
DCA (gradient lengths)					
	Ace	1.655	1.444	1.423	1.067
	Smith	1.439	1.251	1.170	0.969
	Combined	1.468	1.230	1.244	1.290
PCA					
	Ace	0.212	0.148	0.103	0.093
	Smith	0.149	0.121	0.082	0.075
	Combined	0.165	0.096	0.079	0.077

6.4.3.1 Smith Lake

A total of 48 taxa and 31 samples were used in the PCA from Smith L.. Table 6.2 shows the eigenvalues for each principal component (PC) for PCA. PC1 had an eigenvalue of 0.149 and explained 14.9% of the variance in the data. Figure 6.9 shows the PCA axis 1 and 2 sample scores at Smith L.. The results highlighted three clusters of samples; the main group of samples along axis 1, and three samples which had high axis 2 scores. Sample 11-5 is outside 2 SDs of the mean of axis 1 whilst samples 11-8, 11-9 and 11-10 are more than 2 SDs from the mean of axis 2. The cluster analysis in figure 6.10 was completed using the same chironomid assemblage data as was used for PCA. In general the clusters are similar to those visually placed using the PCA axes scores. Samples 11-10, 11-9 and 11-8 were placed in a new cluster at a similarity of 0.5. The remaining samples from the thermokarst zone were clustered within a large group with a similarity of 0.56.

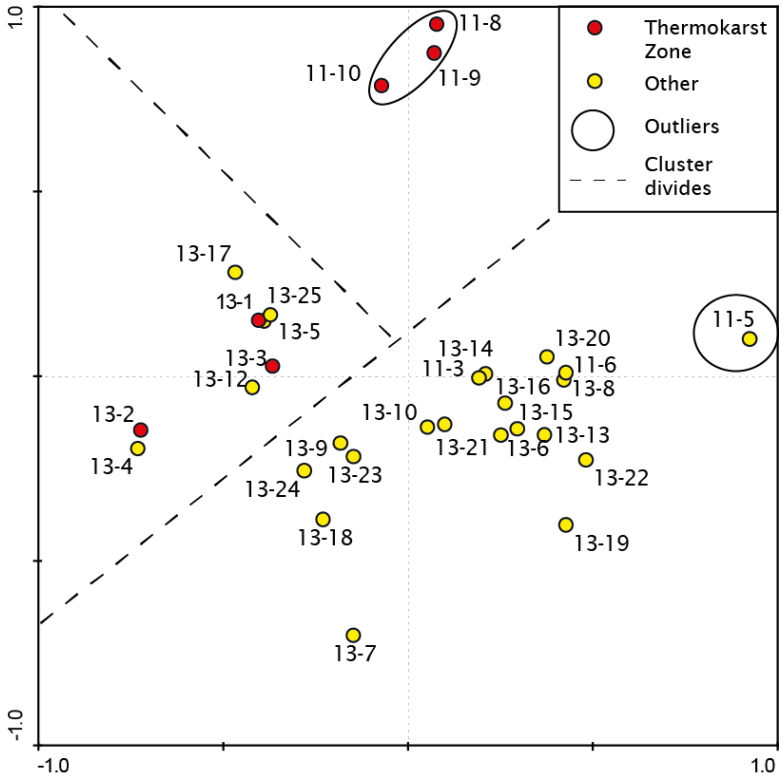

Figure 6.9 PCA axis 1 and 2 sample scores from Smith L.

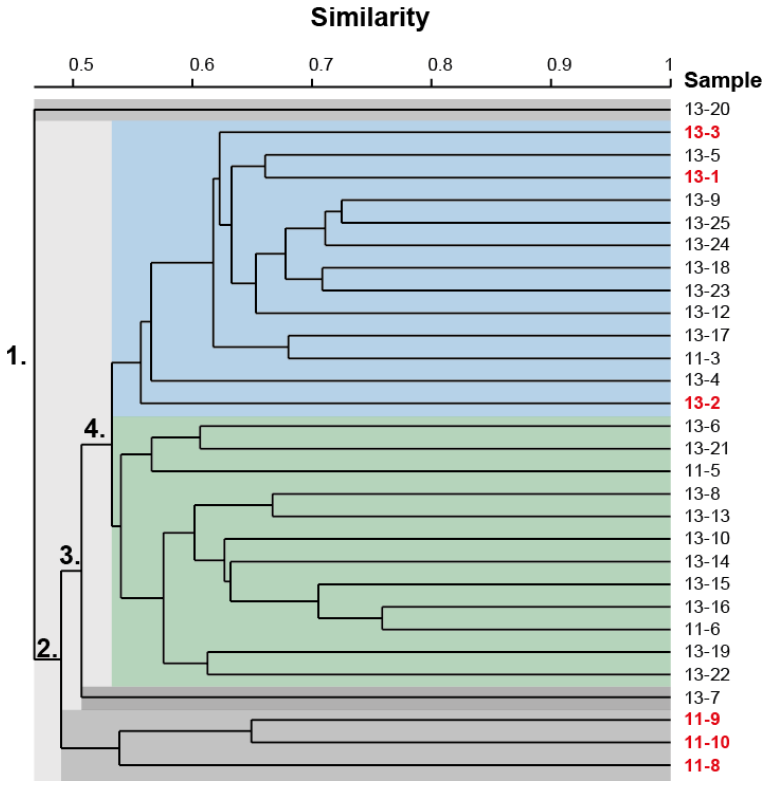

Figure 6.10 Dendrogram from cluster analysis based on a Bray-Crutis similarity matrix of samples at Smith L. according to chironomid assemblage composition

Figure 6.11 shows the axis 1 and 2 species scores for Smith L.. Taxa with low axis 1 scores include: *Psectrocladius spp.*, *C. edwardsi*-type *and Cricotopus spp.*, whilst taxa with high axis 1 scores include: *Zalutchia spp.*, *T. lugens*-type and *Procladius.* Taxa that were closely correlated to axis 2 include: *Paratanytarsus spp.*, and *Zalutchia spp.* The correlation to the axes is identified by the position of the arrows and the relative angles to the axes. Other taxa which had high axis 2 scores include: *Tanypodinae* undiff, *Orthocladinae* undiff and 1st instar Chironomini. The numbers of these three taxa were high in samples 11-8, 11-9 and 11-10 causing these samples to be different.

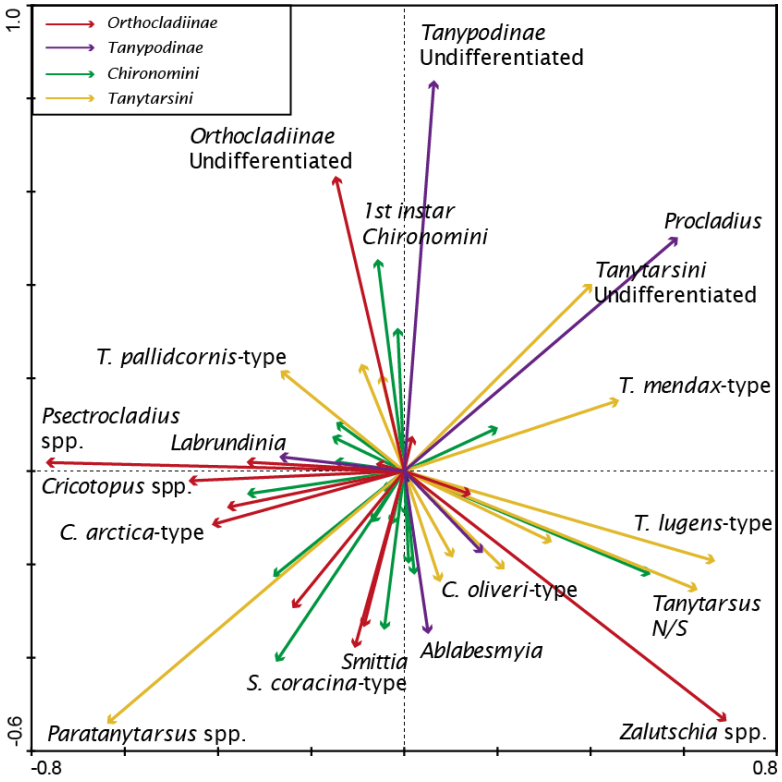

Figure 6.11 PCA axis 1 & 2 species scores, Smith L.

Figure 6.12 shows the results of indirect gradient analysis where environmental variables were included in the PCA (but did not constrain the data). The results suggest axis 1 is most closely correlated with water depth whilst axis 2 is most correlated to TOC. Interestingly, 11-5 has the highest axis 1 score but the water depth is only 1.35m and the water depth gradient max is 3.1m. The cluster of samples with high axis 2 scores are in the thermokarst zone (so were scored yes for methane presence) but had low TOC values and appeared to be more correlated to the latter variable. Most samples were distributed evenly along axis 1 of the PCA. Three clusters of samples were tentatively outlined and the composition of these samples with regard to possible ecological drivers is explored in section 6.6.

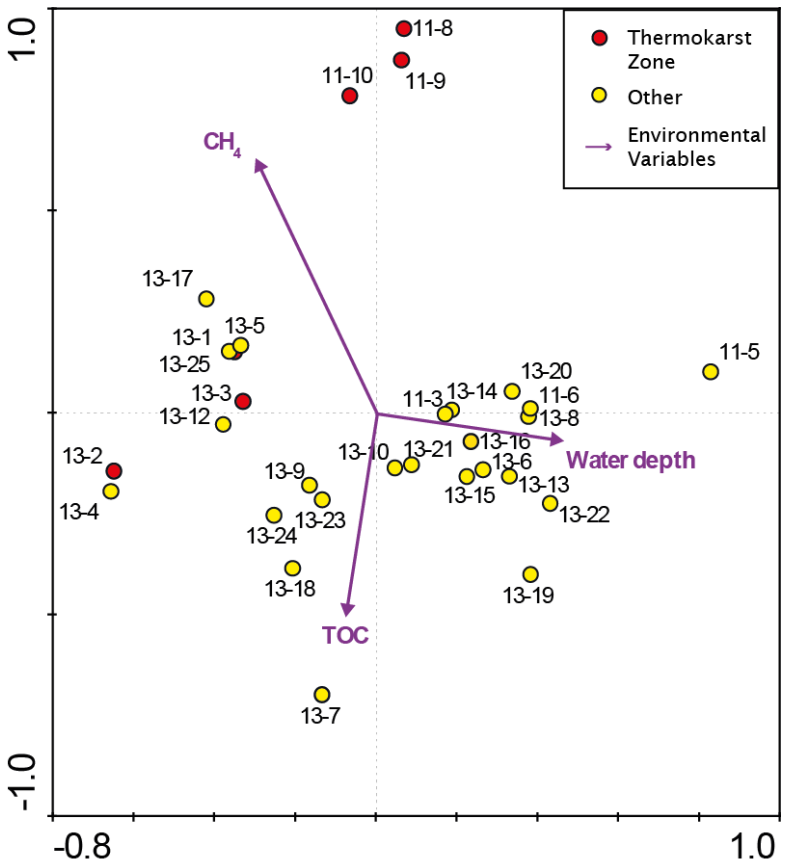

Figure 6.12 PCA sample scores for axes 2 and 3 with the environmental variables plotted at Smith L.

The overall gradient lengths were short suggesting any taxa turnover was relatively small and thus the differences in the samples are subtle. This can also be seen in the chironomid assemblage diagrams where there was little to indicate large changes associated with the thermokarst zone or with any of the other measured variables. The samples from the thermokarst zone were not all clustered together suggesting methane presence did not explain the most variance in the data. However three of the six samples were very different from the rest of the samples and the other three were part of the small cluster with low axis 1 scores. The reasons for the differences in these samples are explored further in the discussion section.

6.4.3.2 Ace Lake

A total of 53 taxa and 18 samples were used in the PCA from Ace L.. Table 6.2 shows the eigenvalues for PC 1-4 at Ace L.. PC1 and PC 2 had eigenvalues of 1.655 and 1.444 respectively. The PCA sample scores highlight three clusters of samples: two samples with low axis 1 scores and high axis 2 scores, a group with low scores for both axes 1 and 2 and samples with a high PC1 score. 13-23 was separate from the other samples and was 2 SDs from the mean (figure 6.13). The cluster analysis in figure 6.14 shows the similarity scores for samples in Ace L. At a similarity of 0.4, two clusters were identified: samples 13-5, 13-12 and 13-23 and the remaining samples. At a similarity of ~0.49 the remaining samples were split into two clusters which are identical to the visual divides, except for sample 13-17.

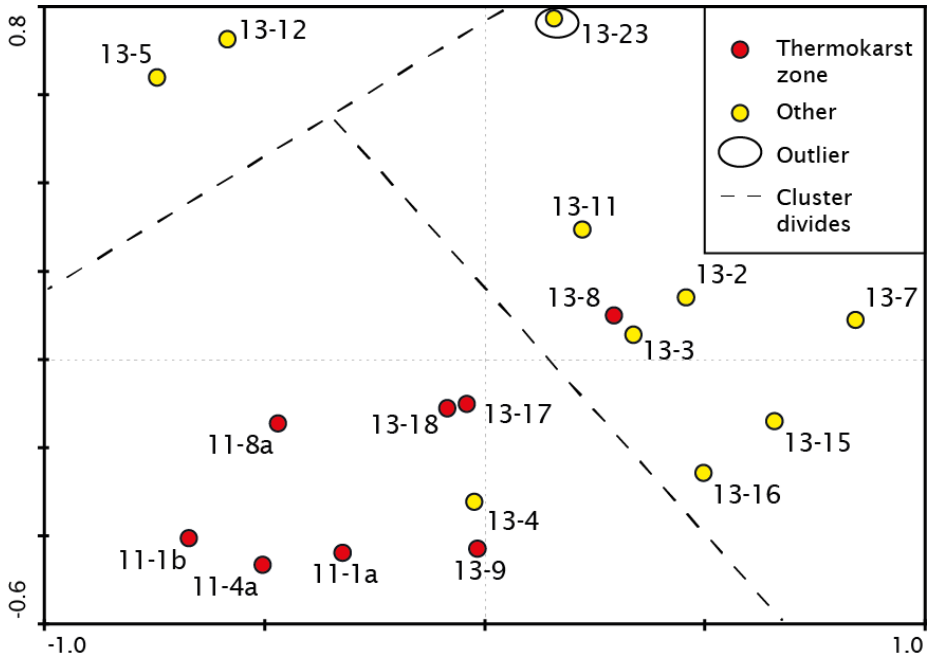

6.13 PCA sample scores, Ace L..

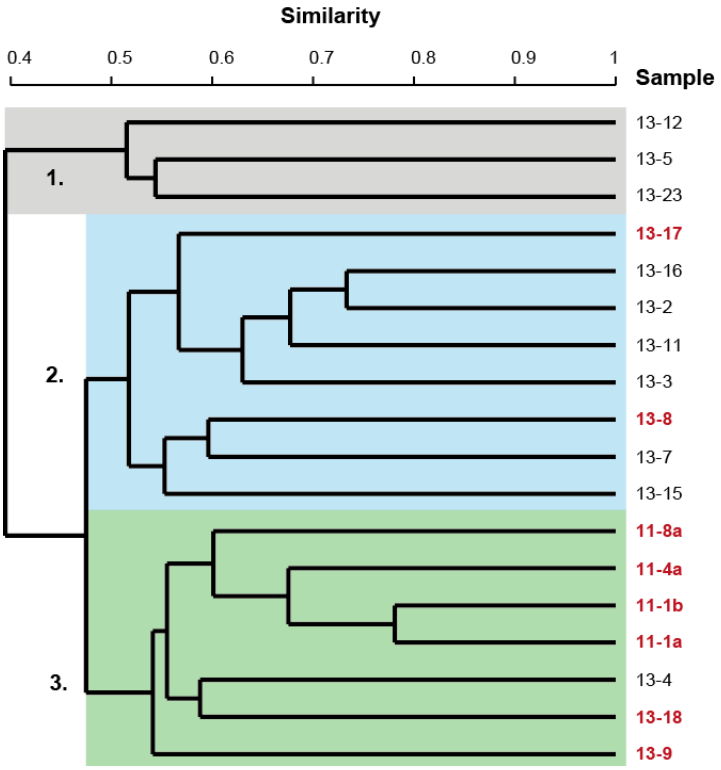

Figure 6.14 Dendrogram from cluster analysis based on a Bray-Crutis similarity matrix of samples at Ace L. according to chironomid assemblages

Figure 6.15 shows PCA species scores at Ace L.. Samples 13-5 and 13-12 had high relative abundances of *C. anthracinus*-type and *T. lugens*-type whilst those samples with low PC 1 and PC2 scores had higher relative abundances of *Dicrotendipes* spp. and *P. nubifer*-type among others. The cluster of samples with high PC1 scores had high relative abundances of *C. plumosus*-type, *P. nubeculosum*-type and *Paratanytarsus* spp.. Interestingly a number of taxa, which might often be grouped together in assemblage diagrams or in transfer functions, plotted in opposite directions suggesting differences in their ecological preferences. For example, *C. anthracinus*-type and *C. plumosus*-type were the taxa with the lowest and highest PC1 scores respectively which suggest that in Ace L. they might be correlated to the same environmental variable but are at different ends of the gradient.

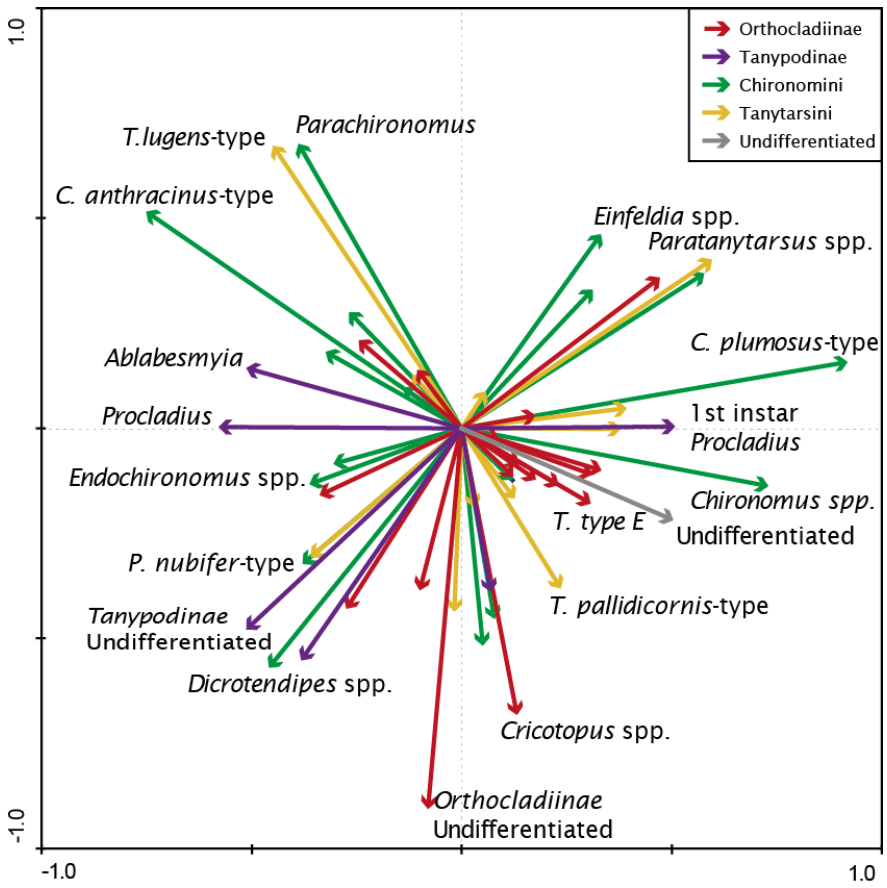

6.15. PCA species scores, Ace L..

Seven environmental variables were identified as potentially important for within-lake variations in chironomid assemblages: %DO, macrophyte presence, water temperature, TOC, methane presence, water depth and conductivity. It was considered highly likely that many of the variables would exhibit co-variance as no variable is truly independent. For example, %DO and water temperature normally decrease with increasing water depth and would therefore share a similar gradient direction in statistical analyses. Without ecological knowledge of chironomid taxa, it would be difficult to decipher which was driving any changes in the chironomid assemblages along the co-varying gradient. The environmental variables were tested using ordination methods to attempt to establish the co-variance. Figure 6.16 shows the environmental variable scores from RDA using automatic forward selection. It highlighted that five of the measured variables were highly co-varying. Of the seven variables measured, only four were considered statistically significant: methane presence, water temperature, TOC and macrophyte presence (P = <0.05 in all instances).

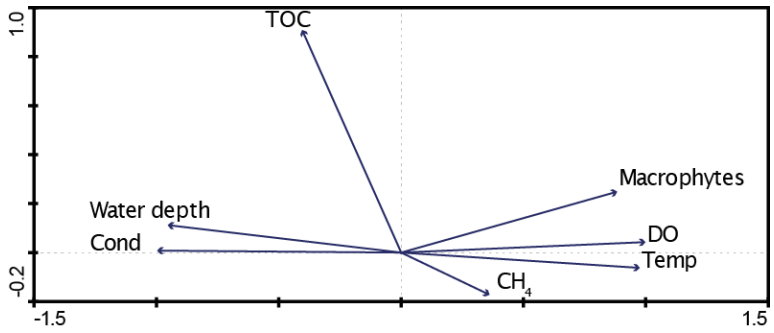

Figure 6.16 RDA environmental variables, Ace L.

Following the RDA, PCA was completed with the environmental variables included (indirect gradient analysis) to establish any correlation between the environmental variables and the PCs in spite of some co-variation (figure 6.17). In this instance, the statistically significant variables were considered independent whilst those which weren't significant were viewed as group. Using PCA instead of RDA meant the environmental variables could be viewed against the samples without constraining the data. Again the co-variance was apparent between most of the variables and the biplot suggested most of the variables were not correlated to either PC1 or PC 2 (figure 6.17).

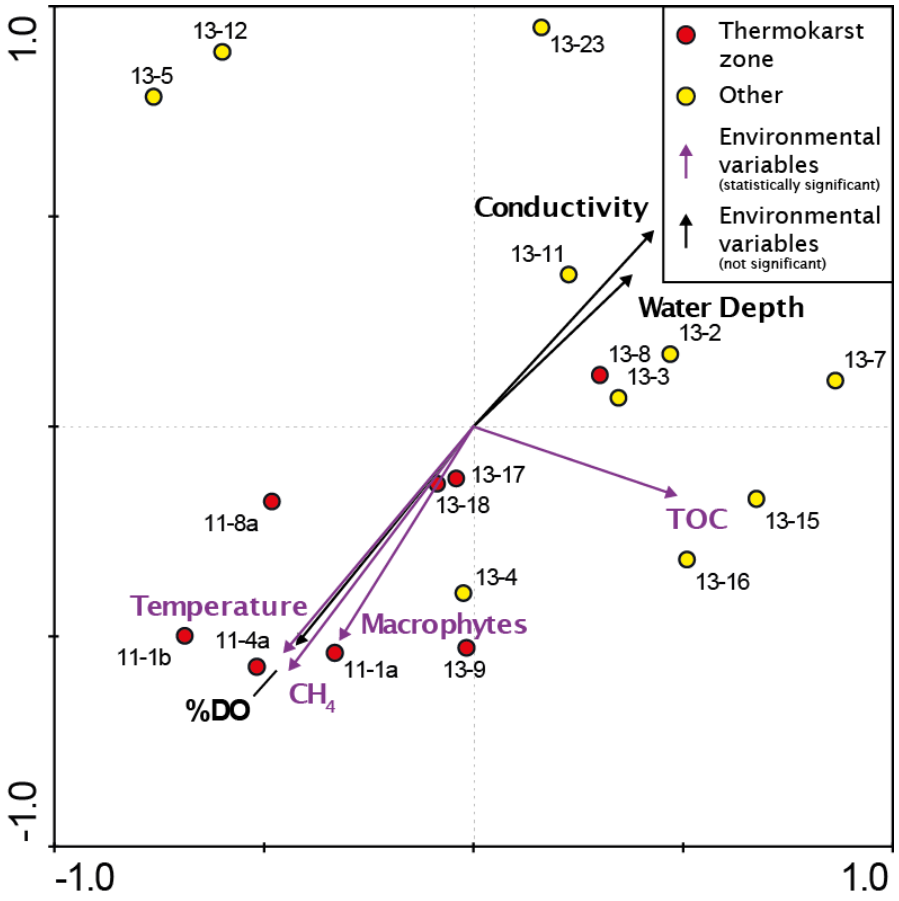

Figure 6.17 PCA axis 1 and 2 sample scores plotted with the environmental variables at Ace L..

The ordination analyses highlighted that all but one of the samples from the thermokarst zone were clustered together. The PCA with environmental variables plotted highlighted these samples were correlated with methane presence, however, macrophyte presence, water temperature and %DO all had a similar gradient trajectory suggesting samples could be equally correlated to these variables. Although water depth was included as an independent variable alongside the other measured variables, in this instance it more likely to be a driver of changes in the other variables. Therefore it could be argued that shifts in the chironomid communities are most closely linked to water depth.

Linear regression was used as a means of testing the correlation (and therefore the co-variance) between environmental variables. Concentration of HCs per dry gram (HCs/dg) was also tested as a means of highlighting changes in chironomid assemblages across the lake that might be associated

with the environmental variables. This testing was only completed on samples that were included in the statistical analysis and not the full dataset. Linear correlation was used to test this variable alongside the other environmental variables measured. Table 6.3 shows the correlation coefficients of HCs against the environmental variables. The results show that HCs/dg has a poor relationship with all measured variables. Although a correlation to variables such as conductivity would be surprising (it is difficult to see why a change in conductivity would lead to a change in the relative abundance of chironomids), the lack of any significant correlation to variables such as water depth or macrophyte abundance is surprising.

Overall the results from Ace L. suggest a heterogeneous intra-lake chironomid assemblage composition. The taxon diversity and species turnover was higher than in Smith (total identified taxa, including rare species: n = 86 and 92 for Smith and Ace respectively), however, the dataset still had a short gradient length overall. The results highlighted three clusters of samples; a small group which was different from the others due to higher relative abundances of *C. anthracinus*-type among other taxa, and two other clusters which appeared to be correlated to opposing ends of the large majority of the measured environmental variables. It is likely that the overarching variable which explains the variance in the data is water depth, however the data show that all but one of the samples located in the thermokarst zone occupy the same ordination space. Reasons for why the thermokarst zone samples are clustered together, including the influence of methane, will be discussed in section 6.6.

Table 6.3 Linear correlation matrix table, Ace L.. Statistically significant relationships are highlighted in red. P values are above the diagonal.

	TOC	CH_4	Cond	%DO	W Depth	W Temp	Macros	HCs/dg
TOC		0.30	0.08	0.29	0.04	0.11	0.54	0.88
CH_4	-0.26		0.16	0.13	0.32	0.09	0.44	0.22
Cond	0.42	-0.34		< 0.01	< 0.01	< 0.01	< 0.01	0.98
%DO	-0.26	0.37	-0.94		< 0.01	< 0.01	< 0.01	0.65
W Depth	0.49	-0.25	0.95	-0.79		< 0.01	< 0.01	0.64
W Temp	-0.39	0.42	-0.99	0.93	-0.93		< 0.01	0.91
Macros	-0.16	0.19	-0.84	0.92	-0.69	0.84		0.92
HCs/dg	0.04	-0.30	0.00	-0.12	-0.12	-0.02	-0.03	

.

6.4.3.3 Inter-lake comparison

A total of 48 samples were analysed as a single dataset using PCA to compare chironomid-environment relationships which might overlap between the lakes. Table 6.1 shows the summary of the percentage of variance explained by PC 1-4 for all analyses completed. PC 1 explained 16.5% of the variance in species data whereas PC2 explained 9%. Sample scores suggested differences between lakes, with Smith samples having low PC1 scores and Ace samples having high scores. Those samples which were located in the thermokarst zones were spread along PC 2, however the majority had high PC1 and PC 2 scores (Figure 6.18). The results of the cluster analysis with combined datasets highlighted a number of small clusters but the thermokarst zone samples did not cluster together on any level (Figure 6.20).

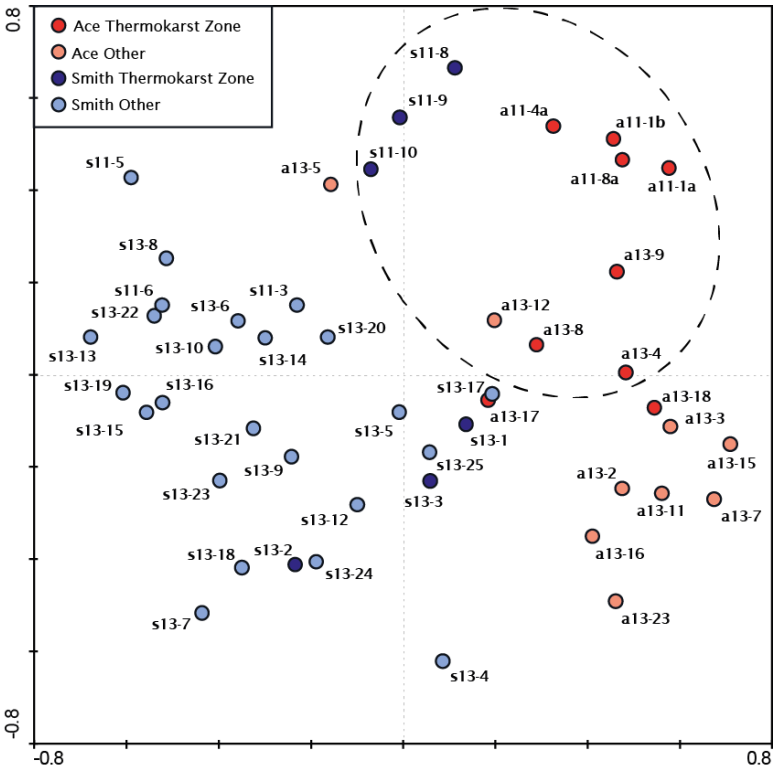

Figure 6.18. PCA P1 and PC1 sample scores for the combined dataset.

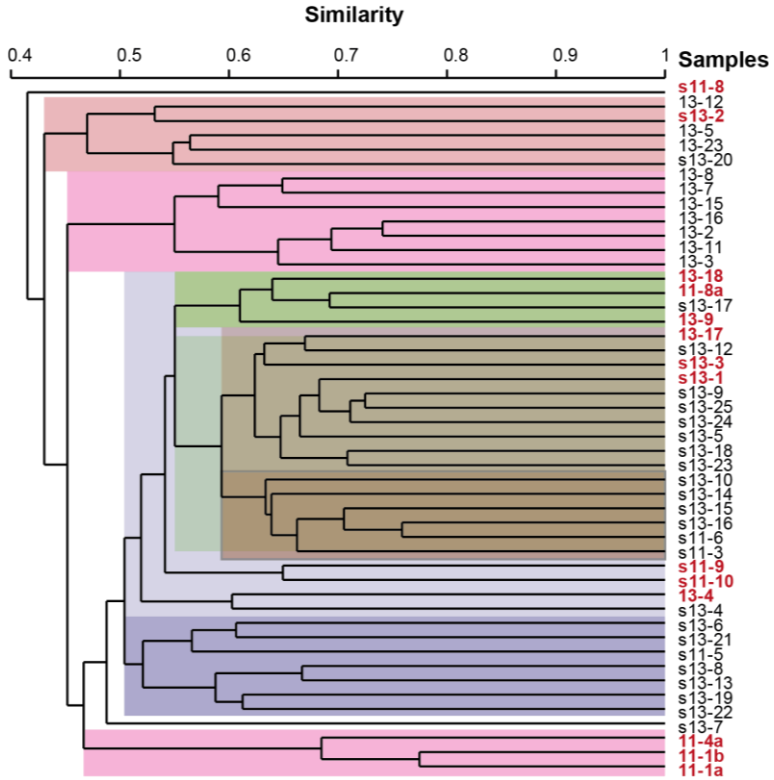

Figure 6.19 Dendrogram from cluster analysis based on a Bray-Crutis similarity matrix of combined Ace and Smith samples according to chironomid assemblages

Figure 6.20 shows the species scores from the combined dataset. The results highlighted the tribe Tanytarsini had low PC 1 scores and a large number of the Orthoclaiinae had high PC1 scores. The Chironomini had both low and high PC 1 scores. *Paratanytarsus* spp. had low PC2 scores whilst the Tanytarsini Undiff, *Procladius* and Tanypodinae Undiff all had high PC2 scores. Again *C. anthracinus*-type has the opposite trajectory to the other *Chironomus* group (in this instance this group consisted of *C. plumosus*-type and *Chironomus* undiff), and these taxa are not correlated to PC1 or PC2. The results show that samples from the thermokarst zone that were clustered together (top-right segment of figure 6.18) had a higher relative abundance of Tanpodinae undiff and Orthocladiinae Undiff, *Endochironomus* spp., 1st instar *Chironomini* and Chironomini Undiff.

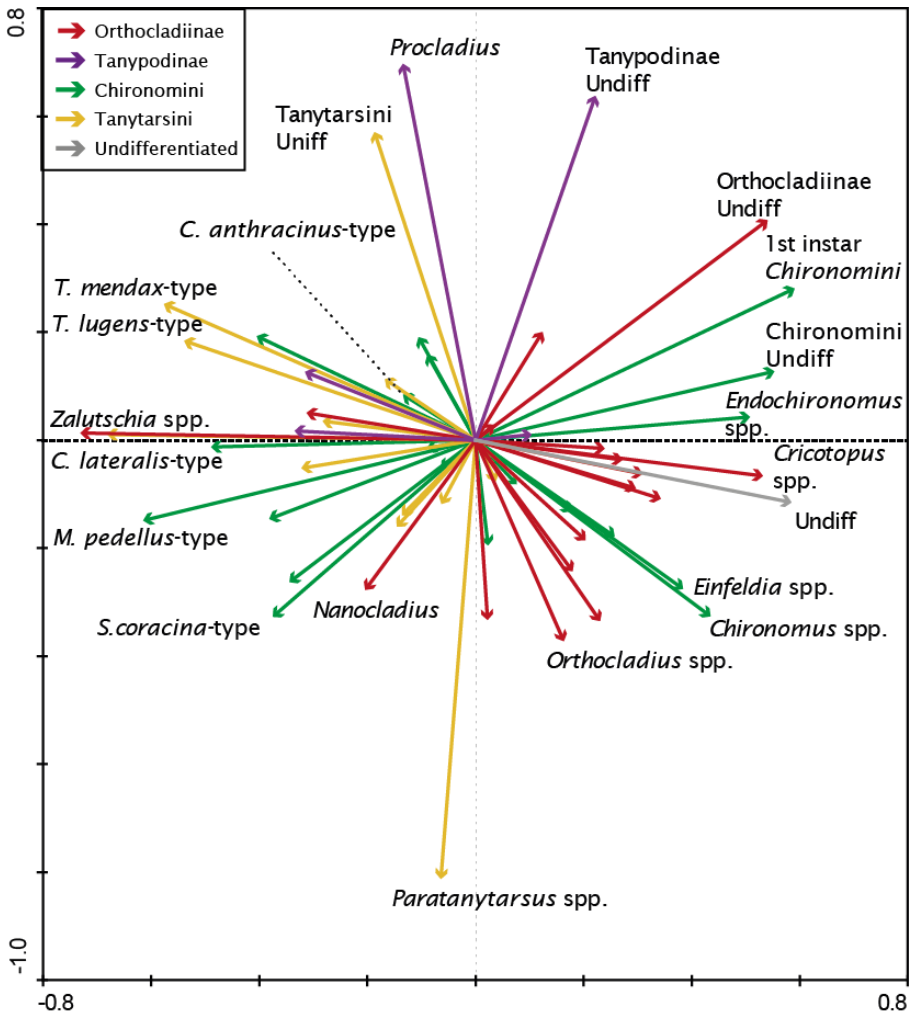

Figure 6.20 PCA spp. scores of the combined dataset

6.4.3.3.1 Inter-lake summary

Overall the inter-lake comparison showed that the two lakes plotted in different areas of the PCA which suggests the assemblages differ between the lakes, however the overall gradients of both lakes were low. The significance of the separation when compared to other lakes is likely to be minimal. Overall the results of the combined PCA indicated a possible grouping of samples from the thermokarst zones of both lakes; the ecological interpretation of the taxa within the samples is discussed in section 6.6. The study lakes showed differing results with regards to the thermokarst zone, with Ace L. having a clearer clustering of samples when using PCA. Reasons for the differences between the lakes are discussed below.

6.5 Discussion

6.5.1 Within-lake chironomid assemblage concentrations and distributions

Overall, Ace L. had a higher number of taxa both in the original, and the reduced dataset (89 and 53) compared to Smith L. (75 and 48); however, Smith L. showed a higher percentage of taxa across the whole lake. The concentration of HCs was also less variable between samples at Smith L. Reasons for the differences in taxa and concentrations of chironomids are discussed below.

The concentration of HCs in the full assemblage datasets ranged from 3 to 781 HC/g. Ace L. showed higher overall variability in the concentrations of HCs which might be a result of the difference in water depth profiles between the lakes. A linear regression using all samples (and not just those considered reliable for ordination analysis) showed that HC/g at Ace L. had a weak, negative but statistically significant correlation to water depth (r^2 = 0.2, p = 0.005; not displayed in graphical form) whereas Smith L. showed no correlation (r^2 = 3.82E-07, p = 0.99; not displayed in graphical form). Fossil chironomid assemblages represent the larvae which develop close to the area of deposition (Walker, 1987). However, redeposition of HCs from shallow to deeper sediments is not uncommon (Brodersen and Lindegaard, 1999; Heiri, 2004; van Hardenbroek et al., 2011). Taxa such as *Endochironomus* and *Dicrotendipes* are commonly associated with macrophytes (Brodersen et al., 2001; Merritt et al., 2008) and the high relative abundance of these taxa in deeper water, which is unlikely to support macrophytes, might indicate sediment transportation. On the other hand taxa such as *Glyptotendipes,* which is also associated with macrophytes (Brodersen et al., 2001), had the highest relative abundance in shallow samples (predominantly those in the thermokarst zone) suggesting that redeposition is not occurring. If sediment focusing were occurring at Ace L., the intermediate or deepest water depths would show the highest diversity (Heiri et al., 2004) however this is not the case. Understanding of the living chironomid larvae and their within-lake distribution would allow a more definitive understanding of the sediment deposition of Ace L..

Taxa occurring in low numbers such as *Labrundinia, C. oliveri* and *Pseudochironomus* may have been underrepresented due to low numbers of samples. In Ace L., samples from deep water depths (>6m) are missing completely, especially in the dataset used for statistical analysis , while the low number of HCs identified in some samples was one of the reasons they were excluded from further analysis. However, the numbers of HCs identified in Smith samples were almost always over the limit deemed reliable for representing the dominant taxa (Quinlan and Smol, 2001). Given that the same taxa had low occurrences in both lakes, it is reasonable to suggest that they are rare taxa.

The taxonomic composition of the chironomid assemblages at the study sites was similar to other high-latitude lakes. Taxa such as *M.pedellus-type* (*Microtendipes), Procladius* and *Dicrotendipes* had high relative abundances in lakes from the boreal forest zone of northwestern Québec (Larocque et al., 2006). A similar set of dominant taxa were found in the surface sample of Screaming Lynx Lake, which included taxa such as *Endochironomus* and *Polypedilum* as well as those mentioned above (Clegg et al., 2011). The distribution of specific taxon within both lakes in this study has been acknowledged previously in other investigations. *T. lugens*-type is considered a cold stenotherm often occupying the profundal areas of lakes (Brundin 1956 in: Hofmann 1998). However, in subarctic regions this taxon can be found in littoral environments (Walker 1987). Conversely, the assemblages in this study are different to those identified from a set of Maar lakes in western Alaska (Kurek et al., 2009). Although these lakes are geographically closer than those in identified in northwestern Québec, the geological and limnological properties of Maar lakes mean that a different chironomid assemblage in these lakes would not be unreasonable. Interestingly, another reason for the discrepancies between lakes in general might be to do with variation in taxonomic classification and resolutions. Unless the exact same system of identification is implemented, some variation in chironomid assemblage composition is possible.

Taxa present in Smith L. in high relative abundance such as *Chironomus, Sergentia* and *Z. zalutschicola*-type are often associated with coloured lakes (Brundin 1949 in: Heiri 2004). Smith L. is surrounded by peatlands and boreal forest vegetation and erosion of this material into the lakes was directly

observed during fieldwork. This will contribute acid humus to the lake which is a common characteristic of dystrophic lakes (Hansen, 1962). The consistent presence (but low relative abundance) Reduced light penetration due to brown water was observed at both lakes (Seccii depth = 0.7m) which might increase the likelihood of anoxic bottom waters (Williamson et al., 1999). Along with the reduction in %OC due long periods of ice cover, these factors might explain the relatively even distribution across all water depths of the taxa mentioned above at Smith L., although, it does not explain the absence of *Z. zalutschicola*-type from samples in the thermokarst zone. Interestingly, the dystrophic-like conditions as described above are also similar in Ace and yet *Sergentia* and *Z. zalutschicola*-type were not found in this lake. It is difficult to see why these taxa might be absent, although the difference might tentatively be associated with more important environmental variables controlling chironomid assemblages at Ace L.. Water depth is unlikely as *Z. zalutschicola*-type is found below 5 m water depth in other studies (Engels et al., 2012) and this would not stop these taxa being present in the shallow water samples. The reasons for the differences between the lakes remain unknown.

6.5.2 Factors explaining chironomid distributions

Overall, the results of the ordination testing showed that the lakes were similar. However, a number of differences lead to the segregation of samples in PCA using the combined data (Figure 6.17). The study sites also had different chironomid assemblages in the thermokarst zones compared to the rest of the lake. The similarities and differences between the lakes are discussed below.

A key difference between the lakes is the bathymetry and overall water depth profiles. Smith L. is a shallow, flat bottomed lake with a small catchment and a homogenous aquatic macrophyte distribution. At Ace L. the samples were more heterogeneous but were still distributed along fairly short gradients (DCA axis lengths <2 SDs). Despite differences in the range of water depths, the results of PCA analysis highlight that water depth an important variable in explaining within-lake distributions of chironomids (although it is not statistically significant in Ace L.). At Ace L., all but one of the environmental variables strongly co-varied with water depth and none were correlated to axis 1 or 2 (Figure 6.17)

Although water depth is included as an independent variable, it is unlikely that changes in water depth will drive chironomid assemblage alterations directly. Other variables such as %DO, water temperature and macrophyte abundance all alter with water depth and are more likely to have a direct ecological impact on biological communities (Juggins, 2013). This strong co-variation between a number of independent variables and water depth is clearly seen in Ace L. (Figure 6.16), creating an intricate environmental gradient where it is difficult to tease apart the exact causal relationship (Juggins 2013). The lack of direct ecological impact of water depth on chironomid assemblages might be highlighted by taxa in Smith L.. Engels et al. (2012) developed a water depth inference model using lakes of a similar size (but greater depth profiles) to those in the present study. Their study highlighted *Z. zalutschicola* had highest relative abundances in the deepest samples (below 5m) whereas this taxa had a high relative abundance across Smith L., where maximum water depth was ~4 m. Engels et al. (2012) describe their study lakes as oligotrophic, having steep littoral slopes and large flat benthic areas leading to accumulation of organics in the deepest areas. In comparison, Smith L. is highly productive and more eutrophic (Alexander and Barsdate, 1971) which leads to high organic accumulation across the lake. This might suggest that this taxon is correlated to substrate composition, more specifically high organic content rather than water depth. In the lakes used by Engels et al. (2012) the relationship between water depth and organic matter content appears to be more linear than it is in Smith L.

Although the chironomid assemblages at the study sites show both similarities and differences when compared to other high-latitude lakes, most of these are qualitative observations. In order to place the study sites in context in a more quantitative manner, the samples from the study sites were analysed alongside samples taken from lakes from variable geomorphic settings in Alaska and from thermokarst lakes in Siberia using DCA (Figure 6.21). Interestingly, the samples from the lakes in this study plotted closest to the lakes from the discontinuous permafrost zone. As the study sites are located in the discontinuous zone also, this result is somewhat unsurprising. The DCA results did, however, show that Ace and Smith L.s have chironomid assemblages which are more representative of boreal forest lakes which are different from the Siberian thermokarst lakes tested here. This raises an

important question associated with the high variability in thermokarst lakes and whether a single classification is enough. Thermokarst lakes have recently been divided based on methane emissions into yedoma lakes and non-yedoma lakes (Walter et al., 2008b; Brosius et al., 2012; Gao et al., 2013; Sepulveda-Jauregui et al., 2014) and the large variations between thermokarst lakes in different geographical regions is recognised through region-specific investigations of thermokarst lakes (Jorgenson and Shur, 2007; Grosse et al., 2008; West and Plug, 2008). This is an important factor when considering the use of chironomid assemblage compositions for understanding methane cycling in thermokarst lakes. The results highlight that a number of different types of thermokarst lakes should be examined to investigate whether chironomid assemblage compositions can be assigned to sub-categories within the broader theme of thermokarst lakes.

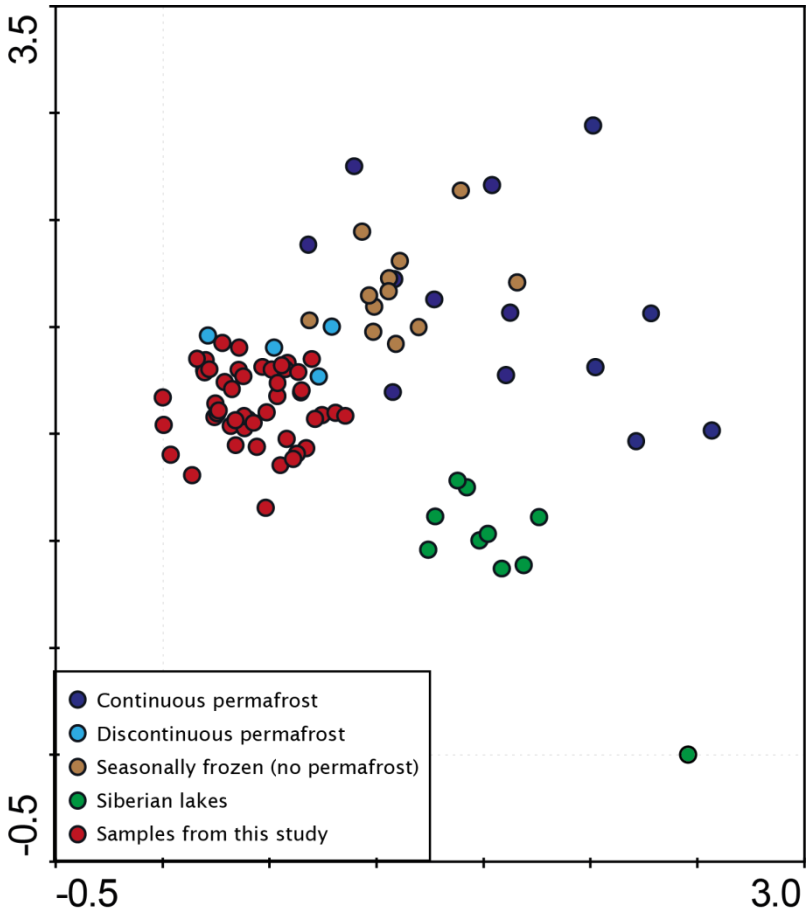

Figure 6.21 DCA of every sample from Ace and Smith compared to lakes from other regions.

6.5.3 The relationship between chironomids and methane

In order for chironomid assemblages to be used as a proxy for methane production areas in thermokarst lakes, any relationships should be observed over a number of lakes and importantly, should be large enough to be picked out above variation caused by other environmental variables.

At Ace L., samples in the thermokarst zone are clustered together and PCA with the environmental variables showed that these samples are characterised by high %DO, shallow water depths, methane presence, macrophyte presence and high water temperatures. Taxa such as *P. nubifer*-type and *Dicrotendipes* are associated with littoral zones and macrophytes (Merritt et al., 2008) and they are dominant taxa in the thermokarst zone samples. The main differences between the thermokarst zone and the rest of the lake was the higher numbers of undifferentiated HCs. Tanypodinae Undiff and Orthocladiinae Undiff were high in the thermokarst zone samples. Within the thermokarst zone of Smith L. the number of undifferentiated HCs also increased, although samples from this zone do not cluster as distinctively as those from Ace L. (three of six samples are different from the rest). The increase in the number of specimens that could not be identified is likely to be linked to a decrease in the preservation of HCs in this zone or the 'cleanliness' of the HCs after chemical treatment. The good condition of the other HCs in the samples suggests the latter is most likely. It is difficult to draw a link between the increase in sediment inside HCs and methane production or methane release from the sediments; however, it might tentatively be linked back to methane ebullition altering the physical structure of sediments preventing consolidation of sediment as it settles on the lake bed.

Although the results showed the samples from the thermokarst zone are similar, an ecological rationale for this is difficult to formulate. The results also highlight some of the limitations of applying ordination statistics to small datasets. In this instance it is likely to lead to over-interpretation of relationships when the full variability in the data might not been captured or differences in what are actually comparatively homogeneous lake sediments.

6.6 Conclusions

The overall taxonomic compositions of chironomid assemblages at the study sites were similar, especially when considered in the context of other lakes. Within-lake variability in chironomid assemblages was larger in Ace L. than in Smith, which is likely due to the larger environmental gradients associated with increased water depth in Ace L.. The chironomid communities across the study sites were similar to the assemblages found in other high-latitude lakes. Quantitative assessment indicated the study sites were similar to other lakes situated in the boreal zone as opposed to other thermokarst lakes. This highlighted the need for further investigation into more refined classification of thermokarst lakes in order to better characterise the chironomid assemblages within them.

At Smith L. three of the samples from the thermokarst zone were clustered together, however the other three plotted with the rest of the lake samples making it difficult to suggest that differences were due to conditions exclusive to the thermokarst zone. At Ace L., almost all of the thermokarst zone samples were clustered together. The main difference between these and the rest of the samples was the increase in the number of undifferentiated specimens in the thermokarst zone.

Overall, the results from both lakes provide a mixed signal with regards to the ability of chironomid assemblages to reflect methane cycling in thermokarst lakes. The results from Ace L. suggest a pattern linked to the thermokarst zone but further work is needed in order to understand if this due to methane ebullition or environmental conditions created specifically by thermokarst erosion and methane processes. If so, and if this pattern is consistent and unaffected by changes in composite variables such as water depth, chironomid assemblages might be able to highlight conditions associated with high level methane ebullition flux.

Chapter 7: Stable isotope signatures of taxon-specific chironomid samples as indicators of methane supply to the lake food web in thermokarst lakes

7.1 Outline

This chapter presents results and interpretation of stable carbon isotope values of chironomid remains in relation to areas of high methane production. Firstly a review of methane production and supply regions in the study lakes is provided, along with the chapter-specific sampling strategy and relevant methods. Following this, the results are presented for each lake separately to describe the site-specific patterns, then as a comparative dataset to assess inter-lake similarities and differences. Finally, a number of factors are considering including: the contribution of methane-derived carbon to chironomid $\delta^{13}C$ values and the use of chironomid $\delta^{13}C$ values as proxies for methane availability.

7.2 Introduction

Methane emissions from thermokarst and thermokarst-affected lakes in high-latitude regions may contribute more substantially towards atmospheric methane than was previously thought (Walter et al., 2007b). Increased understanding of the longevity and dynamics of methane cycling in high-latitude wetlands, and more specifically thermokarst lakes, is necessary to establish how important these emissions actually are. The majority of current estimates of the contribution of thermokarst lake methane emissions are based on modern measurements obtained over the past decade (e.g. Walter et al., 2007b); however, long term methane fluxes are less well understood. In the absence of direct long term methane flux measurements, a proxy for palaeo methane cycling would assist with advancing the current understanding of carbon cycling in thermokarst lakes over time (e.g. Wooller et al., 2012). However, in order to develop such a proxy, a greater understanding of the

interaction between methane production, oxidation and potential uptake by higher organisms in the food web must be obtained.

The full overview of thermokarst lake-specific methane production is outlined in chapter 2; however, the important points that contribute to the understanding of the results in this chapter are reiterated below.

Figure 2.2 highlights the main methane production areas and emission pathways in thermokarst lakes. As well as production in anoxic surface sediments (which is common in many lake types), thermokarst lakes have additional, spatially-explicit, methane production sites near the margins. These production zones are associated with the thawing of permafrost underneath the lake (exposing older labile carbon in the talik bulb) and at the thermokarsting margins (that causes the slumping of younger, but not usually modern, material; Kessler et al. 2012). Thermokarst lakes which produce methane from Pleistocene-age sediments in the deep talik bulb, termed yedoma-lakes, often have higher ebullition flux rates than other types of thermokarst lakes (Walter Anthony and Anthony, 2013).

After the methane is produced it can be transported via ebullition (bubbling); turbulent diffusion; and plant mediated transport (Bastviken, 2004). Methane in solution that diffuses from the sediments is oxidised by methane-oxidising bacteria (MOB), and at this point the carbon is recycled in the lake. The amount of methane that is oxidised is highly variable and often depends on the limnological system; however, values between 30 and 99% have been reported in other studies (Rudd and Taylor, 1980; Bastviken et al., 2002; Kankaala et al., 2006).

Thermokarst lake-specific methane production was first observed due to large numbers of bubbles trapped in winter ice (Zimov et al 1997, Walter et al., 2006). Walter et al. (2008a) estimated that almost all (95%) thermokarst lake-specific methane is transported to the atmosphere via bubble tubes, or methane ebullition-seeps as they are defined in this study. Much of the current research has focused on monitoring this ebullition flux as it reaches the surface water-air interface (Walter Anthony and Anthony, 2013; Greene et al., 2014; Sepulveda-Jauregui et al., 2014).

As yet little work has been done to investigate thermokarst lake-specific methane supply rate to the lake water column (and potentially the atmosphere) via diffusion from the sediments. Methane transported via the ebullition pathway by-passes the lake system. Methane that is contained within a bubble cannot be accessed by lake organisms, and unless water depths are great enough to allow dissolution of a bubble as it travels through the lake water (> than 50% dissolution in water deeper than 20m; Ostrovsky et al., 2008), it will reach the surface water-air interface without being altered. So, unless thermokarst-specific methane is also transported via diffusion, it will not be recycled within the lake via MOB. Therefore, if thermokarst-specific methane transport occurs solely by ebullition and is not contributing to the internal lake carbon cycle then there is little potential for developing a proxy for past thermokarst-specific methane production. The results of chapter 5 suggested the amount of methane that diffuses from the sediment is highly variable, even between samples within close proximity to one another. In Ace L., the area dominated by methane ebullition-seeps (the thermokarst zone) had some of the highest methane oxidation (and by extension high supply rate) suggesting a correlation between high methane flux from ebullition-seeps and high diffusion of methane from sediments. In Smith L., this relationship was not clear, and here the results suggested the highest supply of methane for MO, were in the centre of the lake; the area with next to no methane flux from ebullition-seeps. The thermokarst zone in Smith L. has the lowest interpreted supply rate of methane for MO.

The spatial variability in methane oxidation at the study sites is important for the interpretation of the data derived in this chapter. It is likely that the variability in the $\delta^{13}C$ signatures of MOB will be reflected in the $\delta^{13}C$ values of chironomid larvae.

7.2.1 Linking methane to the lake food web

The stable carbon isotope values of biogenic methane are very low in comparison to the source material (Whiticar 1999). These distinctively low values can be traced through the food web if organisms assimilate methane (Figure 7.1). Previous studies have linked depletion in the $\delta^{13}C$ values at various stages in the food web to the incorporation of carbon from MOB (Hershey et al., 2006; Deines et al., 2007a; Sanseverino et al., 2012). In thermokarst lakes,

low $\delta^{13}C$ values in chironomid larvae and fossil head capsules have been linked to increased methane flux (van Hardenbroek et al., 2013). Wooller et al. (2012) also interpret negative shifts in $\delta^{13}C$ values of fossil chironomids and *Daphnia* as an increase in methane production.

Two studies have investigated the relationship between methane production and $\delta^{13}C$ of chironomid remains in thermokarst lakes (van Hardenbroek et al. 2012a; Wooller et al. 2012). These studies assessed changes in past methane availability based on the stable isotope composition of invertebrate remains. van Hardenbroek et al. (2012a) highlight a correlation between more depleted $\delta^{13}C$ values of Chironomini Tanytarsini and *Daphnia* and high levels of diffusive flux suggesting methane availability affects the stable carbon isotopes of these invertebrates. Wooller et al. (2012) show evidence for low $\delta^{13}C$ values of invertebrates. In both instances, the sampling site did not correspond to the area of highest methane flux from ebullition-seeps and therefore it is difficult to attribute the changes in invertebrate $\delta^{13}C$ values with thermokarst-specific methane production. A greater understanding of the spatial patterns of thermokarst-specific methane production, concentration of dissolved methane and utilisation by lake organisms is necessary in order to establish what fossil invertebrate remains are truly reflecting. The aim of this chapter, therefore, is to try to understand the controls on $\delta^{13}C$ values of fossil chironomids across a within-lake sample distribution to establish the influence of thermokarst-specific methane production.

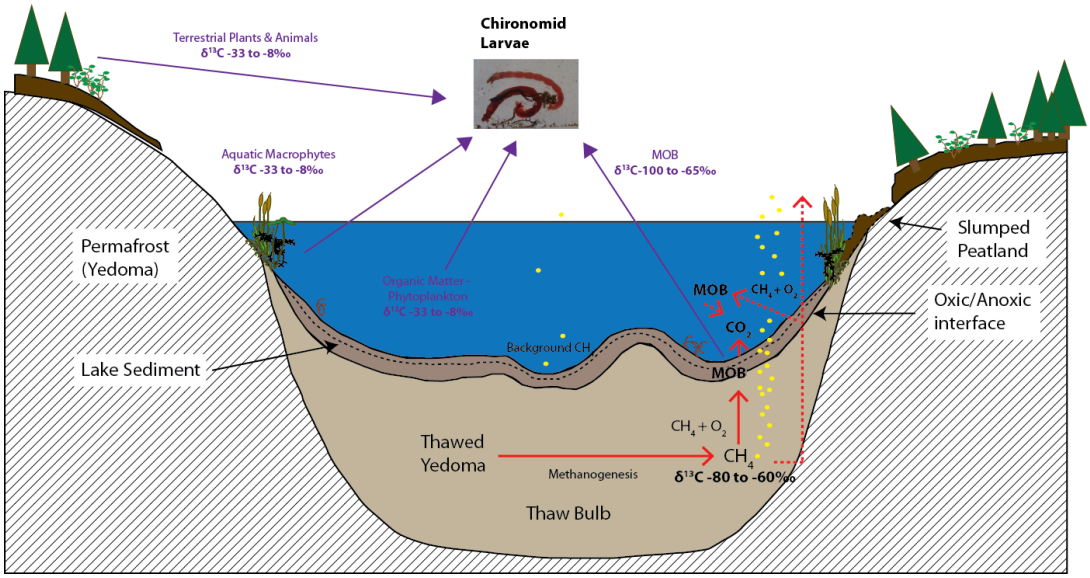

Figure 7.1 Stable isotope signatures of potential food sources for chironomids in lakes. Adapted from Walter et al. (2008a) and $\delta^{13}C$ values are derived from the literature (Grey and Jones, 1999; Hornibrook et al., 2000; Jones and Grey, 2011)

7.3 Design

Few studies have been completed on the interactions between thermokarst-specific production, oxidation and consumption of methane across different spatial scales in modern thermokarst lake environments. The main objective of this chapter is to establish the potential carbon sources for chironomid larvae and their respective stable isotope signatures in two thermokarst lakes. In order to achieve this, the taxon-specific isotope signatures will be used to asses potential input of methane-derived carbon for two chosen taxa. Using the datasets other chapters and this one, the variation in the $\delta^{13}C$ values in lake organisms will be established in order to understand the links between thermokarst-specific methane production zones, dissolved methane concentrations and methane-derived contributions to the lake food web. The results of this chapter will allow a critical assessment of the use of fossil chironomid $\delta^{13}C$ values as a proxy of thermokarst-specific methane availability in thermokarst lakes.

7.3.1 Sampling Strategy

A detailed description of the study sites can be found in chapter 3. Figure 7.2 shows the sample points (with corresponding codes) and the designated spatial zones which have been used in this study. A total of 26 and 17 sample locations were analysed from Smith and Ace respectively. A number of samples were used for replicate measurements, or where possible, larval samples. Samples were selected based on both its location within the lake and it's richness (the number of HCs available).

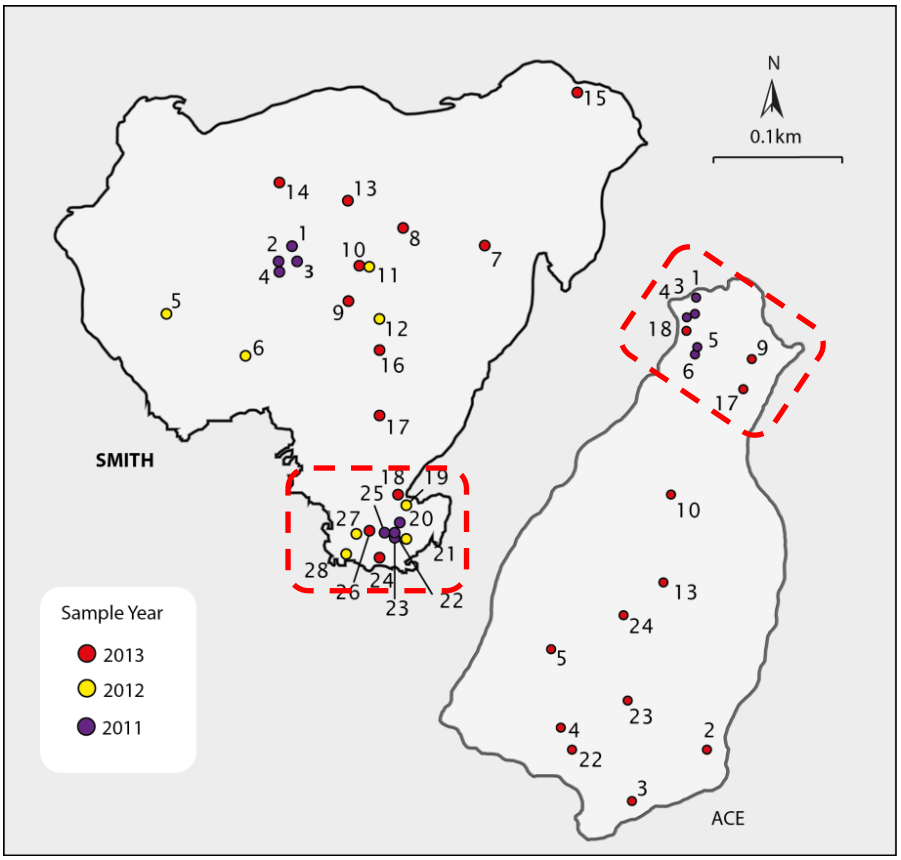

Figure 7.2 Locations of stable carbon isotope samples at the study sites. Different sampling years are indicated by different coloured filled circles. Dashed red boxes indicate the thermokarst zone.

7.3.2 Methods

7.3.2.1 Chironomid head capsule identification

Head capsules (HCs) were processed for isotope analysis either using a mild chemical pre-treatment or with no chemical pre-treatment. Heiri et al. (2012) have shown that standard chemical treatment of HCs for chironomid assemblage analysis (e.g. heating in mild KOH) has little discernible impact on the $\delta^{13}C$ values of the HCs samples. Where a chemical pre-treatment was used, sub samples were placed in 10-20ml of KOH (5%) and gently heated for 5 minutes. Samples were gently washed using nested sieves (180 and 90μm respectively) and the retained fractions were placed in sample tubes until HCs were processed.

Two taxa from each were chosen for stable isotope analysis: *Chironomus* was abundant in both lakes and consisted of *C. anthracinus*-type and where

numbers were low *C. plumosus*-type; in Ace L. the second taxon was *Endochironomus* which was comprised of *E. albipennis*-type and in Smith L. the second taxon was *M.pedellus-type* (termed *Microtendipes* hereafter). HCs were identified using a stereoscope under x100 magnification. Specimens that could not be clearly identified under at the low power were placed onto a microscope slide in distilled water and observed using a high powered microscope at x1000 magnification. From here, HCs were transferred into tin capsules and, once dry; the capsules were crushed and placed into sorted trays. The numbers of HCs were recorded for each sample, with a minimum of 15 HCs which was considered a large enough sample size to meet the minimum weight needed for accurate stable isotope analyses (>20μg; van Hardenbroek et al. 2010).

7.3.2.2 Instrumental analysis

All isotope samples were analysed at the NERC Isotope Geosciences Laboratory (NIGL). The $\delta^{13}C$ values were measured using the standard lab protocol for small samples. Percentage carbon (%C) was measured using a Carlo Erba 1500 elemental analyser, calibrated against an Acetanilide standard. Replicate analysis of well-mixed samples indicated a precision better than 0.1‰. $^{13}C/^{12}C$ analyses were performed also using the Carlo Erba 1500 on-line to a VG TripleTrap (plus secondary cryogenic trap in the mass spectrometer for these very low carbon content samples) and Optima dual-inlet mass spectrometer, with $\delta^{13}C$ values calculated to the VPDB scale using a within-run laboratory standard (BROC1) calibrated against NBS 19 and NBS 22. Replicate analysis of well-mixed samples indicated a precision better than 0.1‰ (1 SD). A standard error of 0.1‰ was applied to all stable isotope samples.

Isotopic values are expressed in the delta notation as per mille (‰) relative to the standard Pee Dee Belemnite (VPDB):

$$\delta^{13}C = (^{13}R_{SA}/^{13}R_{PDB}\text{-}1) \times 10^3 \qquad \text{(EQ 7.1)}$$

Where $^{13}R_{SA}$ and $^{13}R_{PDB}$ represent the $^{13}C/^{12}C$ abundance ratios of the sample and standard respectively.

7.4 Results

7.4.1 Methane production, distribution and oxidation

A detailed description of the methane dynamics at Ace and Smith L. is found in chapter 5. Briefly, the thermokarst zone in both lakes had high concentrations of methane ebullition-seeps (2.27 seeps m^2 and 4.2 seeps m^2 for Smith and Ace respectively). Seep ebullition flux in the thermokarst zones was 85 and 151mg CH_4 m^{-2} d^{-1} (Figure 5.1) and had stable carbon isotope values of -60.9 and -64.6‰ for Smith and Ace, respectively. Methane ebullition (but not ebullition-seep) flux measurements from the lake centres was 6mg and 20mg CH_4 m^{-2} d^{-1} for Smith and Ace, respectively. The bacterial biomarker diploptene was present across almost all samples analysed. The $\delta^{13}C$ values were highly variable indicating differences in the contribution of diploptene derived from MOB across all samples. Ace L. thermokarst zone and the centre of Smith L. had the lowest $\delta^{13}C$ values in the dataset. The areas with the lowest $\delta^{13}C$ values of diploptene were interpreted as having the highest contributions of MOB therefore the areas with the highest dissolved methane available for oxidation. Smith L. thermokarst zone had the highest $\delta^{13}C$ values of the whole dataset and this is interpreted as the area with the lowest concentrations of dissolved methane.

7.4.2 Potential food sources for chironomids

The bulk sediment and vegetation stable carbon isotope results are described in detail in chapter 4. Figure 7.3 is reproduced from figure 4.3 for ease of comparison with other data in this chapter. Terrestrial and aquatic vegetation $\delta^{13}C$ values range between -37 and -21‰. *Sparganium* sp. and brown moss had very different values to the rest of the measured vegetation.

The $\delta^{13}C$ values of bulk sediment have a larger range at Ace L. and on average are more depleted here than at Smith L.. The $\delta^{13}C$ values of bulk sediment are consistently lower than the average $\delta^{13}C$ values of plant material except for brown moss (-36.8‰). Bulk sediment $\delta^{13}C$ values have a negative correlation with water depth at Ace L. ($r^2 = 0.62$, $p = <0.01$) with the deepest sample locations having the most negative bulk sediment $\delta^{13}C$ values (Figure 7.4) but there is no correlation between these values at Smith L..

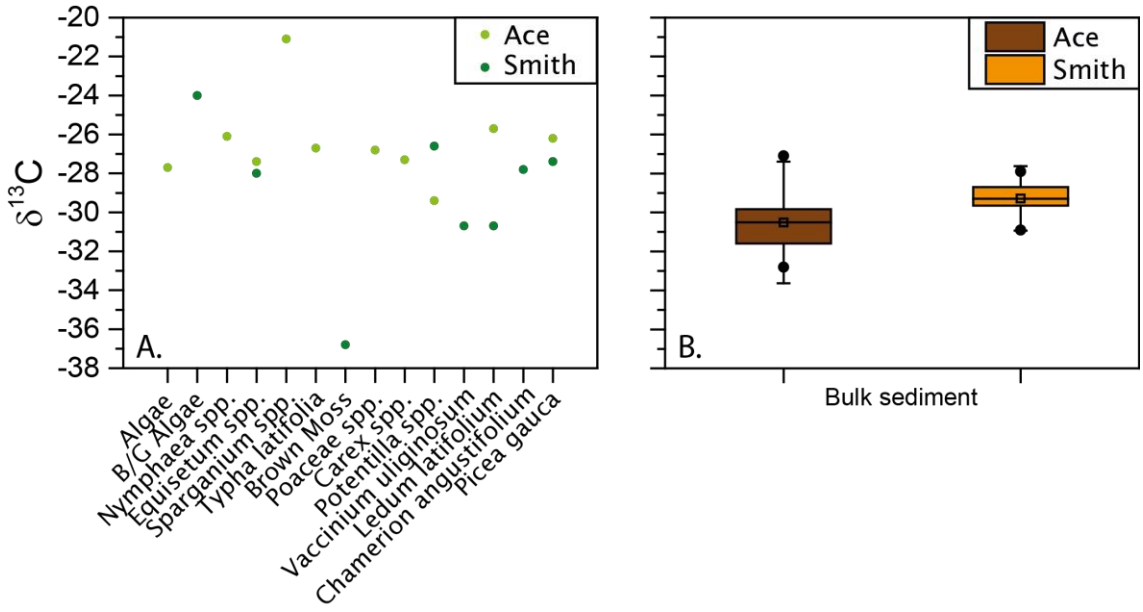

Figure 7.3. Stable isotope values of potential chironomid food sources.

a) Common vegetation at the sites **b**) Box plot of bulk sediment $\delta^{13}C$ values across both lakes. Whisker lines represent 1.5 SDs from the mean and the dots are minimum and maximum values. At Ace L. bulk sediment $\delta^{13}C$ values are more ^{13}C-depleted than individual vegetation components whereas the bulk sediment $\delta^{13}C$ values at Smith L. lie within the range seen in plant material.

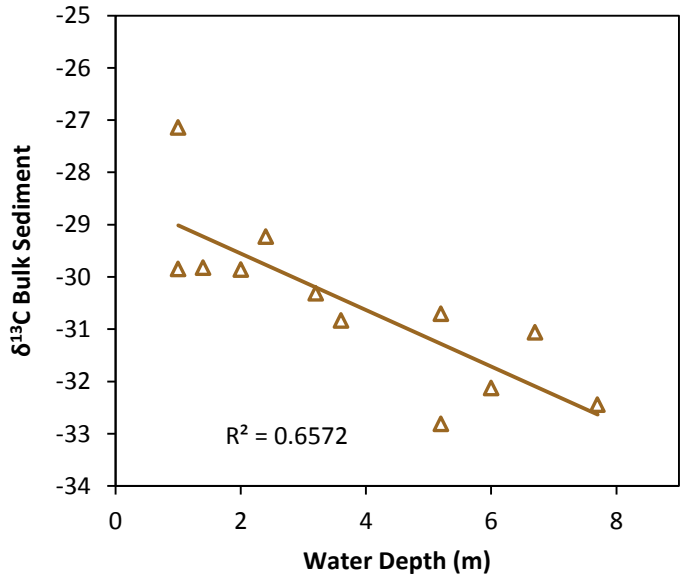

Figure 7.4 Bulk sediment $\delta^{13}C$ values plotted against water depth at Ace L.. The r^2 value is significant at the 0.05 confidence level.

7.4.3 Chironomid $\delta^{13}C$ values in lake surface sediments

A summary table of stable carbon isotopes in chironomids for both lakes is presented in table 7.1.

The stable carbon isotope values for *Chironomus* and *Microtendipes* at Smith L. are presented in graphical form in figures 7.5. The $\delta^{13}C$ values are plotted against distance from the thermokarst zone along a scale of sample numbers. The range of $\delta^{13}C$ values in chironomid HCs from the surface sediments of Smith L. varied both within an individual taxon and between the chosen taxa. *Chironomus* had both the lowest and the highest $\delta^{13}C$ of the studied taxa, with a range of 6.3‰ (from -35.9 and -29.6‰). The $\delta^{13}C$ values of *Microtendipes* have a narrower range than *Chironomus* of 2.4‰ from -32.7 to -30.3‰. The mean $\delta^{13}C$ value of *Microtendipes* was higher than *Chironomus* with at least a 1‰ difference between the two taxa.

Statistical testing (Mann-Whitney U) between the *Chironomus* samples in the centre of the lake and those in the thermokarst zone indicated that the populations are not statistically different. The same testing between all *Chironomus* and all *Microtendipes* samples from Smith L. indicated these populations are statistically different.

The stable carbon isotope values for *Chironomus* and *Endochironomus* in Ace L. are presented in graphical form in figure 7.6. The $\delta^{13}C$ values are plotted against water depth and are colour coded based on their location within the lake.

At Ace L., the overall number of chironomid HCs was low, therefore, many of the samples collected did not contain enough HCs for stable isotope analysis. The number of any single taxon that could be identified from samples in the centre of Ace L. was below the limits of methods (at least 10-15 large HCs required). Therefore samples from the littoral zone are compared to the thermokarst zone in Ace L.

The $\delta^{13}C$ values of *Endochironomus* in the littoral zone are consistent, ranging from -32.4 to -30.2‰. Only one sample contained enough HCs of *Endochironomus* in the thermokarst zone for stable carbon isotope analysis. *Endochironomus* from sample A11-4 in the thermokarst zone had a low $\delta^{13}C$ signal (-38.6‰) and this one of the lowest values observed across the whole

lake. The $\delta^{13}C$ values of *Chironomus* are more variable than *Endochironomus*, ranging from -40.2 to -32.4‰. The highest amount of variation in the $\delta^{13}C$ values of *Chironomus* is found in the thermokarst zone. Statistical testing (Mann-Whitney U) between *Chironomus* samples in the littoral zone and the thermokarst zone indicated the values are not statistically different. Statistical testing between all *Chironomus* samples and all *Endochironomus* samples at Ace L. indicated the populations are statistically different. A large amount of variability can be seen in the repeat samples of the same taxon from the same sediment core and in some instances the same depth slice. A maximum range of 4.3‰ was identified for within taxon variability within a single lake.

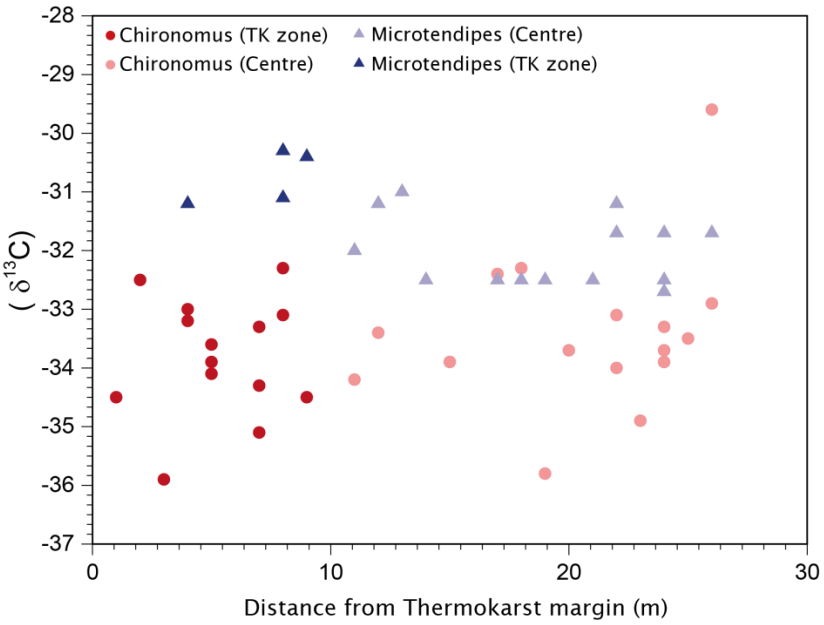

Figure 7.5 Stable carbon isotope results from Smith L.. Chironomid HC samples from both E-S and non E-S zones. A standard error of ± 0.1‰ was applied to all samples.

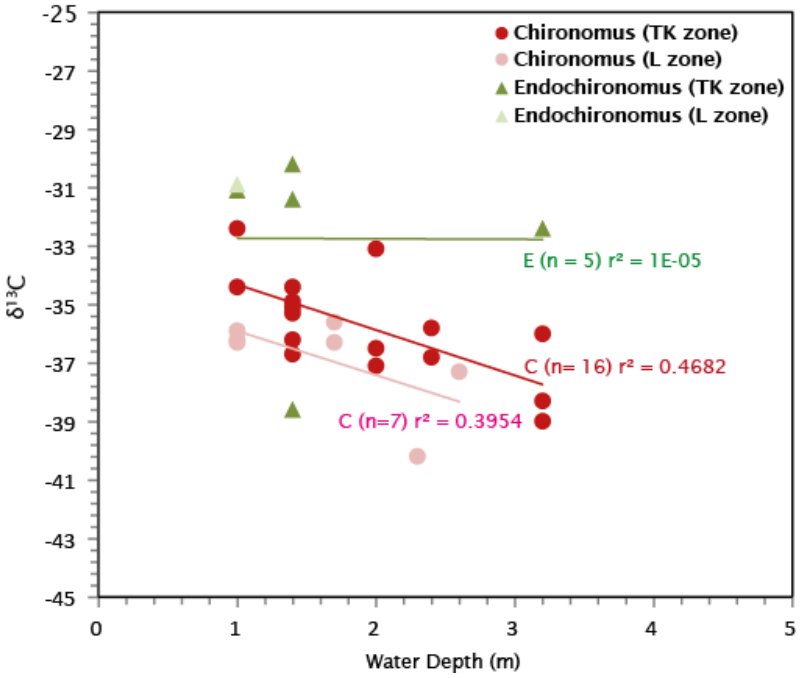

Figure 7.6 Stable carbon isotope results from Ace L..

.

7.4.3.1 Modern larval measurements

At Smith L., 20 sediment samples from the 2012 sampling year were sieved for modern chironomid larvae; however only a few larvae were found. No *Chironomus* larvae were found in the thermokarst zone. The $\delta^{13}C$ of the different chironomid larvae showed high variability, ranging from -38.2 to 32.7‰ (Figure 7.7). One sample of mixed larvae had a considerably lower $\delta^{13}C$ signal; however, even with this sample included, the $\delta^{13}C$ values of the larvae from the thermokarst zone are not significantly different to the larvae from the centre according to a Mann-Whitney u test.

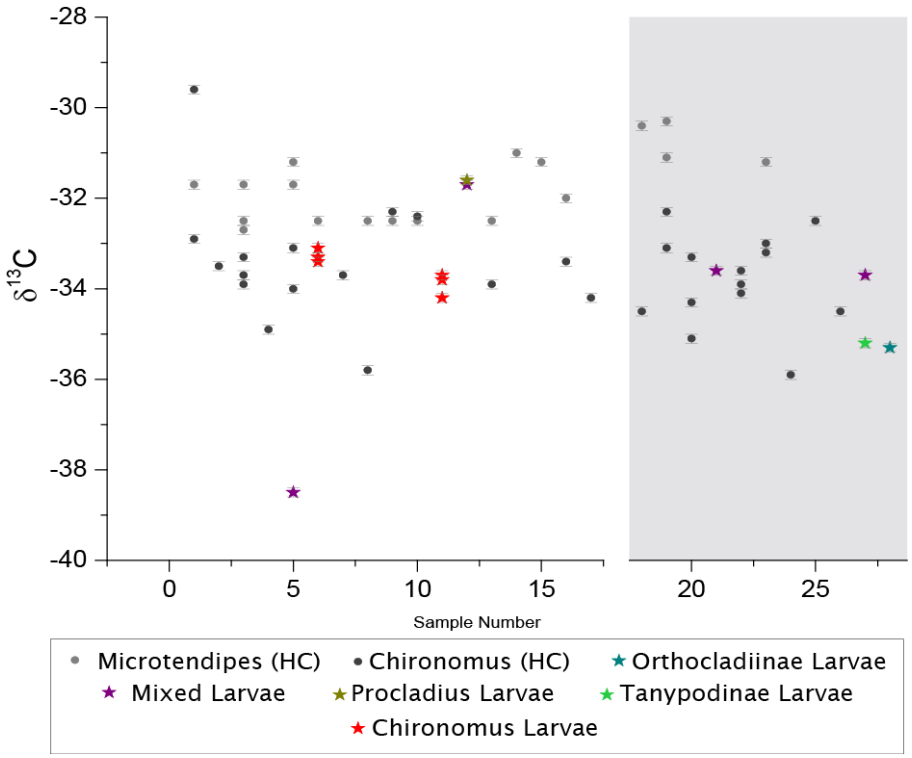

Figure 7.7 Stable carbon isotope values of chironomid larvae in Smith L.. $\delta^{13}C$ values of chironomid HCs are also plotted to compare to chironomid larvae. The grey box represents the thermokarst zone

The contents of the guts were removed from all larvae prior to isotope sampling. Two samples were large enough for stable carbon isotope analysis. The larvae are offset from the gut content by approximately 3‰ (Figure 7.8). The $\delta^{13}C$ values of the gut content are lower than bulk sediment $\delta^{13}C$ values indicating the potential for a secondary contribution beyond sedimentary detritus to the diet of the sampled larvae.

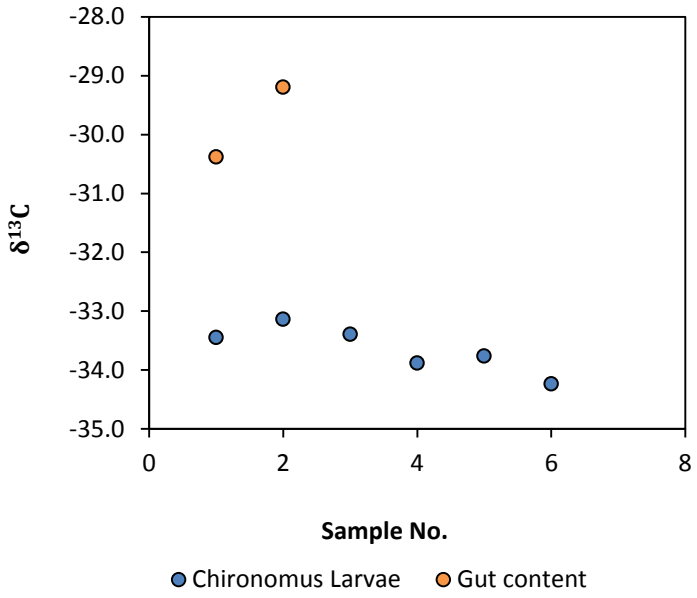

Figure 7.8 Stable isotope values of *Chironomus* larvae and gut content at Smith L.

At Smith L., $\delta^{13}C$ values of both chironomid taxa are more depleted than those of vegetation and bulk sediment (Figure 7.9). In the thermokarst zone, $\delta^{13}C$ of *Microtendipes* are on average 2‰ more depleted than $\delta^{13}C$ of bulk sediment. This is within the range that can be expected due to trophic discrimination (although often the values are less than 2‰; e.g. Goedkoop et al., 2006). All other sample groups in the dataset have $\delta^{13}C$ values which are lower than most of *Microtendipes* in the thermokarst zone.

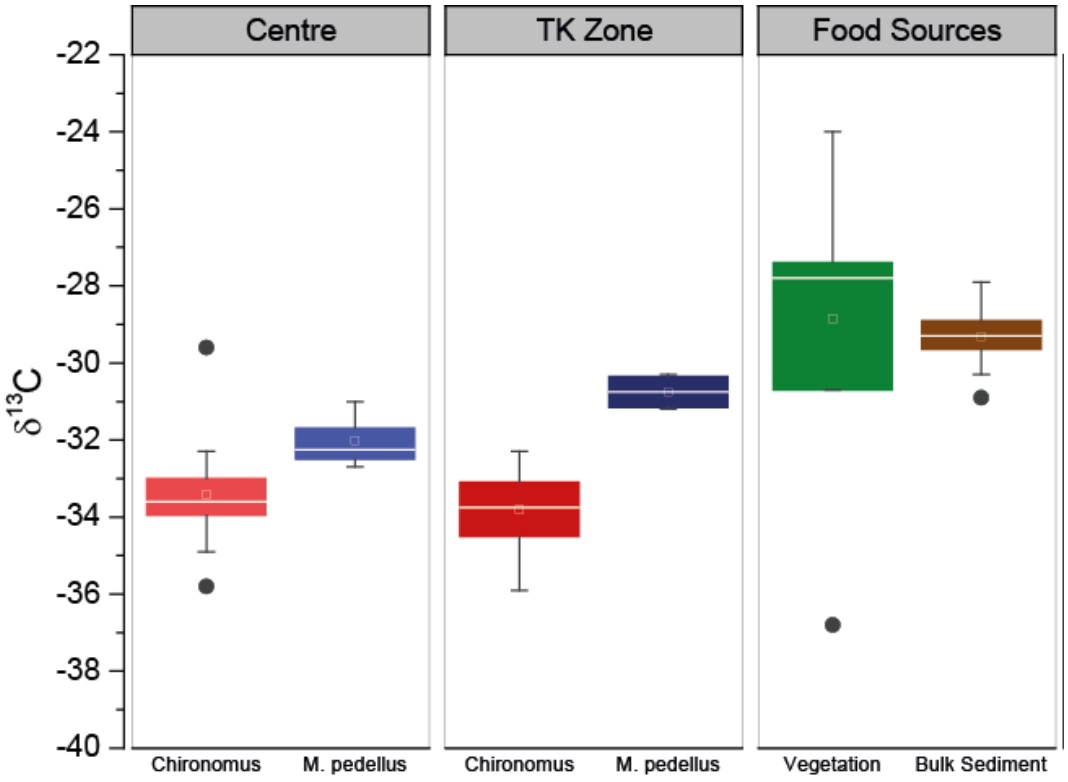

Figure 7.9 Chironomid HC samples and food sources at Smith L.. Outliers are plotted as filled circles. The white lines highlight median values. The whiskers represent the range within 1.5 of the inter quartile range.

The $\delta^{13}C$ values of vegetation, POM and bulk sediment at Ace L. show that the bulk sediment is likely composed of a mixture of POM and higher plant material (Figure 7.10. The $\delta^{13}C$ of *Endochironomus* is very similar to the mean $\delta^{13}C$ of bulk sediment and is higher than the average for POM. The $\delta^{13}C$ values of *Chironomus* are lower than all plant material (except for brown moss), POM and bulk sediment by at least 2‰.

Statistical testing between *Chironomus* and *Microtendipes* from samples within the thermokarst zone and in the centre indicated, in both cases, that the populations were significantly different to one another. Statistical testing between *Chironomus* and *Endochironomus* from samples within the thermokarst zone indicated that the populations were significantly different to one another.

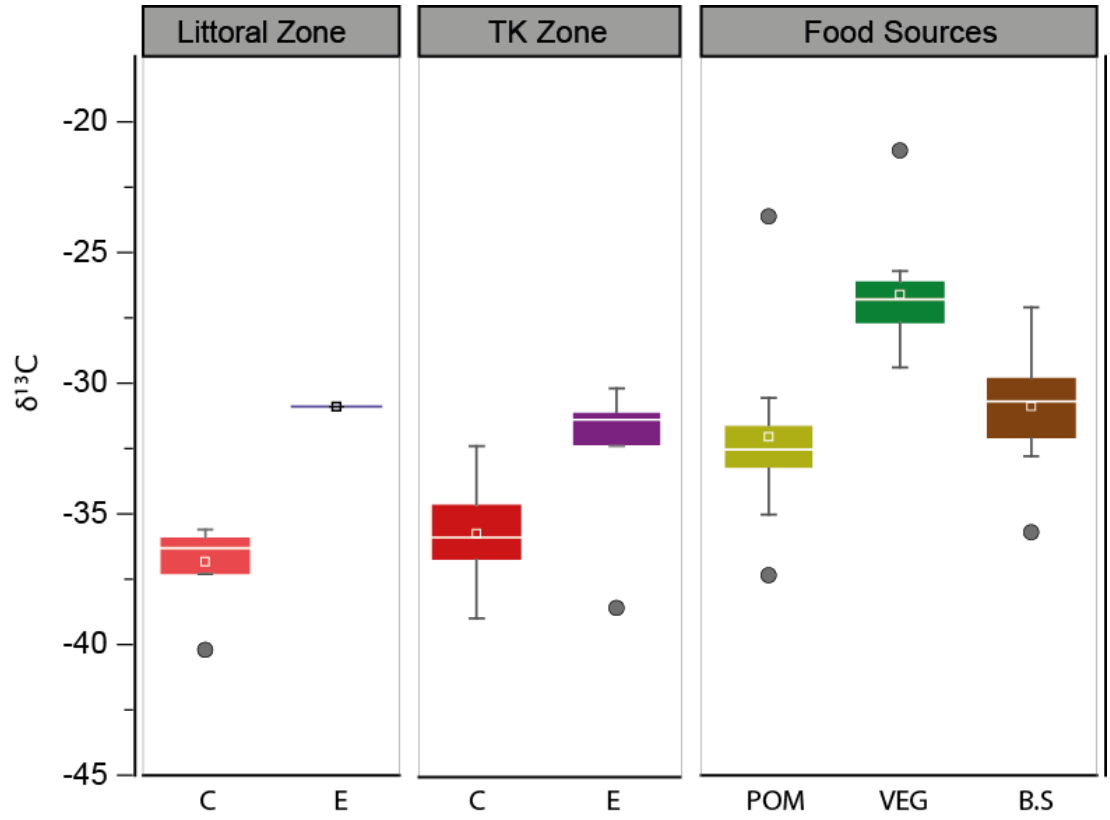

Figure 7.10 A boxplot of $\delta^{13}C$ values of chironomid HC samples and food sources at Ace L.. C = *Chironomus* E = *Endochrionomus*. The outliers are plotted as circles, The white lines highlight median values. The whisker lines show the range within 1.5 of the inter quartile range

Table 7.1 Stable isotope $\delta^{13}C$ values from different sources at both lakes and as a combined dataset

		Mean (‰)	Median (‰)	Standard Deviation (S.D)	n
Chironomus (TK zone)					
	Ace	-35.8	-35.9	1.7	16
	Smith	-33.8	-33.8	1.4	14
	Combined	-34.6	-34.3	1.9	30
Chironomus (non TK Zone)					
	Ace	-36.8	-36.3	1.6	7
	Smith	-33.4	-33.6	1.3	16
	Combined	-34.9	-34.6	1.9	23
Chironomus Larvae					
	Ace	--	--	--	
	Smith	-33.6	-33.6	0.4	6
	Combined	--	--	--	
All chironomid larvae					
	Ace	--	--	--	
	Smith	-34.2	-33.7	2.4	7
	Combined	--	--	---	
Other Taxon (TK Zone)					
	Ace	-31.2	-31.4	3.4	5
	Smith	-30.8	-30.8	0.5	4
	Combined	-31.8	-31.1	2.8	9
Other Taxon (non TK Zone)					
	Ace	--	--	--	
	Smith	-32.0	-32.3	0.6	14
	Combined	--	--	--	
Bulk Sediment					
	Ace	-30.9	-30.7	2.1	
	Smith	-29.3	-29.3	0.8	
	Combined	-30.1	-29.8	1.8	
Vegetation					
	Ace	-26.6	-26.8	2.1	
	Smith	-28.9	-27.9	3.4	
	Combined	-26.7	-27.4	3.0	
POM					
	Ace	-32	-32.5	3.8	
	Smith	--	--	--	
	Combined	--	--	--	

7.5 Discussion

7.5.1 The contribution of MOB to chironomid $\delta^{13}C$ values

The $\delta^{13}C$ of biological consumers in lakes typically reflect the $\delta^{13}C$ values of their food source, although a 0-1‰ shift might be expected due to trophic level discrimination and changing trophic levels (Peterson and Fry, 1987; Zanden and Rasmussen, 2001).

In this study the $\delta^{13}C$ values of *Chironomus* are significantly lower than the $\delta^{13}C$ values of both bulk sediment and the measured plant types. Previous studies have shown this genus to have low $\delta^{13}C$ values in comparison to bulk sediment which have been attributed to the consumption of MOB (Jones et al., 2008). The $\delta^{13}C$ values of *Chironomus* from this study are not as low as those in some studies but fit well within the range of values reported in the literature that also suggest assimilation of MOB (Jones and Grey 2011, van Hardenbroek et al., 2012), especially when comparing only the fossil data from the literature and not larval values. This genus builds tubes in surface sediments and the feeding habits of many species within the genus allow access to MOB and methane-derived carbon (Deines et al., 2007b). *C. anthracinus*-type contains species which are filter feeders, consuming mostly detritus that reaches the tube, whilst *C. plumosus*-type contains species which are predominantly detrital feeders, sweeping and consuming detritus surrounding the tube (Brooks et al., 2007). The lower $\delta^{13}C$ values of *Chironomus* might be expected if *Chironomus* are consuming a ^{13}C-dpleted food source such as MOB.

Further evidence supporting the theory that *Chironomus* might be utilising MOB is provided by Belle et al. (2014), who show evidence for the preferential assimilation of type I MOB over type II MOB by chironomids. He et al. (2012), found that type I MOB were more dominant in the upper most lake sediments (0-1 cm) in the thermokarst lakes in their study. Lake Killarney (~1km in between both lakes) was analysed by He et al. (2012). It is similar morphometrically, and therefore, it would be reasonable to assume a similar MOB profile at the lakes in this study.

The relationship between low $\delta^{13}C$ values of *Chironomus* and consumption of MOB can be tested using the $\delta^{13}C$ values of diploptene from chapter 5. A direct

comparison between the $\delta^{13}C$ values of both *Chironomus* and diploptene can be made where the same sample was analysed for both proxies. Two regions are compared: Ace L. thermokarst zone and the centre of Smith L.. The results from a regression analysis between the selected variables are presented in figure 7.11. If *Chironomus* consumption of MOB is based on the concentration of bacteria in the surrounding sediment, it might be expected that samples with the highest concentrations of MOB would correlate to the lowest $\delta^{13}C$ values of *Chironomus*. A strong correlation between *Chironomus* and diploptene $\delta^{13}C$ values is identified in Ace L. thermokarst but there is no correlation between the $\delta^{13}C$ values of diploptene and *Chironomus* in the centre of Smith L.. Whilst a correlation is identified in the thermokarst zone at Ace L. it should be noted that repeat samples of *Chironomus* highlight a 3-5 ‰ range which adds large uncertainty to the relationship.

At Ace L., the low $\delta^{13}C$ values of diploptene suggest a link between high methane flux from ebullition-seep areas and diffusion of methane from the sediments (see chapter 5 for full interpretations). The strong correlation between *Chironomus* and diploptene $\delta^{13}C$ values highlight that the carbon isotope signature of *Chironomus* larvae could be linked to methane ebullition-seeps.

The results from chapter 5 show that the diploptene $\delta^{13}C$ values at Smith L. are lower in the centre than in the thermokarst zone. This is interpreted as higher concentrations of MOB (and therefore higher supply) in the centre of the lake away from the site of methane ebullition seeps. The diploptene patterns at Smith L. suggest that the supply to the water column and therefore the level of methane diffusion from the sediment is not linked to methane ebullition-seep areas.

Even in Ace L. thermokarst zone where there is a strong correlation, the uncertainty is such that there is a 3-5‰ envelope at individual sample locations, which represents a significant range in the fossil record. Furthermore, the lack of correlation between *Chironomus* and diploptene $\delta^{13}C$ values (although this is a small sample size) in the centre of Smith L. suggests that shifts in the stable isotope composition of *Chironomus* are not linked to changes in the concentration of MOB in the surface sediments. This is important when considering the use of chironomids for reconstructing past

methane dynamics. Wooller et al. (2012) interpret downcore fluctuations in the $\delta^{13}C$ of bulk fossil chironomid samples as periods of higher methane availability from increased methane flux. The range of $\delta^{13}C$ values of bulk chironomids downcore in the study is the same as is evidenced within a single surface sample in this study (repeat samples from the same core and in most cases over between 0-1.5 cm depth). This raises the question of what the fluctuations seen in the Wooller et al. (2012) are truly representing and whether the signal to noise ratio in their study is small enough to truly highlight methane availability.

The same lake which is used in the Wooller et al. (2012) study was investigated by He et al. (2012) who, showed evidence for highest methane oxidation potential at the ebullition-seep site (when compared to other sites in the lake). In theory, it is possible that shifts towards lower chironomid $\delta^{13}C$ values are indicative of increased methane flux from ebullition-seeps in the study by Wooller et al. (2012). However, the sampling site for downcore chironomid reconstructions was not located near to the ebullition-seep area. The downcore reconstruction site used in Wooller et al. (2012) had a lower potential for methane oxidation in the surface sediment according to He et al. (2012). The results from Smith L. in this study suggest little connection between areas of highest methane ebullition flux, diffusion of methane from the sediments and chironomid $\delta^{13}C$ values. If lower $\delta^{13}C$ values of *Chironomus* cannot conclusively be linked to areas of high methane oxidation which, in turn, cannot be linked to areas of high methane flux from ebullition-seeps in contemporary environments, it is difficult to see how these variables can be linked in the fossil record.

In summary, the $\delta^{13}C$ values of *Chironomus* are lower than those of bulk sediment of measured plant types. When compared to other research, the low $\delta^{13}C$ values of *Chironomus* could be attributed to consumption of methane-derived carbon, however, when compared to the results from chapter 5 the connection is not as clear. In Ace L. thermokarst zone the low $\delta^{13}C$ values of *Chironomus* are well correlated with high supply of diffusive methane, whereas there is no correlation between areas of high supply and *Chironomus* $\delta^{13}C$ values in Smith L. Alternative explanations for low $\delta^{13}C$ values of *Chironomus* need to be considered and are discussed below.

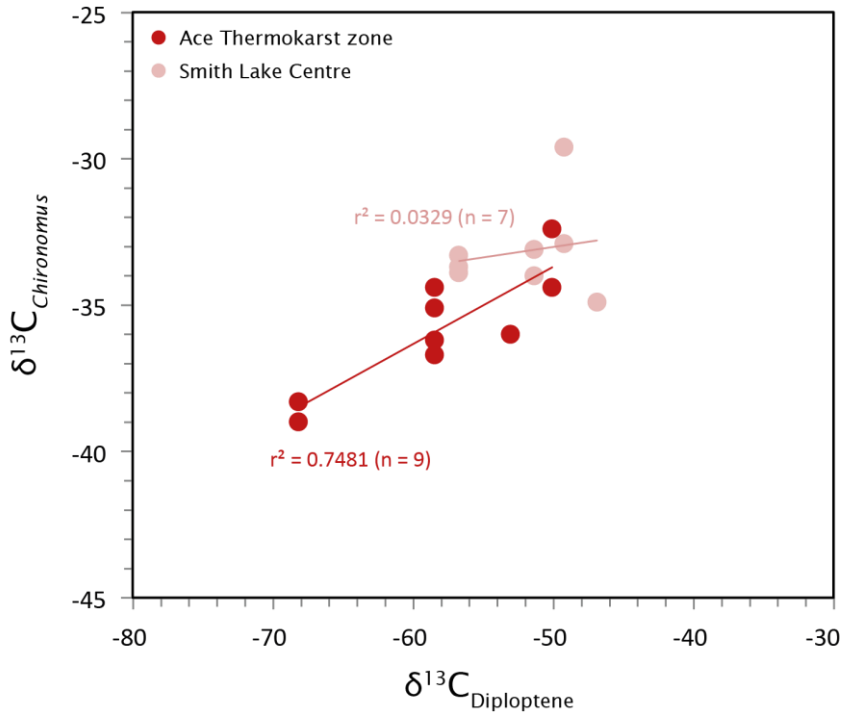

Figure 7.11 Linear regression between chironomus and diploptene $\delta^{13}C$ values from the same samples.

7.5.2 Alternative reasons for low $\delta^{13}C$ values of *Chironomus*

Lower $\delta^{13}C$ of *Chironomus* relative to the *Edochironomus/Microtendipes* $\delta^{13}C$ values due to the incorporation of ^{13}C-depleted food sources other than MOB cannot be ruled out, especially in Smith L. From the measured carbon sources in this study, two alternative sources of ^{13}C-depleted carbon can be identified that might contribute to low $\delta^{13}C$ values in *Chironomus*. Consumption of both POM and brown moss had lower $\delta^{13}C$ values than bulk sediment and could cause *Chironomus* $\delta^{13}C$ values to be low.

In Smith L., the $\delta^{13}C$ values of *Chironomus* are heterogeneous across the lake and do not appear to show a pattern that could be linked to the thermokarst zone. Another reason for the low $\delta^{13}C$ values of *Chironomus* in this lake could be due to the consumption of ^{13}C-depleted brown moss. A single stable isotope measurement of unidentified brown moss was analysed at Smith L. and had a surprisingly low $\delta^{13}C$ value (-36.8‰) when compared to values of identified

types in the literature (*Scorpidium scorpiodes:* -34 to -30‰; Liebner et al., 2011, -34‰; Rundel et al., 1979, Unidentified brown moss: -29‰; Hornibrook et al., 2000). If the sample that was analysed was contaminated with high levels of MOB, this could cause a lowering of the $\delta^{13}C$ value of the sample and the brown moss would appear to be depleted in ^{13}C. Liebner et al. (2011) highlight that MOB are closely associated with submerged brown mosses. If this is the case at the margins of Smith L., then bacterial contamination could be possible. In this instance, if *Chironomus* were consuming large amounts of brown moss, a lowering of its $\delta^{13}C$ value would still be due to the consumption of MOB and therefore this source of depletion can be ruled out as an alternative mechanism.

Alternatively, the heterogeneity in the $\delta^{13}C$ values of *Chironomus* and the similarities in the average $\delta^{13}C$ values between the thermokarst zone and other areas of the lake could be linked to the consumption of ^{13}C-depleted POM.

POM $\delta^{13}C$ values were not available for Smith L., however a study by Gu et al. (1996) studied Smith L. and found seasonally low $\delta^{13}C$ values of POM (-41.3 to -30.1‰). Whilst no spatial data is available, the results of previous research indicate the available and therefore the possibility of low $\delta^{13}C$ values of *Chironomus* due to ^{13}C-depleted POM.

At Ace L., *Chironomus* samples taken from the littoral zone had $\delta^{13}C$ values which were as low as those measured in the thermokarst zone (and include some of the lowest for the whole dataset). Due to the correlation between *Chironomus* $\delta^{13}C$ values and diploptene in the thermokarst zone, two possibilities as to why the $\delta^{13}C$ values are as low as they are in the littoral zone are proposed: that the lower $\delta^{13}C$ values of *Chironomus* are due to the assimilation of ^{13}C-depleted carbon from a different source, or that methane production and oxidation in this littoral zone is occurring to a greater degree than was previously thought. The possibilities are discussed below.

The $\delta^{13}C$ values of *Chironomus* across Ace L. are within the range of POM $\delta^{13}C$ values and at the lower limits of the bulk sediment $\delta^{13}C$ values. POM is often largely composed of phytoplankton is these lakes, especially in summer months (Gu and Alexander 1994). Finney et al. (2012) show evidence for even lower $\delta^{13}C$ values of POM in a number of lakes in Alaska, including Ace L.. They argue that catchment-derived groundwater which has ^{13}C-depleted DIC and

high pCO_2 can lead to low phytoplankton $\delta^{13}C$ values and therefore low POM $\delta^{13}C$ values. Although their study is largely based on Dune Lake, samples from Ace L. provide evidence towards the proposed idea (Figure 7.12). It is postulated that the low $\delta^{13}C$ values of *Chironomus* could be derived from consumption of ^{13}C-depleted POM. If this were the case, given that the similar feeding preferences of *Endochironomus/Microtendipes,* it might be expected that these taxa would demonstrate a similar stable isotope composition to *Chironomus*. So whilst consumption of ^{13}C-depleted POM cannot be ruled out, it seems unlikely as the other taxa in the study are not affected.

Alternatively, the low $\delta^{13}C$ values of *Chironomus* could be associated with higher levels of methane production and oxidation in the littoral zone than previously thought. The littoral zone at Ace L. is dominated by submerged and emergent aquatic vegetation such as *Nymphaea* (water Lilly) and *Typha* (Bull rush). The total area which is covered by these vegetation types is higher in this zone than in other areas of the lake due to the gentle bathymetric profile. (Chanton et al., 1992) showed evidence for MOB communities in sediments in the plant rhizosphere due to root ventilation. Therefore a macrophyte rich zone may also have higher concentrations of MOB. Agasild et al. (2013) showed evidence for very low $\delta^{13}C$ values of *C. plumosus* larvae (-63‰) in the macrophyte covered area of the lake which they attribute to the contribution of methane-derived carbon. The production level of methane in the littoral zone at Ace L. is unknown. This area could be a second zone of methane production in the talik bulb. This area of the lake is the input zone for inflow from the seasonally active water channels which might cause the thaw of underlying ice in this region. Alternatively, methane which is oxidised in the upper surface sediments could be from production in the anoxic surface sediments immediately below the oxic layer, although, at this time there is no way to test this hypothesis.

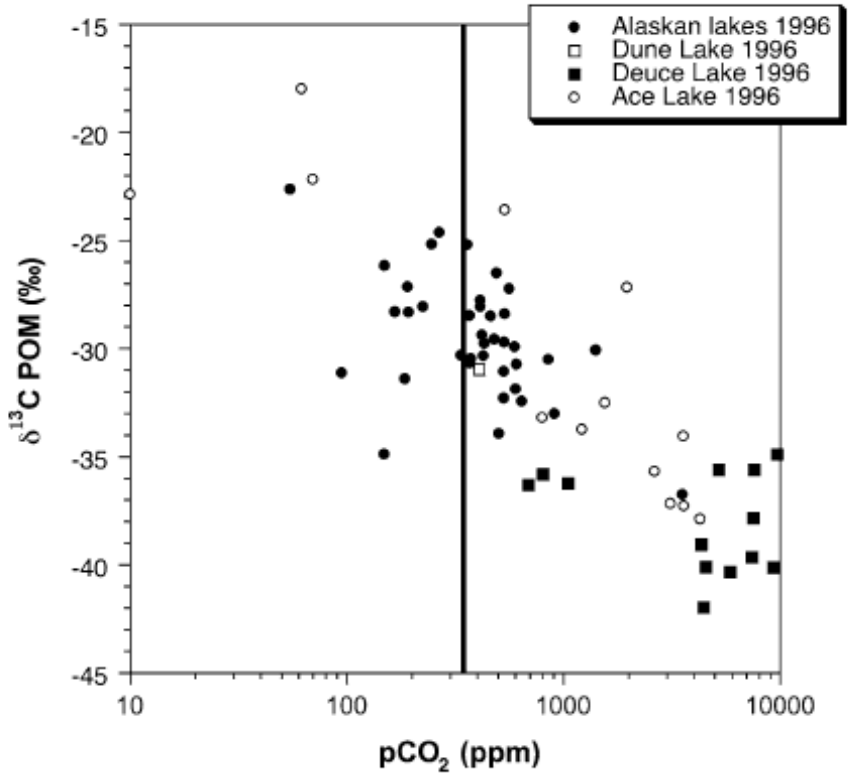

Figure 7.12 Partial pressure of CO_2 (pCO_2) in lake surface water and the $\delta^{13}C$ values of particulate organic matter (POM) from different lakes across Alaska. Ace L. was included in the study. Figure reproduced from Finney et al. (2012).

7.5.3 The importance of sample size and high taxonomic resolution for stable isotope studies of chironomids

Measurements of stable carbon isotope ratios of chironomids from surface sediments are based on many HCs (on average 15-20 HCs). If a large number of individual chironomids had $\delta^{13}C$ values that reflected bulk sediment and only a few incorporated a ^{13}C-depleted carbon source, $\delta^{13}C$ values lower than bulk sediment could reflect selective utilisation of MOB by a number of individuals in the integrated sample.

The results of the stable isotope analysis highlighted that the two chosen taxa were significantly different from each other (both in whole lake and within-zone comparisons). The $\delta^{13}C$ values of taxon-specific chironomid HCs samples are highly variable both within taxon and between taxa. The range of $\delta^{13}C$

values of *Chironomus* in this study is bigger than that of many downcore investigations using both bulk chironomid HCs (Wooller et al., 2012) and taxon-specific samples (Belle et al., 2014, van Hardenbroek et al., 2012). Although the variation in stable isotope composition of *Endochironomus/Microtendipes* is not usually as big as *Chironomus* there is still a 1-2‰ variation. Samples from this study also show large variation within-taxon within the same sample (4.3‰ range).

This study has highlighted that in some regions, despite a high level of noise in the data, correlations between chironomid and MOB $\delta^{13}C$ values can be seen. Within this correlation however, large uncertainties exist due within-taxon variability of $\delta^{13}C$ values. This suggests that although previous studies have evidence to link shifts in chironomid $\delta^{13}C$ values to changes in methane availability, caution is needed in interpretation of the relationships, especially downcore. Further work is needed in order to strengthen the relationship between low $\delta^{13}C$ values of *Chironomus* and MOB communities so it can be identified even in a noisy dataset.

7.5.4 Sources of carbon in chironomid diets

One of the aims of this chapter was to identify sources of carbon which could contribute to the $\delta^{13}C$ signatures of chironomid remains in lakes. A number of publications are available which give the expected range of $\delta^{13}C$ values from carbon sources such as terrestrial and aquatic vegetation (as highlighted in figure 7.2), however, often these ranges are wide which makes interpreting the specific contributions to $\delta^{13}C$ values of detritivores difficult. The $\delta^{13}C$ values of vegetation highlight that the bulk sediment $\delta^{13}C$ is predominantly derived from terrestrial and aquatic vegetation. This is not unexpected; however, the data are important for narrowing the range of values that are present in the literature. Understanding the catchment-specific $\delta^{13}C$ values highlighted that whilst most values appear to conform to those found by other researchers, some values were different.

The $\delta^{13}C$ values of POM highlight large seasonal variability but are overall lower than the $\delta^{13}C$ values of terrestrial and aquatic vegetation. Previous studies of POM at Ace L. have also found low $\delta^{13}C$ values, (Finney et al., 2012, figure 7.12). These low $\delta^{13}C$ values POM are a source of carbon which lowers the

average $\delta^{13}C$ values of the bulk sediment organic matter at Ace L.. POM was not measured at Smith L., but the average $\delta^{13}C$ values for bulk sediment suggest it is derived mostly from terrestrial and aquatic plant material.

In order to try to further disentangle the different carbon sources for chironomid diets, the relationships between a number of variables were assessed. The lakes were combined in order to increase the statistical significance of findings. However it should be noted that the correlations were consistently better in Ace L.. In fact all correlations presented in table 7.2 are applicable to Ace L., whilst only a few were apparent in Smith L., when the datasets were considered independently. Statistical testing (linear regression) highlighted the $\delta^{13}C$ values of *Chironomus* had a weak correlation ($p = >0.3$) with bulk sediment $\delta^{13}C$ values, C/N ratios, LOI, TOC and diploptene $\delta^{13}C$ values. This suggests that the $\delta^{13}C$ values of *Chironomus* might be driven by a numbers of factors but that diploptene $\delta^{13}C$ values are important in controlling *Chironomus* isotope signatures in Ace L..

Overall the stable carbon isotope data highlight that bulk sediment and all plant matter contained therein (terrestrial, aquatic and algal) have a statistically different stable carbon isotope signature to that of diploptene and therefore the MOB bacteria which contribute to the diploptene signal. The results did highlight that brown moss and POM had low $\delta^{13}C$ values. Consumption of these carbon sources by *Chironomus* could also explain the lower $\delta^{13}C$ values compared to the other carbon sources. Consumption of these carbon sources as opposed to MOB does not explain why *Endochironomus/microtendipes* do not also have depleted $\delta^{13}C$ values and therefore they are less likely explanations than the consumption of MOB

7.5.5 Chironomid $\delta^{13}C$ values as proxies for methane availability

This study investigated the relationships between methane production, oxidation and potential incorporation into the lake food web in a different system to those studied previously. The scale of methane production in thermokarst lakes is much greater than other lake systems and it was hypothesised that the scale of oxidation and incorporation into the food web would also be greater. The results from this research suggest that even in an environment with the potential to have a strong relationship with methane

production, and consumption by organisms, this is not always the case. In Ace L., a correlation between the $\delta^{13}C$ values of *Chironomus* and diploptene suggest that with high MOB concentrations, the $\delta^{13}C$ values of *Chironomus* will be significantly lower than bulk sediment $\delta^{13}C$ values which might be traced through downcore sediments. However, both the high within-taxon, within-sample variability and the lack of connection between *Chironomus* and diploptene in Smith L. counteract this argument and highlight the need for caution when attributing low $\delta^{13}C$ values in chironomids to consumption of methane-derived carbon.

Table 7.2 Linear regression values. between: water depth, sediment geochemistry (bulk sediment $\delta^{13}C$ values, C/N ratio, loss-on-ignition (LOI), total organic carbon (TOC), $\delta^{13}C$ values of *Chironomus* (Chiro $\delta^{13}C$), $\delta^{13}C$ values of *Endochironomus/Microtendipes* (2nd taxon). Bottom left = regression values. Top right = statistically significant at the 0.05 confidance interval, Yes (Y), No (N) or not enough data (N/A).

	Water Depth	**$\delta^{13}C$ Bulk**	**C/N ratios**	**LOI**	**TOC**	**$\delta^{13}C$ Dip**	**$\delta^{13}C$ Chiro**	**2nd Taxon**
Water Depth	-	Y	Y	N	N	Y	Y	N
$\delta^{13}C$ Bulk	0.62	-	Y	N	N	N/A	Y	N/A
C/N ratios	0.32	0.68	-	N	N	N/A	Y	N/A
LOI	0.04	0.00	0.01	-	Y	N	Y	Y
TOC	0.05	0.00	0.02	0.97	-	N/A	Y	N/A
$\delta^{13}C$ Dip	0.41	N/A	N/A	0.32	N/A	-	Y	N
$\delta^{13}C$ Chiro	0.13	0.32	0.35	0.38	0.48	0.58	-	N
2nd taxon	0.02	N/A	N/A	0.26*	N/A	0.01	0.00	-

7.6 Conclusions

This chapter investigated whether taxon-specific chironomids were assimilating methane in a measureable way that could be linked with patterns of methane ebullition flux from the lakes.

The $\delta^{13}C$ values of *Chironomus* were correlated with diploptene $\delta^{13}C$ values in Ace L. thermokarst zone suggesting a link between *Chironomus* stable isotope compositions and high levels of methane flux from ebullition-seeps in this lake. The $\delta^{13}C$ values of *Chironomus* in Smith L. were not correlated with diploptene $\delta^{13}C$ values and therefore could not be linked to high methane oxidation. Overall the $\delta^{13}C$ values of *Chironomus* were highly heterogeneous but no distinction between zones could be made on the basis of $\delta^{13}C$ values alone. In Ace L., the similarity in $\delta^{13}C$ values in both zones was attributed to higher than expected methane oxidation in the littoral zone. The patterns of MO across thermokarst lakes might be reflected in the low $\delta^{13}C$ values of *Chironomus* that are significantly different to *Endochironomus/Microtendipes* and bulk sediment. However, the within-lake, within taxon variability is very high, making it difficult to extract the relationships. Other carbon sources which might lower the $\delta^{13}C$ values still need to be investigated also.

Taxon-specific samples are important in order to highlight patterns of different carbon sources. Amalgamation of different taxa will result in the dampening of a strong signal to any individual taxon.

As the data stand, there is a correlation between the stable carbon isotope values of diploptene and *Chironomus* Ace L. but not in Smith L. and the large range of $\delta^{13}C$ values for *Chironomus* mean that there is a high signal to noise ratio. Further work needs to be completed to fully understand the complex relationships between methane production, transport, oxidation and consumption by organisms in the lake food web.

Chapter 8: Discussion and Conclusions

8.1 Introduction

Wetlands, which include lakes and ponds, are an important component of the land surface in permafrost environments (Muster et al., 2013). Ice-rich permafrost regions are susceptible to thaw due to increased temperatures and precipitation associated with future climate change (Colins et al., 2013) and the total number of small lakes is likely to increase (Grosse et al., 2008). In the decade prior to the initiation of this research project, methane emissions from wetland environments and more specifically, thermokarst lakes, became a prominent aspect of high-latitude, permafrost-based research (see section 2.5 for full reference list). A number of fundamental research papers were published highlighting the importance of these environments for the arctic carbon cycle (Zimov et al., 1997; Walter et al., 2006; Grosse et al., 2008; Walter et al., 2008a).

Zimov et al. (1997) and Schuur et al. (2008) suggest 450 and 407 Gt respectively, of carbon is currently stored in frozen northern Siberian yedoma deposits. Active thermokarst lakes in northern Siberia and Alaska that have developed in yedoma sediments (yedoma lakes) can cause the thaw of underlying and surrounding frozen sediments. This exposes the highly labile yedoma carbon to processes of anaerobic decomposition such as methanogenesis. The newly generated methane comes out in solution or in bubbles which are transported to the atmosphere via ebullition from the sediments through the overlying lake water column (Walter Anthony et al., 2010). As a result thermokarst lakes have been identified as potential sources of high methane production (Walter et al., 2006; Zimov et al., 2006a; Walter et al., 2007b).

A conceptual model for the evolution of yedoma thermokarst lakes suggests that methane is emitted from the active thermokarst margins (Walter et al., 2006, 2008a), therefore as the lake expands, the zone of methane production should migrate with the shoreline. A proxy for the presence of large scale methane production and emission, or for the zone of methane production (e.g. the active thermokarst margin) and the temporal rate at which it migrates in

thermokarst lakes would allow a greater understanding of temporal evolution of thermokarst lake dynamics. This may provide a valuable insight into the degree to which the rate and magnitude of carbon release varies within a thermokarst lake through time.

Large uncertainties exist in our understanding of the spatial and temporal complexity of methane emissions (and therefore quantification of methane emissions) from thermokarst lakes. Empirical flux measurements are difficult to make, and they vary seasonally and with the weather. Spatially, ebullition is apparent in certain marginal zones, but upscaling the patchy occurrence of ebullition is difficult, as although evidence of ebullition is obvious (e.g. bubbles trapped in ice), capturing the full extent of methane emissions is difficult (Walter Anthony et al., 2010). Initial work by Zimov et al. (1997) estimated that northern Siberian thermokarst lakes contribute ~2 Tg CH_4 yr^{-1} to the annual atmospheric methane concentration. Following this, Walter et al. (2006) re-evaluated the same lakes and suggested a higher contribution of 3.7 Tg CH_4 yr^{-1}. The results of both these studies have been subsequently used as regional estimates of the permafrost carbon stock (e.g., O'Connor et al. 2010) or used in studies attempting to understand regional methane emissions (e.g., McGuire et al., 2010). A later publication by van Huissteden et al. (2011) highlighted that methane emissions from thermokarst lakes in northern Siberia might be significantly lower than those estimated previously, due in part, to the incorporation of lake drainage into their calculations; a process excluded in previous studies.

Greater understanding of contemporary methane dynamics is vital for the accurate estimation of contributions to the carbon cycle. To improve our understanding it is important to increase the overall number of fine resolution (site-specific) studies, utilising a range of methodologies (e.g. differing biogeochemical proxies). The knowledge gained from such research can then be up-scaled to provide more robust estimates of carbon contributions to regional and global carbon cycles.

Not only is it important to understand contemporary methane dynamics over highly resolved spatial scales, it is imperative that a clearer understanding of temporal variability in methane emissions in these lake environments is gained. The current spatial heterogeneity affects the accuracy of emission

predictions, and also the understanding of changes in historical carbon stocks. A better understanding of methane cycling in thermokarst lakes may also further our knowledge of limnological processes and improve our ability to make future predictions. Methane emissions from a single lake depend on a number of criteria, including total lake area, lake expansion rates, and potentially on the thermokarst zone migration (as described above). They may also depend upon climate and it affects in the thermokarst landscape, for example, wind, or lake features ultimately depend on climate, such as water depth or water temperature. Some idea of temporal variability would be beneficial, as would tracing the displacement of ebullition zones (if they were possible to identify from sediments).

8.2 Empirical findings and implications

The main findings of this research project are chapter-specific and detailed discussions and conclusions are found within the respective chapters (Chapters 4 to 7). This section will draw upon the findings from all the chapters to answer the primary research question of this thesis: **to investigate the biogeochemical interactions between methane and organisms within the food web of thermokarst lakes.**

In order to answer the given research aim, it was important to establish the basic limnological profile of the lakes in order to assess the viability of the lakes as sites in which to study thermokarst lake carbon cycling. This included establishing the methane emission profiles and basic limnological functioning, assessing the study lake similarities and differences comparing these lakes with other thermokarst lakes from different regions (sections 8.2.1 and 8.2.2). Sections 8.2.3 and 8.2.4 highlight the complicated nature of the findings with regard to answering the research question.

8.2.1 Methane emissions from Ace and Smith Lakes

The lakes in this study were chosen for a number of reasons that are detailed in chapter 3, however, of upmost importance was a clear indication that the lakes were producing and emitting methane on a large enough scale for ebullition to be observed and quantified. Both these lakes were not only easily accessible, but both are part of ongoing research into GHG emissions from

thermokarst lakes (Sepulveda-Jauregui et al., 2014). Secondary data on methane dynamics were readily available, and whilst validation of the secondary data was important, its availability meant this study could focus on developing a method of detecting the source areas of methane using biogeochemical proxies from lake sediments rather than collecting data on methane emissions. The data which were available prior to initiation of the project quantified the amount of methane emissions from a single ebullition-seep in the thermokarst zone of each lake (Figure 5.2; K M Walter Anthony). Further to these initial data, the methane emission profiles from both lakes were developed through qualitative observation of the thermokarst and non thermokarst zones and quantified bubble counts (Figure 5.3; this project), qualitative observations of the thermokarst zones in this project and via newly published data on methane emissions from a number of lakes including Ace L. and Smith L. (Sepulveda-Jauregui et al., 2014).

Although both lakes were identified as having high methane emissions (85 and 151mg CH_4 m^{-2} d^{-1}), differences in their methane dynamics were identified. A key difference was the ^{14}C radiocarbon age of the methane emitted at ebullition-seeps in the thermokarst zone. The data suggest that the methane from ebullition-seeps at Ace L. is Pleistocene in age (Walter Anthony *pers comm*), whilst the methane from ebullition-seeps at Smith L. is late Holocene in age (2.5ka). The difference in ages of the methane has been attributed to a difference in the source carbon being used in methanogenesis. The old age of the methane at Ace L. indicates an old carbon source, most likely Pleistocene Yedoma sediments in the deep talik bulb (Walter Anthony *pers comm*). Methanogenesis in the thermokarst zone at Smith L., on the other hand, could be derived from Holocene material slumped in at the thermokarst edge.

Both lakes are formed in loess (or loess-related deposits) which were deposited in the Late Quaternary (Muhs and Budahn, 2006) and re-transported from the hill slopes to the valley bottoms via colluvial processes (Pewé 1955). Ace L. is approximately 80m higher in elevation than Smith L. and lies almost on the top of Gold Hill, a local high point underlain by *in situ* and/or lightly retransported loess (Pewé 1975). This portion of the landscape fits well a definition of yedoma (although it is far less rich in massive ground ice than Siberian equivalents; M. Edwards, *pers comm*). However, Smith L. lies in a low saddle between higher loess-mantled slopes, which may have previously been the

drainage for Happy Creek. Reworking and/or removal of loess in this location may have further reduced the ice content and replaced the older carbon with younger deposits. In this case, the capacity for thermal erosion could have been reduced, along with the overall carbon content, thus reducing the capacity for methanogenesis in the underlying talik.

8.2.2 Lake classification: how representative are the study sites of thermokarst lakes?

When considering the methane emission data only, both study lakes appear to be comparable to other thermokarst or thermokarst-affected lakes both locally and in other geographically distant regions (Sepulveda-Jauregui et al., 2014). However, when the rest of the results are considered, it is clear that Ace and Smith L.s differ from each other in several ways. As described above, the methane from the lakes is likely produced in different sediments, resulting in different methane ebullition rates. Through the analysis of many different biogeochemical aspects of these lakes a more refined classification can be made. Ace L. can be classified as a Yedoma-type thermokarst lake. Alexander and Barsdate (1974) suggest that Ace L. was formed due to thawing of ice-rich permafrost. Its bathymetry is similar to that of lakes found in Northern Siberia and Seward Peninsula in Alaska (Walter et al., 2008a, West and Plug 2008), with a deep (9m) centre and steep sides (especially those close to the current thermokarst margin). Furthermore, its high inorganic content and terrestrial input at the thermokarst margin add weight to the argument that Ace L. can be classified as a yedoma thermokarst lake.

Smith L. however, is representative of a shallow, stable, thermokarst-affected lake. The results of the organic lake sediment analysis (Chapter 4) highlighted that there was little terrestrial sediment entering the lake which indicates that the thermokarst margin is not as active as it is in Ace L.. This suggests higher stability of the lake margin as there is less thermal erosion. Although the lake is thought to have formed through thermokarst action (Alexander and Barsdate, 1971), it is postulated that a lower ground-ice content due to re-working in the lower areas of Happy Creek (described above) reduced the thermokarst activity over time. Other lakes with similar morphometries occur in lowlands and valleys in the interior of Alaska where the original Pleistocene loess has undergone reworking and erosion.

This research has highlighted that even within a small geographic area and similar underlying substrates, lakes differ in properties and processes. It is therefore crucial to understand the basic limnological profile of a lake if it is to be used as a type site or in any upscaling exercises. In a complex topographical region like Interior Alaska, lakes can occasionally be located on high ground that has suffered little erosion, but they are more typically on surfaces that have undergone erosion and/or deposition (like Smith L.). It is likely that the ice content and carbon content, susceptibility to bank erosion, age and labiality of carbon will vary spatially and therefore interpretations of results should be done so with this in mind.

8.2.3 A sediment-based proxy for methane in thermokarst lakes

Through the increased understanding of the limnological and ecological functioning of the study lakes, a more detailed and accurate understanding of lake carbon cycling with regard to biological proxies has been gained. In order to understand how well the chosen proxies reflect large-scale methane supply, properties of sediments and microfossils were interpreted in relation to the observed methane emission patterns. An important question was: can the thermokarst zone be distinguished from other areas of the lake using lake organisms?

It was hypothesised that a thermokarst zone might be distinguished in a number of ways. Firstly, diploptene $\delta^{13}C$ values in this zone would be markedly low and indicate the presence of MOB; secondly, fossil chironomid samples (both head capsules and larvae) would have lower $\delta^{13}C$ values than vegetation and bulk sediment, reflecting partial consumption of MOB, and finally, the fossil chironomid assemblage in the thermokarst zone would be different from that of the rest of the lake. All three datasets appear to show a similar pattern with regard to the thermokarst zone in Ace L..

The diploptene $\delta^{13}C$ values were low in the thermokarst zone at Ace L.. Previous studies have attributed similar ^{13}C-depleted values of diploptene to high levels of MOB in other environments (Spooner et al., 1994, van Winden 2010, Zheng et al., 2014). Therefore it is argued that in the Ace L. thermokarst zone, there is a high amount of MOB, and by extension, a higher supply rate of

methane in this zone: large enough to constitute a difference in diploptene $\delta^{13}C$ values (when compared with the other samples in the dataset).

In the Ace L. thermokarst zone, the $\delta^{13}C$ values of diploptene and *Chironomus* are positively correlated, suggesting a relationship between an area of higher methane supply and increased consumption of MOB by *Chironomus* larvae. Thus, from Ace data, a proxy-isotope indicator of high emissions appears plausible. Developmental preferences of *Chironomus* such as tube building and aeration of the tube are conducive to the growth of MOB, as highlighted in a number of studies previously (Jones and Grey 2011). Previous studies have argued that $\delta^{13}C$ values of chironomids (Larvae and head capsules samples) can be attributed to the assimilation of methane-derived carbon via consumption of MOB (Jones and Grey 2011). However, others have pointed out that lower $\delta^{13}C$ values in chironomids than in detritus and bulk sediment can also be due to other causes, such as consumption of isotopically depleted POM. Belle et al. (2014) suggest that the stable carbon isotope values of chironomids alone may not be enough to definitively argue for the consumption of MOB. They suggest other lines of evidence should be used when only a moderate depletion in $\delta^{13}C$ values is seen in chironomids. Using both the diploptene and chironomid $\delta^{13}C$ values in conjunction may be a good method for detecting MOB in lake sediments. Interestingly, one sample of *Endochironomus* HCs also showed a low $\delta^{13}C$ value in Ace L. thermokarst zone, hinting that methane assimilation, whilst not the norm, might occur in other taxa in locations where large amounts of MOB are present.

The results from chapter 6 highlight that the chironomid assemblages in samples from the thermokarst zone are more similar to each other than those in the rest of the lake. This clustering was driven mostly by a larger number of undifferentiated specimens in thermokarst zone samples compared to the rest of the lake. Many of the head capsules were either damaged or not clean enough to allow identification. The reasons for the increase in numbers of damaged or dirty head capsules in this zone are not fully understood, however, this increase could be used as a means for distinguishing the thermokarst zone.

Therefore, analysis of organisms (and/or their $\delta^{13}C$ signatures) in Ace L. the thermokarst zone highlight the potential of using multiple lines of evidence to

distinguish an area of high methane production within a single lake. The fact that all three lines of evidence appear to show a similar pattern with regard to this zone increases the confidence that can be placed in the results. These findings have important implications as they indicate that with further development the methods might be good proxies for methane ebullition-seeps. However, all proxies show high variability in sample values; although broad trends are detectable, relationships are noisy. At present, a conservative position would be that none of the proxies could reliably be used on its own to differentiate a zone of methane ebullition from other areas of a lake.

8.2.4 Complexities of estimating methane derived carbon in the lake food web

Although the evidence from the Ace L. thermokarst zone suggests that the approaches used in this study might indicate a difference in supply rates of methane (possibly linked to high methane ebullition flux), the results from the rest of the lake need to be considered in order to contextualise and validate these findings.

The results from the littoral zone of Ace L. show that the stable carbon isotopes of *Chironomus* are similar to those in the thermokarst zone. Two possible ideas of why this might be are presented below.

If the initial assumption that the rest of the lake area has a relatively low level of methane production compared to the thermokarst zone is correct, then the low $\delta^{13}C$ of *Chironomus* from the littoral zone would have to be linked to a different ^{13}C-depleted carbon source. This would invalidate the correlation between the proxies in the thermokarst zone. One explanation for the similarity in $\delta^{13}C$ values of *Chironomus* in the littoral and thermokarst zones has been developed through this research. Low stable carbon isotope values *Chironomus* could be linked to the consumption of ^{13}C-depleted POM. This idea is discussed in detail in chapter 7. It was concluded that if *Chironomus* were consuming ^{13}C-depleted POM then it would be expected that *Endochironomus* would have low $\delta^{13}C$ values also. On average, *Endochironomus* $\delta^{13}C$ values reflected the consumption of bulk sediment and were not low, suggesting a difference in feeding mechanisms between the two taxa. Therefore an alternative explanation was sought.

Another explanation is that the supply of dissolved methane is high in this zone also. High amounts of methane diffusing from the sediments could be linked to either high surface production or a second site of deeper, talik bulb methane production not characterised by ebullition-seeps. This idea is discussed in detail in chapter 6. It was postulated that methane might be produced in anoxic surficial sediments. The littoral zone is dominated by aquatic and emergent vegetation, more so than the thermokarst zone (due to the shallow bathymetric profile across a large area in the littoral zone as a whole). This allows both plant-mediated transport of methane produced in the anoxic surface sediments but can also increase the MOB community (Agasild et al., 2014). Bastviken et al. (2008) show evidence for the importance of the shallow-littoral zone for non-plant mediated methane flux and others have argued that these areas are important for plant-mediated flux also (Kankaala et al., 2003). It was concluded in chapter 7 that it is difficult to differentiate surface methane production from deep thaw bulb production in the current dataset. If methane is being produced in the littoral zone, there is currently, little evidence for methane ebullition, although ebullition has been observed infrequently in this zone (Walter Anthony *Pers comm* 2015). One approach to distinguish between deep or surficial methane production might be to compare the $\delta^{13}C$ values of both the methane and the diploptene from different regions of the lake (with more data than was available here). Walter et al. (2008a) highlights that the different zones of methane production (surface or yedoma sediments) use different pathways (acetate fermentation in surface sediments and CO_2 reduction from deep sources) and therefore the corresponding $\delta^{13}C$ values will be different. Further work is required in order to understand the methane dynamics in the littoral zone, thereby increasing our knowledge of the total lake potential methane production zones.

It is important to also consider Smith L., which has an altogether different pattern to Ace L. At Smith L. diploptene is present in both the centre and the thermokarst zone, while the low $\delta^{13}C$ values of diploptene relative to bulk sediment values suggest that MOB are likely contributing to the diploptene signal to some degree in both areas (although the contribution is very small in some samples). The $\delta^{13}C$ values of diploptene are lower in the centre than in the thermokarst zone, which is assumed to reflect a higher abundance of MOB and therefore evidence for more MO in the centre relative to the thermokarst

Zone. This fits well with evidence from Sepulveda-Jauregui et al. (2014): diffusive methane flux measured in the centre of Smith L. was relatively high compared with values in other non-yedoma lakes in the same study.

In Smith L., the average $\delta^{13}C$ values of *Chironomus* are similar in the thermokarst zone and the rest of the lake. Low $\delta^{13}C$ values of diploptene and *Chironomus* are not strongly linked at the sample level. The results presented in chapter 5 suggest high supply of dissolved methane in the centre of Smith L. where diploptene concentrations are higher (which is also seen by Sepulveda-Jauregui et al., 2014). It is hypothesised the high diffusion of methane in the centre of Smith L. is linked to high levels of surface methane production, as there are no visible signs of ebullition in the centre. However, the $\delta^{13}C$ values of *Chironomus* are statistically indistinguishable between the areas. It is therefore difficult to argue the *Chironomus* $\delta^{13}C$ values reflect increased utilisation of MOB.

Chapter 7 highlights the high within-lake, within-taxon variability of the $\delta^{13}C$ values in the surface sediment samples from Ace L. and Smith L. The range in $\delta^{13}C$ values seen in the surface sediments is similar to the range in values identified downcore in other lakes (e.g. Wooller et al., 2012). This large contemporary variation, together with rather limited correlation between $\delta^{13}C$ values and observed levels of methane production, means that down-core variations in stable isotope values should be interpreted with extreme caution. The variability recorded downcore may be a record of the small-scale spatial heterogeneity observed in modern sediments and not a reflection of temporal shifts in methane availability that could be extended to a whole lake.

8.3 Limitations and future research

This research project employed robust techniques in novel ways and led to the identification of several limitations in relation to methane proxies. However, it also points to future research that could be employed to overcome those limitations. The following section outlines three main areas where improvements could be made in order to increase our knowledge of biogeochemical interactions in thermokarst lakes. These include: sampling strategy and resolution, the choice of study site and alternative proxies for methane in lakes.

8.3.1 Sampling strategy and resolution: increasing sample points and coverage

Firstly, a confounding factor that limits the ability to thoroughly assess some of the datasets is the lack of data from the rest of the Ace L. (e.g. the central deeper region). There were very low concentrations of chironomid HCs in almost all samples from the centre of Ace L., and often all the collected sediment was exhausted with little to show in the way of chironomid totals. The sampling strategy employed for the analysis of lipid biomarkers (which was restricted by available resources) was to focus on samples where $\delta^{13}C$ measurements on chironomid head capsules were also possible. This meant that no diploptene $\delta^{13}C$ values were available from the centre of the lake, and therefore the MOB concentrations in this area are unknown. Furthermore, the lipid biomarker analysis was completed prior to obtaining samples from the littoral zone at Ace L. which meant diploptene values could not be assessed for this region either. More samples from other areas of the lake, especially diploptene $\delta^{13}C$ values, would allow a better comparison of whole lake methane cycling.

Further to improving the coverage of specific lake areas (e.g. the deep centre and the littoral zone), the number of overall samples per lake could be increased. The sampling strategy employed aimed to analyse the highest number of samples possible without compromising on the quality of the data. Despite this, the spatial resolution at which samples are retrieved from a single site and the number of study sites which are analysed will always be restricted by the time and resources available. More samples would allow more robust statistical testing and reduce the uncertainty in the relationships. For example, the relationship between the datasets in the Ace thermokarst zone is based on a very small dataset (n=4). This makes any inference relating to an apparent relationship between the variables very sensitive to erroneous data points. The same numbers of data points were available in Smith L. also.

Having argued for an increase in sample numbers in a single study site, it should be highlighted that multiple samples were taken within each experimental zone. Calibration of downcore patterns with modern data is essential, and this is the first study (as far as is known) to look at highly resolved within-lake variability in measured variables that might be applied as

downcore proxies. Reconstructions will often use a single core on which evidence is based; analysis of multiple samples per experimental zone meant the reliability of a palaeo approach was adequately tested. The data show that the variability of downcore reconstructions of isotope values is no greater than modern within-lake variability.

A compromise needs to be made between gaining enough samples necessary for reliable results and the time and resources available with which to gather and analyse the samples. Organic geochemical analysis of lipid biomarkers is time consuming and expensive, and whilst stable isotope analysis of bulk material is less so, both analyses are expensive in comparison to traditional palaeoenvironmental techniques. This study analysed a large dataset in comparison to other studies, although the aims the other studies were very different and often other studies drew on multiple lines of evidence. For instance Belle et al. (2014) analysed six chironomid HC samples, whilst Sanseverino et al. (2009) only compared two samples of Chironomidae. Had more resource been available, increasing the number of lipid biomarker samples would be beneficial to this study. As described above, increasing the coverage of samples in underrepresented zones of the lake would allow a better understanding of whole lake methane dynamics.

8.3.2 Thermokarst lake classification

This research project has highlighted that there is a need to classify thermokarst lakes to a greater degree, especially when considering their biogeochemical cycles. Section 8.2.2 reviews the chosen study sites with regard to how well they represent thermokarst lakes. The applicability of the study is discussed in more detail here in the context of a need for increased understanding of thermokarst lakes in general.

The lakes in this study were chosen for a number of reasons. Both lakes were not only easily accessible but both are part of ongoing research into GHG from thermokarst lakes. Secondary data on methane dynamics was readily available which meant this study could focus on developing a method of detecting the source areas of methane. However, although the lakes were suitable study sites, their geographical location mean they are somewhat different to thermokarst lakes from other, more northerly, regions. A number of previous

studies detail the criteria that lakes should have in order to be classified as thermokarst lakes (Jorgensen and Shur 2007, West and Plug 2008). However, these studies use lakes from localised geographical areas, meaning their definitions are biased towards the lakes in the chosen study region. Others have divided thermokarst lakes in two groups: yedoma and non-yedoma lakes (Brosisus et al., 2012, Jorgensen et al., 2012), although the rationale is different in each instance. The results of chapter 6 highlighted that the chironomid assemblages found across the surface of the study lakes were different from those of Siberian thermokarst lakes, but are similar to those from lakes located close to the study sites (Fairbanks and the surrounding area) which are also thermokarst in origin (Figure 6.21). The differences between the Siberian thermokarst lakes and the lakes from Interior Alaska were attributed to differences in physical and chemical variables such as catchment topography, air and lake temperature and nutrient input (due to different vegetation biomes), many of which would be different regardless of the fact that all these lakes are thermokarst in origin. Therefore it is important to understand the environment from which the samples are being taken, in this instance this refers to both the within lake environment and the surrounding catchment.

Despite a similar genesis for the initial development of thermokarst lakes (e.g. thaw of ice-rich permafrost), a number of factors can mean thermokarst lakes can evolve in very different ways over time, in terms of not only methane production, but methane processing within the lake. The study sites provide a good example of this. The lakes have been classified differently and the evidence in this project highlights differences between the lakes (e.g. methane emission and oxidation rates), despite a similar initiation in what can be considered fairly similar underlying surficial geologies (when compared with other regions, such as the Arctic Coastal Plain, for example). At the study sites, factors such as ground ice content have a big impact on the evolution and the final classification of the lakes. If the chosen lake environments differ greatly from one another for reasons such as differences in organic carbon substrate in the lake, thermal regimes or ground ice content (reasons which may or may not be associated with thermokarst), then the biological organisms within them are likely to differ due to these factors. This may make establishing a single proxy difficult as differences in biological communities due to methane cycling

might be masked by more influential variables. Replication of the methods across a number of contemporary thermokarst lakes from several different regions would allow a greater understanding of methane cycling and the biological communities. In turn this will allow a more accurate interpretation of the interaction of organisms within a lake with methane cycling through time.

8.3.3 Alternative proxies for methane

During the course of the study it became clear that a level of uncertainty is associated with the ability to pinpoint methane production in a lake. Although this study focused on MOB and chironomids, other lines of evidence are available that can highlight methane production and cycling through the food web. These include proxies for methanogenesis and other organisms which might consume ^{13}C-depleted MOB.

This study focused on understanding methanotrophic communities; however, assessing methanogenic organisms (archaea and bacteria), at least in the anoxic surface sediments, would allow a more definitive conclusion as to the source of methane used by MOB. A number of recent studies have quantified archaeal lipids, which produced by methanogenic archaea, in peatlands (Pancost et al., 2000b; Pancost and Sinninghe Damsté, 2003) and permafrost environments (Liebner and Wagner, 2007), highlighting the applicability ofassessing methane production using this methods. Furthermore, quantification of biomarker concentrations will also help assess the levels of methane production and oxidation in the surface sediments, an important step in determining the importance of deeper methane production (e.g. in the talik bulb).

Multiple lines of evidence are useful in validating observed patterns and as such, different organisms which highlight the consumption of MOB would provide more insight into methane cycling. The stable carbon isotope compositions of organisms such as cladocera (water fleas) have been studied previously as they are considered effective bacterial feeders (Kankaala et al., 1988). Studies have demonstrated the assimilation of methane-derived carbon through the δ^{13}C values of cladocera (Kankaala et al., 2006) whilst others have attributed low δ^{13}C values of cladocera to changes in the utilisation of MOB over time (Wooller et al., 2012). Certainly this organism shows a similar

potential to chironomids. It would be useful to explore this further in environments with abundant methane production and a high concentration of dissolved methane versus an environment with low methane levels.

8.4 The significance of the research

The results of this study highlight the complexities of methane production, distribution, oxidation and utilisation by chironomid larvae in thermokarst lakes. The importance of this research within the wider scientific community is discussed below in the context of previous research and addresses those in the community who may benefit from the findings.

Research into biogeochemical interactions between methane cycling and organisms within lakes is relative new and there is still a lot to understand. This work is of the upmost importance as it challenges the conception that the relationship between methane production and subsequent processes is linear. In other words, an increase in the amount of methane that is oxidised does not relate directly to a decrease in the stable isotope values of the potential consumers of methane-derived carbon. Studies have begun to use changes in chironomid $\delta^{13}C$ values (among other proxies) to suggest changes in methane availability (e.g. Wooller et al. 2012; van Hardenbroek et al. 2012a) over time; suggesting lower $\delta^{13}C$ values in chironomids reflect higher methane availability. The lowest chironomid $\delta^{13}C$ values in this study do not always reflect the highest methane production or even methane oxidation areas (assumed to indicate highest methane availability) and therefore, this highlights the need for increased understanding of the relationships between a proxy and the variable which is being reconstructed. Furthermore, the results in this study suggest methane oxidation is correlated with supply rate, but the relationship between methane ebullition-seeps and diffusive methane is still to be fully understood. Clarification and comprehension of the source of methane production (surficial or deep) is imperative for understanding methane availability.

In non-specific research fields (those not dealing with thermokarst lake methane cycling and biological organisms), this work will be of interest to researchers who want to understand the dynamics of methane over both short (decadal and centennial) and longer (millennial or longer) temporal scales, not

just in thermokarst lakes but in other freshwater environments. It will also be of interest to ecologists concerned with understanding lake food web interactions and methods with which to highlight carbon pathways through different trophic levels.

It is important to understand fully the patterns of methane emissions from thermokarst lakes over time in order to contextualise their current role in the global carbon cycle. Predictions of future climate change suggest high latitudes will become increasingly warmer (Vaughan et al., 2013). In continuous permafrost regions, this could lead to increased thaw and a possible increase in the number of thermokarst lakes. The results of increasing the total number of thermokarst lakes are twofold: the total number of lakes that produce methane may increase, but higher temperatures may mean that the amount of methane that is produced per lake may also increase (as methanogenesis is linked to temperature). Detailed knowledge of the longevity of past carbon sources will allow more accurate assessments of these future emissions scenarios.

8.5 Concluding remarks

This research set out to evaluate a number of potential proxies that might be used to highlight methane ebullition-seeps in thermokarst lakes. Whilst some of the results appear promising, the heterogeneity across the proxies evidenced in this research project highlight the complex nature of methane production, oxidation and utilisation by organisms within the lake. It is argued that currently, none of the chosen organisms provide a clear enough relationship to methane-ebullition seeps to be used as proxies. It is clear that there is far more work to be completed on biogeochemical cycling in thermokarst lakes with regard to methane dynamics. Furthermore, this research has highlighted a clear need for the increased understanding of the relationship between methane production and the different transport pathways (e.g. ebullition and diffusive flux). It is this link that will provide the key to establishing the importance of within-lake recycling of methane-derived carbon and establishing a quantifiable and robust proxy for methane cycling in thermokarst lakes.

Appendices

Appendix A

Apolar fraction integrated peaks. The peak height and retention times are included for reference. Solid lines indicate the table margins whilst dashed lines indicate the table continues below.

	Diploptene			c-15		
Code	Peak area	Peak height	RT	Peak area	Peak height	RT
A1	145804564.9	42357775.87	41.23			0
A2	90241854.78	24988863.73	39.31	0	.	0
A3	63846023.06	18692178.32	41.23	0		0
A4	378595250.6	98653540.41	39.32	0	.	0
S12-N1	89140659.48	27564774.32	41.23	0		
S12-N2	73177404.61	22452799.41	41.23	0		
S12-N3	194285721.6	53701370.87	39.3	0	.	0
S12-N4	118651129.4	33425384.32	39.31	0	.	0
S12-N5	66248144.82	18083551.14	39.28	0		0
S11-N6	60056281.81	18013886.43	41.22	0		
S11-N7	268980558.1	72580584.73	39.31	0	.	0
S11-N8	417636793.8	114791554.3	39.32	0	.	0
S12-N9	70753876.13	19242809.51	39.29	0	.	0
S12-N10	54629547.59	15994871.35	41.21	0		0
S12-N11	1.49E+08	41550522.03	39.31	0	.	0
S12-N12	114137528.8	31384422.49	39.3	0	.	0
S12-N13	5893796.559	1618617.189	39.3	0	.	0
S11-N14	217394601.9	61236326.22	39.31	0	.	0

Appendix A

c-16			C-17		
Peak area	Peak height	RT	Peak area	Peak height	RT
567550.71	451046.857	10.41	28791189.99	11904025.97	12.42
0	0	.	0	.	.
0	0	.	0	.	.
0	0	.	6419336.398	2407667.027	10.72
0	0	.	7185629.509	3078047.918	12.44
0	0	.	0	.	.
2241103.357	814235.081	8.78	1964223.56	998701.622	10.72
0	0	.	0	.	.
0	0	.	0	.	.
0	0	.	6660368.467	2715197.032	12.44
0	0	.	14033563.59	5255532.973	10.71
0	0	.	9761954.034	3609308.405	10.72
0	0	.	0	.	.
0	0	.	0	.	.
0	0	.	0	.	.
1346981.838	490298.703	8.78	0	.	.
0	0	.	0		
0	0	.	11864785.45	4686859.676	10.72

c-18			c-19		
Peak area	Peak height	RT	Peak area	Peak height	RT
5049842.065	2149768.33	14.58	17860138.32	5471675.733	16.74
0	.	.	825017.29	368604.405	15.02
0	.	.	2198180.786	911357.613	16.76
0	.	.	0	.	.
2972406.528	1378333.638	14.59	9454132.423	3686864.533	16.75
995648.59	597743.619	14.6	5763906.85	2213828.698	16.76
4343774.19	1541293.189	12.82	7958795.12	2717104.378	14.99
0	.	.	0	.	.
0	.	.	0	.	.
1757798.275	830413.829	14.59	4980541.279	1876783.2	16.75
5014348.162	1691366.108	12.82	15571154.48	5107103.838	14.99
6213745.642	2124937.081	12.81	22883968.87	6931587.838	14.99
0	.	.	0	.	.
0	.	.	14785695.92	5173539.556	16.75
0	.	.	5050523.593	2087692.297	15.01
2162500.756	787991.189	12.81	3412006.341	1129716.486	14.99
0			0		
6113551.018	2643215.135	12.82	15632586.67	5773148.541	15.01

c-20			c-21		
Peak area	**Peak height**	**RT**	**Peak area**	**Peak height**	**RT**
19494066.57	4756625.778	18.99	53665826.13	18944021.99	21.16
1729353.403	571344.595	17.2	7671742.968	2342405.135	19.36
2365993.812	1143241.956	19	14317360.53	5295558.933	21.17
8808734.03	3062605.946	17.19	48746371.55	16148359.22	19.35
7938277.035	2985826.997	19	72552311.55	24999479.82	21.18
6875483.049	2240562.921	19.01	34004380.99	11614923.24	21.18
10885384.92	3652871.162	17.19	68053957.6	21967239	19.35
4439419.569	1566249.946	17.18	32735593.59	10442633.68	19.35
2426031.677	925228.973	17.17	16627835.32	5622925.962	19.33
5511407.455	1923330.781	19.01	20890225.47	7161653.46	21.17
14086703.39	4873181.054	17.18	112827380.6	37366604	19.35
25474103.78	8413450.946	17.18	129600847.3	41945508	19.35
7483086.175	2684693.622	17.18	118129540.4	36838950.89	19.34
3310690.33	1130292.267	18.99	22791743.58	8004683.378	21.16
8000649.701	2718290.642	17.19	55279094.04	18050527.3	19.35
5289427.372	1777557.297	17.19	33617485.86	11390410.22	19.35
19100069.93	6161089.189	17.19	104116108.7	34165831.38	19.35

c-22			c-23		
Peak area	**Peak height**	**RT**	**Peak area**	**Peak height**	**RT**
33395555.51	11073755.05	23.28	173192655.2	58487804.01	25.33
4880778.86	1494278.953	21.47	20929915.98	6369629.189	23.51
9292713.903	3585745.092	23.29	51354691.25	17385721.13	25.35
28908116.99	9413704.216	21.46	137223015.2	43685812	23.52
27068308.26	9819638.4	23.29	219703200.6	75719572.86	25.36
17753367.46	5807795.81	23.29	82032099.46	29060690.5	25.35
34632251.41	10503086.76	21.47	199097800.8	64809006.41	23.52
16163343.47	4823669.189	21.46	83500255.72	25745336	23.51
11705722.82	3731286.136	21.45	65011768.18	21051496	23.49
11752704.95	4282700.952	23.29	49738759.51	16811911.01	25.35
43975153.32	14316912.03	21.46	255304618.7	81306466.78	23.52
74456181.07	23099958.22	21.46	317709362.6	95541716	23.52
36836789.6	11393191.3	21.45	385840748.7	114333735.5	23.52
10696870.23	3711888.711	23.28	72876299.23	24287869.94	25.33
28605190.09	9201428.757	21.46	166720575	52600299.95	23.52
18622159.28	5899607.459	21.46	108992664.6	35958254.03	23.51
			8465482.277	2108747.135	23.51
65909408.3	20906796	21.46	305690237.3	94585624.38	23.53

c-24			c-25		
Peak area	Peak height	RT	Peak area	Peak height	RT
47096157.87	14745293.92	27.31	366858269.9	113258153.2	29.25
7786438.753	2434600.432	25.5	45078605.86	13171490.41	27.42
16794077.98	5349727.289	27.33	128056624.3	40243356.1	29.25
44756757.88	14943837.98	25.5	295290418.8	94737264.81	27.44
28089333.33	9150302.578	27.32	160354005.8	51927742.78	29.25
22358638.17	7022100.317	27.33	106657695.4	34542025.55	29.24
53115462.4	16862668.54	25.5	347501416.3	100382954.8	27.44
21863625.08	6712688.432	25.49	132539614.5	39322036	27.42
23362517.69	7182067.514	25.48	125147648.2	37353259.91	27.4
14788716.13	4908374.044	27.32	91454923.19	30514360.06	29.24
70800357.28	21855825.14	25.5	397001837.7	121721888.9	27.43
106341505.4	33007356.43	25.49	590128658	161719793.4	27.44
41618104.57	11774062.7	25.47	186682371.6	56615218.46	27.4
12633754.88	4189613.206	27.31	88488008.23	28986143.86	29.23
51696443.85	16216165.14	25.49	360157079.5	106966536.5	27.44
28888064.78	9260870.757	25.49	187656223.9	58807361.92	27.43
8465482.277	2108747.135	25.49	17671945.25	5375045.351	27.41
95674076.51	29938546.92	25.5	601242416.6	170713285.8	27.46

c-26			c27		
Peak area	Peak height	RT	Peak area	Peak height	RT
54779634.99	14406174.79	31.08	614946201.8	171285193.8	32.9
7553513.117	2153430.811	29.27	76532272.54	21145699.7	31.07
17502264.6	5187336.762	31.09	192478783.9	61084221.49	32.89
48905216.79	14422726.76	29.27	443867943	123607822.5	31.09
18049798.27	5874923.022	31.09	227947501.1	68061176.66	32.88
18613952.5	5851387.238	31.09	150377815	45898775.41	32.89
56206513.23	15859328.92	29.27	501187488.3	137924494.1	31.09
19527071.43	5925143.162	29.26	169722223.4	49630454.76	31.07
25681589.11	7758844.189	29.25	196220610.5	58165140	31.06
14200160.42	4435092.622	31.09	164962928.4	50314171.14	32.88
76714866.85	22078573.92	29.26	694890696.7	176245828.8	31.1
112062362	32965953.81	29.26	968753794.8	233436286.6	31.11
26096672.6	7855649.324	29.25	239487674.8	67234820	31.05
11711891.73	3698437.867	31.07	126797730	39803538.16	32.87
64371356.94	18662943.24	29.27	632051459.8	170261697.2	31.1
31945737.59	9171861.351	29.26	300121235.9	91643991.49	31.08
3221340.791	955191.838	29.28	40262009.84	11245109.41	31.06
105923749.4	31232920	29.27	979425432.4	252894716.8	31.13

c-28			c29		
Peak area	**Peak height**	**RT**	**Peak area**	**Peak height**	**RT**
50285781.69	12565574.03	34.59	406755483.2	105551836	36.29
14687716.6	3250771.243	32.82	57817202.52	15698528.38	34.47
12085842.9	3975014.997	34.6	116575600.7	30775129.3	36.27
46448819.48	13316852.22	32.79	310909096.7	88411564.35	34.49
15771387.76	4849468.47	34.6	139080660.3	41151336.91	36.27
18343233.1	4537654.553	34.6	118292907.3	32886739.41	36.27
75941281.98	18007336.54	32.79	385109735.8	104941501.2	34.48
27311546.41	6317570.189	32.8	110613073.7	29817122.03	34.46
39624797.13	9405162.162	32.78	189891399.1	51977443.95	34.46
15774188.31	4633709.714	34.6	142753053	42124923.93	36.27
202078763.5	49768663.51	32.79	909159463.7	225874658.6	34.52
144890716.2	38446377.08	32.79	910716126.9	214502908	34.51
38274907.22	8828711.784	32.77	221275481.6	63924420	34.45
			98726939.85	29344758.26	36.26
73466345.96	20012690.19	32.78	545628812.5	149433226.1	34.51
44953421.3	9998315.081	32.8	262044475.2	72291536	34.48
11239929.83	2509409.189	32.8	39882956.15	10729551.84	34.46
118829333.8	33186612.92	32.8	945286586.3	222942520.2	34.54

c-30			c31		
Peak area	**Peak height**	**RT**	**Peak area**	**Peak height**	**RT**
0	.	.	298159238.7	61201377.02	39.45
2122866.049	756767.478	36.11	46534169.44	11718346.38	37.67
0	.	.	70823247.08	16157801.91	39.45
15424605.4	4335237.521	36.11	292418087.4	77143998.89	37.69
0	.	.	85056278.54	22238704.46	39.45
0	.	.	105672748.6	26061065.27	39.45
34871039.53	8467003.459	36.08	396545545.5	101406813.6	37.67
8980189.321	2638792.054	36.1	108948700.9	28653140.41	37.66
18828109.75	4994504.595	36.07	253530445.5	68705584	37.65
0	.	.	98217828.17	25655136.72	39.45
69128237.7	19411488.11	36.08	996685198.4	231295468	37.72
74698929.79	19626558.65	36.1	805517371.4	201059701.5	37.71
13669351.5	3831728	36.07	223393432.2	60956744.11	37.65
0	.	.	76947720.37	20219376.32	39.44
41699060.77	11139630.43	36.08	588783902.7	156237867.2	37.71
23293317.39	5486357.162	36.1	283546486.8	82601472.97	37.69
1117305.783	668361.486	36.08	39626318.85	10071634	37.66
63847337.77	18252965.32	36.1	1019641792	234716016.4	37.73

c-32			c-33		
Peak area	**Peak height**	**RT**	**Peak area**	**Peak height**	**RT**
0	.	.	36213204.74	9915877.79	42.43
0			9279864.831	1865451.378	40.68
0	.	.	0	.	.
0	.	.	69719130.38	17653241.92	40.68
0	.	.	7703190.793	3682889.424	42.43
0	.	.	21241481.63	5372701.054	42.44
10527940.4	3744726.351	39.18	100686276.97	25757525.19	40.67
0	.	.	25338362.42	5542800.216	40.66
8594840.789	2900077.135	39.17	76348956.94	19715940	40.65
0	.	.	21462059.29	5054700.597	42.43
22649342.22	6713236.553	39.18	347713542.3	85026564	40.68
18790798.75	5455316.324	39.17	243227112.2	60838116	40.67
5959573.643	1823428.767	39.16	70116421.68	16501987.57	40.66
0	.	.	0	.	.
15719085.89	5012611.784	39.18	167966795.4	44075458.6	40.68
7723807.822	2407930.514	39.18	81089687.58	18781168.95	40.68
0	.	.	8465482.277	2108747.135	40.67
24977215.39	7396438.054	39.18	301379682	79839923.27	40.68

Appendix B

Chironomid assemblage counts, Ace L. (pp 231 - 238), Smith L. (pp 239 - 2. Solid Lines represent the margins of the table. Dashed lined indicate where the table continues to the next page. Taxa codes are located at the end of each table.

Sample code	1	2	3	4	5	6	7	8	9	10	11	12	13	14	15	16	17	18
11-1a	11	4	6	1	1	1	3	4				20			2			9
11-1b	43		19	1	5		2	13	1			57				4		26
11-2a	6	1		2				1	1			1			5			7
11-3a	27	1			2			1				8	1		2			1
11-4a	9	2					1	3				9			1			
11-5a	10	5	7		1		2	3				2						3
11-6a	29	3		9	1		1	2				1		1	6			1
11-6b	25	3	6					1	1			14						6
11-7a	5	2	10				2					1						
11-8a	8	2	13				1	1				2		2	1			2
11-8b	2	2	3		1	1												
11-9a		2	2					1										1
11-9b			4									2						
11-10a			1				1											1
11-11a	1							1	1				1					
11-11b	7		6									2						
11-12a			6									1						
13-2	4	12	2	6	1			1			1	6						
13-3	4	9	4	2	1						1	14						
13-4	7	2	1	1	1	1	3	1				4			2			
13-5	13	1	3				1					3						1
13-6	1	1	2	1								3						
13-7	0	11	1	1								1						1
13-8	1	10	4	4			1	1				1						1
13-9	2	6	10		2		2					5				1		1
13-11	4	9	1	1				1		1		4		1		1		
13-12	6		5			1						2						
13-15	0	9	4	3								1						
13-16	1	10		4	1		1					5		1				
13-17	2	4	2	2	2		2					1			2	1		1
13-18	4	2	4	2			1					5						
13-23	14	10	2								1	6						1

Appendix B

19	20	21	22	23	24	25	26	27	28	29	30	31	32	33	34	35	36	37	38
1	1		2			2				3						1	12		
	1					8		1		5			1			1	19		
										1							4		
	1	1		1	2			1		1							15		
	2		1			2				1				1			2		
	2					1	1										5		
	2					1				3							11		
	1					2											4		
2																	3		
										1							3		
	1																		
																	4		
																	2		
	1				2			1		1							3	4	
	4				2					1							4		1
	2																1		
	2					1				2									
																		2	
					2														
	1									1							1	1	
	5					2											11		
						1				2							3		
	1									2									
																	1		
	3				1	1				1							2		
	6					1				1									
	2					3											3		
	2				4					3							1	1	

39	40	41	42	43	44	45	46	47	48	49	50	51	52	53	54	55	56	57	58
									1	1			1				4		
													3				16		
						1					1						9		
								3	1		1					1	10		
									1		1	1					3		3
									1			2	1				3		
	1					1		1	1							1	6		
													1			2	13		
		1																	
											1		2	1			3		
																	2		
														1			2		
																	2		
																	1		
																	4		
	1					1													
	1		1			2			2	1			2						
1	1		1							2	1		1						
		1	1	2								1	1				2	2	
								3	5				2				2		
									1				3						
			1													2	2	1	
									1		1					2	2		
1			1				1		2		3	1					2		
			2					1	1	1									
	1							2											
	2		1								1		3						
			1						2	1	1	1	1	1					
									1				2						
	1											2				1			
			4										1						

Appendix B

59	60	61	62	63	64	65	66	67	68	69	70	71	72	73	74	75	76	77	78
2	10			4				28						1			1		
1	21			8	1	4		41											1
	1			2				15					1						
1								13											
	1					3		8											
2	1							6				1							
1				4				4											
1	4							6											
								4											2
	4							2					1						2
				1				2											1
	2			1				2						1					
	2							1											1
1	3							2											
						1													
	1							2											
1				2		1										4			
1	4		2	2										1			1		
	2			2					1										
1	3			1				3	1								1		
2						1													
			1							1						1			
	2			2				1							2	3		1	
	2			1				2					1	1					
2	2			1		1		3		1	1								
2	2		2	3					1		1						1		
				1									1			1			
	1			3													1		
1	5		1	3										1					
1	2		1	2									1						
2							1	1					1						
1			1	1												1			

79	80	81	82	83	84	85	86	87	88	89	90	91	92	93	94	95	96	97	98
1		6											21	3			10	2	4
2		20											25	10		6	15		14
		1	4										9	1			2		
		3	8										7			2	7		
		11	3										10	3		1	8		2
		5											11	2		1	3		
		1	4										18	1		2	10		1
1		8	6										11	3		2	2		3
		3	1										10			1	1		1
		11	2										3	2		3	3		1
		5											3						
		4											5						
																	1		
		2	1										1	1			1		
		1											3			1			
																1			1
		5	1							1			1		1	1	1	1	1
	1	10		1	1				1				3				1	2	1
1		16	2	1	1			1					8	1					
		1												1			4		
1		3						1	1				5						
		4											1	1				1	
		4									1		0	2		1	1	1	
		7								1	1		7	1		2		1	1
		9														1	1	1	
		7												1			1		
		7				3		2					2			1	2		
		6	1										3			1			
		7	1			2	1						1						1
		9				1							3	1		1	1		
		2												2					

Appendix B

99	100	Total HC
4	4	192
11		406
3	4	83
15	17	154
7		100
4	1	86
9	24	161
6		132
		49
1		78
		23
2		17
1		23
		11
1	3	19
		29
		19
		78
	2	82
3	5	85
		48
3	2	33
	2	43
	0	50
1	2	93
		58
1		33
1	1	49
	1	62
1		51
		51
	1	59

Number	Sample code
1	C.anthracinus-type
2	C.plumosus-type
3	1st instar chironomini
4	Chironomus spp.
5	C.lateralis-type
6	Cryptochironomus
7	D.nervosus-type
8	D.notatus-type
9	Dicrotendipes spp.
10	E.Dissidens-type
11	E.pagana
12	Endochironomus albipennis-type
13	Endochironomus pagana-type
14	Endochironomus tendens-type
15	Endochironomus spp.
16	Glytotendipes-barbipes
17	Glytotendipes-severini
18	Glyptotendipes pallens-type
19	Lauterborniella
20	Microtendipes pedellus-type
21	Phaenospectra flavipes-type
22	Phaenospectra type A
23	Phaenospectra spp.
24	Polypedilum nubeculosum-type
25	Polypedilum nubifer-type
26	Polypedilum sordens-type
27	Polypedilum spp.
28	Pseudochironomus
29	Parachironomus varus-type
30	Parachironomus vitiosus
31	Parachironmus spp.
32	Sergentia coracina-type
33	Stenochironomus-type
34	Stempellinella
35	Xenochironomus
36	Chironomini Undifferentiated
37	Neozavrelia
38	C.oliveri
39	C.mancus
40	Paratanytarsus penicillatus-type
41	Paratanytarsus austriacus-type
42	Paratanytarsus sp.
43	Rheotanytarsus
44	Tanytarsus chinyensis-type
45	Tanytarsus glabrescens-type
46	Tanytarsus lactesens
47	Tanytarsus lugens-type
48	Tanytarsus mendax-type
49	Tanytarsus nemorosus-type
50	Tanytarsus pallidicornis-type
51	Tanytarsus-type W/S
52	Tanytarsus-type N/S
53	Microspectra radilias

54	Microspectra insigulobus-type
55	Microspecta spp.
56	Tanytarsini Undifferentiated
57	Chaetocladius
58	Corynoneura edwardsi-type
59	Corynoneura arctica-type
60	Cricotopus bicinctus-type
61	Cricotopus type P
62	Cricotopus cylindraceus-type
63	Cricotopus (Isocladius) intersectus-type
64	Cricotopus laricomalis-type
65	Cricotopus obnixus-type
66	Cricotopus type C
67	Cricotopus (Isocladius) spp.
68	Doncricotopus
69	Georthocladius
70	Heterotrissocladius grimshawi-type
71	Heterotrissocladius marcidus-type
72	Lymnophyes
73	Nanocladius
74	Orthocladius oliveri
75	Orthocladius type S
76	Orthocladius spp.
77	Paracladius
78	Parakiefferiella bathophila-type
79	Psectrocladius (Mesopsectrocladius) barbatipes-type
80	Psectrocladius septentrionalis
81	Psectrocladius (Psectrocladius) sordidellus-type
82	Psectrocladius (Psectrocladius) spp.
83	*Propsilocerus type N*
84	Pseudosmittia
85	Smittia
86	Synorthocladius
87	Thienemanniella type E
88	Trissocladius
89	Tvetenia bavarica
90	Zalutschia type B
91	Z.zalutcola
92	Orthocladiinae Undifferentiated
93	Ablabesmyia
94	Macropelopia
95	Labrundinia
96	Procladius
97	Procladius 1st instar
98	Thienemannimyia
99	Tanypodinae undifferentiated
100	Undifferentiated

Sample code	1	2	3	4	5	6	7	8	9	10	11	12	13	14	15	16	17	18	19
13-1	7	3		1				1				3				1	1		
13-2	7								2			1							
11-8		1		1				2	2						3				
11-9	12	3		3		3		3	2						1				
11-10	7	1		1					1										1
13-3	5	1				2						3							
13-4	5	2					1	3	3		1	6							1
13-5	7	3						3	1			1							
13-6	16	2		2				1	1			3							
13-7	3					1		2								2		1	2
13-8	2					1		6	1			2							2
13-9	8	3		2		2	1	4	1			4				2			1
13-10	8	1				1		4	2			2				6		2	
13-11	2											2							
13-12	6	2				1		1	2			4				2			1
13-13	1					1		4				1					1	1	2
13-14	3	1				2		1				3				4		1	
13-15	4	1		1		2		1				2				1			
13-16	3	1				9		4				1				2			
13-17	3	3		5					1			3						1	1
13-18	1	3				1	1	3	2			2				1			1
13-19	3					1		4				6							
13-20	11	3		4		2						2							
13-21	9	2		1		2		2				3							2
13-22	7	1				2		1	1			2				1			
11-3	3	1		1		1		1				3				1		2	
11-5	4	1				3	1	1				3							
11-6	9	7				4		3	1			2						1	
13-23	5	1		1		1	1	4				3				1			3
13-24	4	4				1						3				2			1
13-25	8	5		2		3		1	1			2				1			1

Appendix B

20	21	22	23	24	25	26	27	28	29	30	31	32	33	34	35	36	37	38	39
4																1			
4	1				1							2							2
4			1	2															
6		1			2				1										
2					2				1					1					
2					1				1										
1					2			1	2	1									9
4									1							2			1
5							2	1				1				2		4	
3	1								1		1								5
6					3			1	1							2			
10					6				3			2				2			6
4	1				5							1		1		2		1	3
1												1							
8					2				1			2							2
6									1							1			1
3	1							1											
5					2			1											1
9					5				1										2
2					1			2	1										2
6					2			1	2			2					1		2
2					3			2				1							
					1				1										
10					4							1							4
3								1	1			1					1	3	
3																			
3																			
11					2													1	
8					1			1				1			1	1			3
5							3					3							3
5					1			1	1										3

40	41	42	43	44	45	46	47	48	49	50	51	52	53	54	55	56	57	58	59
	2					1		2	1	1					2		1	1	1
						1		3	1							1			
	1				1	2		1	1					1			1		1
					1	5	2	1	3	3				5			2		
						1	1	3	1	4				2					
1	2					1			3	1				2		1			
	8			1			2	3		2	2			1	1		1		
						1	3	2	2	1				1		1	1		
1					9	1	2	1	1	4				1					
	1				3					1							3		
					1	6			1	11				2					
	5				1	2		6	3	9				2			2		
						1		1	2	4	1			2			1		
						1										1			
	1					1		1		2									
				1	1	5	2	3	2	8	1			6					
						1	1	1	3	4	2			1					
						3		3		5	1			1					
		1		1	1	2		5	4	8	3			1		1			
						2		2		1	1			2		1	1		
	3				1	3	1	2	1	3	1					1			
	4				2	2				8	1			1			1		
	2				4		1	1	1	8	2			2					
					16	2				2	2					1	1		
	2			1	6	6			1	10				2			1		
1					1	1		1		2	1	3		1		1	1		
					10	3		1		2				1					
			1		3	5		5	1	7	1	2		5		1			
	2				2	5		3	1	5						2	1		
	4							1	2	3				1		1	2		
	3						1	2		2				2		1	2		

Appendix B

60	61	62	63	64	65	66	67	68	69	70	71	72	73	74	75	76	77	78	79
2	1			1					2			1	1	9					
	1							1	1				1	6					
				1									2	9					4
2		1					2						2	22					7
2				2			2							3					2
4								1					1	6					3
8		1		1			1		1				1	19	1	1			
2				2			1		1		1			17					1
2									1			1		11				9	2
1				1			1	3	1				1	6			1	5	
1				1	2		1		1				1	9				4	2
6	1	1			1		1		3				1	27			1	2	2
			1				1						1	12				4	
														4				1	
1				1										9		1			2
2							1							8				5	
2									1				1	6				2	2
							3	1						6				3	
3				1			1	1					1	13				2	
3		1					2	1						10					2
8													1	11				3	1
1							2	1	3					6				8	
2														3				2	
3								3	2				1	12					
11		1									1		1	7				4	
1				2			1	1						5				3	1
1														2				3	
1	1	1		2			3	1						13				4	1
1				2			2							9					
5				1									1	17				2	
5							2		1					15					1

80	81	82	83	84	85	86	87	Total HC
1			1		2	2		57
1		1						38
1			20			12		74
		1	8		1	13		118
		1	3			2		46
1		1			3			46
								93
3		3	1		4			71
2		1	1		3			93
1								51
7			5					82
15		1	4		5			158
6		4	4		5	1		95
1			1			1		16
		1	1					55
	1		1		5			72
			1		2			50
2		1	1					51
5			6		7	1		105
2		2				2		60
4		2			1			78
5		1	7		1			76
2			1			1		56
3		2	4	1	2	1		98
2		1	7		2			91
3		1	2			1		50
			4		1	1		45
6			5		2			112
3			1		1			76
1			3		2			75
3			2		1	2		80

Appendix B

Number	Taxon code
1	Chironomus anthracinus-type
2	Chironomus plumosus-type
3	1st Instar Chironomus
4	1st instar chironomini
5	Chironomus spp.
6	Cladoplema lateralis-type
7	Cryptochironomus
8	Dicrotendipes nervosus-type
9	Dicrotendipes notatus-type
10	Dicrotendipes spp.
11	Einfeldia Dissidens-type
12	Endochironomus albipennis-type
13	Endochironomus pagana-type
14	Endochironomus tendens-type
15	Endochironomus spp.
16	Glytotendipes-barbipes
17	Glytotendipes-severini
18	Glyptotendipes pallens-type
19	Lauterborniella
20	Microtendipes pedellus-type
21	Phaenospectra flavipes-type
22	Phaenospectra type A
23	Phaenospectra spp.
24	Polypedilum nubeculosum-type
25	Polypedilum nubifer-type
26	Polypedilum sordens-type
27	Polypedilum spp.
28	Pseudochironomus
29	Parachironomus varus-type
30	Parachironomus vitiosus
31	Parachironmus spp.
32	Sergentia coracina-type
33	Stenochironomus-type
34	Stempellinella
35	Xenochironomus
36	Chironomini Undifferentiated
37	C.oliveri
38	C.mancus
39	Paratanytarsus penicillatus-type
40	Paratanytarsus austriacus-type
41	Paratanytarsus sp.
42	Rheotanytarsus
43	Tanytarsus chinyensis-type
44	Tanytarsus glabrescens-type
45	Tanytarsus lugens-type

46	Tanytarsus mendax-type
47	Tanytarsus nemorosus-type
48	Tanytarsus pallidicornis-type
49	Tanytarsus-type W/S
50	Tanytarsus-type N/S
51	Microspectra radilias
52	Microspectra insigulobus-type
53	Microspecta spp.
54	Tanytarsini Undifferentiated
55	Corynoneura edwardsi-type
56	Corynoneura arctica-type
57	Cricotopus bicinctus-type
58	Cricotopus type P
59	Cricotopus cylindraceus-type
60	Cricotopus (Isocladius) intersectus-type
61	Cricotopus laricomalis-type
62	Cricotopus obnixus-type
63	Cricotopus type C
64	Cricotopus (Isocladius) spp.
65	Heterotrissocladius grimshawi-type
66	Heterotrissocladius marcidus-type
67	Lymnophyes
68	Nanocladius
69	Orthocladius type S
70	Orthocladius spp.
71	Paracladius
72	Parakiefferiella bathophila-type
73	Psectrocladius (Mesopsectrocladius) barbatipes-type
74	Psectrocladius (Psectrocladius) sordidellus-type
75	Psectrocladius (Psectrocladius) spp.
76	Pseudosmittia
77	Smittia
78	Z.zalutcola
79	Orthocladiinae Undifferentiated
80	Ablabesmyia
81	Macropelopia
82	Labrundinia
83	Procladius
84	Procladius 1st instar
85	Thienemannimyia
86	Tanypodinae undifferentiated
87	Undifferentiated

References

Agasild H, Zingel P, Tuvikene L, Tuvikene A, Timm H, Feldmann T, Salujõe J, Toming K, Jones RI, Nõges T (2014) Biogenic methane contributes to the food web of a large, shallow lake. *Freshwater Biology* 59:272–285. doi: 10.1111/fwb.12263

Akerblom N, Goedkoop W (2003) Stable isotopes and fatty acids reveal that Chironomus riparius feeds selectively on added food in standardized toxicity tests. *Environmental toxicology and chemistry / SETAC* 22:1473–80.

Alexander V, Barsdate RJ (1971) Physical Limnology, Chemistry and Plant Productivity of a Taiga Lake. *Int Revue ges Hydrobiol* 56:825–872.

Alexander V, Barsdate RJ (1974) Limnological Studies of a Subarctic Lake System. *Int Revue ges Hydrobiol* 59:737–753.

Alperin MJ, Hoehler TM (2010) Anaerobic methane oxidation by archaea/sulfate-reducing bacteria aggregates: 1. Thermodynamic and physical constraints. *American Journal of Science* 309:869–957. doi: 10.2475/10.2009.01

Anderson PM, Brubaker LB (1994) Vegetation history of northcentral Alaska: A mapped summary of Late-Quaternary pollen data. *Quaternary Science Reviews* 13:71–92.

Anderson PM, Edwards ME, Brubaker LB (2003) Results and paleoclimate implications of 35 years of paleoecological research in Alaska. *Developments in Quaternary Science* 1:427–440. doi: 10.1016/S1571-0866(03)1019-4

Armitage PD, Cranston PS, Pinder LC V. (1995) The Chironomidae: the biology and ecology of non-biting midges. Chapman and Hall, London, UK

Barber KE, Langdon PG (2007) What drives the peat-based palaeoclimate record? A critical test using multi-proxy climate records from northern Britain. *Quaternary Science Reviews* 26:3318–3327. doi: 10.1016/j.quascirev.2007.09.011

Barber V a, Juday GP, Finney BP (2000) Reduced growth of Alaskan white spruce in the twentieth century from temperature-induced drought stress. *Nature* 405:668–73. doi: 10.1038/35015049

Barber VA, Finney BP (2000) Late Quaternary paleoclimatic reconstructions for interior Alaska based on paleolake-level data and hydrologic models *. *Journal of Paleolimnology* 24:29–41.

Bartlein PJ, Anderson PM, Edwards ME, Mcdowell PF (1991) A framework for interpreting paleoclimatic variations in Eastern Beringia. *Quaternary International* 10-12:73–83.

References

Bastviken D (2009) Methane. Encyclopedia of Inland Waters 783–805.

Bastviken D (2004) Methane emissions from lakes: Dependence of lake characteristics, two regional assessments, and a global estimate. *Global Biogeochemical Cycles* 18:GB4009. doi: 10.1029/2004GB002238

Bastviken D, Cole JJ, Pace ML, Van de Bogert MC (2008) Fates of methane from different lake habitats: Connecting whole-lake budgets and CH 4 emissions. *Journal of Geophysical Research* 113:G02024. doi: 10.1029/2007JG000608

Bastviken D, Ejlertsson J, Sundh I, Tranvik L (2003) Methane as a source of carbon and energy for lake pelagic food webs. *Ecology* 84:969–981. doi: 10.1890/0012-9658(2003)084[0969:MAASOC]2.0.CO;2

Bastviken D, Ejlertsson J, Tranvik L (2002) Measurement of methane oxidation in lakes: a comparison of methods. *Environmental science & technology* 36:3354–61.

Bastviken D, Tranvik LJ, Downing JA, Crill PM, Enrich-prast A (2011) Freshwater Methane Emissions Offset the Continental Carbon Sink. *Science* 331:50.

Belle S, Parent C, Frossard V, Verneaux V, Millet L, Chronopoulou P-M, Sabatier P, Magny M (2014) Temporal changes in the contribution of methane-oxidizing bacteria to the biomass of chironomid larvae determined using stable carbon isotopes and ancient DNA. *Journal of Paleolimnology* 52:215–228.

Berg MB (1995) Larval food and feeding behaviour. In: Armitage P, Cranston P, Pinder LC V (eds) The Chironomidae: Biology and Ecology of Non-biting Midges. Springer Netherlands, pp 136–168

Birgel D, Peckmann J (2008) Aerobic methanotrophy at ancient marine methane seeps: A synthesis. *Organic Geochemistry* 39:1659–1667. doi: 10.1016/j.orggeochem.2008.01.023

Birks HJB (1998) DG Frey and ES Deevey Review 1: Numerical tools in palaeolimnology–Progress, potentialities, and problems. *Journal of Paleolimnology* 20:307–332.

Bligh EG, Dyer WJ (1959) A rapid method of total lipid extraction and purification. *Canadian journal of biochemistry and physiology* 37:911–917.

Briggs BR, Pohlman JW, Torres M, Riedel M, Brodie EL, Colwell FS (2011) Macroscopic biofilms in fracture-dominated sediment that anaerobically oxidize methane. *Applied and environmental microbiology* 77:6780–7. doi: 10.1128/AEM.00288-11

Brodersen KP, Lindegaard C (1997) Significance of subfossile chironomid remains in classification of shallow lakes. Shallow Lakes' 95. Springer, pp 125–132

Brodersen KP, Lindegaard C (1999) Mass occurrence and sporadic distribution of Corynocera ambigua Zetterstedt (Diptera , Chironomidae) in Danish lakes . Neo- and palaeolimnological records. *Journal of Paleolimnology* 22:41–52.

Brodersen KP, Odgaard B V., Vestergaard O, Anderson NJ (2001) Chironomid stratigraphy in the shallow and eutrophic Lake Sobygaard, Denmark: chironomid-macrophyte co-occurrence. *Freshwater Biology* 46:253–267. doi: 10.1046/j.1365-2427.2001.00652.x

Brodersen KP, Quinlan R (2006) Midges as palaeoindicators of lake productivity, eutrophication and hypolimnetic oxygen. *Quaternary Science Reviews* 25:1995–2012. doi: 10.1016/j.quascirev.2005.03.020

Brooks S (1996) Three Thousand Years of Environmental History in a Cairngorms Lochan Revealed by Analysis of Non-biting Midges (Insecta: Diptera: Chironomidae). *Botanical Journal of Scotland* 48:89–98. doi: 10.1080/03746609609480376

Brooks S., Langdon P., Heiri O (2007) The Identification and Use of Palaearctic Chironomidae Larvae in Palaeoecology. Quaternary Research Association, London

Brooks SJ (2006) Fossil midges (Diptera: Chironomidae) as palaeoclimatic indicators for the Eurasian region. *Quaternary Science Reviews* 25:1894–1910. doi: 10.1016/j.quascirev.2005.03.021

Brooks SJ, Bennion H, Birks HJB (2001) Tracing lake trophic history with a chironomid-total phosphorus inference model. *Freshwater Biology* 46:513–533. doi: 10.1046/j.1365-2427.2001.00684.x

Brooks SJ, Birks HJ. (2001) Chironomid-inferred air temperatures from Lateglacial and Holocene sites in north-west Europe: progress and problems. *Quaternary Science Reviews* 20:1723–1741. doi: 10.1016/S0277-3791(01)00038-5

Brooks SJ, Birks HJB (2000) Chironomid-inferred Late-glacial air temperatures at Whitrig Bog, Southeast Scotland. *Journal of Quaternary Science* 15:759–764. doi: 10.1002/1099-1417(200012)15:8<759::AID-JQS590>3.0.CO;2-V

Brooks SJ, Lowe J, Mayle F (1997a) The Late Devensian Lateglacial palaeoenvironmental record from Whitrig Bog, SE Scotland. 2. Chironomidae (Insecta: Diptera). *Boreas* 26:279–295. doi: 10.1111/j.1502-3885.1997.tb00857.x

Brooks SJ, Mayle FE, Lowe JJ (1997b) Chironomid-based Lateglacial climatic reconstruction for southeast Sctoland. *Journal of Quaternary Science* 12:161–167.

Brosius LS, Walter Anthony KM, Grosse G, Chanton JP, Farquharson LM, Overduin PP, Meyer H (2012) Using the deuterium isotope composition of permafrost meltwater to constrain thermokarst lake contributions to

atmospheric CH 4 during the last deglaciation. *Journal of Geophysical Research: Biogeosciences* 117:n/a–n/a. doi: 10.1029/2011JG001810

Brown JB, Ferrians OJ, Melnikov ES (1997) Circum-arctic map of permafrost and ground-ice conditions. U.S. Geol. Survey.,

Brundin L (1956) Zur Systematik der Orthocladiinae (Dipt. Chironomidae). publisher not identified

Brundin L (1949) Chironomiden und andere Bodentiere der südschwedischen Urgebirgsseen: ein Beitrag zur Kenntnis der bodenfaunistischen Charakterzüge schwedischer oligotropher Seen. Bloms

Bunn SE, Boon PI (1993) What sources of organic carbon drive food webs in billabongs? A study based on stable isotope analysis. *Oecologia* 96:85–94.

Butler MG (1982) A 7-year life cycle for two Chironomus species in arctic Alaskan tundra ponds (Diptera: Chironomidae). *Canadian Journal of Zoology* 60:58–70. doi: 10.1139/z82-008

Chanton JP, Martens CS, Kelley CA, Crill PM, Showers WJ (1992) Methane transport mechanisms and isotopic fractionation in emergent macrophytes of an Alaskan tundra lake. *Journal of Geophysical Research: Atmospheres (1984–2012)* 97:16681–16688.

Chappellaz J, Barnola JM, Raynaud D, Korotkevich YS, Lorius C (1990) Ice-core record of atmospheric methane over the past 160,000 years. *Nature* 345:127–131.

Chase M, Bleskie C, Walker IR, Gavin DG, Hu FS (2008) Midge-inferred Holocene summer temperatures in Southeastern British Columbia, Canada. *Palaeogeography, Palaeoclimatology, Palaeoecology* 257:244–259. doi: 10.1016/j.palaeo.2007.10.020

Clark Jr RC, Blumer M (1967) Distributions of nlparaffins in marine organisms and sediment1. *Limnology and Oceanography* 12:79–87.

Clegg BF, Kelly R, Clarke GH, Walker IR, Hu FS (2011) Nonlinear response of summer temperature to Holocene insolation forcing in Alaska. *Proceedings of the National Academy of Sciences of the United States of America* 108:19299–304. doi: 10.1073/pnas.1110913108

Coffman WP (1995) Conclusions. In: Armitage PD, Cranston PS, Pinder LC V. (eds) The Chironomidae: the biology and ecology of non-biting midges. Chapman and Hall, London, UK, pp 436–447

Colins M, Knutti R, Arblaster J, Dufresne JL, Fichefet T, Friedlingstein P, Gao X, Gutowski WJ, Johns T, Krinner G, Shongwe M, Tebaldi C, Weaver AJ, Wehner M (2013) Long-term Climate Change: Projections, Commitments and Irreversibility. In: Stocker TF, Qin D, Plattner G-K, Tignor M, Allen SK, Boschung J, Nauels A, Y X, Bex V, Midgley PM (eds) Climate Change 2013: The Physical Science Basis. Contribution of the working group I to the Fifth Assessment Report of the intergovernmental Panel on Climate Change.

Cambridge University Press, Cambridge, United Kingdom and New York, USA,

Collister JW, Rieley G, Stern B, Eglinton G, Fry B (1994) Compound-specific δ 13 C analyses of leaf lipids from plants with differing carbon dioxide metabolisms. *Organic Geochemistry* 21:619–627.

Conrad R (1999) Contribution of hydrogen to methane production and control of hydrogen concentrations in methanogenic soils and sediments. *FEMS Microbiol Ecol* 28:193–202.

Conrad R, Chan O-C, Claus P, Casper P (2007) Characterization of methanogenic Archaea and stable isotope fractionation during methane production in the profundal sediment of an oligotrophic lake (Lake Stechlin, Germany). *Limnology and Oceanography* 52:1393–1406. doi: 10.4319/lo.2007.52.4.1393

Cranston PS (1995) Biogeography. In: Armitage PD, Cranston PS, Pinder LC V. (eds) The Chironomidae: Biology and Ecology of Non-biting Midges. Chapman and Hall, London, UK, pp 62–84

Cranwell PA, Eglinton G, Robinson N (1987) Lipids of aquatic organisms as potential contributors to lacustrine sediments—II. *Organic Geochemistry* 11:513–527.

Damste JSS, Rijpstra WIC, Schouten S, Fuerst JA, Jetten MSM, Strous M (2004) The occurrence of hopanoids in planctomycetes: implications for the sedimentary biomarker record. *Organic Geochemistry* 35:561–566.

Data UC (2015) Climate Fairbanks - Alaska. http://www.usclimatedata.com/. Accessed 18 Jun 2015

Davis TN (2001) Permafrost. University of Alaska, Press, Fairbanks, Alaska

Deines P, Bodelier PLE, Eller G (2007a) Methane-derived carbon flows through methane-oxidizing bacteria to higher trophic levels in aquatic systems. *Environmental microbiology* 9:1126–34. doi: 10.1111/j.1462-2920.2006.01235.x

Deines P, Grey J, Richnow H-H, Eller G (2007b) Linking larval chironomids to methane: seasonal variation of the microbial methane cycle and chironomid δ13C. *Aquatic Microbial Ecology* 46:273–282. doi: 10.3354/ame046273

Deines P, Wooller MJ, Grey J (2009) Unravelling complexities in benthic food webs using a dual stable isotope (hydrogen and carbon) approach. *Freshwater Biology* 54:2243–2251. doi: 10.1111/j.1365-2427.2009.02259.x

Delsontro T, Kunz MJ, Kempter T, Wehrli B, Senn DB (2011) Spatial Heterogeneity of Methane Ebullition in a Large Tropical Reservoir. *Environmental science & technology* 45:9866–9873.

References

DeNiro MJ, Epstein S (1978) Influence of diet on the distributions of carbon isotopes in animals. *Geochimica et Cosmochimica Acta* 42:495–506.

Denman KL, Brasseur G, Chidthaisong A, Ciais P, Cox PM, Dickinson RE, Hauglustaine D, Heinze C, Holland E, Jacob D, Lohmann U, Ramachandran S, Dias PL da S, Wofsy SC, Zhang X (2007) Couplings Between Changes in the Climate System and Biogeochemistry. Climate Change 2007: The Physical Science Basis. Contribution of Working Group I to the Fourth Assessment Report of the Intergovernmental Panel on Climate Change [Solomon, S., D. Qin, M. Manning, Z. Chen, M. Marquis, K.B. Averyt, M.Tignor and H.L. Miller. Cambridge University Press, Cambridge, UK,

Doi H, Kikuchi E, Takagi S, Shikano S (2007) Changes in carbon and nitrogen stable isotopes of chironomid larvae during growth , starvation and metamorphosis. *Rapid communications in mass spectrometry : RCM* 21:997–1002. doi: 10.1002/rcm

Edwards M (2001) Potential analogues for paleoclimatic variations in eastern interior Alaska during the past 14,000yr: atmospheric-circulation controls of regional temperature and moisture responses. *Quaternary Science Reviews* 20:189–202. doi: 10.1016/S0277-3791(00)00123-2

Eglinton G, Calvin M (1967) Chemical fossils. *Scientific American* 216:32–43.

Eglinton G, Hamilton RJ (1967) Leaf epicuticular waxes. *Science* 156:1322–1335.

Elias SA, Brigham-Grette J (2004) Late Pleistocene Events in Beringia. Encyclopedia of Quaternary Science 1057–1066.

Eller G, Deines P, Grey J, Richnow H-H, Krüger M (2005) Methane cycling in lake sediments and its influence on chironomid larval delta13C. *FEMS microbiology ecology* 54:339–50. doi: 10.1016/j.femsec.2005.04.006

Eller G, Deines P, Krüger M (2007) Possible sources of methane-derived carbon for chironomid larvae. *Aquatic Microbial Ecology* 46:283–293. doi: 10.3354/ame046283

Elvert M, Greinert J, Suess E, Whiticar MJ (2001a) Carbon Isotopes of Biomarkers Derived from Methane Oxidizing Microbes at Hydrate Ridge, Cascadia Convergent Margin. *Natural Gas Hydrates: Occurrence, Distribution, and Detection* 115–129.

Elvert M, Niemann H (2008) Occurrence of unusual steroids and hopanoids derived from aerobic methanotrophs at an active marine mud volcano. *Organic Geochemistry* 39:167–177. doi: 10.1016/j.orggeochem.2007.11.006

Elvert M, Whiticar M., Suess E (2001b) Diploptene in varved sediments of Saanich Inlet: indicator of increasing bacterial activity under anaerobic conditions during the Holocene. *Marine Geology* 174:371–383. doi: 10.1016/S0025-3227(00)00161-4

Engels S, Cwynar LC, Rees ABH, Shuman BN (2012) Chironomid-based water depth reconstructions: an independent evaluation of site-specific and local inference models. *Journal of Paleolimnology* 48:693–709. doi: 10.1007/s10933-012-9638-x

Ferrington LC (2008) Global diversity of non-biting midges (Chironomidae; Insecta-Diptera) in freshwater. *Hydrobiologia* 595:447–455. doi: 10.1007/s10750-007-9130-1

Ficken KJ, Barber KE, Eglinton G (1998) Lipid biomarker , d13C and plant macrofossil stratigraphy of a Scottish montane peat bog over the last two millennia.

Ficken KJ, Li B, Swain DL, Eglinton G (2000) An n-alkane proxy for the sedimentary input of submerged/ floating freshwater aquatic macrophytes. *Organic Geochemistry* 31:745–749.

Finney BP, Bigelow NH, Barber V a., Edwards ME (2012) Holocene climate change and carbon cycling in a groundwater-fed, boreal forest lake: Dune Lake, Alaska. *Journal of Paleolimnology* 48:43–54. doi: 10.1007/s10933-012-9617-2

Fischer W, Summons R, Pearson A (2005) Targeted genomic detection of biosynthetic pathways : anaerobic production of hopanoid biomarkers by a common sedimentary microbe. *Geobiology* 3:33–40.

Freeman KH, Wakeham SG, Hayes JM (1994) Predictive isotopic biogeochemistry: hydrocarbons from anoxic marine basins. *Organic geochemistry* 21:629–44.

French HM (2007) The Periglacial Environment, 3rd edn. Wiley and Sons Ltd., Chichester

Gannon JE (1971) Two counting cells for the enumeration of zooplankton micro-crustacea. *Transactions of the American Microscopical Society* 486–490.

Gao X, Adam Schlosser C, Sokolov A, Anthony KW, Zhuang Q, Kicklighter D (2013) Permafrost degradation and methane: low risk of biogeochemical climate-warming feedback. *Environmental Research Letters* 8:035014. doi: 10.1088/1748-9326/8/3/035014

Goedkoop W, Akerblom N, Demandt MH (2006) Trophic fractionation of carbon and nitrogen stable isotopes in Chironomus riparius reared on food of aquatic and terrestrial origin. *Freshwater Biology* 51:878–886. doi: 10.1111/j.1365-2427.2006.01539.x

Goedkoop W, Johnson RK (1992) Modelling the importance of sediment bacterial carbon for profundal macroinvertebrates along a lake nutrient gradient. *Netherlands Journal of Aquatic Ecology* 26:477–483. doi: 10.1007/BF02255278

References

Gorham E (1991) Northern peatlands: Role in the carbon cycle and probable response to climatic warming. *Ecological applications : a publication of the Ecological Society of America* 1:182–195.

Green P (1992) Taxonomy of Methylotrophic Bacteria. In: Murrell JC, Dalton H (eds) Methane and Methanol Utilizers SE - 2. Springer US, pp 23–84

Greene S, Walter Anthony KM, Archer D, Sepulveda-Jauregui a., Martinez-Cruz K (2014) Modeling the impediment of methane ebullition bubbles by seasonal lake ice. *Biogeosciences Discussions* 11:10863–10916. doi: 10.5194/bgd-11-10863-2014

Greinert J, Lewis KB, Bialas J, Pecher I a., Rowden a., Bowden D a., De Batist M, Linke P (2010) Methane seepage along the Hikurangi Margin, New Zealand: Overview of studies in 2006 and 2007 and new evidence from visual, bathymetric and hydroacoustic investigations. *Marine Geology* 272:6–25. doi: 10.1016/j.margeo.2010.01.017

Grey J, Deines P (2005) Differential assimilation of methanotrophic and chemoautotrophic bacteria by lake chironomid larvae. *Aquatic Microbial Ecology* 40:61–66. doi: 10.3354/ame040061

Grey J, Jones R (1999) Carbon stable isotopes reveal complex trophic interactions in lake plankton. *Rapid communications in mass spectrometry : RCM* 13:1311–1314. doi: 10.1002/(SICI)1097-0231(19990715)13:13<1311::AID-RCM545>3.0.CO;2-P

Grey J, Jones RI, Sleep D (2001) Seasonal changes in the importance of the source of organic matter to the diet of zooplankton in Loch Ness, as indicated by stable isotope analysis. *Limnology and Oceanography* 46:505–513. doi: 10.4319/lo.2001.46.3.0505

Grey J, Kelly A, Jones RI, Jones RL (2004a) High Intraspecific variability in carbon and nitrogen stable isotope ratios of lake chironomid larvae. *Limnology and Oceanography* 49:239–244.

Grey J, Kelly A, Jones RI, Jones RL (2011) High intraspecfic variability in carbon and nitrogen stable isotope ratios of lake chironomid larvae. *Limnology and Oceanography* 49:239–244.

Grey J, Kelly A, Ward S, Sommerwerk N, Jones RI (2004b) Seasonal changes in the stable isotope values of lake-dwelling chironomid larvae in relation to feeding and life cycle variability. *Freshwater Biology* 49:681–689. doi: 10.1111/j.1365-2427.2004.01217.x

Grimalt J, Albaigés J (1987) Sources and occurrence of C 12□ C 22 n-alkane distributions with even carbon-number preference in sedimentary environments. *Geochimica et Cosmochimica Acta* 51:1379–1384.

Grosse G, Romanovsky V, Walter K, Morgenstern A, Lantuit H, Zimov S (2008) Distribution of Thermokarst Lakes and Ponds at Three Yedoma Sites in Siberia. Proceedings of the Ninth International Conference on Permafrost. Fairbanks, Alaska,

Gu B, Schell DM, Alexander V (1994) Stable Carbon and Nitrogen Isotopic Analysis of the Plankton Food Web in a Subarctic Lake.

Gu B, Schelske CL, Brenner M (1996) Relationship between sediment and plankton isotope ratios (d13C and d15N) and primary productivity in Florida lakes. *Canadian Journal of Fisheries and Aquatic Sciences* 53:875–883.

Hamburger K, Dall PC, Lindegaard C (1995) Effects of oxygen deficiency on survival and glycogen content of Chironomus anthracinus (Diptera, Chironomidae) under laboratory and field conditions. *Hydrobiologia* 297:187–200. doi: 10.1007/BF00019284

Hansen K (1962) The dystrophic lake type. *Hydrobiologia* 19:183–190.

Hayes JM (1993) Factors controlling 13 C contents of sedimentary organic compounds: principles and evidence. *Marine Geology* 113:111–125.

He R, Wooller MJ, Pohlman JW, Quensen J, Tiedje JM, Leigh MB (2012) Shifts in identity and activity of methanotrophs in arctic lake sediments in response to temperature changes. *Applied and environmental microbiology* 78:4715–23. doi: 10.1128/AEM.00853-12

Heiri O (2004) Within-lake variability of subfossil chironomid assemblages in shallow Norwegian lakes. *Journal of Paleolimnology* 32:67–84. doi: 10.1023/B:JOPL.0000025289.30038.e9

Heiri O, Schilder J, Hardenbroek M Van (2012) Stable isotopic analysis of fossil chironomids as an approach to environmental reconstruction : state of development and future challenges. Proceedings of the 18th International Symposium on Chironomidae - Fauna norvegica. pp 7–18

Hershey AAE, Beaty S, Fortino K, Kelly S, Keyse M, Luecke C, Brien WJO, Whalen C (2006) Stable isotope signatures of benthic invertebrates in Arctic Lakes Indicate Limited coupling to Pelagic Production. *Limnology and Oceanography* 51:177–188.

Hinkel KM, Eisner WR, Bockheim JG, Nelson FE, Peterson KM, Dai X (2003) Spatial Extent, Age, and Carbon Stocks in Drained Thaw Lake Basins on the Barrow Peninsula, Alaska. *Arctic, Antarctic, and Alpine Research* 35:291–300. doi: 10.1657/1523-0430(2003)035[0291:SEAACS]2.0.CO;2

Hinkel KM, Frohn RC, Nelson FE, Eisner WR, Beck R a. (2005) Morphometric and spatial analysis of thaw lakes and drained thaw lake basins in the western Arctic Coastal Plain, Alaska. *Permafrost and Periglacial Processes* 16:327–341. doi: 10.1002/ppp.532

Hinzman LD, Bettez ND, Bolton WR, Chapin FS, Dyurgerov MB, Fastie CL, Griffith B, Hollister RD, Hope A, Huntington HP, Jensen AM, Jia GJ, Jorgenson T, Kane DL, Klein DR, Kofinas G, Lynch AH, Lloyd AH, McGuire a. D, Nelson FE, Oechel WC, Osterkamp TE, Racine CH, Romanovsky VE, Stone RS, Stow D a., Sturm M, Tweedie CE, Vourlitis GL, Walker MD, Walker D a., Webber PJ, Welker JM, Winker KS, Yoshikawa K (2005) Evidence and

Implications of Recent Climate Change in Northern Alaska and Other Arctic Regions. *Climatic Change* 72:251–298. doi: 10.1007/s10584-005-5352-2

Hofmann W (1998) Cladocerans and chironomids as indicators of lake level changes in north temperate lakes. *Journal of Paleolimnology* 19:55–62.

Hopkins DM (1982) Aspects of paleogeography of Beringia during the late Pleistocene. In: Hopkins DM, Matthews J V., Schweger CE, Young SB (eds) Palaeoecology of Beringia. Academic Press, pp 3–28

Hornibrook ERC, Longstaffe FJ, Fyfe WS (2000) Evolution of stable carbon isotope compositions for methane and carbon dioxide in freshwater wetlands and other anaerobic environments. *Geochimica et cosmochimica acta* 64:1013–1027.

Hunter J, MacAulay H, Gagne R, Burns R, Harrison T, J. Hawkins (1981) Drained lake experiment for investigation of growth of perma-frost at Illisarvik, Northwest Territories—Initial geophysical results. Cur-rent Research, Part C, Pap. 81-1C, Geol. Surv. of Can., Ottawa

Iovino AJ (1975) Extant chironomid larval populations and the representativeness and nature of their remains in lake sediments. Indiana University Press, Bloomington

Jahnke LL, Summons RE, Hope JM, Des Marais DJ (1999) Carbon isotopic fractionation in lipids from methanotrophic bacteria II : The effects of physiology and environmental parameters on the biosynthesis and isotopic signatures of biomarkers. *Geochimica et Cosmochimica Acta* 63:79–93.

Johnson RK (1987) Seasonal variation in diet of Chironomus plumosus (L.) and C. anthracinus Zett. (Diptera: Chironomidae) in mesotrophic Lake Erken. *Freshwater Biology* 17:525–532. doi: 10.1111/j.1365-2427.1987.tb01073.x

Jones MC, Yu Z (2010) Rapid deglacial and early Holocene expansion of peatlands in Alaska. *Proceedings of the National Academy of Sciences of the United States of America* 107:7347–52. doi: 10.1073/pnas.0911387107

Jones RI, Carter CE, Kelly A, Ward S, Kelly DJ, Grey J (2008) Widespread contribution of methane-cycle bacteria to the diets of lake profundal chironomid larvae. *Ecology* 89:857–64.

Jones RI, Grey J (2004) Stable isotope analysis of chironomid larvae from some Finnish forest lakes indicates dietary contribution from biogenic methane. *BOREAL ENIVIRONMENT RESEARCH* 9:17–23.

Jones RI, Grey J (2011) Biogenic methane in freshwater food webs. 213–229. doi: 10.1111/j.1365-2427.2010.02494.x

Jorgenson MT, Shur Y (2007) Evolution of lakes and basins in northern Alaska and discussion of the thaw lake cycle. *Journal of Geophysical Research* 112:1–12. doi: 10.1029/2006JF000531

Jorgenson MT, Shur YL, Pullman ER (2006) Abrupt increase in permafrost degradation in Arctic Alaska. *Geophysical Research Letters* 33:2–5. doi: 10.1029/2005GL024960

Joyce J, Jewell PW (2003) Physical Controls on Methane Ebullition from Reservoirs and Lakes. *Environmental and Engineering Geoscience* IX:167–178.

Juggins S (2007) Software: C2 Data Analysis. Version 1.5. 1.

Juggins S (2013) Quantitative reconstructions in palaeolimnology: new paradigm or sick science? *Quaternary Science Reviews* 64:20–32.

Kamal S, Varma A (2008) Peatland Microbiology. In: Dion P, Nautiyal C (eds) Microbiology of Extreme Soils SE - 9. Springer Berlin Heidelberg, pp 177–203

Kankaala P, Huotari J, Peltomaa E, Saloranta T, Ojala A (2006) Methanotrophic activity in relation to methane efflux and total heterotrophic bacterial production in a stratified, humic, boreal lake. *Limnology and Oceanography* 51:1195–1204. doi: 10.4319/lo.2006.51.2.1195

Kankaala P, Makela S, Bergstrom I, Huitu E, Kaki T, Ojala A, Rantakari M, Kortelainen P, Arvola L (2003) Midsummer spatial variation in methane efflux from stands of littoral vegetation in a boreal meso-eutrophic lake. *Freshwater Biology* 48:1617–1629.

Kaufman D (2004) Holocene thermal maximum in the western Arctic (0–180°W). *Quaternary Science Reviews* 23:529–560. doi: 10.1016/j.quascirev.2003.09.007

Kaushal S, Binford MW (1999) Relationship between C:N ratios of lake sediments , organic matter sources , and historical deforestation in Lake Pleasant , Massachusetts , USA. 1:439–442.

Kelly A, Jones RI, Grey J (2004) Stable isotope analysis provides fresh insights into dietary separation between Chironomus anthracinus and C. plumosus. *Journal of the North American Benthological Society* 23:287–296. doi: 10.1899/0887-3593(2004)023<0287:SIAPFI>2.0.CO;2

Kennett JP, Cannariato KG, Hendy IL, Behl RJ (2003) Methane Hydrates in Quaternary Climate Change: The Clathrate Gun Hypothesis. AGU, Washington, DC

Kessler M a., Plug LJ, Walter Anthony KM (2012) Simulating the decadal- to millennial-scale dynamics of morphology and sequestered carbon mobilization of two thermokarst lakes in NW Alaska. *Journal of Geophysical Research: Biogeosciences* 117:n/a–n/a. doi: 10.1029/2011JG001796

Kirschke S, Bousquet P, Ciais P, Saunois M, Canadell JG, Dlugokencky EJ, Bergamaschi P, Bergmann D, Blake DR, Bruhwiler L, Cameron-Smith P, Castaldi S, Chevallier F, Feng L, Fraser A, Heimann M, Hodson EL,

Houweling S, Josse B, Fraser PJ, Krummel PB, Lamarque J-F, Langenfelds RL, Le Quéré C, Naik V, O'Doherty S, Palmer PI, Pison I, Plummer D, Poulter B, Prinn RG, Rigby M, Ringeval B, Santini M, Schmidt M, Shindell DT, Simpson IJ, Spahni R, Steele LP, Strode S a., Sudo K, Szopa S, van der Werf GR, Voulgarakis A, van Weele M, Weiss RF, Williams JE, Zeng G (2013) Three decades of global methane sources and sinks. *Nature Geoscience* 6:813–823. doi: 10.1038/ngeo1955

Kiyashko S, Narita T, Wada E (2001) Contribution of methanotrophs to freshwater macroinvertebrates: evidence from stable isotope ratios. *Aquatic Microbial Ecology* 24:203–207. doi: 10.3354/ame024203

Klene AE, Nelson FE, Shiklomanov NI, Hinkel KM (2001) The n-factor in natural landscapes: Variability of air and soil-surface temperatures, Kuparuk River Basin, Alaska, USA. *Arctic, Antarctic, and Alpine Research* 140–148.

Kling GW, Kipphut GW, Miller MC (1992) The flux of CO 2 and CH 4 from lakes and rivers in arctic Alaska. *Hydrobiologia* 240:23–36.

Knittel K, Lösekann T, Boetius A, Kort R, Amann R (2005) Diversity and Distribution of Methanotrophic Archaea at Cold Seeps. *Applied and environmental microbiology* 71:467–479. doi: 10.1128/AEM.71.1.467

Kohzu a, Kato C, Iwata T, Kishi D, Murakami M, Nakano S, Wada E (2004) Stream food web fueled by methane-derived carbon. *Aquatic Microbial Ecology* 36:189–194. doi: 10.3354/ame036189

Kurek J, Cwynar LC (2009) The potential of site-specific and local chironomid-based inference models for reconstructing past lake levels. *Journal of Paleolimnology* 42:37–50. doi: 10.1007/s10933-008-9246-y

Kurek J, Cwynar LC, Vermaire JC (2009) A late Quaternary paleotemperature record from Hanging Lake, northern Yukon Territory, eastern Beringia. *Quaternary Research* 72:246–257. doi: 10.1016/j.yqres.2009.04.007

Lambeck K, Esat TM, Potter E-K (2002) Links between climate and sea levels for the past three million years. *Nature* 419:199–206. doi: 10.1038/nature01089

Langdon PG, Caseldine CJ, Croudace IW, Jarvis S, Wastegård S, Crowford TC (2011) A chironomid-based reconstruction of summer temperatures in NW Iceland since AD 1650. *Quaternary Research* 75:451–460. doi: 10.1016/j.yqres.2010.11.007

Langdon PG, Ruiz Z, Brodersen KP, Foster IDL (2006) Assessing lake eutrophication using chironomids: understanding the nature of community response in different lake types. *Freshwater Biology* 51:562–577. doi: 10.1111/j.1365-2427.2005.01500.x

Langdon PG, Ruiz Z, Wynne S, Sayer CD, Davidson T a. (2010) Ecological influences on larval chironomid communities in shallow lakes: implications for palaeolimnological interpretations. *Freshwater Biology* 55:531–545. doi: 10.1111/j.1365-2427.2009.02345.x

Larocque I, Hall R (2003) Chironomids as quantitative indicators of mean July air temperature: validation by comparison with century-long meteorological records from northern Sweden. *Journal of Paleolimnology* 475–493.

Larocque I, Hall R, Grahn E (2001) Chironomids as indicators of climate change: a 100 lake training set from a subarctic region of northern Sweden (Lapland). *Journal of Paleolimnology* 26:307–322.

Leng MJ (2006) Isotopes in Palaeoenvironmental Research. Springer, Dordrecht

Liebner S, Wagner D (2007) Abundance, distribution and potential activity of methane oxidizing bacteria in permafrost soils from the Lena Delta, Siberia. *Environmental microbiology* 9:107–17. doi: 10.1111/j.1462-2920.2006.01120.x

Liebner S, Zeyer J, Wagner D, Schubert C, Pfeiffer E, Knoblauch C (2011) Methane oxidation associated with submerged brown mosses reduces methane emissions from Siberian polygonal tundra. *Journal of Ecology* 99:914–922.

Little JL, Smol JP (2001) A chironomid-based model for inferring late- summer hypolimnetic oxygen in southeastern Ontario lakes. *Journal of Paleolimnology* 26:259–270.

Livingstone DM, Lotter AF (1998) The relationship between air and water temperatures in lakes of the Swiss Plateau: a case study with pal\ sgmaelig; olimnological implications. *Journal of Paleolimnology* 19:181–198.

Lotter a (1999) An intercontinental comparison of chironomid palaeotemperature inference models: Europe vs North America. *Quaternary Science Reviews* 18:717–735. doi: 10.1016/S0277-3791(98)00044-4

Loulergue L, Schilt A, Spahni R, Masson-Delmotte V, Blunier T, Lemieux B, Barnola J-M, Raynaud D, Stocker TF, Chappellaz J (2008) Orbital and millennial-scale features of atmospheric CH4 over the past 800,000 years. *Nature* 453:383–6. doi: 10.1038/nature06950

Lowe JJ, Birks HH, Brooks SJ, Coope GR, Harkness DD, Mayle FE, Sheldrick C, Turney CSM, Walker MJC (1999) The chronology of palaeoenvironmental changes during the Last Glacial-Holocene transition: towards an event stratigraphy for the British Isles. *Journal of the Geological Society* 156:397–410. doi: 10.1144/gsjgs.156.2.0397

Maciolek J a. (1989) Tundra ponds of the Yukon Delta, Alaska, and their macroinvertebrate communities. *Hydrobiologia* 172:193–206. doi: 10.1007/BF00031622

Mackey A (1977) Growth and development of larval Chironomidae. *Oikos* 28:270–275.

References

Madigan MT, Martinko JM (2006) Brock Biology of Microorganisms, 11th edn. Pearson Education LTD, Upper Saddle River, NJ

Martens CPS, Klump JVAL (1980) Biogeochemical cycling in an organic-rich coastal marine basin-I . Methane sediment-water exchange processes. *Geochimica et Cosmochimica Acta* 44:471–490.

Martinez-Cruz K, Sepulveda-Jauregui A, Walter Anthony K, Thalasso F (2015) Geographic and seasonal variation of dissolved methane and aerobic methane oxidation in Alaskan lakes. *Biogeosciences Discussions* 12:4213–4243. doi: 10.5194/bgd-12-4213-2015

Mayer T, Johnson MG (1994) History of anthropogenic activities in Hamilton Harbour as determined from the sedimentary record. *Environmental Pollution* 86:341–347.

Mazéas O, von Fischer JC, Rhew RC (2009) Impact of terrestrial carbon input on methane emissions from an Alaskan Arctic lake. *Geophysical Research Letters* 36:1–5. doi: 10.1029/2009GL039861

McGuire a D, Macdonald RW, Schuur EA, Harden JW, Kuhry P, Hayes DJ, Christensen TR, Heimann M (2010) The carbon budget of the northern cryosphere region. *Current Opinion in Environmental Sustainability* 2:231–236. doi: 10.1016/j.cosust.2010.05.003

McGuire a. D, Chapin FS, Walsh JE, Wirth C (2006) Integrated Regional Changes in Arctic Climate Feedbacks: Implications for the Global Climate System *. *Annual Review of Environment and Resources* 31:61–91. doi: 10.1146/annurev.energy.31.020105.100253

Meehl G a., Covey C, Taylor KE, Delworth T, Stouffer RJ, Latif M, McAvaney B, Mitchell JFB (2007) THE WCRP CMIP3 Multimodel Dataset: A New Era in Climate Change Research. *Bulletin of the American Meteorological Society* 88:1383–1394. doi: 10.1175/BAMS-88-9-1383

Megonigal JP, Vann CD, Wolf A a. (2005) Flooding constraints on tree (Taxodium distichum) and herb growth responses to elevated CO2. *Wetlands* 25:430–438. doi: 10.1672/17

Merritt RW, K CW, Berg MB (2008) An Introduction to the Aquatic Insects of North America, 4th edn. Kendall/Hunt Publ. Co.,, Dubuque, IA

Meyers P a (2003) Applications of organic geochemistry to paleolimnological reconstructions: a summary of examples from the Laurentian Great Lakes. *Organic Geochemistry* 34:261–289. doi: 10.1016/S0146-6380(02)00168-7

Meyers PA (1994) Preservation of elemental and isotopic source identification of sedimentary organic matter. *Chemical Geology* 114:289–302.

Meyers PA, Ishiwatari R (1993) Lacustrine organic geochemistry - an overview of indicators of organic matter sources and diagenesis in lake sediments. *Organic geochemistry* 20:867–900.

Meyers PA, Lallier-Verges E (1999) Lacustrine sedimentary organic matter records of Late Quaternary paleoclimates. *Journal of Paleolimnology* 21:345–372.

Miller GH, Brigham-Grette J, Alley RB, Anderson L, Bauch H a., Douglas MSV, Edwards ME, Elias S a., Finney BP, Fitzpatrick JJ, Funder SV, Herbert TD, Hinzman LD, Kaufman DS, MacDonald GM, Polyak L, Robock a., Serreze MC, Smol JP, Spielhagen R, White JWC, Wolfe a. P, Wolff EW (2010) Temperature and precipitation history of the Arctic. *Quaternary Science Reviews* 29:1679–1715. doi: 10.1016/j.quascirev.2010.03.001

Muri G, Wakeham SG, Pease TK, Faganeli J (2004) Evaluation of lipid biomarkers as indicators of changes in organic matter delivery to sediments from Lake Planina, a remote mountain lake in NW Slovenia. *Organic Geochemistry* 35:1083–1093.

Murton JB (1996) Near-Surface Brecciation of Chalk , Isle of Thanet , South-East England a Comparison with Ice-Rich Brecciated Bedrocks in Canada and Spitsbergen. *Permafrost and Periglacial Processes* 7:153–164.

Muster S, Heim B, Abnizova A, Boike J (2013) Water Body Distributions Across Scales: A Remote Sensing Based Comparison of Three Arctic TundraWetlands. *Remote Sensing* 5:1498–1523. doi: 10.3390/rs5041498

Naeher S, Niemann H, Peterse F, Smittenberg RH, Zigah PK, Schubert CJ (2014) Tracing the methane cycle with lipid biomarkers in Lake Rotsee (Switzerland). *Organic Geochemistry* 66:174–181. doi: 10.1016/j.orggeochem.2013.11.002

O'Connor FMO, Boucher O, Gedney N, Jones CD, Folberth GA, Coppell R, Friedlingstein P, Collins WJ, Chappellaz J, Ridley J, Johnson CE (2010) Possible role of wetlands, permafrost and methane hydrates in the methane cycle under future climate change: A review. *Reviews of Geophysics* 48:1–33. doi: 10.1029/2010RG000326.1.INTRODUCTION

Oba M, Sakata S, Tsunogai U (2006) Polar and neutral isopranyl glycerol ether lipids as biomarkers of archaea in near-surface sediments from the Nankai Trough. *Organic geochemistry* 37:1643–1654.

Oechel WC, Callaghan T, Gilmanov T, Holten JI, Maxwell B, Molau U, Sveinbjornsson B (1997) Global Climate and Arctic Terrestrial Ecosystems. Springer, New York

Oliver DR, Dillon ME (1997) Chironomids (Diptera: Chironomidae) of the Yukon Arctic North Slope and Herschel Island. Insects of the Yukon. Biological Survey of Canada (Terrestrial Arthropods), Ottawa,.

Oliver DR, Roussel ME (1983) The insects and arachnids of Canada. Part 11. The genera of larval midges of Canada. Diptera: Chironomidae. Minister of Supply and Services

Osterkamp T (2005) The recent warming of permafrost in Alaska. *Global and Planetary Change* 49:187–202. doi: 10.1016/j.gloplacha.2005.09.001

References

Ostrovsky I, Mcginnis DF, Lapidus L, Eckert W (2008) Quantifying gas ebullition with echosounder: the role of methane transport by bubbles in a medium-sized lake. *Limnology and Oceanography: Methods* 6:105–118.

Ourisson G, Rohmer M, Poralla K (1987) Prokaryotic hopanoids and other polyterpenoid sterol surrogates. *An Rev Microbiol* 41:301–33.

Pancost R., Hopmans E., Sinninghe Damsté J. (2001) Archaeal lipids in Mediterranean cold seeps: molecular proxies for anaerobic methane oxidation. *Geochimica et Cosmochimica Acta* 65:1611–1627. doi: 10.1016/S0016-7037(00)00562-7

Pancost RD, Baas M, Van B, Sinninghe JS (2003) Response of an ombrotrophic bog to a regional climate event revealed by macrofossil, molecular and carbon isotopic data. *The Holocene* 13:921–932. doi: 10.1191/0959683603hl674rp

Pancost RD, Damsté JSS, De S, Maarel MJEC Van Der, Gottschal JC (2000a) Biomarker Evidence for Widespread Anaerobic Methane Oxidation in Mediterranean Sediments by a Consortium of Methanogenic Archaea and Bacteria. *Applied and environmental microbiology* 66:1126–1132. doi: 10.1128/AEM.66.3.1126-1132.2000.Updated

Pancost RD, Geel B Van, Baas M, Sinninghe Damsté JS (2000b) d13C values and radiocarbon dates of microbial biomarkers as tracers for carbon recycling in peat deposits. *Geology* 28:663–666. doi: 10.1130/0091-7613(2000)28<663

Pancost RD, Sinninghe Damsté JS (2003) Carbon isotopic compositions of prokaryotic lipids as tracers of carbon cycling in diverse settings. *Chemical Geology* 195:29–58. doi: 10.1016/S0009-2541(02)00387-X

Pearson EJ, Farrimond P, Juggins S (2007) Lipid geochemistry of lake sediments from semi-arid Spain: Relationships with source inputs and environmental factors. *Organic Geochemistry* 38:1169–1195. doi: 10.1016/j.orggeochem.2007.02.007

Peterson BJ, Fry B (1987) Stable Isotopes in Ecosystem Studies. *Annual Review of Ecology and Systematics* 18:293–320. doi: 10.1146/annurev.es.18.110187.001453

Péwé TL (1975) Quaternary geology of Alaska.

Pienitz R, Doran PT, Lamoureux SF (2008) Origin and geomorphology of lakes in the polar regions. *Polar Lakes and RiverseLimnology of Arctic and Antarctic Aquatic Ecosystems Oxford University Press, Oxford, UK* 25–41.

Pitcher A, Hopmans EC, Schouten S, Damsté JSS (2009) Separation of core and intact polar archaeal tetraether lipids using silica columns: insights into living and fossil biomass contributions. *Organic Geochemistry* 40:12–19.

Porinchu DF, Macdonald GM (2003) The use and application of freshwater midges (Chironomidae: Insecta: Diptera) in geographical research.

Progress in Physical Geography 27:378–422. doi: 10.1191/0309133303pp388ra

Prowse TD (1990) Northern Hydrology: an overview. In: Prowse TD, Ommanney CS. (eds) Northern Hydrology, Canadian Perspectives, NHRI Scien. Sakatchewan, pp 1–36

Prowse TD, Wrona FJ, Reist JD, Gibson JJ, Hobbie JE, Lévesque LMJ, Vincent WF (2006) Climate change effects on hydroecology of arctic freshwater ecosystems. *Ambio* 35:347–58.

Quinlan R, Paterson MJ, Smol JP (2012) Climate-mediated changes in small lakes inferred from midge assemblages: the influence of thermal regime and lake depth. Journal of Paleolimnology. doi: 10.1007/s10933-012-9585-6

Quinlan R, Smol J (2001) Setting minimum head capsule abundance and taxa deletion criteria in chironomid-based inference models. *Journal of Paleolimnology* 327–342.

Rau G (1978) Carbon-13 depletion in a subalpine lake: carbon flow implications. *Science (New York, NY)* 201:901–2. doi: 10.1126/science.201.4359.901

Ravinet M, Syväranta J, Jones RI, Grey J (2010) A trophic pathway from biogenic methane supports fish biomass in a temperate lake ecosystem. *Oikos* 119:409–416. doi: 10.1111/j.1600-0706.2009.17859.x

Reddy KR, DeLaune R (2008) Biogeochemistry of Wetlands: Science and applications. CRC Press, USA

Reeburgh WS (2007) Oceanic methane biogeochemistry. *Chemical reviews* 107:486–513. doi: 10.1021/cr050362v

Reyes A V, Cooke CA (2011) Northern peatland initiation lagged abrupt increases in deglacial atmospheric CH 4. *PNAS* 108:4748–4753. doi: 10.1073/pnas.1013270108/-/DCSupplemental.www.pnas.org/cgi/doi/10.1073/pnas.1013270108

Rohmer M, Knani M, Simonin P, Sutter B, Sahm H (1993) Isoprenoid biosynthesis in bacteria: a novel pathway for the early steps leading to isopentenyl diphosphate. *The Biochemical journal* 295 (Pt 2:517–24.

Rouse WR, Douglas MS V, Hecky RE, Hershey AE, Kling GW, Lesack L, Marsh P, Mcdonald M, Nicholson BJ, Roulet NT, Smol JP (1997) Effects of climate change on the freshwaters of arctic and subarctic North America. *Hydrological Processes* 11:873–902.

Rudd JWM, Taylor CD (1980) Methane cycling in aquatic environments. *Adv Aquat Microbiol* 2:77–150.

References

Ruiz Z, Brown A, Langdon P (2006) The potential of chironomid (Insecta: Diptera) larvae in archaeological investigations of floodplain and lake settlements. *Journal of Archaeological Science* 33:14–33. doi: 10.1016/j.jas.2005.05.015

Rundel PW, Stichler W, Zander RH, Ziegler H (1979) Carbon and hydrogen isotope ratios of bryophytes from arid and humid regions. *Oecologia* 44:91–94.

Sakata S, Hayes JM, McTaggart a R, Evans R a, Leckrone KJ, Togasaki RK (1997) Carbon isotopic fractionation associated with lipid biosynthesis by a cyanobacterium: relevance for interpretation of biomarker records. *Geochimica et cosmochimica acta* 61:5379–89.

Sanseverino AM, Bastviken D, Sundh I, Pickova J, Enrich-Prast A (2012) Methane carbon supports aquatic food webs to the fish level. *PloS one* 7:e42723. doi: 10.1371/journal.pone.0042723

Scandella BP, Varadharajan C, Hemond HF, Ruppel C, Juanes R (2011) A conduit dilation model of methane venting from lake sediments. *Geophysical Research Letters* 38:n/a–n/a. doi: 10.1029/2011GL046768

Schirrmeister L, Froese D, Tumskoy V, Grosse G, Wetterich S (2013) Yedoma. Encyclopedia of Quaternary Science 3:542–552.

Schirrmeister L, Kunitsky V, Grosse G, Wetterich S, Meyer H, Schwamborn G, Babiy O, Derevyagin a., Siegert C (2011) Sedimentary characteristics and origin of the Late Pleistocene Ice Complex on north-east Siberian Arctic coastal lowlands and islands – A review. *Quaternary International* 241:3–25. doi: 10.1016/j.quaint.2010.04.004

Schirrmeister L, Meyer H, Wetterich S, Siegert C, Kunitsky V, Grosse G, Kuznetsova T, Dereviagin A (2008) The Yedoma Suite of the Northeastern Siberian Shelf Region : Characteristics and Concept of Formation. Ninth International Conference on Permafrost. pp 1595–1600

Schleusner P, Biskaborn BK, Kienast F, Wolter J, Subetto D, Diekmann B (2015) Basin evolution and palaeoenvironmental variability of the thermokarst lake El'gene-Kyuele, Arctic Siberia. *Boreas* 44:216–229. doi: 10.1111/bor.12084

Schuldt RJ, Brovkin V, Kleinen T, Winderlich J (2012) Modelling holocene carbon accumulation and methane emissions of boreal wetlands – an earth system model approach. *Biogeosciences Discussions* 9:12667–12710. doi: 10.5194/bgd-9-12667-2012

Schuur E a. G, Bockheim J, Canadell JG, Euskirchen E, Field CB, Goryachkin S V., Hagemann S, Kuhry P, Lafleur PM, Lee H, Mazhitova G, Nelson FE, Rinke A, Romanovsky VE, Shiklomanov N, Tarnocai C, Venevsky S, Vogel JG, Zimov S a. (2008) Vulnerability of Permafrost Carbon to Climate Change: Implications for the Global Carbon Cycle. *BioScience* 58:701. doi: 10.1641/B580807

Sepulveda-Jauregui a., Walter Anthony KM, Martinez-Cruz K, Greene S, Thalasso F (2014) Methane and carbon dioxide emissions from 40 lakes along a north-south latitudinal transect in Alaska. *Biogeosciences Discussions* 11:13251–13307. doi: 10.5194/bgd-11-13251-2014

Sepulveda-Jauregui a., Walter Anthony KM, Martinez-Cruz K, Greene S, Thalasso F (2015) Methane and carbon dioxide emissions from 40 lakes along a north-south latitudinal transect in Alaska. *Biogeosciences* 12:3197–3223. doi: 10.5194/bg-12-3197-2015

Sher A V. (1971) Mammals and Late Pleistocene Stratigraphy of the Northeast USSR and of North America. Nauka(in Russian), Moscow

Shirokova LS, Pokrovsky OS, Kirpotin SN, Desmukh C, Pokrovsky BG, Audry S, Viers J (2012) Biogeochemistry of organic carbon, CO2, CH4, and trace elements in thermokarst water bodies in discontinuous permafrost zones of Western Siberia. *Biogeochemistry* 113:573–593. doi: 10.1007/s10533-012-9790-4

Silliman JE, Schelske CL (2003) Saturated hydrocarbons in the sediments of Lake Apopka, Florida. *Organic Geochemistry* 34:253–260. doi: 10.1016/S0146-6380(02)00169-9

Smith LC, MacDonald GM, Velichko a a, Beilman DW, Borisova OK, Frey KE, Kremenetski K V, Sheng Y (2004) Siberian peatlands a net carbon sink and global methane source since the early Holocene. *Science (New York, NY)* 303:353–6. doi: 10.1126/science.1090553

Smith LC, Sheng Y, MacDonald GM, Hinzman LD (2005) Disappearing Arctic lakes. *Science (New York, NY)* 308:1429. doi: 10.1126/science.1108142

Sobek S (2014) Climate science: Cold carbon storage. *Nature* 511:415–417.

Soja AJ, Tchebakova NM, French NHF, Flannigan MD, Shugart HH, Stocks BJ, Sukhinin AI, Parfenova EI, Chapin FS, Stackhouse PW (2007) Climate-induced boreal forest change: Predictions versus current observations. *Global and Planetary Change* 56:274–296. doi: 10.1016/j.gloplacha.2006.07.028

Spooner N, Rieley G, Collister JW, Lander IM, Cranwell IPA, Maxwell JR (1994) Stable carbon isotopic correlation of individual biolipids in aquatic organisms and a lake bottom sediment. *Organic Geochemistry* 21:823–827.

Stuiver M, Polach HA (1977) Discussion; reporting of C-14 data. *Radiocarbon* 19:355–363.

Sundh I, Bastviken D, Tranvik LJ (2005) Abundance, activity, and community structure of pelagic methane-oxidizing bacteria in temperate lakes. *Applied and environmental microbiology* 71:6746–6752.

References

Talbot HM, Farrimond P (2007) Bacterial populations recorded in diverse sedimentary biohopanoid distributions. *Organic Geochemistry* 38:1212–1225. doi: 10.1016/j.orggeochem.2007.04.006

Tarnocai C, Canadell JG, Schuur E a. G, Kuhry P, Mazhitova G, Zimov S (2009) Soil organic carbon pools in the northern circumpolar permafrost region. *Global Biogeochemical Cycles* 23:1–11. doi: 10.1029/2008GB003327

Templeton AS, Chu K-H, Alvarez-Cohen L, Conrad ME (2006) Variable carbon isotope fractionation expressed by aerobic CH4-oxidizing bacteria. *Geochimica et Cosmochimica Acta* 70:1739–1752. doi: 10.1016/j.gca.2005.12.002

Tenzer GE, Meyers PA, Knoop P (1997) Sources and distribution of organic and carbonate carbon in surface sediments of pyramid lake, Nevada. *Journal of Sedimentary Research* 67:884–890.

Ter Braak CJF, Smilauer P (2002) Canoco for Windows version 4.5.

Thiel V, Blumenberg M, Pape T, Seifert R, Michaelis W (2003) Unexpected occurrence of hopanoids at gas seeps in the Black Sea. *Organic Geochemistry* 34:81–87. doi: 10.1016/S0146-6380(02)00191-2

Tokeshi M (1995) Life cycles and population dynamics. In: Armitage PD, Cranston PS, Pinder LC V. (eds) he Chironomidae: Biology and Ecology of Non-biting Midges. Chapman and Hall, London, UK, pp 225–268

Trotsenko Y a, Khmelenina VN (2005) Aerobic methanotrophic bacteria of cold ecosystems. *FEMS microbiology ecology* 53:15–26. doi: 10.1016/j.femsec.2005.02.010

Valdes PJ (2005) The ice age methane budget. *Geophysical Research Letters* 32:L02704. doi: 10.1029/2004GL021004

Van Der Meer MT, Schouten S, van Dongen BE, Rijpstra WI, Fuchs G, Damste JS, de Leeuw JW, Ward DM (2001) Biosynthetic controls on the 13C contents of organic components in the photoautotrophic bacterium Chloroflexus aurantiacus. *The Journal of biological chemistry* 276:10971–6. doi: 10.1074/jbc.M009701200

Van Hardenbroek M, Heiri O, Grey J, Bodelier PLE, Verbruggen F, Lotter AF (2010) Fossil chironomid d13C as a proxy for past methanogenic contribution to benthic food webs in lakes? *Journal of Paleolimnology* 43:235–245. doi: 10.1007/s10933-009-9328-5

Van Hardenbroek M, Heiri O, Parmentier FJW, Bastviken D, Ilyashuk BP, Wiklund J a., Hall RI, Lotter AF (2012a) Evidence for past variations in methane availability in a Siberian thermokarst lake based on d13C of chitinous invertebrate remains. *Quaternary Science Reviews* 1–11. doi: 10.1016/j.quascirev.2012.04.009

Van Hardenbroek M, Heiri O, Wilhelm MF, Lotter a. F (2011) How representative are subfossil assemblages of Chironomidae and common benthic

invertebrates for the living fauna of Lake De Waay, the Netherlands? *Aquatic Sciences* 73:247–259. doi: 10.1007/s00027-010-0173-4

Van Hardenbroek M, Lotter AF, Bastviken D, Duc NT, Heiri O (2012b) Relationship between δ13C of chironomid remains and methane flux in Swedish lakes. *Freshwater Biology* 57:166–177. doi: 10.1111/j.1365-2427.2011.02710.x

Van Huissteden J, Berrittella C, Parmentier FJW, Mi Y, Maximov TC, Dolman a. J (2011) Methane emissions from permafrost thaw lakes limited by lake drainage. *Nature Climate Change* 1:119–123. doi: 10.1038/nclimate1101

Van Winden JF, Kip N, Reichart G-J, Jetten MSM, Camp HJMO Den, Damsté JSS (2010) Lipids of symbiotic methane-oxidizing bacteria in peat moss studied using stable carbon isotopic labelling. *Organic Geochemistry* 41:1040–1044. doi: 10.1016/j.orggeochem.2010.04.015

Varadharajan C (2009) Magnitude and spatio-temporal variability of methane emissions from a eutrophic freshwater lake. Massachusetts Institute of Technology

Vaughan DG, Comiso JC, Allison I, Carrasco G, Kaser G, Kwok R, Mote P, Murray T, Paul F, Ren J, Rignot E, Solomina O, Steffen K, Zhang T (2013) Observations: Cryosphere. In: Stocker TF, Qin D, Plattner G-K, Tignor M, Allen SK, Boschung J, Nauels A, Xia Y, Bex V, Midgley PM (eds) Climate Change 2013: The Physical Science Basis. Contribution of the working group I to the Fifth Assessment Report of the intergovernmental Panel on Climate Change. Cambridge University Press, Cambridge, United Kingdom and New York, USA,

Vincent WF, Hobbie JE, Laybourn-Parry J (2008) Introduction to the limnology of high-latitude lake and river ecosystems. In: Vincent W, Laybourn-Parry J (eds) Polar Lakes and Rivers. Oxford University Press, New York, pp 1–23

Vincent WF, Laurion I, Pienitz R, Anthony KMW (2013) Climate Impacts on Arctic Lake Ecosystems. In: Goldman CR, Kumagai M, Robarts RD (eds) Climatic Change and Global Warming of Inland Waters: Impact and Mitigation for Ecosystems and Societies, 1st edn. John Wiley & Sons, Ltd,

Vuorio K, Meili M, Sarvala J (2006) Taxon-specific variation in the stable isotopic signatures (delta13C and delta15N) of lake phytoplankton. *Freshwater Biology* 51:807–822. doi: 10.1111/j.1365-2427.2006.01529.x

Wakeham SG (1990) Algal and bacterial hydrocarbons in particulate matter and interfacial sediment of the Cariaco Trench. *Geochimica et Cosmochimica Acta* 54:1325–1336. doi: 10.1016/0016-7037(90)90157-G

Walker DA, Jia GJ, Epstein HE, Raynolds MK, Chapin III FS, Copass C, Hinzman LD, Knudson J a., Maier H a., Michaelson GJ, Nelson F, Ping CL, Romanovsky VE, Shiklomanov N (2003) Vegetation-soil-thaw-depth relationships along a low-arctic bioclimate gradient, Alaska: synthesis of information from the ATLAS studies. *Permafrost and Periglacial Processes* 14:103–123. doi: 10.1002/ppp.452

References

Walker I (2001) Midges: Chironomidae and Related Diptera. In: Smol J, Birks HJ, Last W (eds) Tracking Environmental Change Using Lake Sediments SE - 3. Springer Netherlands, pp 43–66

Walker I, Levesque A, Cwynar L, AF (1997) An expanded surface-water palaeotemperature inference model for use with fossil midges from eastern Canada. *Journal of Paleolimnology* 165–178.

Walker I, MacDonald G (1995) Distributions of Chironomidae (Insecta: Diptera) and other freshwater midges with respect to treeline, Northwest Territories, Canada. *Arctic and Alpine Research* 27:258–263.

Walker IR (1987) Chironomidae (Diptera) in paleoecology. *Quaternary Science Reviews* 6:29–40. doi: 10.1016/0277-3791(87)90014-X

Walker IR, Smol JP, Engstrom DR, Birks HJB (1991) An Assessment of Chironomidae as Quantitative Indicators of Past Climatic Change. *Canadian Journal of Fisheries and Aquatic Sciences* 48:975–987. doi: 10.1139/f91-114

Walshe BM (1951) The feeding habits of certain chironomid larvae (subfamily Tendipedinae). Proceedings of the Zoological Society of London. Wiley Online Library, pp 63–79

Walter Anthony KM, Anthony P (2013) Constraining spatial variability of methane ebullition seeps in thermokarst lakes using point process models. *Journal of Geophysical Research: Biogeosciences* 118:1015–1034. doi: 10.1002/jgrg.20087

Walter Anthony KM, Vas DA, Brosius L, Iii FSC, Zimov SA, Zhuang Q (2010) Estimating methane emissions from northern lakes using ice- bubble surveys. *Limnology and Oceanography: Methods* 8:592–609.

Walter Anthony KM, Zimov S a, Grosse G, Jones MC, Anthony PM, Chapin FS, Finlay JC, Mack MC, Davydov S, Frenzel P, Frolking S (2014) A shift of thermokarst lakes from carbon sources to sinks during the Holocene epoch. *Nature* 511:452–6. doi: 10.1038/nature13560

Walter BP, Heimann M, Matthews E (2001) Modeling modern methane emissions from natural wetlands 1 . Model description and results. *Journal of Geophysical Research* 106:34,189 – 34,206.

Walter KM, Chanton JP, Chapin FS, Schuur E a. G, Zimov S a. (2008a) Methane production and bubble emissions from arctic lakes: Isotopic implications for source pathways and ages. Journal of Geophysical Research. doi: 10.1029/2007JG000569

Walter KM, Edwards ME, Grosse G, Zimov SA, Chapin FS (2007a) Thermokarst lakes as a source of atmospheric CH4 during the last deglaciation. *Science (New York, NY)* 318:633–6. doi: 10.1126/science.1142924

Walter KM, Engram M, Duguay CR, Jeffries MO, Chapin FS (2008b) The Potential Use of Synthetic Aperture Radar for Estimating Methane Ebullition From

Arctic Lakes 1. *JAWRA Journal of the American Water Resources Association* 44:305–315. doi: 10.1111/j.1752-1688.2007.00163.x

Walter KM, Smith LC, Chapin FS (2007b) Methane bubbling from northern lakes: present and future contributions to the global methane budget. *Philosophical transactions Series A, Mathematical, physical, and engineering sciences* 365:1657–76. doi: 10.1098/rsta.2007.2036

Walter KM, Zimov SA, Chanton JP, D. V, Chapin III FS (2006) Methane bubbling from Siberian thaw lakes as a positive feedback to climate warming. *Nature* 443:71–5. doi: 10.1038/nature05040

West JJ, Plug LJ (2008) Time-dependent morphology of thaw lakes and taliks in deep and shallow ground ice. *Journal of Geophysical Research* 113:1–14. doi: 10.1029/2006JF000696

Wetzel RG (2001) Limnology: lake and river ecosystems. Gulf Professional Publishing

Whiticar MJ (1996) Stable isotope geochemistry of coals, humic kerogens and related natural gases. *International Journal of Coal Geology* 32:191–215.

Whiticar MJ (1999) Carbon and hydrogen isotope systematics of bacterial formation and oxidation of methane. *Chemical Geology* 161:291–314. doi: 10.1016/S0009-2541(99)00092-3

Wiederholm T (1983) Chironomidae of the Holarctic. Keys and diagnoses. Part 1. Larvae, 19th edn. Entomologica Scandinavica Supplement, Lund, Sweden

Wik M, Crill PM, Varner RK, Bastviken D (2013) Multiyear measurements of ebullitive methane flux from three subarctic lakes. *Journal of Geophysical Research: Biogeosciences* 118:n/a–n/a. doi: 10.1002/jgrg.20103

Williams PJ, Smith MW (1989) The frozen earth: Fundamentals of geocryology. Cambridge University Press, Cambridge

Williamson CE, Morris DP, Pace ML, Olson OG (1999) Dissolved organic carbon and nutrients as regulators of lake ecosystems: Resurrection of a more integrated paradigm. *Limnology and Oceanography* 44:795–803.

Wooller MJ, Pohlman JW, Gaglioti B V., Langdon P, Jones M, Walter Anthony KM, Becker KW, Hinrichs K-U, Elvert M (2012) Reconstruction of past methane availability in an Arctic Alaska wetland indicates climate influenced methane release during the past ~12,000 years. *Journal of Paleolimnology* 48:27–42. doi: 10.1007/s10933-012-9591-8

Yu Z, Loisel J, Brosseau DP, Beilman DW, Hunt SJ (2010) Global peatland dynamics since the Last Glacial Maximum. *Geophysical Research Letters* 37:L13402. doi: 10.1029/2010GL043584

References

Zanden M, Rasmussen JB (2001) Variation in d15N and d13C trophic fractionation: implications for aquatic food web studies. *Limnology and oceanography* 46:2061–2066.

Zhang T, Barry RG, Knowles K, Heginbottom JA, Brown J (1999) Statistics and characteristics of permafrost and ground - ice distribution in the Northern Hemisphere I. *Polar Geography* 23:37–41.

Zheng Y, Singarayer JS, Cheng P, Yu X, Liu Z, Valdes PJ, Pancost RD (2014) Holocene variations in peatland methane cycling associated with the Asian summer monsoon system. *Nature communications* 5:4631. doi: 10.1038/ncomms5631

Zhuang Q, Melack JM, Zimov S, Walter KM, Butenhoff CL (2009) Global methane emissions from wetlands , rice paddies , and lakes. *Earth and Atmospheric Science Faculty Publications* 1–5.

Zimov SA, Davydov SP, Zimova GM, Davydova a. I, Schuur E a. G, Dutta K, Chapin FS (2006a) Permafrost carbon: Stock and decomposability of a globally significant carbon pool. *Geophysical Research Letters* 33:0–4. doi: 10.1029/2006GL027484

Zimov SA, Schuur EAG, Chapin III FS (2006b) Permafrost and the Global Carbon Budget. *Science* 312:1612–1613.

Zimov SA, Voropaev Y V, Semiletov IP, Davidov SP, Prosiannikov SF, Iii FSC, Chapin MC, Trumbore S, Tyler S (1997) North Siberian Lakes: A Methane Source Fueled by Pleistocene Carbon. *Science* 277:800–802. doi: 10.1126/science.277.5327.800

Zundel M, Rohmer M (1985) Prokaryotic triterpenoids. 3. The biosynthesis of 2 beta-methylhopanoids and 3 beta-methylhopanoids of Methylobacterium organophilum and Acetobacter pasteurianus ssp. pasteurianus. *European journal of biochemistry/FEBS* 150:35–39.